

A new species of *Eurytoma* (Hymenoptera, Chalcidoidea, Eurytomidae) from South Korea, feeding on seeds of *Prunus tomentosa* Thunb. (Rosaceae)

Duk-Young Park¹, Seunghwan Lee^{1,2}

1 *Insect Biosystematics Laboratory, Department of Agricultural Biotechnology, Seoul National University, Seoul, 08826, Republic of Korea* **2** *Research Institute for Agricultural and Life Sciences, Seoul National University, Seoul, 08826, Republic of Korea*

Corresponding author: Seunghwan Lee (seung@snu.ac.kr)

Academic editor: Petr Janšta | Received 26 February 2021 | Accepted 10 July 2021 | Published 31 August 2021

<http://zoobank.org/D3E967BF-0D9D-476A-9E6D-7E696C6218C8>

Citation: Park D-Y, Lee S (2021) A new species of *Eurytoma* (Hymenoptera, Chalcidoidea, Eurytomidae) from South Korea, feeding on seeds of *Prunus tomentosa* Thunb. (Rosaceae). *Journal of Hymenoptera Research* 85: 1–9. <https://doi.org/10.3897/jhr.85.64925>

Abstract

Eurytoma tomentosae **sp. nov.**, included in the *Eurytoma amygdali* species-group, is described from South Korea. This species could potentially be an economically important pest, as it interferes with reproduction by attacking the seeds of the garden plant *P. tomentosae*. A key to the two *Eurytoma* species feeding on *Prunus* in South Korea is provided.

Keywords

Chalcidoidea, parasitoids, pests, *Prunus tomentosa*, phytophagy

Introduction

Genus *Eurytoma* Illiger is the largest genus constituting approximately 700 species in the family Eurytomidae. Approximately 300 species have been recorded in the Palearctic region, 100 species in the Nearctic region, 80 species in Neotropical and Oriental regions, 70 species in the Australasian region, and 45 species in the Afro-tropical region. They are well known for their diverse natural histories. Most species are parasitoids of larvae of Coleoptera, Diptera, Hymenoptera, and Lepidoptera; oth-

ers are hyperparasitoids of larvae of Ichneumonoidea (Hymenoptera) and Tachinidae (Diptera); and others are phytophagous on seeds or flesh of fruits of various plants (e.g., Asphodelaceae, Campanulaceae, Euphorbiaceae, Fabaceae, Rosaceae) (Noyes 2020).

In the Palearctic region, Lotfalizadeh et al. (2007) reported that the genus *Eurytoma* is polyphyletic based on phylogenetic analysis based on morphology. Additionally, they divided *Eurytoma sensu stricto* into 11 species-groups depending on morphological characteristics. In addition, Zerova (2010) divided them into 15 species-groups using 225 Palearctic species based on morphological characteristics. Among them, the *E. amygdali* species-group, which is common to the opinions of two authors (Lotfalizadeh et al. 2007 and Zerova 2010), is restricted by an antenna with a 6-segmented funicle and a one-segmented clava in the female and lack of the postgenal depression by Lotfalizadeh et al. (2007). Zerova (2010) described this species-group with a comparatively large body size (approximately 5 mm), elongated body with a long metasoma, antenna with 6-segmented funicle in the female and 7-segmented funicle in the male, lower genal carina, and diameter of eyes shorter than length of gena.

The *E. amygdali* species-group is known for larvae that develop within seeds of Rosaceae. In particular, *E. amygdali* Enderlein, *E. schreineri* Schreiner, *E. samsonowi* Vassiliev, and *E. maslovskii* Nikol'skaya are pests that produce critical economic damage on cultivated trees of the genus *Prunus* L. (Zerova and Fursov 1991). In South Korea, *E. maslovskii*, first recorded by Tachikawa (1979), is a well-known pest of apricots (*P. armeniaca*), plums (*P. mume*), and peaches (*P. persica*). Above all, it is causing severe harm to plums every year, and even some farms that heavily damaged have suffered up to 90 percent (Lee et al. 2014).

In this study, we found an undescribed *Eurytoma* species associated with planted *Prunus tomentosa* Thunb. (Rosaceae). Larvae and pupae of the new species were discovered in seeds of host plants, and ovipositing behavior of adult females to premature fruits were observed (Fig. 2E–G). Their host, Nanking cherry (*P. tomentosa*), is a significant horticultural plant grown for ornamental purposes in urban areas. However, we found that seeds of the Nanking cherry can be attacked by this new *Eurytoma* species, resulting in an economic influence on the horticultural industry by disturbing plant reproduction. Though there have been no reports of severe damage to Nanking cherry, this new pest species requires attention. Here we describe a new species damaging *P. tomentosa* with a key to South Korean *Eurytoma* species associated with *Prunus*.

Materials and methods

Adult samples were collected by direct sweeping. Some fruits damaged by the immatures were also brought to the laboratory for rearing. Specimens are deposited at the Laboratory of Insect Biosystematics, Seoul National University (SNU). Most morphological terms follow Delvare et al. (2019).

Specimens were examined with an Olympus SZ61 stereomicroscope and photographed with a DMC 5400 digital camera attached to a Leica Z16 APO motorized

macroscope. Serial images were combined using Zerene Stacker and digitally retouched using Adobe Photoshop CS6.

Abbreviations used in this paper as follows: **SNU**, Seoul National University, Seoul, South Korea; **cl1–3**, clava segment 1–3; **F1–F6**, funicular segment 1–6; **MPS**, multiporous plate sensilla(e); **POL**, the distance between posterior ocelli; **LOL**, distance between anterior and posterior ocellus; **OOL**, minimal distance between posterior ocellus and inner orbit; **MPOD**, maximum diameter of posterior ocellus; **cc**, costal cell; **mv**, marginal vein; **pmv**, postmarginal vein; **stv**, stigmal vein; **Gt1–Gtx**, gaster tergites 1 to x.

Taxonomy

Key to South Korean species of *Eurytoma* associated with *Prunus*

- 1 Antenna with F1–6 cylindrical; with setae as long as half-length of funicular segment (Figs 1B, 3B); petiole of metasoma wider than long (Fig. 1G)..... **female 2**
- Antenna with F1–5 or 6 petiolate; with setae as long as length of funicular segment (Figs 2B, 3F); petiole of metasoma at least 2× longer than wide (Figs 2D, 3H)..... **male 3**
- 2 Head with temples 0.4× as long as length of eye in dorsal view (Fig. 3C); first funicular approximately 3× as long as wide, F2–6 about 2× longer than wide (Fig. 3B); OOL 2.5–2.8× as long as MPOD (Fig. 3C); propodeum without straight carina medially; metasoma 1.16–1.17× as long as head+mesosoma, syntergum as long as Gt6 and upturned; body length more than 6 mm. On apricots (*P. armeniaca*), plums (*P. mume*), and peaches (*P. persica*) ***Eurytoma maslovskii* Nikol'skaya**
- Head with temples 0.32–0.33× length of eye in dorsal view (Fig. 1D); F1 approximately 1.5× as long as wide, F2–6 about 1.1× longer than wide (Fig. 1B); OOL 2.0× as long as MPOD (Fig. 1D); propodeum with distinctly straight carina anterior margin to middle of propodeum (Fig. 1G); metasoma 0.90–0.93× as long as head+mesosoma; syntergum as half as length of Gt6 and not upturned; body length less than 5 mm. On Nanking cherry (*P. tomentosa*) ***Eurytoma tomentosae* sp. nov.**
- 3 Head with temples 0.55–0.56× length of eye in dorsal view (Fig. 1D); antenna with F1–5 petiolate; OOL 3.1× as long as MPOD (Fig. 3G); propodeum without straight carina medially, petiole more carinate (Fig. 3H); body length more than 5 mm. On apricots (*P. armeniaca*), plums (*P. mume*), and peaches (*P. persica*) ***Eurytoma maslovskii* Nikol'skaya**
- Head with temples 0.32–0.33× length of eye in dorsal view (Fig. 1D); antenna with F1–6 petiolate; OOL 2.0–2.3× as long as MPOD (Fig. 2C); propodeum with distinctly straight carina medially, petiole less carinate to coriaceous (Fig. 2D); body length more than 4 mm. On Nanking cherry (*P. tomentosa*) ***Eurytoma tomentosae* sp. nov.**

***Eurytoma tomentosae* sp. nov.**

<http://zoobank.org/178DA8C6-4A0B-49C3-9F05-0C666838B14E>

Figs 1A–H, 2A–G

Type material. *Holotype* female; SOUTH KOREA: Incheon, Yeonsu-gu, Solsaem-ro 43beon-gil, 42, Mt. Cheongnyang, 37°25'20.6"N, 126°39'50.7"E, 12.v.2019, found on fruits of *Prunus tomentosa*, Duk-Young Park (in SNU). *Paratype*. 7 females, 10 males, same data as holotype, 5 females, 16 males (in SNU); same data as holotype except 11.v.2019, Jihwan Park (in SNU).

Etymology. The species is named after the host plant, *Prunus tomentosa*.

Diagnosis. This new species differs from others of *amygdali* species-group in the comparatively small body length, short funicular segments, metasoma shorter than head+mesosoma, especially the syntergum half as long as Gt6 and not upturned.

Description. **FEMALE** (Fig. 1A, habitus). Body length 4.61–4.74 mm, including ovipositor. Antenna (Fig. 1B) black except radicle and clava dark brown; scape sparsely setose, spindle-like. Body black except mandible reddish-brown to dark apically, labial and maxillary palpi (Fig. 1C) black basally to apical tips yellowish-brown, knees brown to whitish-yellow medially, tibiae narrowly apically brown, ovipositor sheaths pale; with hair-like to slightly lanceolate yellow setae. Fore wing (Fig. 1H) pale yellowish, but deeply yellow infuscated below apical half of submarginal vein to stigmal vein; veins brownish-yellow and setae yellow. Hind wing yellowish-hyaline with pale-yellow setae.

Head 1.87–1.97× as wide as long and temples as long as one third of eye length in dorsal view (Fig. 1D); 1.39–1.52× as wide as high in frontal view (Fig. 1C); OOL:POL:LOL:MPOD = 2.0:2.5–2.6:1.0–1.1:1.0; scrobal depression adjoined from anterior ocellus, somewhat strigulate, carinate laterally and ground-shaped bottle in form; frons with yellowish lanceolate setae except between eyes and ocelli. Malar space 0.70× as long as height of eye. Mandible 3-toothed. Vertex and upper face entirely areolate except between eyes and ocelli coriaceous-punctured; lower face areolate-strigose converged towards clypeus, but clypeus smooth to somewhat strigose; malar sulcus shallowly and widely grooved. Lateral outline of gena distinctly convex in frontal view; genal carina present.

Antenna (Fig. 1B). Scape slightly swollen anteromedially; 3.67–3.75× as long as wide. Pedicel short, 0.9–0.95× as long as wide. Anellus 0.6–0.66× as long as wide. Funicle 6-segmented; F1 approximately 1.5× as long as wide; F2–F6 slightly longer than wide; each funicular with two rows of MPS; all setae subdecumbent. Clava 1-segmented; 2.87–2.99× as long as wide.

Mesosoma (Fig. 1E, F). In dorsal view, mesosoma 1.60–1.61× as long as wide; pronotum, and mesoscutum respectively 2.22× and 1.5× as wide as long; mesoscutellum 1.11× as long as wide. Propodeum approximately 125° angle to the plane of scutellum. Pro- and mesonotum densely coriaceous-punctured except anterior area of mesoscutal lateral lobe smooth in dorsal view and neck alutaceous. Sides of pronotum straight, not convex. Notauli distinctly impressed, narrow. Axilla clearly separated from scutellum by impressed axillar groove. Propodeum with irregularly rugulose-areolate and concave mesal area bearing distinct median carina on anterior half, lateral area areolate (Fig. 1G). Prepectus smooth except medial area to anterior and anteroventral margin rugulose.

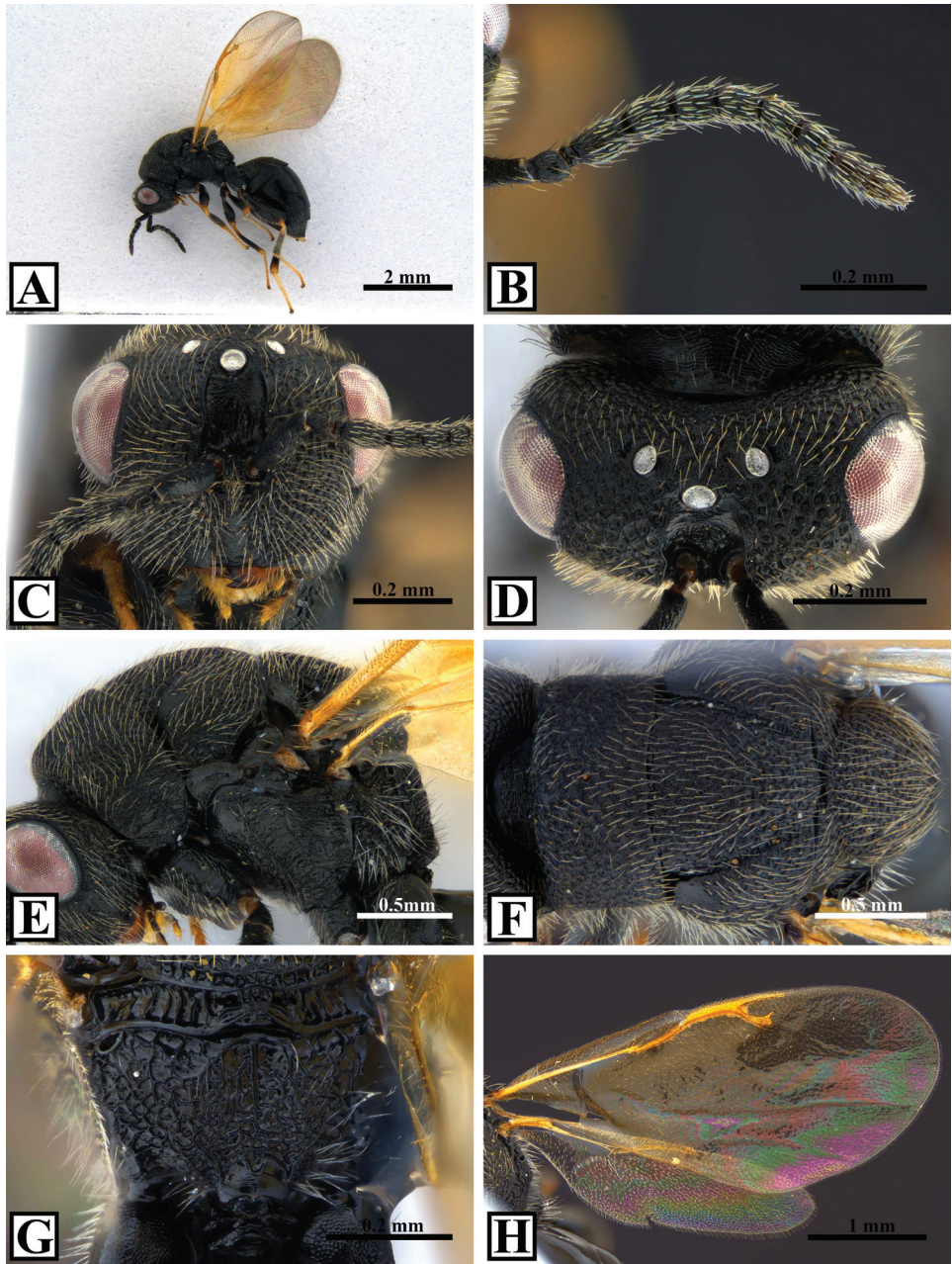


Figure 1. A–H *Eurytoma tomentosae*, female **A** habitus **B** antenna **C** head, frontal view **D** head, dorsal view **E** mesosoma, lateral view **F** mesosoma, dorsal view **G** propodeum **H** wing.

Tegula entirely smooth except posterior and ventral margin imbricate; with 2 distinct setae. Epicnemium hardly margined laterally by low epicnemial carina. Mesosternal shelf absent. Mesepisternum with variously smooth to strigose upper one-fourth and confused-areolate in lower three-fourth; adscrobal carina delimiting anteriorly femoral

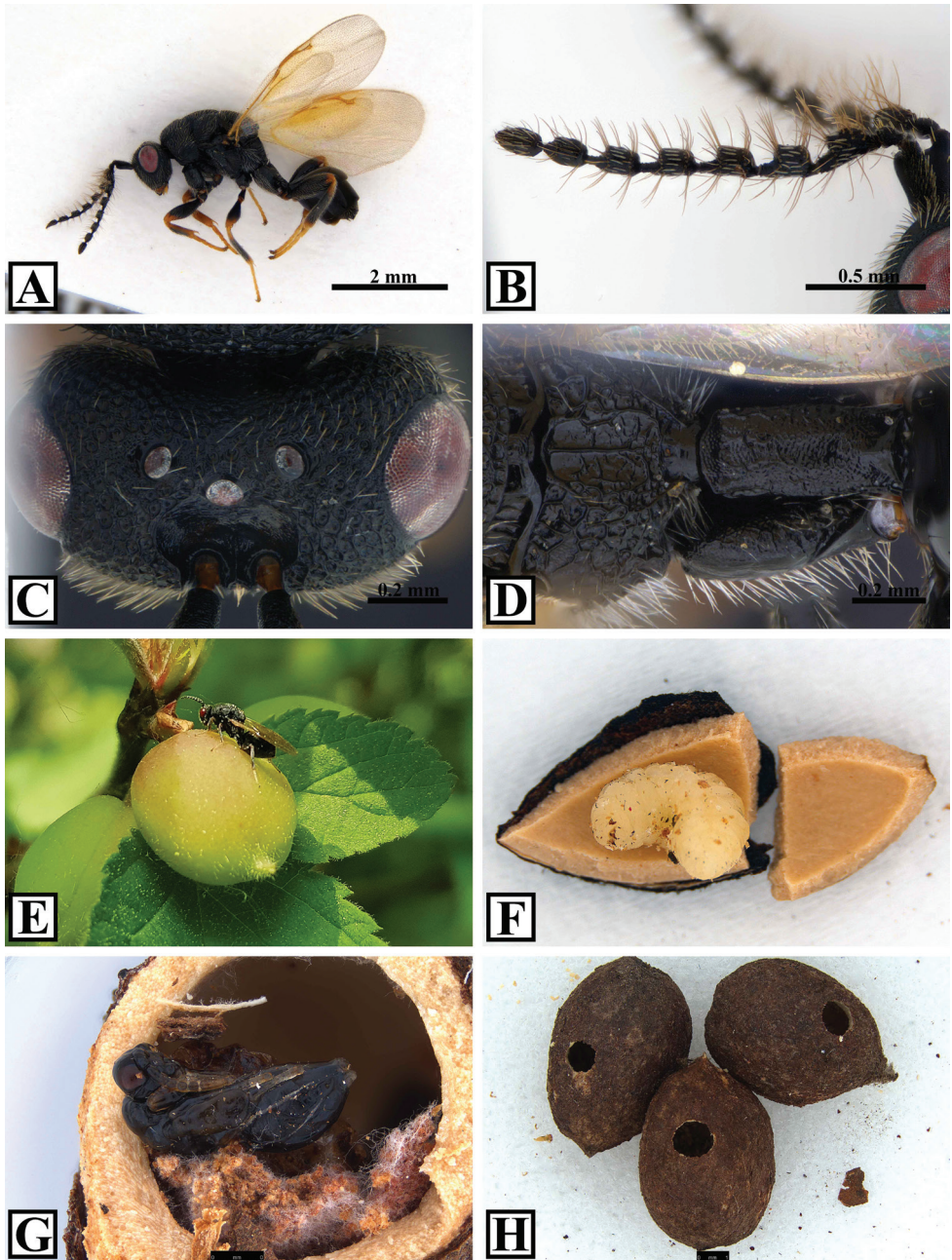


Figure 2. A–H *Eurytoma tomentosae* A–D male A habitus B antenna C head, dorsal view D propodeum and petiole E ovipositing behavior of female F larva in seed G pupa in seed H seed of *P. tomentosa* after adults of *E. tomentosae* emerged.

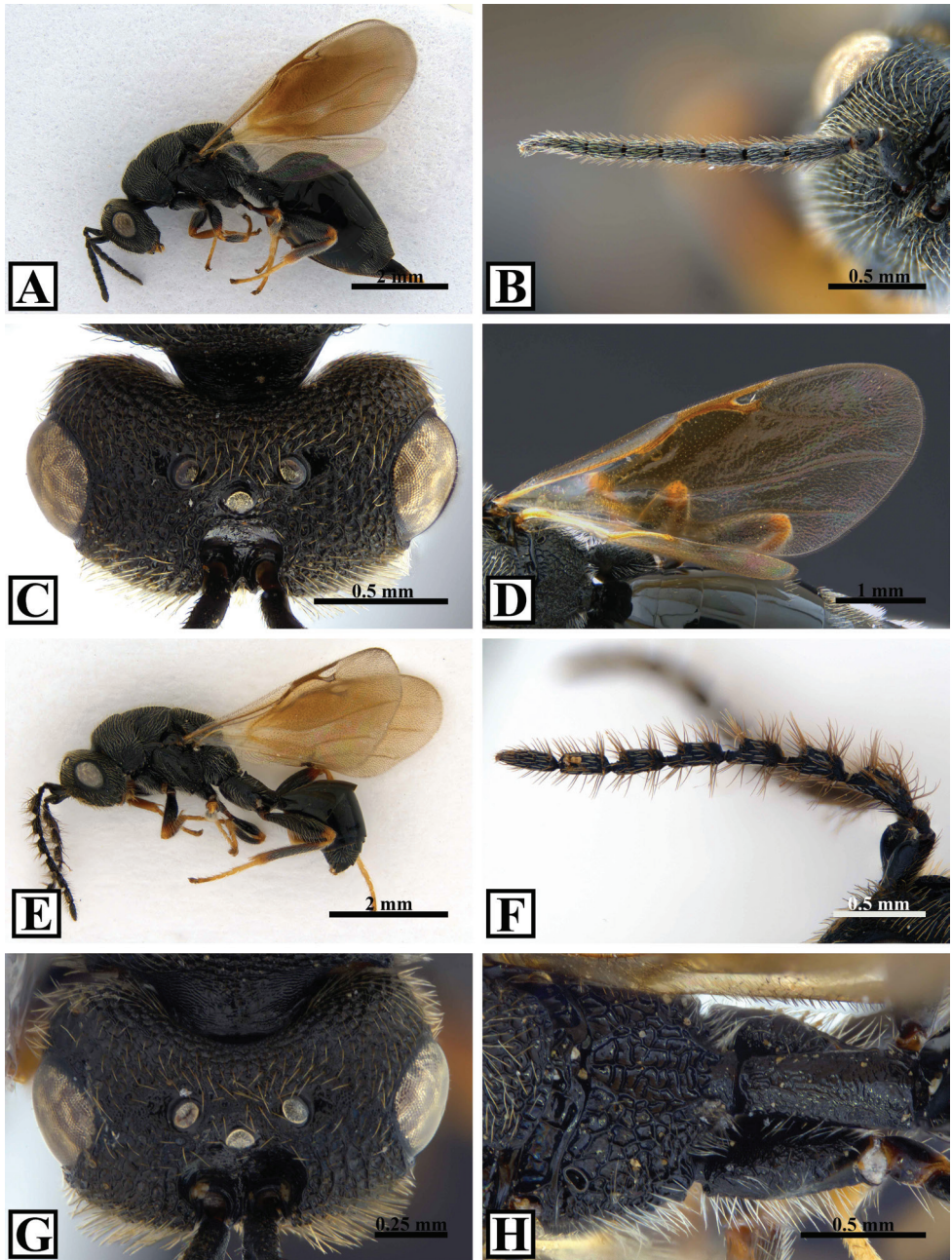


Figure 3. A–D *Eurytoma maslovskii* female A habitus B antenna C head, dorsal D wing E–H *E. maslovskii* male E habitus F antenna G head, dorsal H propodeum to petiole.

depression and reaching ventrally the mesocoxal foramen; femoral depression and mesepimeron with irregular carinulae, but the latter with smooth posterior margin. Metepimeron areolate and bearing long and thin erect setae, merging to propodeum posteriorly. **Legs.** Procoxa imbricate except smooth medially, without carina; setation bare medially. Mesocoxa without lamella. Metacoxa bare dorsally at base. **Fore wing** (Fig. 1H) $2.34\text{--}2.39\times$ as long as wide, cc: mv: pmv: stv = $5.3\text{--}5.5: 1.3\text{--}1.4: 1.2\text{--}1.4: 1.0$. Stigmal vein approximately an angle of 35° with the postmarginal vein. Stigma with sharp uncus.

Metasoma. Petiole wider than long, with slightly rough-coriaceous dorsal surface and highly raised carina transversally. Gaster ovate and smooth, about $1.59\text{--}1.74\times$ as long as length and $1.75\text{--}1.82\times$ as long as width. Gt4 slightly longer than Gt3; with short setae on anterior admarginal area. Gt5 and Gt6 similar in length; with hair-like yellow setae. Syntergum short and not upturned. Apex of ovipositor sheath round.

Male (habitus Fig. 2A). Body length $3.99\text{--}4.0$ mm. Morphologically similar to females except the following. Antenna (Fig. 2B) with funicle 6-segmented and clava 1-segmented; funicular segments petiolate, the bodies almost square. Head (Fig. 2C) with OOL: POL: LOL: MPOD = $2.0\text{--}2.3: 2.8: 1.2: 1.0$. Propodeum (Fig. 2D) less rugulose-areolate than female. Metasoma with long petiole punctured and less rugulose (Fig. 2D).

Host. *Prunus tomentosa* Thunb. (Rosaceae).

Biology. Adults of this species were observed emerging from seeds and mating in May. After mating, females oviposit inside premature fruits, and hatching larvae develop by eating the insides of seeds. They overwinter in a larval stage and pupate in spring before escaping from the seeds.

Distribution. South Korea.

Discussion

Eurytoma tomentosae sp. nov., is included in the *E. amygdali* species-group according to the definition provided by Lotfalizadeh et al. (2007) and Zerova (2010) based on a comparatively large body size (approximately 5 mm), antenna with 6-segmented funicle in the female and 7-segmented funicle in the male, lack of postgenal depression, lower genal carina.

The new species would be keyed out as *E. schreineri* using the key of Zerova and Fursov (1991) and Zerova (2010), because the metasoma is slightly longer than the mesosoma, the marginal vein is longer than the stigmal vein, and the syntergum is not upturned. However, it is distinguished from *E. schreineri* in having the metasoma shorter than the head plus mesosoma, the syntergum half as long as Gt6, and all funiculars with comparatively long setation in males. In addition, this species might be confused with the geographically close species *E. maslovskii*, distributed in Far East regions (Shandong, China; Japan; Korea; Primor'ye Kray, Russia) (Noyes 2020). However, *E. tomentosae* differs from *E. maslovskii* in having a distinctly shorter body length, less than 5 mm in the female and at most 4 mm in the male, comparatively short funicular segments in both sexes, OOL at most $2.0\times$ (female)

and 2.0–2.3× (male) as long as MPOD, propodeum with distinctly straight carina, metasoma at most slightly longer than mesosoma, and syntergum not upturned and half as long as Gt6.

Acknowledgements

We thank Jihwan Park for giving us the information on collecting the location of specimens. This work was supported by a grant from the National Institute of Biological Resources (NIBR) funded by the Ministry of Environment (MOE) of the Republic of Korea (NIBR202002205 and NIBR202130203), by Basic Science Research Program through the National Research Foundation of Korea (NRF) funded by the Ministry of Education (NRF-2020R111A2069484), and by Survey and identification of insect pests of small area-cultivated crops in central areas of Korean peninsula (Project Code PJ01450704) supported by Rural Development Administration, South Korea.

References

- Delvare G, Ribes Escolà A, Stojanova AM, Benoit L, Lecomte J, Askew RR (2019) Exploring insect biodiversity: the parasitic Hymenoptera, chiefly Chalcidoidea, associated with seeds of asphodels (Xanthorrhoeaceae), with the description of nine new species belonging to Eurytomidae and Torymidae. *Zootaxa* 4597(1): 001–090. <https://doi.org/10.11646/zootaxa.4597.1.1>
- Lee SM, Kim SJ, Yang CY, Shin JS, Hong KJ (2014) Host Plant, Occurrence, and Oviposition of the Eurytomid wasp *Eurytoma maslovskii* in Korea. *Korean Journal of Applied Entomology* 53(4): 381–389. <https://doi.org/10.5656/KSAE.2014.10.0.047>
- Lotfalizadeh H, Delvare G, Rasplus J-Y (2007) Phylogenetic analysis of Eurytominae (Chalcidoidea: Eurytomidae) based on morphological characters. *Zoological Journal of the Linnean Society* 151: 441–510. <https://doi.org/10.1111/j.1096-3642.2007.00308.x>
- Noyes JS (2020) Universal Chalcidoidea Database. World Wide Web electronic publication. <http://www.nhm.ac.uk/chalcidoids>
- Tachikawa (1979) *Eurytoma marlovskii* Nikolskaja newly discovered from Korea (Hymenoptera: Chalcidoidea – Eurytomidae). *Transactions of the Shikoku Entomological Society* 14(3–4): 181–183.
- Zerova MD (2010) Palaearctic species of the genus *Eurytoma* (Hymenoptera, Chalcidoidea, Eurytomidae): morphological and biological peculiarities, trophical associations and key to determination [In Russian]. *Vestnik Zoologii, Kiev* 24, 203 pp.
- Zerova MD, Fursov VN (1991) The Palaearctic species of *Eurytoma* (Hymenoptera: Eurytomidae) developing in stone fruits (Rosaceae: Prunoideae). *Bulletin of Entomological Research* 81(2): 209–219. <https://doi.org/10.1017/S0007485300051294>

Comparative biology of four *Rhodanthidium* species (Hymenoptera, Megachilidae) that nest in snail shells

Lucie Hostinská¹, Petr Kuneš², Jirí Hadrava^{3,4},
Jordi Bosch⁵, Pier Luigi Scaramozzino⁶, Petr Bogusch¹

1 Department of Biology, Faculty of Science, University of Hradec Králové, Rokytanského 62, CZ-500 03 Hradec Králové, Czech Republic **2** Department of Botany, Faculty of Science, Charles University, Benátská 433/2, CZ-128 01 Praha 2, Czech Republic **3** Biology Centre of the Czech Academy of Sciences, Institute of Entomology, Branišovská 1160/31, CZ-370 05, České Budějovice, Czech Republic **4** Department of Zoology, Faculty of Science, Charles University, Viničná 7, CZ-128 44 Praha 2, Czech Republic **5** CREAM – Ecological and Forestry Application Research Centre, Edifici C Campus de Bellaterra, 08193, Barcelona, Spain **6** Department of Agriculture, Food and Environment, University of Pisa, Via del Borghetto, 56124, Pisa, Italy

Corresponding author: Lucie Hostinská (lucie.hostinska@uhk.cz)

Academic editor: Christopher K. Starr | Received 26 March 2021 | Accepted 11 June 2021 | Published 31 August 2021

<http://zoobank.org/53AD3706-AEA6-4645-A3C7-B6A9D53C8525>

Citation: Hostinská L, Kuneš P, Hadrava J, Bosch J, Scaramozzino PL, Bogusch P (2021) Comparative biology of four *Rhodanthidium* species (Hymenoptera, Megachilidae) that nest in snail shells. Journal of Hymenoptera Research 85: 11–28. <https://doi.org/10.3897/jhr.85.66544>

Abstract

Some species of two tribes (Anthidiini and Osmiini) of the bee family Megachilidae utilize empty gastropod shells as nesting cavities. While snail-nesting Osmiini have been more frequently studied and the nesting biology of several species is well-known, much less is known about the habits of snail-nesting Anthidiini. We collected nests of four species of the genus *Rhodanthidium* (*R. septemdentatum*, *R. sticticum*, *R. siculum* and *R. infuscatum*) in the Czech Republic, Slovakia, Catalonia (Spain) and Sicily (Italy). We dissected these nests in the laboratory and documented their structure, pollen sources and nest associates. The four species usually choose large snail shells. All four species close their nests with a plug made of resin, sand and fragments of snail shells. However, nests of the four species can be distinguished based on the presence (*R. septemdentatum*, *R. sticticum*) or absence (*R. siculum*, *R. infuscatum*) of mineral and plant debris in the vestibular space, and the presence (*R. septemdentatum*, *R. infuscatum*) or absence (*R. sticticum*, *R. siculum*) of a resin partition between the vestibular space and the brood cell. *Rhodanthidium septemdentatum*, *R. sticticum* and *R. siculum* usually build a single brood cell per nest, but all *R. infuscatum* nests studied contained two or more cells. For three of the species (*R. siculum*, *R. septemdentatum* and *R. sticticum*) we confirmed overwintering in the adult stage. Contrary to *R. siculum*, *R. septemdentatum* and *R. sticticum* do not hide their nest shells and usually use shells under the stones or hidden in crevices

within stone walls. Nest associates were very infrequent. We only found two *R. sticticum* nests parasitized by the chrysidid wasp *Chrysura refulgens* and seven nests infested with pollen mites *Chaetodactylus* cf. *anthidii*. Our pollen analyses confirm that *Rhodanthidium* are polylectic but show a preference for Fabaceae by *R. sticticum*.

Keywords

Anthidiini, bees, ecology, nest structure, phenology, pollen specialization

Introduction

There are approximately known 20,000 species of bees worldwide classified into seven families (Michener 2007). Most non-parasitic species (ca. 70%) nest underground. Among bees nesting above ground, a few species, all of them in the family Megachilidae, utilize empty gastropod shells for nesting. Megachilidae comprises approximately 4,000 species classified into seven tribes and more than 70 genera (Michener 2007; Ascher and Pickering 2020). Nesting in gastropod shells has been reported in two tribes (Osmiini and Anthidiini) and five genera (*Osmia* Panzer, *Hoplitis* Klug, *Protosmia* Ducke, *Rhodanthidium* Isensee, and *Afranthidium* Michener). In addition, there is a single record of nesting in gastropod shells for *Megachile* (*Chalicodoma*) *lefebvrei* Lepelletier (tribe Megachilini), which usually builds nests in cavities in or between rocks (Müller et al. 2018).

The largest number of species nesting in snail shells are found in the Osmiini, which includes 52 species from five genera, most of which (43 species) occur in the Palaearctic biogeographic region (Müller et al. 2018). Most species are shell-nesting specialists and only occasionally use other types of cavities. However, a few species (most in the subgenus *Osmia* (*Osmia*)) typically nest in other types of cavities and only occasionally in snail shells (for review, see Müller et al. (2018)). The tribe Anthidiini displays a wide variety of nesting behaviours, including nesting underground, using various types of cavities and building exposed nests (Michener 2007; Litman et al. 2016; Westrich 2018). Nesting in shells in this tribe has been recorded in only four Palaearctic species of *Rhodanthidium* (Erbar and Leins 2017; Baldock et al. 2018; Westrich 2018; Romero et al. 2020) and two Afrotropical species of *Afranthidium* (Gess and Gess 2008, 2014).

The genus *Rhodanthidium* comprises 13 species, eight of which occur in Europe. The genus is divided into three subgenera: *Asianthidium* Popov (three species), *Meganthidium* Mavromoustakis (one species) and *Rhodanthidium* s. str. Isensee (nine species) (Michener 2007; Kasperek 2019; Kuhlmann et al. 2021). Among *Asianthidium*, the nesting biology is known only in *R. caturigense* (Giraud) which occurs in southern and central Europe, North Africa and the Middle East. This species builds nests in soil, often in large aggregations of 130–150 females. Nests of *R. caturigense* usually have 3–6 brood cells at the end of a short burrow. Cells are usually haphazardly oriented and conform to the presence of stones and roots. This species uses plant resin and plant

fibres to build nest plugs and brood cells. Each individual brood cell has two distinct layers – the inner layer of resin and the outer layer of plant fibres (e/g/ from leaves of *Verbascum*). The plug of the nest is built from resin coated with plant fibres (Pasteels 1977; Scheuchl and Willner 2016; Kasperek 2019). The nesting biology of the only *Meganthidium* species (*R. superbum* (Radoszkowski)), which is distributed in Turkey and the Middle East, remains unknown (Kasperek 2019).

The nesting biology of the subgenus *Rhodanthidium* s. str. is only partly known for five of the nine described species. Nothing is known about the nesting biology of *R. acuminatum* (Mocsáry) from Morocco, Sicily, Greece and Turkey, *R. buteum* (Warncke) from eastern Turkey, *R. exsectum* (Pasteels) from the Middle East, and *R. ordonezi* (Dusmet) from Morocco (Kasperek 2019). The nesting biology of *R. rufocinctum* (Alfken) also remains unknown; because of its close phylogenetic relationship to *R. septemdentatum*, it is expected to nest in snail shells (Kasperek 2019). The nesting biology of the other four species has only been partly described. *Rhodanthidium septemdentatum* (Latreille) has a wide distribution across southern and central Europe, North Africa and the Middle East; *R. infuscatum* (Erichson), *R. siculum* (Spinola) and *R. sticticum* (Fabricius) are only distributed in the western part of southern Europe (Portugal to Italy) and North Africa. Erbar and Leins (2017) described the nesting biology and pollen preferences of *R. siculum*. Although various aspects of the nesting biology of the three remaining species can be reconstructed based on several short notes (*R. septemdentatum*: Xambeau 1896; Friese 1911; Armbruster 1913; Grandi 1961; Gogala 1999; Grace 2010; Kasperek 2019; *R. infuscatum*: Pasteels 1977; *R. sticticum*: Schremmer 1960; Pasteels 1977; Ortiz-Sánchez 1990; Bosch et al. 1993; Romero et al. 2020), a comprehensive study of their biology has not yet been published. In particular, the range of snail species used by these species is unknown; the only relevant publication to date is that of Romero et al. (2020), who studied the use of empty gastropod shells by adults during inclement weather and at night.

In this study, we describe the nesting biology of four species of *Rhodanthidium* (*R. septemdentatum*, *R. sticticum*, *R. siculum* and *R. infuscatum*), including the range of snail shells used, the manipulation of shells by females during nesting, the structure of the nest, the main pollen sources collected by nesting females for their brood, the overwintering stage and the nest parasites.

Methods

We collected snail shells containing nests of *Rhodanthidium* in the Czech Republic (two sites in 2017 and 2018), Slovakia (one site), Catalonia (northeastern Spain; various sites in the provinces of Barcelona, Girona and Lleida in 1996, 1999, 2001, and 2018–2021), and Sicily (Italy, one site in 2018) (Suppl. material 1: Table S1, Suppl. material 2: Table S2). A description of all the sites surveyed is provided in Appendix 1.

We dissected the snail shells in the laboratory using thick tweezers, carefully breaking off small fragments of the upper part of the shell from the aperture to the apex.

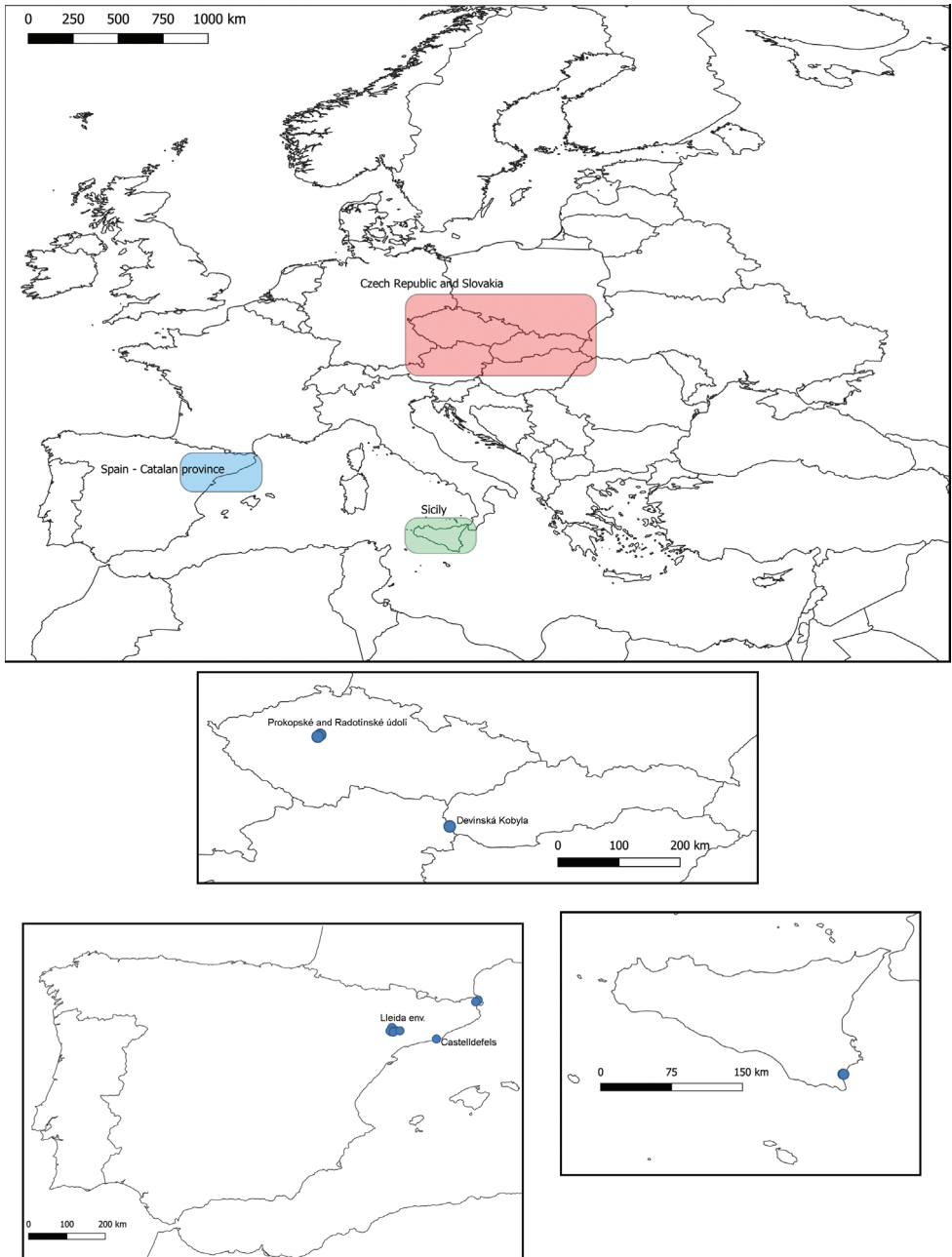


Figure 1. Location of study sites (blue dots) in the three regions surveyed.

We described the structure of the nest, including the number of brood cells and the materials used to make the plug and cell partitions, as well as any loose filling material found in the vestibular cell. We also recorded the developmental stage of the brood.

Larvae (with their food provision) and pupae of nests collected in spring/summer were transferred to microtubes closed with cotton wad and kept under laboratory conditions (20–22 °C, ca. 60% relative humidity). In September, cocoons were dissected to check the developmental stage. Adults were identified, and their sex determined.

We described the structure of the nests, took photos of some of them and made schematic drawings of the structure of nests for the four species. Photos of nests and their contents were taken using a Canon E550d digital camera with a macro lens. Final figures were created from multiple photos stacked by ZERENE STACKER software using the D-Map/P-Max algorithm. The drawings of nests were made by a pen and retouched and coloured in ADOBE PHOTOSHOP.

We took pollen samples of five nests of *R. septemdentatum*, one nest of *R. siculum* and nine nests of *R. sticticum*. Pollen samples were prepared using a standard acetolysis method (Moore et al. 1991) based on 5 min of boiling in an acetolysis mixture of sulfuric acid (H₂SO₄) and acetic anhydride (CH₃CO)₂O at a ratio of 1:9. The sample was then transferred into a mixture of water and glycerol. Slides were observed at 400× magnification using a light microscope. Pollen grains were identified using pollen atlases (Punt and Clarke 1984; Moore et al. 1991; Reille 1992; Beug 2004) and the reference collection of the Department of Botany at Charles University. An overview of the samples and types of pollen found is shown in Suppl. material 3: Table S3.

In our study of the nesting biology of *R. septemdentatum*, we attempted to determine whether females search for nesting snail shells under stones or if they transport snail shells under stones themselves. In 2018, we performed a manipulative experiment with snail shells in the locality Prokopské údolí. Based on our knowledge of the nesting sites of this species from 2017, we placed 16 empty snail shells of *Caucasotachea vindobonensis* (Férussac) on the ground surface around each of four nesting sites: four shells at a distance of up to 50 cm from the centre of the nesting site (marked with a number of the nesting site and letter A), another four shells up to 1 m (B), another four shells up to 2 m (C), and the last four shells up to 4 m (D). The snail shells were placed on 30th April 2018 (before the nesting season) and collected on 29th June (at the end or after the end of the nesting season).

Results

Rhodanthidium septemdentatum (Latreille)

Material examined. 23 nests from five localities in the Czech Republic, Slovakia and Spain (Suppl. material 2: Table S2).

Nest structure. All nests had a subterminal closing plug, a vestibular cell and one or two brood cells (Fig. 2). The vestibular cell was delimited by the closing plug and an inner partition, both made of resin and loosely filled with mineral fragments, soil and plant matter. In nests with two brood cells, there was no partition between the two (Fig. 2B). Nests with two cells appeared to be more frequent in central Europe

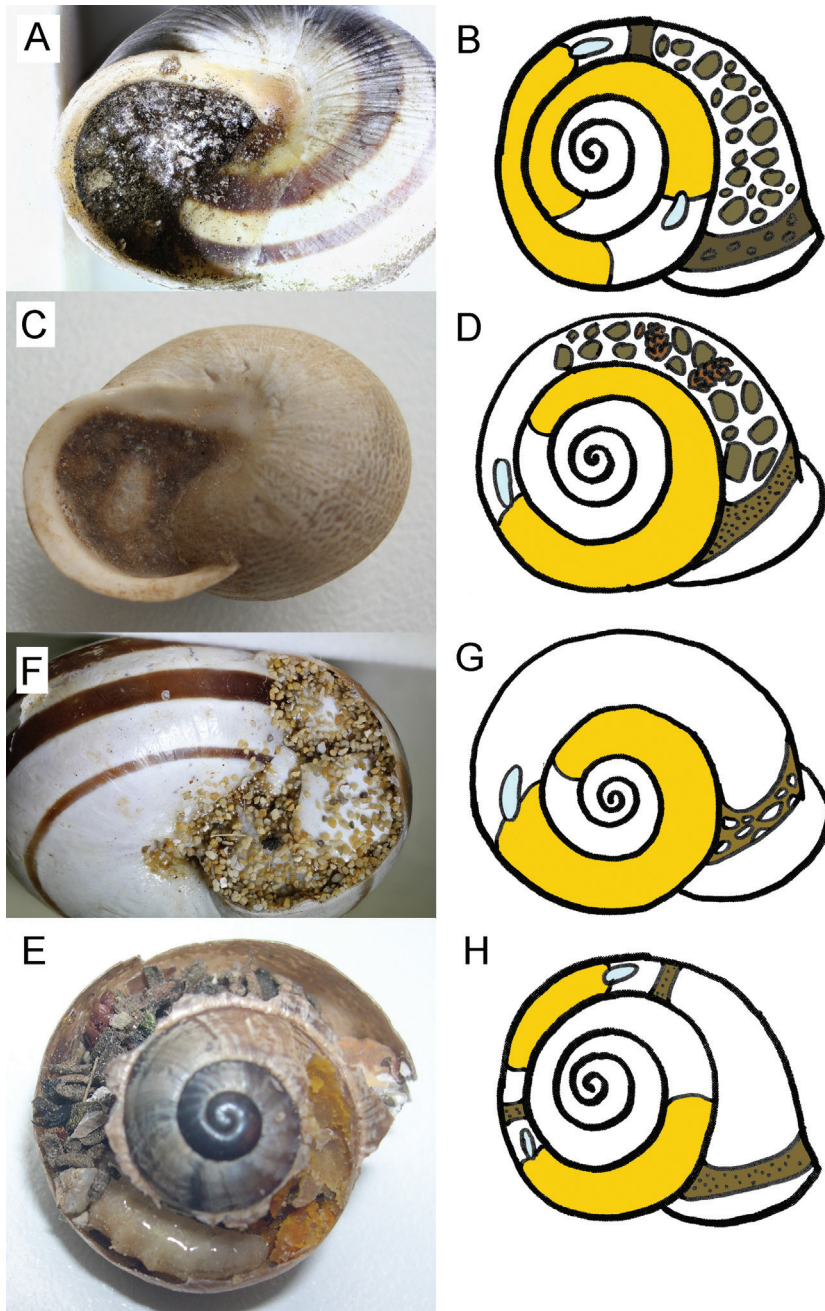


Figure 2. Photos and schematic drawings of nests of four species of *Rhodanthidium*. *Rhodanthidium septemdentatum* **A** shell of *Caucosatachea vindobonensis* with closing plug made of resin **B** schematic drawing of the inner nest structure in the shell. *Rhodanthidium sticticum* **C** shell of *Eobania vermiculata* with closing plug made of resin and soil particles **D** schematic drawing of the inner nest structure in the shell **E** photo of the shell with larva, pollen and filling of stones and plant partitions. *Rhodanthidium siculum* **F** shell of *Eobania vermiculata* with closing plug made of resin, sand and shell particles **G** schematic drawing of the inner nest structure in the shell. *Rhodanthidium infuscatum* **H** schematic drawing of the inner nest structure in the shell.

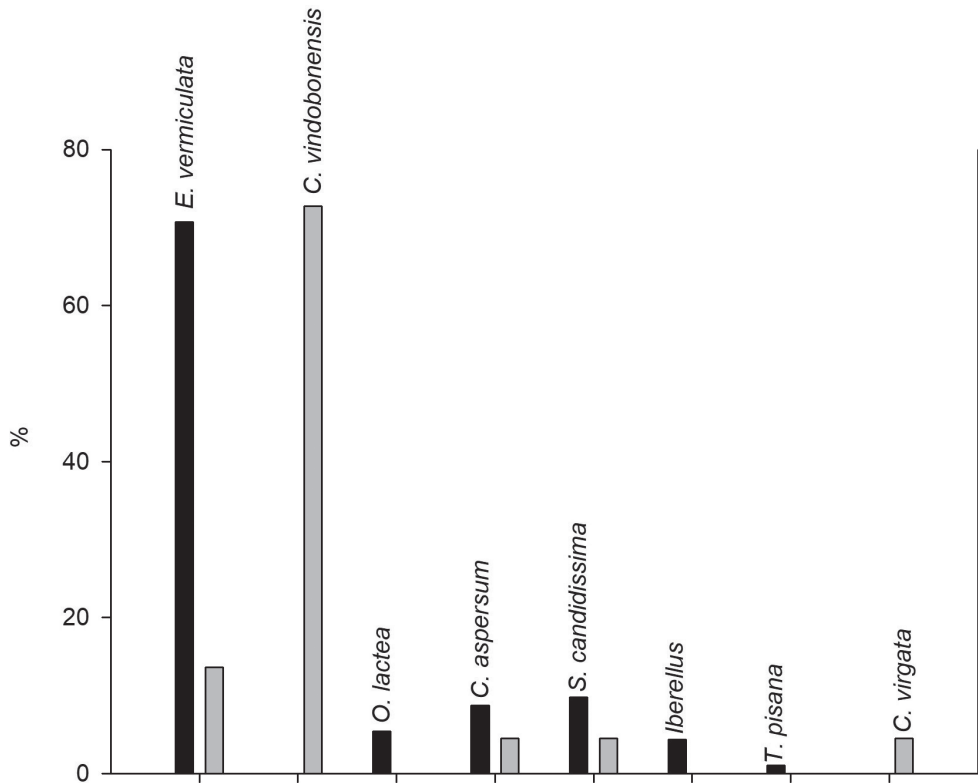


Figure 3. Proportions (in %) of shells used by *Rhodanthidium sticticum* (black columns) and *Rhodanthidium septemdentatum* (grey columns).

(Czech Republic and Slovakia) (11 of 17 nests examined) than in Spain (0 of 6 nests examined). Overall, we obtained 26 adult bees, 15 males and 11 females (M/F sex ratio: 1.4).

Shell choice. All nests from the Czech Republic and Slovakia were built in shells of *C. vindobonensis*, whereas nests from Spain were found in *Eobania vermiculata* (O. F. Müller) (3), *Sphincterochila candidissima* (Draparnaud) (1), *Cerneuella virgata* (Da Costa) (1), and *Cornu aspersum* (O. F. Müller) (1) shells (Fig. 3).

Shell manipulation. Females of *R. septemdentatum* do not move shells. All marked shells from our experiment in Prokopské údolí remained in place with no nesting on the ground surface, and only one shell placed near the centre of the nesting site (group A) was found under the stone with a nest of *R. septemdentatum*. However, we found five unmarked shells with nests under the stones on the same nesting site and suspected that the shell probably fell under the stone because of the climatic conditions before the nesting season of *R. septemdentatum*; alternatively, the space between the stones was utilized as a shelter by snails.

Life cycle. We dissected five nests in September 2017. All of them contained adult bees inside their cocoons. We also found adults in two nests collected during the winter of 2017/2018. In the spring of 2018, 16 young larvae from nine nests were transferred

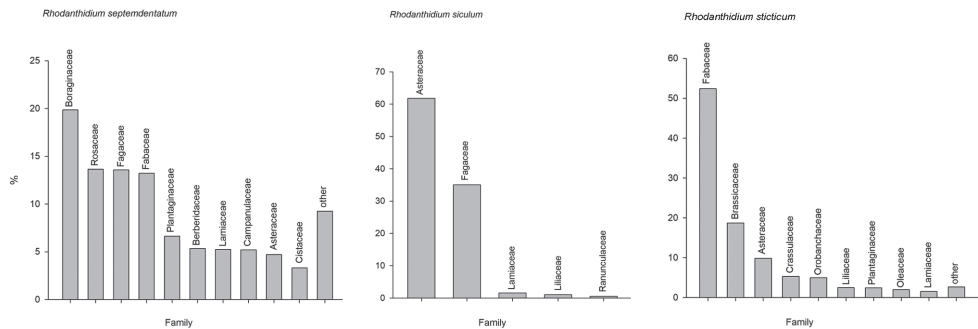


Figure 4. Proportions (in %) of pollen grains of plant families in studied nests of three species of *Rhodanthidium*.

with their pollen and nectar provisions to microtubes. The feeding larval stage lasted 5–8 weeks. Pupation occurred during July and August, and adults eclosed 2–4 weeks after pupation. Five larvae did not pupate and died during the winter. We conclude that *R. septemdentatum* overwinters in the adult stage in both study regions.

Nest associates. There were no nest associates with any of the *R. septemdentatum* nests.

Pollens collected. We analysed pollen samples from five nests from the Czech Republic. We recorded 41 pollen types from 22 plant families. Of these, 13 pollen types representing nine families were recorded in proportions higher than 10%. The most abundant pollen types were of the families Boraginaceae (20%, mostly *Echium vulgare*), Rosaceae (14%, mostly *Rubus* and *Filipendula*), Fagaceae (13%, mostly *Fagus sylvatica*), Fabaceae (11%, mostly *Cytisus*) and Plantaginaceae (7%) (Fig. 4 and Suppl. material 3: Table S3). Individual nests usually contained a mixture of pollen types from unrelated families. Only one nest contained a dominant pollen type (71% *Echium vulgare* pollen). The other nests contained 4–18 pollen types, of which only 2–5 represented more than 10% of the grains identified. These results indicate that *R. septemdentatum* is widely polylectic, and individual females do not specialize on any particular pollen source.

Rhodanthidium sticticum (Fabricius)

Material examined. 95 nests from various locations in Catalonia, north-eastern Spain (Suppl. material 2: Table S2).

Nest structure. The nests of this species have a vestibular cell and one (rarely two) brood cells. The closing plug was made of resin mixed with sand particles and sometimes fragments of snail shells (Fig. 2C). In most cases (62 nests), the closing plug was close to the aperture, but sometimes it was built a few mm inside the shell (33 shells). The vestibular cell was not delimited by a basal partition (Fig. 2D) and was loosely filled with mineral fragments, soil particles and plant debris (Fig. 2D, E). Most nests (90) had only one brood cell. Five nests contained two brood cells, and one

nest contained three brood cells. Overall, we obtained 76 adult bees, 44 males and 33 females (M/F sex ratio: 1.3).

Shell choice. Most nests (67) were built in shells of *E. vermiculata* (65). Other nests were built in shells of *S. candidissima* (9), *C. aspersum* (8, two of which juveniles), *Otala lactea* (O. F. Müller) (5), *Iberellus* sp. (4), and *Theba pisana* (O. F. Müller) (2) (Fig. 3). Multicell nests were found in *E. vermiculata* (two cells) and *O. lactea* (3 cells).

Shell manipulation. Most nests were found in shells hidden within stone walls or under stones. However, despite many hours of observation, we never observed any females dragging or hiding shells.

Life cycle. Eleven larvae from 21 nests collected in 2018 were transferred with their pollen nectar provisions into microtubes 4–10 days after collection. The feeding larval period lasted 3–6 weeks, and the pupal stage lasted 2–4 weeks. Adult eclosion occurred in July and August. Some larvae did not pupate and died during the autumn/winter.

Nest associates. We recorded parasitism by the ruby wasp *Chrysura refulgens* (Spinola) in two nests from Cap Ras (Girona) and by *Chaetodactylus* cf. *anthidii* mites in one nest from Sta. Margarida de Montbui (Barcelona). Overall, the parasitism rate in the nests examined was 3.03%. In addition, the three nests from Lleida (Lleida) and two nests from Òdena (Barcelona) contained low numbers of *C. cf. anthidii*, which did not cause the death of the bee.

Pollens collected. We analysed pollen samples in eight nests from Spain. We recorded 30 pollen types from 19 plant families. Of these, eight pollen types from six plant families were found in proportions greater than 10%. Most pollen grains identified (52%) were of the family Fabaceae (mostly *Cytisus* but also *Trifolium repens*), followed by Brassicaceae (19%) and Asteraceae (10%). Individual nests tended to be provisioned with a dominant (>50%) pollen type: *Cytisus* pollen was dominant in five nests, Brassicaceae pollen in two nests, and *Trifolium repens* pollen in one nest (Fig. 4 and Suppl. material 3: Table S3). These results indicate that *R. sticticum* is a polylectic species with a preference for collecting Fabaceae pollen and that females show a certain level of specialization, probably conditioned by the dominant pollen types in each locality.

Rhodanthidium siculum

Material examined. Two nests from Sicily.

Nest structure. The nests of this species contained only one brood cell. The vestibular space had no inner partition and, unlike the two previous species, was not filled with debris (Fig. 2G). The closing plug was made of resin with small fragments of snail shells and sand particles (Fig. 2F).

Shell choice. One nest was built in an *E. vermiculata* shell, and the other was built in a *T. pisana* shell.

Life cycle. In May, both nests contained young feeding larvae. Adult eclosion occurred in August.

Nest associates. No nest associates were recorded for this species.

Pollens collected. We analysed pollen from one nest. We identified nine pollen types from five plant families. The main plant family was Asteraceae (62%, mostly *Anthemis arvensis* but also *Centaurea jacea*), followed by Fagaceae (32%, mostly *Castanea*) (Fig. 4 and Suppl. material 3: Table S3). These results indicate that this species is also polylectic.

Rhodanthidium infuscatum

Material examined. Four nests from Spain. We found one nest in the city park in Castelldefels (Spain). The snail shell was found in a stone wall, and there were two cocoons, with hatched bees and partitioning in the nest. The structure of the nest was similar to that of the nest of *R. septemdentatum* but did not contain filling in the first empty cell. The other three records were collected in Spain by P. L. Scaramozzino. Two nests contained two individuals, and the third nest contained four individuals (mean 2.5 ± 0.5 SD).

Nest structure. The nests contained 2–4 brood cells and one vestibular cell. Both the brood cells and the vestibular cells were delimited by resin partitions (Fig. 2H). The vestibular cell was not filled with debris. The closing plug was made of resin mixed with small sand particles. Overall, we obtained 8 adult bees, 6 males and 2 females.

Shell choice. The nest found in Castelldefels was built in an *Iberellus* sp. shell and nests from Llanca (Girona) in *E. vermiculata* shells.

Nest associates. No nest associates were recorded for this species.

Discussion

The four species of *Rhodanthidium* studied build their nests in snail shells and use similar nesting materials, but the structures of their nests differ. All four use large snail shells, and the number of brood cells is inversely related to body size. The larger species, *R. septemdentatum*, *R. sticticum* and *R. siculum*, usually build one cell, sometimes two, per nest. By contrast, *R. infuscatum* (body length: 9–11 mm; Kaspárek 2019) builds 2–4 brood cells per nest. Information on the number of cells per nest in this species was hitherto unknown (Pasteels 1977; Ortiz-Sánchez 1990). Most nests from Spain were built in shells of *E. vermiculata*, and most nests from Central Europe were found in similar-sized *C. vindobonensis*. Both these species are similar in size, shape and aperture diameter, and are numerous in steppic habitats. We suppose that nests of these species can also be found in the shells of other large genera, such as *Cepaea* Held and *Helix* Linnaeus. Although all four species are specialized in the use of snail shells as nesting substrates, *R. sticticum* has also been recorded nesting in linear cavities (paper tubes; Bosch et al. 1993).

All four species use fragments of shells, small stones and grains of sand pasted with resin as material for the closing plug, and all nests studied had a long vestibular space

Table 1. Comparison of main characters of nesting biology of four European *Rhodanthidium* species.

Character / Species	<i>R. infuscatum</i>	<i>R. septemdentatum</i>	<i>R. siculum</i>	<i>R. sticticum</i>
Brood cells per nest	2–4	1–2	1	1 (2)
Closing plug	resin + soil particles	resin	resin + shell particles + sand	resin + soil particles
Septa between brood cells	yes	yes	no	no
Filling	no	yes	no	yes
Individual pollen specialisation	N/A	no	no	yes
Moving shells	N/A	no	yes	no

between the plug and the outermost brood cell (Table 1). However, we observed some structural differences among species (Table 1). First, *R. septemdentatum* and *R. infuscatum* build partitions between the outermost brood cell and the closing plug, whereas *R. sticticum* and *R. siculum* do not. Second, *R. septemdentatum* and *R. sticticum* fill the vestibular space with debris, whereas the other two species do not. Therefore, our study provides new information on the behavioural differences across closely related species (*R. septemdentatum* and *R. infuscatum* nests are considered indistinguishable; Pasteels 1977). Interestingly, the nest structure of *R. sticticum* nests built in paper tubes (1–2 cells per nest, lacking a partition between the brood cells and the plug and vestibular space filled with debris; fig. 1 in Bosch et al. 1993) fully coincides with the structure that we observed in nests built in snail shells. The lack of cell partitions is an unusual trait among cavity-nesting megachilid bee species, the vast majority of which build nests with clearly delimited brood cells (e.g., Bosch et al. 1993; Vicens et al. 1993; Müller 2021). It is usually known in one or several species in a group, e.g. *Heriades spiniscutis* (Cameron) is the only species of the genus with known nests without partitions (Michener 1968); *Osmia brevicornis* (Fabricius) does the same (Radchenko 1979, in the study reported as *Metalinella atrocoerulea* Schilling). Although most species of crabronid wasps of the genus *Pemphredon* create nests with partitions in dead wood or plant stems (Blösch 2000), *Pemphredon fabricii* (Müller) nesting in reed stalks and galls creates nests without partitions and female provisions the smallest larvae (Bogusch et al. 2018). Another unusual trait among cavity-nesting megachilid bees is the filling of the vestibular space with loose debris. Bees nesting in empty snail shells usually do not use debris, but several species with well-described nesting behaviour are exceptions (*Osmia bicolor* Schrank and *O. rufobirta* Panzer) (Bellmann 1981; Müller et al. 2018; Heneberg et al. 2020).

Erbar and Leins (2017) reported that *R. siculum* created 1–2 brood cells per nest that were not separated by a partition. The nests studied by us contained the closing plug and pollen inside the shell behind the plug. As Erbar and Leins (2017) did not describe nest structure, this study is the first to describe the nest structures of this species. *R. septemdentatum* and *R. sticticum* nests are known to contain one or two brood cells separated by a transverse partitioning from resin, and the closing plug is made of grains of sand, small stones or plant residues glued together with resin. Grandi (1961) also described the nest construction of *R. septemdentatum* in the snail shell of *T. pisana*: the shell had the closing plug made from pieces of shells glued with resin, followed by a cell filled with various materials (small stones, sand grains, fragments of dry leaves,

bark and moss), a resin layer and then a brood cell with pollen. We confirm these observations provided by both authors. Nests of *R. sticticum* had the space behind the closing plug filled with small stones and plant pieces, followed by pollen with eggs or larvae without any partitions.

Consistent with previous studies (Pasteels 1977; Kaspárek 2019), all nests that we studied in the field were placed under stones or inside stone walls. Despite many hours of observing *R. septemdentatum* and *R. sticticum* nesting females, we never observed any significant manipulation or transportation of shells. Instead, females appeared to choose shells that were already hidden under stones or in spaces in stone walls. This was confirmed by our manipulative experiment with shells of *C. vindobonensis* in Prokopské údolí. In contrast, Erbar and Leins (2017) provided a detailed description of *R. siculum* females transporting and burying nesting shells, usually beneath a plant. Importantly, the *R. siculum* population studied by Erbar and Leins (2017) nested in a sandy area with few stones. Future study of the nesting behaviour of *R. siculum* in stony areas and that of *R. septemdentatum* and *R. sticticum* in sandy areas could help determine whether shell manipulation is a plastic behavioural trait conditioned by the characteristics of the nesting environment.

Parasitism rates were low (3.4% of the cells obtained). We found *C. refulgens* in two nests of *R. sticticum*. *Chrysura refulgens* has been previously recorded from *R. septemdentatum* nests (Xambeau 1896; Friese 1911; Bogusch, unpublished observations in Greece) and probably parasitizes other *Rhodanthidium* species nesting in snail shells (Berland and Bernard 1938), as well as *O. bicolor*, another snail-nesting species (Strumia 1997). *Chrysura refulgens* occurs in southern Europe but does not reach Central Europe (Agnoli and Rosa 2019). We also found three *R. septemdentatum* nests with *Chaetodactylus* cf. *anthidii* (Klimov and O'Connor 2008). In one of these nests, the number of mites was high, and the bee did not develop. The other two nests contained few mites, and the bee larva had developed and spun its cocoon.

Rhodanthidium are polylectic bees (Bosch et al. 1993; Müller 1996; Erbar and Leins 2017; Westrich 2018; Kaspárek 2019). Previous observations have indicated that *R. septemdentatum* females collect pollen for their brood primarily from the Fabaceae and Lamiaceae families (Kaspárek 2019). Our results show that Boraginaceae, Rosaceae and Fagaceae pollen is also preferred. Bosch et al. (1993) found mostly *Cistus* and *Quercus* pollen in nests of *R. sticticum*. In our study, most of the pollen was from Fabaceae, followed by Brassicaceae and Asteraceae. *R. siculum* is known to collect pollen from Asteraceae and Fabaceae (Erbar and Leins 2017). In addition to Asteraceae, we also found Fagaceae pollen. To the best of our knowledge, the origin of the pollen collected by *R. infuscatum* remains unclear. We found that *R. sticticum* and *R. septemdentatum* are both polylectic, but the pollen preferences of individual females significantly differ. Each female of *R. septemdentatum* collected pollen from more species of unrelated plants (Boraginaceae, Rosaceae, Fagaceae, Fabaceae and Plantaginaceae in our surveys) and probably tracked the food supply, similar to *R. siculum* (Erbar and Leins 2017). Compared with this species, females of *R. sticticum* collected pollen from one dominant pollen source, which always made up more than half of all the pollen grains in the nest.

This pollen source differed among localities and among nesting females in one locality and usually belonged to the families Fabaceae, Brassicaceae and Asteraceae. Although we cannot comment on the generality of this individual specialization, our findings indicate that additional studies are needed to examine pollen preferences in both species.

Based on the phylogeny of *Rhodanthidium* (Litman et al. 2016; Kasperek 2019), all species of the subgenus *Rhodanthidium* likely nest in snail shells. According to several authors, a separate subgenus might be warranted for *R. infuscatum* based on its morphological differences (Michener 2007; Kasperek 2019). However, the nest structure of this species is similar to that of its relatives, except for the higher number of brood cells per nest, which appears to be related to the smaller body size of this species. *Rhodanthidium sticticum* and *R. siculum* are morphologically similar, but they differ in nest structure and possibly in nest manipulation (shell burying in *R. siculum* but not in *R. sticticum*) and possibly in pollen preferences (individual specialization in *R. sticticum* in contrast to unspecialized in *R. siculum*). Based on nest structure, *R. septemdentatum* combines the characters of the nesting biology of *R. siculum* and *R. sticticum*, but the main difference is in the presence of partitions or septa between the brood cells or between the empty cell at the closing plug and the first brood cell. Based on morphological traits (Kasperek 2019) and nest structure, *R. septemdentatum* appears to be closer to *R. infuscatum* than to *R. siculum* and *R. sticticum*. According to Litman et al. (2016), the genus *Rhodanthidium* belongs to the *Dianthidium* Cockerell clade, which includes genera that use resin to build their nests, whereas *Afranthidium*, the other genus nesting in snail shells, belongs to the *Anthidium* Fabricius clade, indicating that this behavioural trait evolved at least twice independently in tribe *Anthidiini*.

The majority of bees nesting in snail shells belong to the tribe *Osmiini*. In contrast to *Rhodanthidium*, most of these species use masticated plant leaves or mud to build their nest, but species of the genus *Protosmia* use resin (Müller et al. 2018). Many snail-nesting *Osmiini* have been reported to move their nest shells, and some are known to camouflage them with plant matter or cover them with pine needles or small twigs (e.g., *Osmia bicolor* and *O. rufohirta* Latreille; Bellman 1981; Vereecken and Le Goff 2012; Müller 2021). This behaviour has not been observed in *Rhodanthidium*, and the only species known to bury the shell nest is *R. siculum* (Erbar and Leins 2017). In contrast to *R. sticticum* and *R. siculum*, all snail-nesting bees of the tribe *Osmiini* build partitions between brood cells. Most species nesting in empty shells occur and nest in spring and overwinter as adults (Bellmann et al. 1981; Müller et al. 2018; our study). In Central Europe, only *Osmia spinulosa* (Kirby) nesting later in summer overwinters in prepupal stage (see Müller 1994).

Conclusions

We describe differences in the nesting biology of four closely related species belonging to the same subgenus *Rhodanthidium* (genus *Rhodanthidium*). In general, the nesting biology of all four species is quite similar. All species select shells of larger gastropod

species, collect pollen from multiple plant species, and use resin usually mixed with small soil or shell partitions for making closing plugs and partitions inside the nest. The main differences are in making a partition between the intercalary cell and first brood cell-nests of yellow-coloured species *R. infuscatum* and *R. septemdentatum* include partitions, while nests of orange-coloured species *R. siculum* and *R. sticticum* do not. Only *R. siculum* buries shells with nests in the ground (Erbar and Leins 2017), while *R. septemdentatum* and *R. sticticum* use hidden shells under stones or in stone walls for their nesting. All species are polylectic but individuals of *R. sticticum* show preferences. Using resin in nest supports the position of the genus *Rhodanthidium* in the *Dianthidium* clade as indicated Litman et al. (2016). Additional studies are needed, especially for the species *R. infuscatum*, which is the rarest of the four species studied (Kaspárek 2019). *R. sticticum* and *R. septemdentatum* are common species that form large local populations in southern Europe (Torné-Noguera et al. 2014; Romero et al. 2020) and the latter occurs in steppe habitats of conservation interest in central Europe (Bogusch et al. 2019, 2020).

Acknowledgements

We would like to thank to Georgina Alins and Neus Rodriguez-Gasol (IRTA, Spain) and Klára Daňková (Charles University, Czech Republic) for the help with field studies and Claudia Erbar (Heidelberg University, Germany) for collecting and sending shells of *R. siculum*. The study was supported by the Specific Research Grant of University of Hradec Králové Nr. 2102/2020.

References

- Agnoli GL, Rosa P (2019) Chrysis.net. <https://www.chrysis.net> [Accessed on 10.1.2021]
- Armbruster L (1913) Chromosomenverhältnisse bei der Spermatogenese solitärer Apiden (*Osmia cornuta* Latr.): Beiträge zur Geschlechtsbestimmungsfrage und zum Reduktionsproblem. Archiv für Zellforschung 11: 243–326.
- Ascher J, Pickering J (2020) Bee Species Guide (Hymenoptera: Apoidea: Anthophila). http://www.discoverlife.org/mp/20q?guide=Apoidea_species [Accessed on 18.8.2020]
- Baldock D, Wood TJ, Cross I, Smit J (2018) The Bees of Portugal (Hymenoptera: Apoidea: Anthophila). Entomofauna Supplement 22: 1–164.
- Bellmann H (1981) Zur Ethologie mitteleuropäischer Bauchsammlerbienen (Hymenoptera, Megachilidae): *Osmia bicolor*, *O. aurulenta*, *O. rufobirta*, *Anthidium punctatum*, *Anthidium strigatum*, *Trachusa byssina*. Veröffentlichungen für Naturschutz und Landschaftspflege Baden-Württemberg 53: 477–540.
- Berland L, Bernard F (1938) Hyménoptères vespiformes III (Cleptidae, Chrysidae, Trigonaliidae). Faune de France 34: 1–145.
- Beug HJ (2004) Leitfaden der Pollenbestimmung für Mitteleuropa und angrenzende Gebiete. Verlag Dr. Friedrich Pfeil, München, 542 pp.

- Blösch M (2000) Die Grabwespen Deutschlands—Lebensweise, Verhalten, Verbreitung. Goecke & Evers, Keltern, 480 pp.
- Bogusch P, Havelka J, Astapenková A, Heneberg P (2018) New type of progressive provisioning as a characteristic parental behaviour of the crabronid wasp *Pemphredon fabricii* (Hymenoptera Crabronidae). *Ethology Ecology & Evolution* 30: 114–127. <https://doi.org/10.1080/03949370.2017.1323801>
- Bogusch P, Hlaváčková L, Rodriguez-Gasol N, Alins G, Heneberg P, Bosch J (2020) Near-natural habitats near almond orchards with presence of empty gastropod shells are sufficient for solitary shell-nesting bees and wasps. *Agriculture, Ecosystems and Environment* 299: e106949. <https://doi.org/10.1016/j.agee.2020.106949>
- Bogusch P, Roháček J, Baňář P, Astapenková A, Kouklík O, Pech P, Janšta P, Heller K, Hlaváčková L, Heneberg P (2019) The presence of high numbers of empty shells in anthropogenic habitats is insufficient to attract shell adopters among the insects. *Insect Conservation and Diversity* 12: 193–205. <https://doi.org/10.1111/icad.12335>
- Bosch J, Vicens N, Blas M (1993) Análisis de los nidos de algunos Megachilidae nidificantes en cavidades preestablecidas (Hymenoptera, Apoidea). *Orsis* 8: 53–63.
- Erbar C, Leins P (2017) Sex and breeding behaviour of the Sicilian snail-shell bee (*Rhodanthidium siculum* Spinola, 1838; Apoidea–Megachilidae): preliminary results. *Arthropod-Plant Interactions* 11: 317–328. <https://doi.org/10.1007/s11829-016-9489-x>
- Friese H (1911) Hymenoptera. Apidae I. Megachilinae. In: *Das Tierreich. Eine Zusammenstellung und Kennzeichnung der rezenten Tierformen*. 28. Lieferung. De Gruyter, Berlin and Leipzig, 440 pp.
- Gess SK, Gess FW (2008) Patterns of usage of snail shells for nesting by wasps (Vespidae: Masarinae and Eumeninae) and bees (Megachilidae: Megachilinae) in southern Africa. *Journal of Hymenoptera Research* 17: 86–109.
- Gess SK, Gess FW (2014) Wasps and bees in southern Africa. SANBI Biodiversity Series 24. Pretoria: South African National Biodiversity Institute.
- Gogala A (1999) Bee fauna of Slovenia: checklist of species (Hymenoptera: Apoidea). *Scopolia* 42: 1–79.
- Grace A (2010) *Introductory Biogeography to Bees of the Eastern Mediterranean and Near East*. Bexhill Museum, Sussex.
- Grandi G (1961) *Studi di un entomologo sugli imenotteri superiori*. Calderini ed., Bologna, 660 pp.
- Heneberg P, Bogusch P, Hlaváčková L (2020) Experimental confirmation of empty snail shells as limiting resources for specialized bees and wasps. *Ecological Engineering* 142: e105640. <https://doi.org/10.1016/j.ecoleng.2019.105640>
- Kaspárek M (2019) Bees in the genus *Rhodanthidium*: A review and identification guide. *Entomofauna, Supplement* 24: 1–132.
- Klimov PB, O'Connor BM (2008) Morphology, evolution, and host associations of bee-associated mites of the family Chaetodactylidae (Acari: Astigmata), with a monographic revision of North American taxa. *Miscellaneous Publications Museum of Zoology University of Michigan* 199: 1–243.
- Kuhlmann M et al. (2021) Checklist of the Western Palaearctic Bees (Hymenoptera: Apoidea: Anthophila). <http://westpalbees.myspecies.info> [Accessed on 25.2.2021]

- Litman JR, Griswold T, Danforth BN (2016) Phylogenetic systematics and a revised generic classification of anthidiine bees (Hymenoptera: Megachilidae). *Molecular Phylogenetics and Evolution* 100: 183–198. <https://doi.org/10.1016/j.ympev.2016.03.018>
- Moore PD, Webb JA, Collingson ME (1991) *Pollen Analysis*. 2nd edn. Blackwell Scientific Publications, Oxford, 216 pp.
- Michener CD (1968) *Heriades spiniscutis*, a bee that facultatively omits partitions between rearing cells (Hymenoptera, Apoidea). *The Journal of the Kansas Entomological Society* 41: 484–493.
- Michener CD (2007) *The Bees of the World*. 2nd edn. Johns Hopkins University Press, Baltimore, 992 pp.
- Müller A (1994) Die Bionomie der in leeren Schneckengehäusen nistenden Biene *Osmia spinulosa* (Kirby 1802) (Hymenoptera, Megachilidae). *Veröffentlichungen für Naturschutz und Landschaftspflege Baden-Württemberg* 68/69: 291–334.
- Müller A (1996) Host-Plant Specialization in Western Palearctic Anthidine Bees (Hymenoptera: Apoidea: Megachilidae). *Ecological Monographs* 66: 235–257. <https://doi.org/10.2307/2963476>
- Müller A (2021) Palearctic Osmiine Bees. <http://blogs.ethz.ch/osmiini> [Accessed on 12.2.2021]
- Müller A, Praz C, Dorchin A (2018) Biology of Palearctic *Wainia* bees of the subgenus *Caposmia* including a short review on snail shell nesting in osmiine bees (Hymenoptera, Megachilidae). *Journal of Hymenoptera Research* 65: 61–89. <https://doi.org/10.3897/jhr.65.27704>
- Ortiz y Sánchez FJ (1990) Contribución al conocimiento de las abejas del género *Anthidium* Fabricius, 1804 en Andalucía (Hym., Apoidea, Megachilidae). *Boletín de la Asociación Española de Entomología* 14: 251–260.
- Pasteels JJ (1977) Une revue comparative de l'éthologie des Anthidiinae nidificateurs de l'ancien monde. *Annales de la Société Entomologique de France* 13: 651–667.
- Punt W, Clarke GCS (1984) *The Northwest European Pollen Flora, IV*. Elsevier, Amsterdam, 364 pp.
- Radchenko VG (1979) A new type of nest without cells in *Metalinella atrocaerulea* (Hymenoptera, Megachilidae). *Entomological review* 57: 353–355.
- Reille M (1992) *Pollen et spores d'Europe et d'Afrique du nord*. Laboratoire de Botanique Historique et Palynologie, Marseille, 543 pp.
- Romero D, Ornosá C, Vargas P (2020) Where and why? Bees, snail shells and climate: distribution of *Rhodanthidium* (Hymenoptera: Megachilidae) in the Iberian Peninsula. *Entomological Science* 23: 256–270. <https://doi.org/10.1111/ens.12420>
- Scheuchl E, Willner W (2016) *Taschenlexikon der Wildbienen Mitteleuropas. Alle Arten im Porträt*. Quelle and Meyer, Wiebelsheim, 917 pp.
- Schremmer F (1960) Harzbienen – *Anthidium sticticum* als Brutschmarotzer von *Anthidium septemdentatum*. Österreichische Mediathek, vx-02660_01_k02. www.mediathek.at [Accessed on 24.11.2020]
- Strumia F (1997) Alcune osservazioni sugli ospiti di Imenotteri Chrisididi (HYMENOPTERA: CHRYSIDIDAE). *Frustula entomologica* 20(33): 178–183.
- Torné-Noguera A, Rodrigo A, Arnán X, Osorio S, Barril-Graells H, Correia L, Bosch J (2014) Determinants of spatial distribution in a bee community: nesting resources, flower resources, and body size. *PLoS ONE* 9: e97255. <https://doi.org/10.1371/journal.pone.0097255>

- Vereecken NJ, Le Goff G (2012) Observations sur la nidification d'*Osmia* (*Allosmia*) *sybarita* Smith, 1853 (Hymenoptera, Megachilidae) en Crète. *Osmia* 5: 5–7. <https://doi.org/10.47446/OSMIA5.3>
- Vicens N, Bosch J, Blas M (1993) Análisis de los nidos de algunas *Osmia* (Hymenoptera, Megachilidae) nidificantes en cavidades preestablecidas. *Orsis* 8: 41–52.
- Westrich P (2018) Die Wildbienen Deutschlands. Eugen Ulmer, Stuttgart, 824 pp.
- Xambeau V (1896) Moeurs et métamorphoses des *Anthidium oblongatum* et *septemdentatum*, Hyménoptères du group des Apides. Bulletin de la Société Entomologique de France 1896: 328–333.

Appendix I. Description of sites surveyed

CZECH REPUBLIC

Prokopské and Radotínské údolí Nature Reserves in Prague. This area is occupied by hilly steppic grasslands on limestone subsoil, many snail species occur there and a larger amount of empty snail shells is available on the ground surface.

SLOVAKIA

Devínská Kobyla. The site is near the capital Bratislava, on a south-west slope of the hill. This area is occupied by hilly steppic grasslands on limestone subsoil, many snail species occur there and a larger amount of empty snail shells is available on the ground surface.

SPAIN

Lleida. The various sites in Lleida (Juneda, Castellans, Alamús, Aspa, Arbeca) were located in areas occupied by orchards and patches of Mediterranean scrubland vegetation (see Bogusch et al. 2020). Most nests were found in patches of natural habitat surrounding almond orchards. Nests were found within stone-walls and under stones on the ground.

Girona. The two sites in Girona (Cap Ras and Castell de Quermançó) are rocky areas covered by sparse Mediterranean scrubland. The *Rhodanthidium* nests were found within a collapsed stone wall, under the dry basal leaves of Agave plants and under a stone at the base of a bush.

Barcelona. The Garraf Natural Park comprises 123 km² of garrigue-type Mediterranean scrubland dominated by *Quercus coccifera*, *Rosmarinus officinalis* and *Thymus vulgaris* with sparse urban housing and long-time abandoned fields delimited by dry-stone walls.

The Òdena and Sta. Margarida de Montbui sites are located in rural areas of extensive agriculture with wheat fields, old almond orchards and olive groves. All nests were found in field margins and along dirt roads.

ITALY

Sicily. The two sites in Sicily where the *R. siculum* nests were found on a sandy habitat near the sea near Lido di Noto.

Supplementary material 1

Table S1. List of the localities, where nests of *Rhodanthidium* were studied

Authors: Lucie Hostinská, Jordi Bosch, Pier Luigi Scaramozzino, Petr Bogusch

Data type: table of localities (excel table)

Explanation note: This table contains all information to the localities of our studies.

Copyright notice: This dataset is made available under the Open Database License (<http://opendatacommons.org/licenses/odbl/1.0/>). The Open Database License (ODbL) is a license agreement intended to allow users to freely share, modify, and use this Dataset while maintaining this same freedom for others, provided that the original source and author(s) are credited.

Link: <https://doi.org/10.3897/jhr.85.66544.suppl1>

Supplementary material 2

Table S2. List of all studied nests

Authors: Lucie Hostinská, Jordi Bosch, Pier Luigi Scaramozzino, Petr Bogusch

Data type: shells studied (excel table)

Copyright notice: This dataset is made available under the Open Database License (<http://opendatacommons.org/licenses/odbl/1.0/>). The Open Database License (ODbL) is a license agreement intended to allow users to freely share, modify, and use this Dataset while maintaining this same freedom for others, provided that the original source and author(s) are credited.

Link: <https://doi.org/10.3897/jhr.85.66544.suppl2>

Supplementary material 3

Table S3. Pollen contents of nests

Authors: Petr Kuneš, Petr Bogusch

Data type: pollen contents (excel table)

Explanation note: Pollen contents of nests of *Rhodanthidium septemdentatum* (yellow), *R. siculum* (blue) and *R. sticticum* (green). Pollen types with 50% and more in one nest are marked in red, those with 10% and more in one nest are marked orange.

Copyright notice: This dataset is made available under the Open Database License (<http://opendatacommons.org/licenses/odbl/1.0/>). The Open Database License (ODbL) is a license agreement intended to allow users to freely share, modify, and use this Dataset while maintaining this same freedom for others, provided that the original source and author(s) are credited.

Link: <https://doi.org/10.3897/jhr.85.66544.suppl3>

The Waterston's evaporatorium of Ceraphronidae (Ceraphronoidea, Hymenoptera): A morphological barcode to a cryptic taxon

Jonah M. Ulmer¹, István Mikó², Andrew R. Deans³, Lars Krogmann^{1,4}

1 Department of Entomology, State Museum of Natural History Stuttgart, Rosenstein 1, 70191 Stuttgart, Germany **2** Don Chandler Entomological Collection, Department of Biology, University of New Hampshire, Durham, NH, USA **3** Frost Entomological Museum, Department of Entomology, The Pennsylvania State University, University Park, PA, USA **4** Institute of Biology, Systematic Entomology (190n), University of Hohenheim, 70593 Stuttgart, Germany

Corresponding author: Jonah M. Ulmer (jonah.ulmer@gmail.com)

Academic editor: Michael Ohl | Received 23 April 2021 | Accepted 20 July 2021 | Published 31 August 2021

<http://zoobank.org/B229BB82-83B9-485A-A43E-902F7601C950>

Citation: Ulmer JM, Mikó I, Deans AR, Krogmann L (2021) The Waterston's evaporatorium of Ceraphronidae (Ceraphronoidea, Hymenoptera): A morphological barcode to a cryptic taxon. *Journal of Hymenoptera Research* 85: 29–56. <https://doi.org/10.3897/jhr.85.67165>

Abstract

The Waterston's evaporatorium (=Waterston's organ), a cuticular modification surrounding the opening of an exocrine gland located on metasomal tergite 6, is characterized and examined for taxonomic significance within the parasitoid wasp family Ceraphronidae. Modification of the abdominal musculature and the dorsal vessel are also broadly discussed for the superfamily Ceraphronoidea, with a novel abdominal pulsatory organ for Apocrita being discovered and described for the first time. Cuticular modification of T6, due to the presence of the Waterston's evaporatorium, provides a character complex that allows for genus- and species-level delimitation in Ceraphronidae. The matching of males and females of a species using morphology, a long standing challenge for the group, is also resolved with this new character set. Phylogenetic analysis including 19 Waterston's evaporatorium related characters provides support for current generic groupings within the Ceraphronidae and elaborates on previously suggested synapomorphies. Potential function of the Waterston's organ and its effects on the dorsal vessel are discussed.

Keywords

Cryptic species, exocrine, morphological barcode, pulsatory organ

Introduction

Ceraphronoidea is a cosmopolitan group of parasitoid wasps consisting of two extant families: Ceraphronidae and Megaspilidae. Although being one of the most abundantly collected Hymenoptera (Martinez and Murgia 2001; Schmitt 2004), the group currently comprises only about 660 described species worldwide (Johnson 2004). However, current estimates propose a significantly larger species diversity, with an estimated 329 species still unknown in Canada alone (Bennett et al. 2019).

The phylogenetic placement of Ceraphronoidea within Apocrita remains unresolved, with current molecular studies indicating a position as sister to Ichneumonoidea (Peters et al. 2017) or as sister to Evaniidae, in a clade that is sister to Aculeata (Tang et al. 2019). A sister group relationship to Ichneumonoidea is supported by limited morphological data, including the presence of semitransparent patches on the abdominal sternites (Trietsch et al. 2017). Likewise, the presence of numerous plesiomorphic traits, including the presence of a median mesoscutal sulcus, well developed pterostigma, two apical spurs of the foretibia, muscled harpes in the male genitalia, and the presence of T10 among others (Gibson 1985; Mikó et al. 2013), suggest Ceraphronoidea might retain more plesiomorphic features than most other Apocrita.

Phylogenetic relationships within the superfamily are yet to be resolved (Mikó et al. 2018). This uncertainty is due, in part, to a lack of molecular studies within Ceraphronoidea and the great difficulty in morphologically separating genera. Nine of the sixteen known genera of Ceraphronidae, for example, are rare, monotypic taxa, defined primarily by autapomorphies (Masner and Dessart 1967; Dessart and Cancemi 1987). Species-level characterization and delimitation is relatively robust, compared to other Hymenoptera, due to the informative nature of the male genitalia (Dessart 1963a; Mikó et al. 2018; Ulmer et al. 2018). To study the male genitalia of minute specimens, often less than a millimeter in length, is challenging. Many species descriptions, therefore, were based on ambiguous female traits, such as flagellomere ratios (Szelényi 1940), which have been shown to be unreliable due to the pronounced allometry within the group possibly due to their small size or variance in host size. (Dessart 1963b; Mikó et al. 2013). Male genitalia has become increasingly accessible, however, with the application of new imaging methods, such as confocal laser scanning microscopy (CLSM), scanning electron microscopy (SEM), and micro-computer tomography (μ -CT) and the application of glycerol-based preservation of specimens (Mikó et al. 2016).

The development of species concepts based primarily on male specimens, however, makes it difficult for one to identify conspecific females (Dessart 1963b). The matching of males with females within Ceraphronoidea, and Ceraphronidae in particular, has been a long standing issue with over half (60%) of all species descriptions being based solely on females within *Aphanogmus* Thomson, 1858 (46:100) and *Ceraphron* Jurine, 1807 (125:190) combined. This problem is further exacerbated with the monotypic genera, many of which are based only on a single female and hypothesized to simply be highly derived forms of the larger genera (*Retasus ater* Dessart, 1984; for

example, likely being a female *Aphanogmus* with unusual morphology) (Dessart 1984). Likewise, subgenera may be valid genera but lack robust morphological diagnoses of both sexes.

The abdominal Waterston's evaporatorium (=Waterston's organ) (WE) is a cuticular specialization on the sixth metasomal tergite (T6) that is composed of a smooth, concave region which is covered by a reticulate, honeycomb-like structure of cells in many taxa (Fig. 1A–C). The structure is a synapomorphy of Ceraphronidae, and Dessart (1975e, 1992) speculated that it might have potential for generic and even species characterization. Several hypotheses regarding WE function have been proposed since its original discovery by Nees (1834), including mechanosensory (Brues 1902) and respiratory (Waterston 1923), while more recent work suggests that the structure is associated with glands (Ogloblin 1944; Mikó and Deans 2009). Although some species- and genus-level variation in the WE has been recorded (Dessart 1963a, 1965a, 1980e, 1991b), the structure has never been described in detail.

The formation of new structures or changes in size of preexisting structures can often lead to cascading shifts in surrounding morphology (Nijhout and Emlen 1998). Due to internal and external morphology developing largely independently from one another. Alteration in sclerite morphology can alter muscle attachment points which in turn affect the mechanical function of said muscle (Matsuda 1976). Within Hymenoptera, the evolution of the petiole provides numerous examples of shifting musculature morphology in response to restructuring of sclerites (Vilhelmsen et al. 2010). The development of a petiole also leads to internal space constraints leading to novel developmental paths of the dorsal vessel in higher hymenopterans (Willie 1958). Exocrine glands cause both an external modification of the sclerite they are present on as well as an internal space constraint from the glands presence within the body cavity. The dorsomedian position of the Waterston's evaporatorium with its relatively large exocrine glands likely serve as spatial constraints within the ceraphronid metasoma. These in turn may trigger alterations not only in the skeletomuscular system but also structurally influence the dorsally located abdominal circulatory system. Understanding the broader phenotypic alterations in response to the presence of a structure allows for a more thorough morphological and evolutionary analysis of a structure and the taxa as a whole.

In this study, we provide a detailed description of the Waterston's evaporatorium and adjacent structural abdominal modifications and explore their taxonomic utility for genus- and species-level classification of Ceraphronidae. The structure's species specificity and phenotypic consistency between sexes is also investigated in order to facilitate matching males and females.

Materials and methods

Ethanol-preserved and freshly collected and fixed specimens of the present study have been deposited in the Frost Entomological Collection (PSUC). Morphospecies were

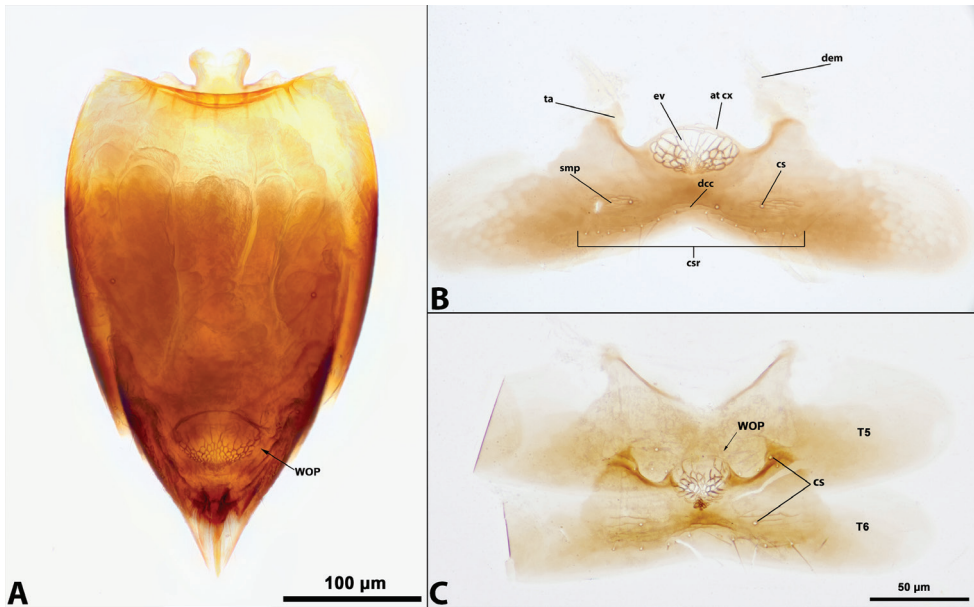


Figure 1. Morphological Terminology and overview of Waterston's evaporatorium (WE) and surrounding tergites in *Ceraphron* (brightfield) **A** metasoma in dorsal view, with WE visible on Mt6 **B** metasomal tergum 6 (T6) and Waterston's evaporatorium **C** metasomal tergum 5 and 6 ta = tergal apodeme ev = evaporatorium at cx = acrotergal calyx ite = intertergal extensor muscle sr ta = sclerotized ridge of tergal apodeme smp = submedial patches dcc = distal crenulate carina cs = campaniform sensilla csr = caudal setal row. Character abbreviations are provided in Appendix 1.

identified using male genitalia. Female specimens were taken from the same collecting event as males, when available. T6 was removed and mounted alongside the specimen.

Morphological terminology (Figs 1B, C; Appendix 1) was matched with concepts from the Hymenoptera Anatomy Ontology (Yoder et al. 2010). Terms referring to anatomical structures appear in bold and a URI table is provided (Suppl. material 2.) for terms in the HAO (<http://portal.hymao.org/projects/32/public/ontology/>). Abbreviations and figure references are given in parenthesis following the term. Abbreviations referring to muscles are italicized. New or modified terms are denoted with an asterisk (*). Skeletomuscular terminology for abdominal segments follows Snodgrass (1931) and Duncan (1939).

Dissections were performed under an Olympus SZX16 stereomicroscope with an Olympus SDF PL APO 1X PF objective (115 \times) and an Olympus SDF PL APO 2X PFC objective (230 \times magnification). Specimens were placed in glycerol, on concave microscope slides (Sail Brand CAT.NO.7103) and dissected with #2 pins and #5SA forceps. Brightfield imaging was performed using an Olympus DP71 digital camera mounted on an Olympus ZX41 compound microscope. All images were aligned and stacked (Pmax) using ZereneStacker v 1.04 (T201404082055). Scale bars were added in Adobe Photoshop 2020 (v 21.2.4).

Sample preparation for CLSM followed Mikó and Deans (2013). Abdomens of ethanol stored specimens were dissected and incubated at room temperature in

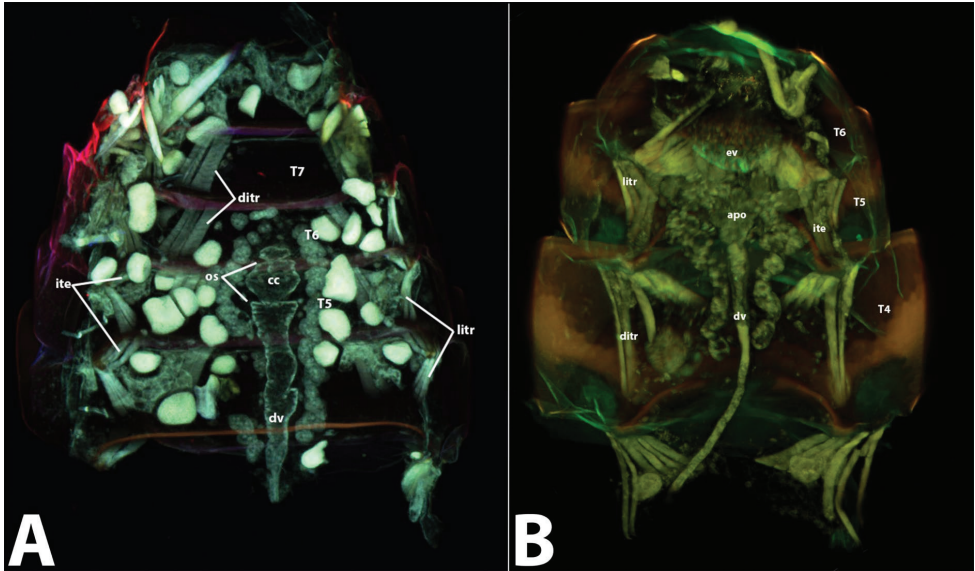


Figure 2. Skeletomusculature of Ceraphronoidea metasoma (CLSM) **A** dorsal view of metasoma of *Conostigmus* sp. showing termination of dorsal vessel into caudal chamber and tergal muscles **B** dorsal view of metasoma of *Ceraphron* sp. showing tergal muscles and termination of dorsal vessel into abdominal pulsatory organ anterior to Waterston's evaporatorium. Ditr = dorsal intertergal retractor muscles; ite = intertergal extensor muscles; litr = lateral intertergal retractor muscles; os = ostia; cc = caudal chamber; dv = dorsal vessel; apo = abdominal pulsatory organ; ev = evaporatorium.

35% hydrogen peroxide solution for 48 hours to bleach melanin-rich structures that may affect autofluorescence. Metasomal T6 of each specimen was then suspended in glycerol between two 0.15 mm thick, 24×50 mm coverslips and imaged with an Olympus FV10i confocal laser-scanning microscope (CLSM, Olympus Corporation of the Americas, Center Valley, PA) at the Microscopy and Cytometry Facility at the Huck Institutes of the Life Sciences at the Pennsylvania State University (Fig. 5C) and with a Nikon A1R-HD CLSM at the University of New Hampshire Instrumentation Center (Figs 2A, B, Figs 5A, B). With the Olympus FV10i, we used three excitation wavelengths, 405, 473, and 559 nm, and detected the autofluorescence using two channels with emission ranges of 490–590 and 570–670 nm (Fig. 2). On the Nikon A1R-HD, we used one excitation wavelength 487 nm laser with emission ranges defined using the A1-DUS spectral detector, 500–560 and 570–630 nm (Figs. 3E and F, and 4–6). The resulting image sets were assigned pseudo-colors that reflected the fluorescence spectra. Volume-rendered micrographs and media files were created using FIJI (Schindelin et al. 2012) and Nikon NIS-Elements AR v. 5.02.01.

SEM micrographs were made with a Hitachi S-3200 Scanning Electron Microscope (wd = 23.5, av = 5 kV) at the Analytical Instrumentation Facility (AIF) of the North Carolina State University. Specimens were critical point dried and coated with palladium prior to imaging.

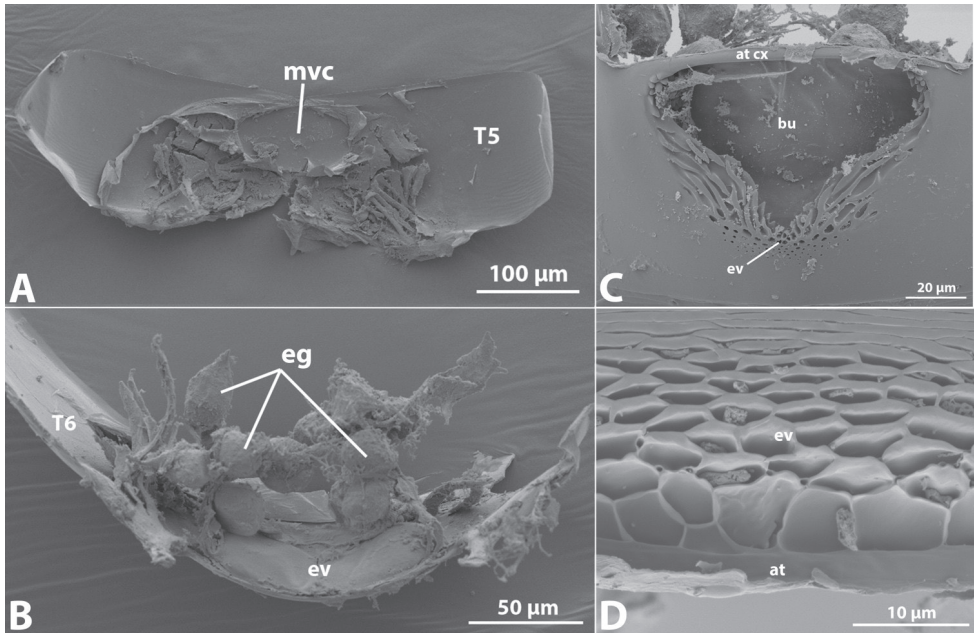


Figure 3. WE glands and sculpture of evaporatorium in Ceraphronidae (SEM) **A** ventral side T5 of *Aphanogmus* sp. showing median-ventral concavity corresponding to position of Waterston's organ on T6. **B** glandular subunits of the Waterston's organ extending into abdominal body cavity from ventral side of T6 and evaporatorium **C** evaporatorium and bulla of *Aphanogmus* **D** evaporatorium topography in *Ceraphron*, a reticulate matrix of empty cells. Mvc = median ventral concavity of T5 eg = evaporatorium glandules ev = evaporatorium at cx = acrotergal calyx bu = bulla; at = acrotergite.

Freshly collected specimens for serial block face scanning electron microscopy (SBFSEM) were dissected in 0.1M cacodylate buffer, fixed in 2.5% glutaraldehyde (in 0.1M cacodylate buffer), and then stained and embedded following Mikó et al. (2017). Specimens were then embedded in colloidal silver and trimmed with a Leica UCT ultramicrotome. Sectioning and imaging was conducted with a Zeiss SIGMA VP-FESEM with a Gatan 3View2 accessory at the Microscopy and Cytometry Facility at the Huck Institutes of the Life Sciences at the Pennsylvania State University. Images were aligned in imageJ (Version 2.0.0).

Characters were encoded within Mesquite Version 3.61 (build 927) then exported to TNT 1.5. The data matrix is available in Supplementary table 2. Cladistic analyses were performed with a traditional search, utilizing sub-tree pruning with all characters unordered. Collapsing rules were set to maximum length = 0. One thousand replications with 1,000 trees saved per replication were run, followed by branch breaking on optimal trees. A strict consensus was then run based on the resulting trees. Bootstrap support values were calculated from 10,000 pseudoreplications. Trees were post-processed in TreeGraph (version 2.15.0-887 beta).

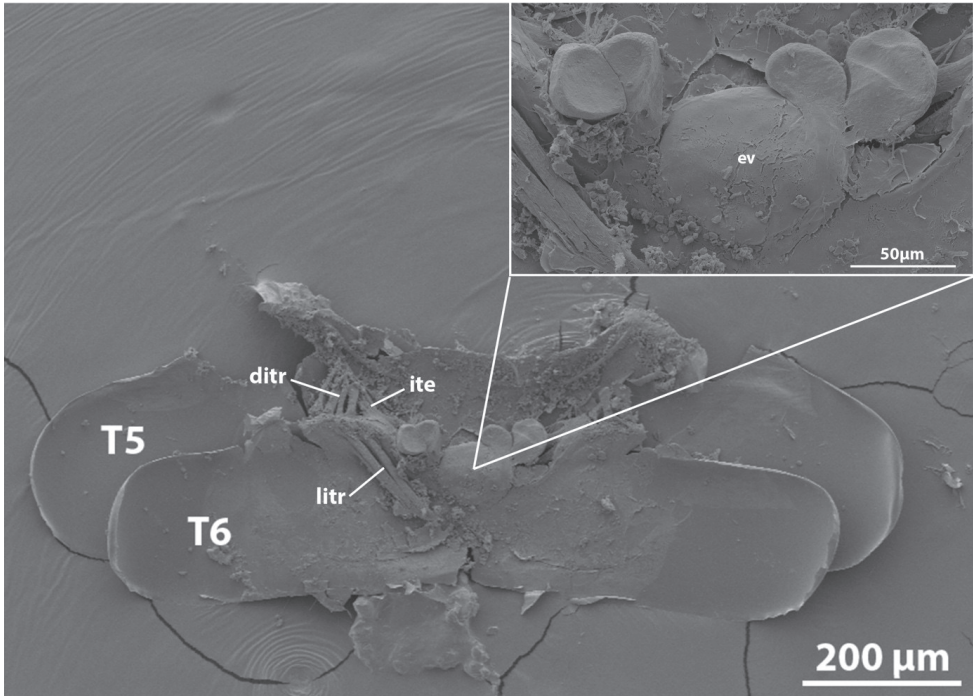


Figure 4. Tergite 5 and 6 of *Ceraphron* (SEM). The evaporatorium is visible ventrally as a plate corresponding to the bulla concavity or reticulate evaporatorium cell matrix. *Ditr* inserting lateral to *ite* on T6. *Litr* of T6 extending towards T7.

Results

Modification of the surrounding tergites and internal structures of Ceraphronidae in relation to the presence of the Waterston's evaporatorium are discussed in the following two subsections, these are provided as a comparative study relative to the sister group Megaspilidae.

T5 and T6 of Ceraphronoidea

The **Waterston's evaporatorium*** (WE) = (Waterston's organ) (Fig. 3B) is a cuticular specialization corresponding to a putative exocrine gland orifice present on the **acrotergite of metasomal tergite 6** (at: Fig. 3D). We use the name Waterston's evaporatorium to refer to the cuticular modification following Mikó et. al. (2009) due to the cuticular structure not falling within the definition of an organ as a multi-tissue structure.

In Megaspilidae, the abdominal tergites retain the plesiomorphic configuration; connected to each other by three muscles, the dorsal intertergal retractor muscle (*ditr*) (muscle 155, in T6; serially homologous with 133 in T4 and 144 in T5), which arises at the antecostal ridge of T5 and inserts medially on the antecostal ridge of T6. The lateral intertergal retractor muscle (*litr*) (muscle 156) (serially homologous with muscles

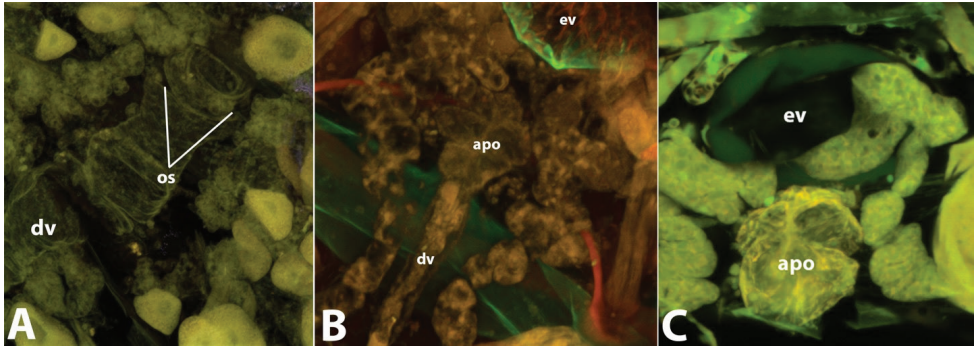


Figure 5. Dorsal vessel termination in Ceraphronoidea (CLSM) **A** dorsal vessel termination of *Conostigmus* sp. **B** dorsal vessel and abdominal pulsatory organ of *Ceraphron* sp. **C** abdominal pulsatory organ and evaporatorium in *Aphanogmus* sp.

134 [T4] and 145 [T5]) arises at the antecostal ridge of T6 diverging posteriorly from muscle 155 and inserts on the lateral edge of the **tergal apodeme (ta)** at the antecostal ridge of T6. The intertergal extensor muscle (*ite*) (muscle 157) (serially homologous with 135 [T4] and 146 [T5]) arises from the posterior margin of T5 and inserts apically on the tergal apodeme of T6. The antecosta does not bear any exocrine glands medially (Fig. 2A).

In Ceraphronidae, due to the presence of the WE, the tergal apodemes shift submedially on T6 and *ditr* is lateral to *ite* and the tergal apodeme (Figs 2B, 4). The **medioventral concavity*** (**mvc**) of T5 is a cuticular concavity on the ventral side of T5 corresponding to the WE of T6 which lies ventrally to the mvc when the *ite* muscles are relaxed. (Fig.3A) and bears campaniform sensilla at the level of the lateral tergal apodemes of the sixth tergite (T5) (Fig.1C). The T5 is not modified in Megaspilidae.

Internal anatomy

The exocrine glands corresponding to the WE are composed of Type III gland cells clustered ventrally to the WE. The glands attach via ductules connected with each glandular subunit which merge into larger ducts attached lateroventrally to the WE; the ducts terminate in the bulla or external reticulate cells of the WE. The glands themselves extend substantially into the abdomen (50–75 μm) (Fig. 3B).

In Megaspilidae, the dorsal vessel consists of a termination of the aorta into an enlarged globular caudal chamber ventral to T6, the caudal chamber contains an anterior and posterior pairing of ostia (os: Figs 2A, 5A). In Ceraphronidae, the dorsal vessel consists of a thin, weakly muscled aorta which abruptly terminates ventral to T6 and anterior to the WE into a large pulsatile organ consisting of 4–6 lobes divided by septa and muscled via broad alary muscles (Figs 2B, 5B, C).

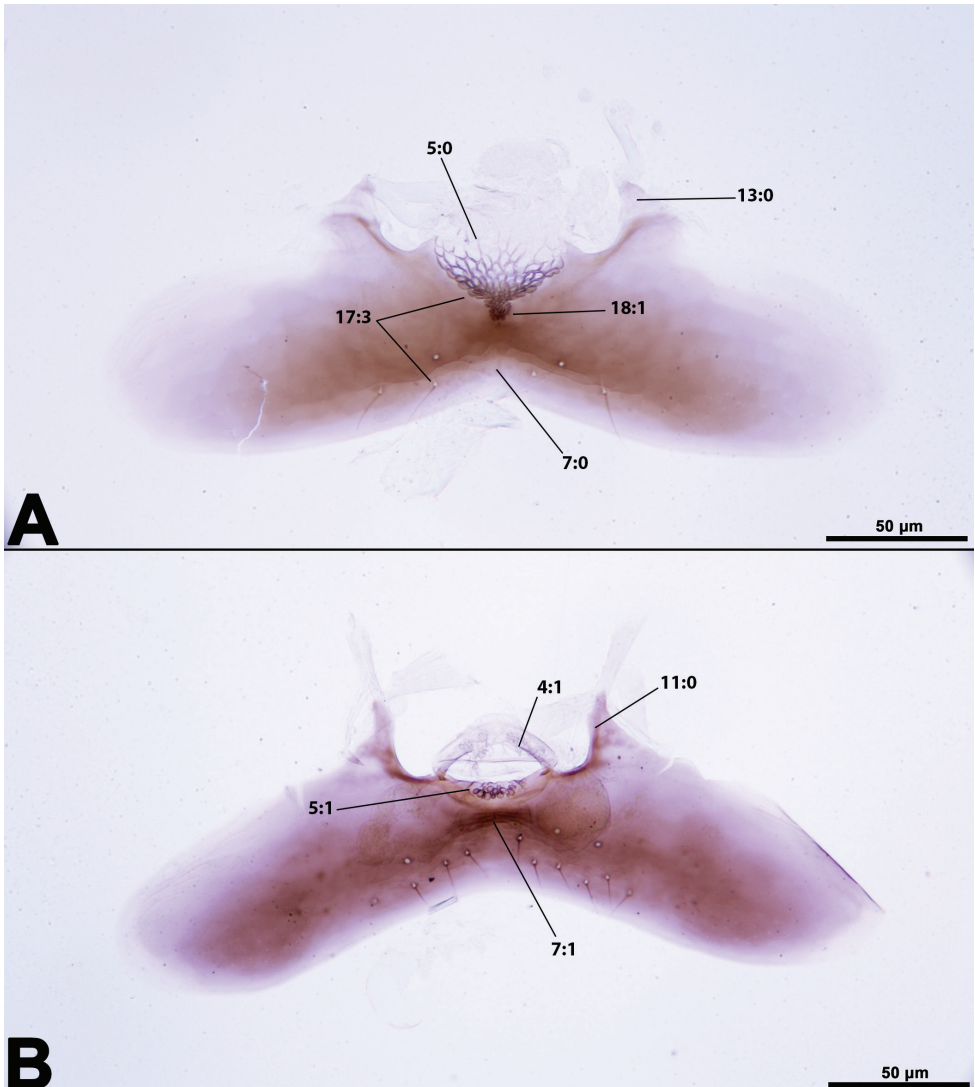


Figure 6. Principle differences between Waterston's evaporatorium in the *Ceraphron* Group and *Aphanogmus* Group (brightfield) **A** *Ceraphron* sp. **B** *Aphanogmus* sp.

Waterston's evaporatorium

The medial margins of the tergal apodemes are sclerotised in all members of the *Aphanogmus* group (Fig. 6B). In the *Ceraphron* group, the median margins of the apodemes are not sclerotized, but a sclerotized line traverses the apodeme basally (Fig. 6A). In *Elysocheraphron* and *Aphanogmus fasciipennis*, both sclerotizations (medial and basal) are present (Figs 7A, 8B; chr. 11). In *Trassedia* and *Masner*, the tergal apodemes are lo-

cated at the lateral edges of the tergum. In other ceraphronid taxa, the tergal apodemes originate at the lateral edges of the **evaporatorium (ev)** within the middle third of the tergite (chr.12). The evaporatorium consists exclusively of the medial reticulate cell structure while the term ‘Waterston’s evaporatorium’ relates to the entire character complex. All Ceraphronidae *sensu stricto* have the tergal apodemes of T6 oriented sub-medially. The tergal apodemes converge or diverge proximomedially or are parallel to each other. Convergence is the only state found in the *Ceraphron* group (Fig.6A). In *Aphanogmus*, apodemes either diverge (Fig.8A) or are parallel (*A. fasciipennis* or *Synarsis*; Figs 8B, 7B; chr.13).

The WE is not reaching the lateral third of T6 in all Ceraphronidae aside from *Trassedia* in which it is present across the entire anterior margin of the T6 (chr. 2). The WE is transversely elongate and at least two times as wide as long in *Trassedia* and *Masner* and as long or longer than wide in Ceraphronidae *s.str.*

The **acrotergal calyx* (at cx)**, the ridge arising medially from the acrotergite, forms the sclerotized distal edge of the **bullae (bul)**, a smooth median concavity, present in all taxa within the *Aphanogmus* group (bul: Fig. 6B). Within the *Ceraphron* group, the bulla can be found only in *Pristomicrops*, *Cyoceraphron*, and *Pteroceraphron* (bul: Fig. 9). Within *Pteroceraphron* and *Pristomicrops*, the WE extends towards the acrotergal calyx (chr. 5:0), either up the lateral edges in *Pteroceraphron* or medially in *Cyoceraphron*. The cells of the evaporatorium extend beyond the acrotergite in all *Ceraphron* group taxa including those which contain an acrotergal calyx and a bulla. In these taxa the cells continue up the lateral edges of the bulla towards the anterior rim. Within the *Aphanogmus* group, the evaporatorium barely extends beyond the lateral walls of the bulla in some genera, e.g., *Synarsis* and *Elysoceraphron* (Fig.7A,B).

The **caudal setal row (csr)**, which arise from the posterior ridge of the tergite, is present in all ceraphronids with the number of setae being highly variable among genera (from 2–30), and intraspecific variation often being a difference of just 1–2 setae. The **distal crenulate carina* (dcc)**, on T6, a carina which arises dorsally to or upon the caudal setal row, is absent in *Ceraphron* (*Pristomicrops*), *Pteroceraphron*, *Gnathoceraphron*, and the examined specimens of *A. fumipennis* and *A. fasciipennis*. Dcc is present in all other genera. In the *Ceraphron* group, the distal crenulate carina always lies upon the caudal setal row when present (Fig. 6A). The position of the distal crenulate carina in many *Aphanogmus* group genera arises dorsally of the caudal setal row (Fig. 6B; chr.7).

The **submedian patches* (smp)** on T6 are located anterolaterally to the WE when present (smp: Fig.1B) (chr.8). The shape of the submedian patches is variable at the species level (chr.9). These patches have the campaniform sensilla within them (Fig. 10A). Submedian patches are only present in the *Ceraphron* group. In *Ceraphron* (*Eulagynodes*) sp. (Fig. 10B), the submedian patches are large and apparently continuous medially; they also connect to the distal crenulate carina which may obfuscate the carina. This is the character state determined for *Trassedia* and *Masner*; in both genera, cuticular sculpturing extends from the posterior edge of the evaporatorium to the distal tergal edge.

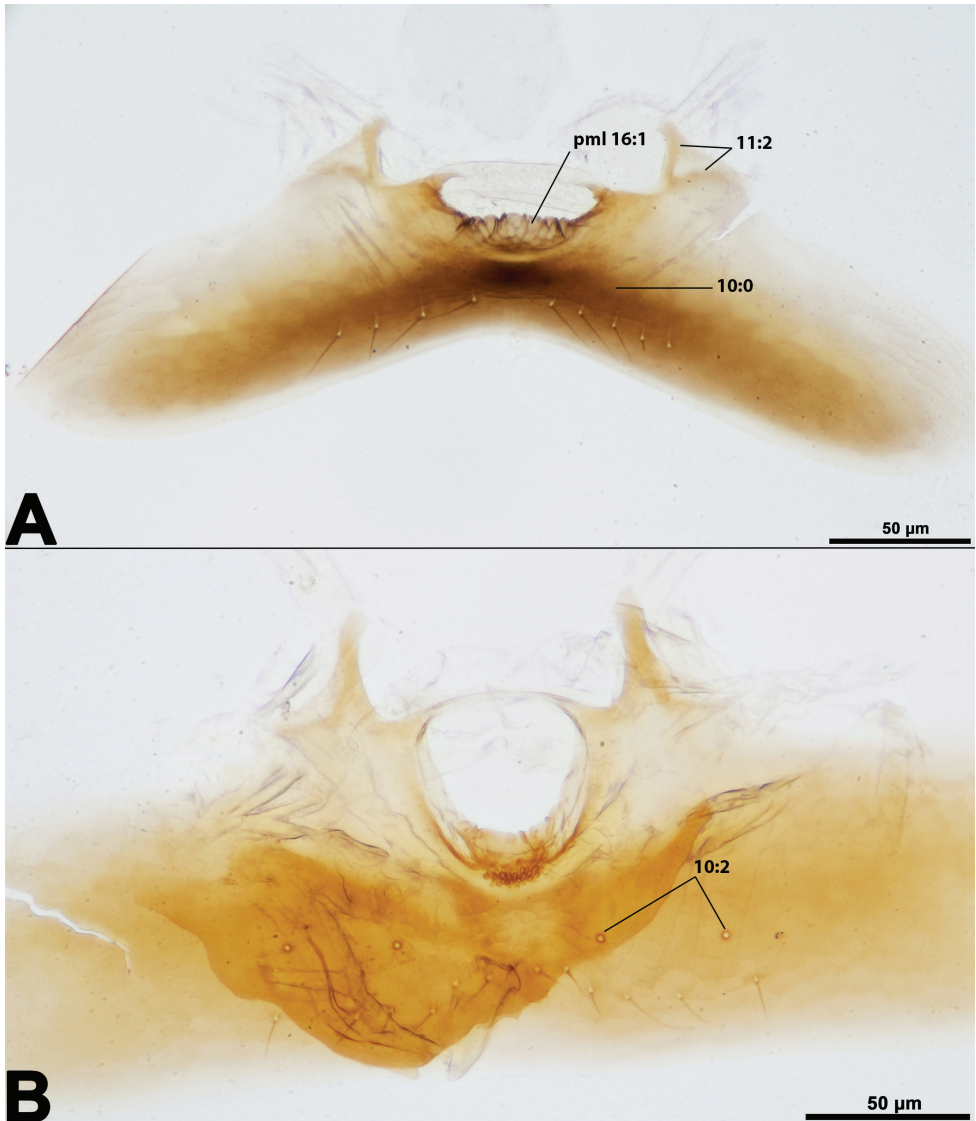


Figure 7. Variation of campaniform sensilla within the *Aphanogmus* Group (brightfield) **A** *Elysocheraphron hungaricus* **B** *Synarsis* sp. Presence of a complete proximomedial lamella (pml) (character 16) in *E. hungaricus* and partial pml in *Synarsis*. *Elysocheraphron* contains both inner marginal sclerotization and transverse sclerotization of the tergal apodeme. Both abnormal states of campaniform sensilla (character 10) are shown, *Synarsis* having two sets of cs, whereas they are entirely absent in *Elysocheraphron*.

A pair of **campaniform sensilla** are present laterally on both T6 and T5 in all Ceraphronidae except *Elysocheraphron* (Fig.7A). *Synarsis* have two sets of campaniform sensilla present on T6 (Fig.7B) (chr.10).

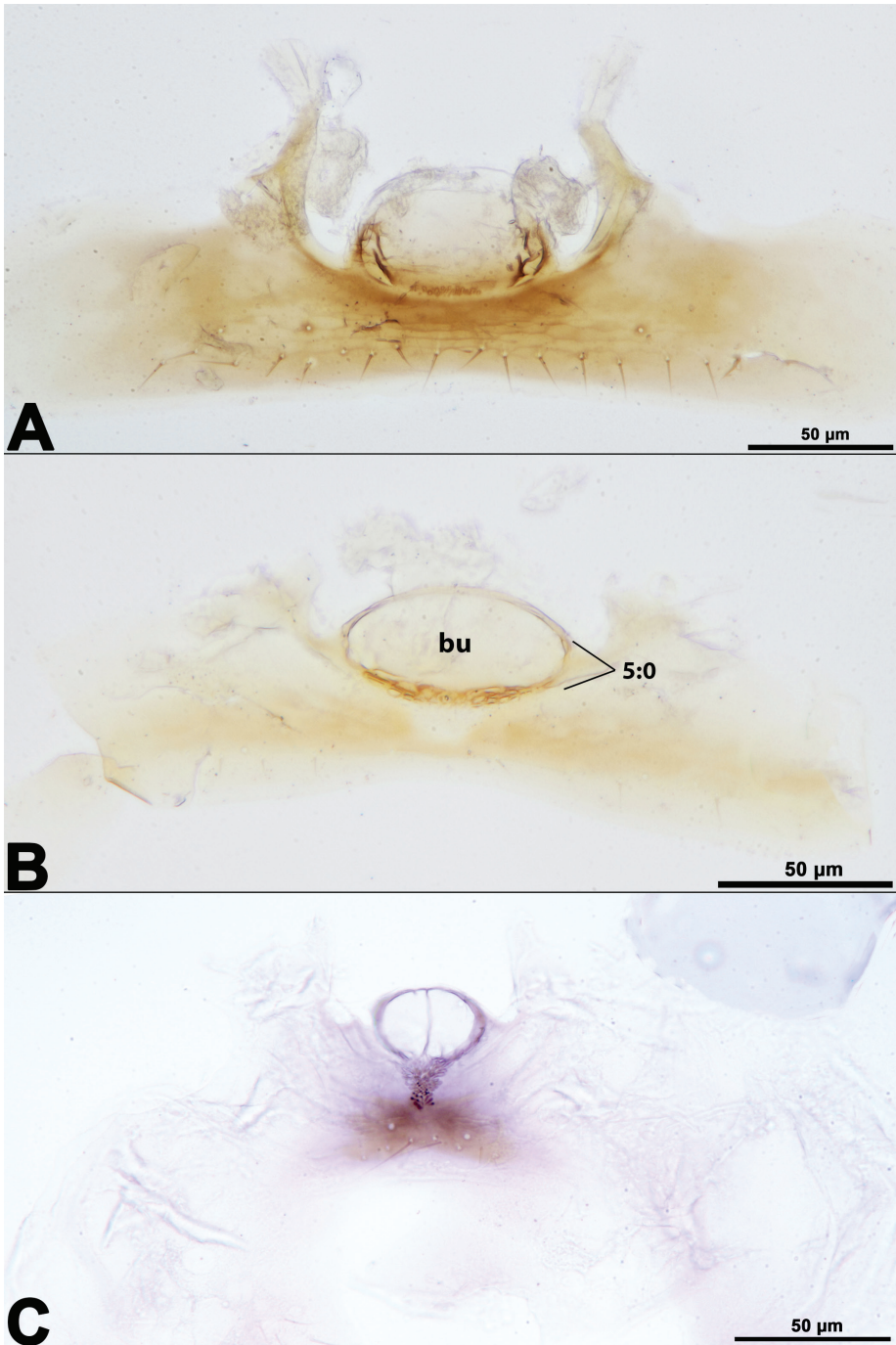


Figure 8. Acrotergal calyx within genera of *Ceraphron* Group (brightfield) **A** *Ceraphron (Pristomicrops)* sp. **B** *Pteroceraphron mirabilipennis* **C** *Cyoceraphron striatopleuralis*. Genera within the *Ceraphron* group which have the acrotergal calyx and bulla (**bu**) well separated. The evaporatorium extends up the lateral walls of the bulla in *P. mirabilipennis* (chr. 5)

Medially, unsculptured regions of the evaporatorium are only seen in some females of *Trassedia*, which, in several species, have a sexually dimorphic WE (chr. 14). Lighter melanization of the WE medial cells is found within *Ceraphron* (*Allomicrops*) (Fig. 10A; chr.15). This is different from char.14 where the evaporatorium is medially bifurcated by unmodified cuticle.

The **proximomedial lamella of the Waterston's evaporatorium*** (**pml**) extends from the base of the evaporatorium. In *Elysoceraphron*, the lamella envelops all cells of the evaporatorium (Fig. 7A). In *Ceraphron* (*Eulagynodes*), the lamella only covers the basal cells of the evaporatorium (10B; chr.16).

The uniformly-sized cells of the evaporatorium are smaller than or equal to the sizes of the setal sockets in *Aphanogmus* (Figs 8A, B). In *Ceraphron*, the cells increase in size as they extend towards the antecostal ridge (Fig. 6A). In *Pteroceraphron mirabilipennis*, the uniformly sized cells are larger than the setal bases (Fig. 9B; chr.17). A basomedial constriction of the WE is seen in many *Ceraphron* with the basal cells reducing greatly in size as they terminate into a single point (Fig. 6A) (chr.18). In the case of *Ceraphron*-type WE, the cells are often a combination of all size ratios, these are scored as polymorphic.

Sexual dimorphism is only found in some species of *Trassedia* where the female evaporatorium is medially unsculptured (Char.19, Mikó et al. 2018).

Character list

1. Evaporatorium: 0, absent; 1, present.
2. Evaporatorium lateral extension: 0, evaporatorium not reaching lateral third of tergite; 1, evaporatorium reaching lateral third of tergite.
3. Evaporatorium shape: 0, transversely elongate, at least twice as wide as long; 1, as long or longer than wide.
4. Acrotergal calyx: 0, absent; 1, present.
5. Evaporatorium cell: 0, cells extend to anterior rim of T6; 1, cells extend only to the edge of the acrotergite.
6. Distal crenulate carina on T6: 0, absent; 1, present.
7. Distal crenulate carina on T6 position: 0, present on caudal setal row; 1, present dorsally to caudal setal row.
8. Submedian patches on T6: 0, absent; 1, present.
9. Submedian patch medially: 0, patches continuous medially; 1, patches medially separated.
10. Campaniform sensilla on T6: 0, absent; 1, single pair present; 2, two pairs present.
11. Sclerotized ridge of the tergal apodeme: 0, present along inner margin; 1, present, traversing base; 2, both.
12. Tergal apodeme shifted medially: 0, absent; 1, present.
13. Tergal apodeme orientation: 0, converging distally; 1, parallel; 2, diverging distally
14. Evaporatorium median unsculptured region female: 0, absent; 1, present.

15. Median cells of evaporatorium melanization: 0, lightly melanized; 1, heavily melanized.

16. Proximomedian lamella of T6: 0, absent; 1, present.

17. Evaporatorium cell size related to setal bases: 0, smaller than setal base; 1, equal to setal base; 2, larger than setal base.

18. Evaporatorium basomedial constriction: 0, absent; 1, present.

19. Dimorphism (Only *Trassedia*): 0, absent; 1, present.

Results of cladistic analysis

Parsimony analysis resulted in 92 trees with a length of 136 steps (Fig. 11). The strict consensus tree retrieved the following relationships:

“*Ceraphron* group”

The *Ceraphron* group is paraphyletic to the *Aphanogmus* group (see below), and includes *Ceraphron sensu stricto*, as well as its included subgenera (*C. (Allomicrops)*, *C. (Pristomicrops)*, *C. (Eulagynodes)*, *Homaloceraphron*, *Pteroceraphron*, *Cyoceraphron*, and *Ecitonetes*). The group is characterized by the absence of an inner marginal sclerotization of the tergal apodeme, with the apodeme being sclerotized transversely across the base and converging distally. The extension of the evaporatorium to the anterior rim of the tergite is also a character shared by members of the group including those genera that have an acrotergal calyx wherein the evaporatorium extends along the edges of the formed bulla.

“*Aphanogmus* group”

The *Aphanogmus* group (*Aphanogmus sensu stricto*, *Synarsis*, *Elysoceraphron*, *Gnathoceraphron*) is supported by the presence of an inner marginal sclerotization of the tergal apodemes and their subsequent distal divergence or straightening. The presence of an acrotergal calyx and the evaporatorium not advancing beyond the acrotergite. This grouping is strongly supported as monophyletic with a bootstrap (BS) value of 89.

“*Trassedia* and *Masner*”

Trassedia is well supported (BS value: 97) and characterized by the presence of dimorphism (chr. 19) and a medially unsculptured region of the evaporatorium in females (chr. 14). *Masner* is present within a trichotomy also comprising *Trassedia* and the rest of Ceraphronidae *sensu stricto*. *Trassedia* and *Masner* are characterized by a lack of tergal apodeme modification as well as a laterally extended evaporatorium present directly along the acrotergite without any modification into a calyx. *Masner lubomirus* (Mikó & Deans, 2009) is only known from male specimens, so the presence of dimorphism is unknown for the genus.

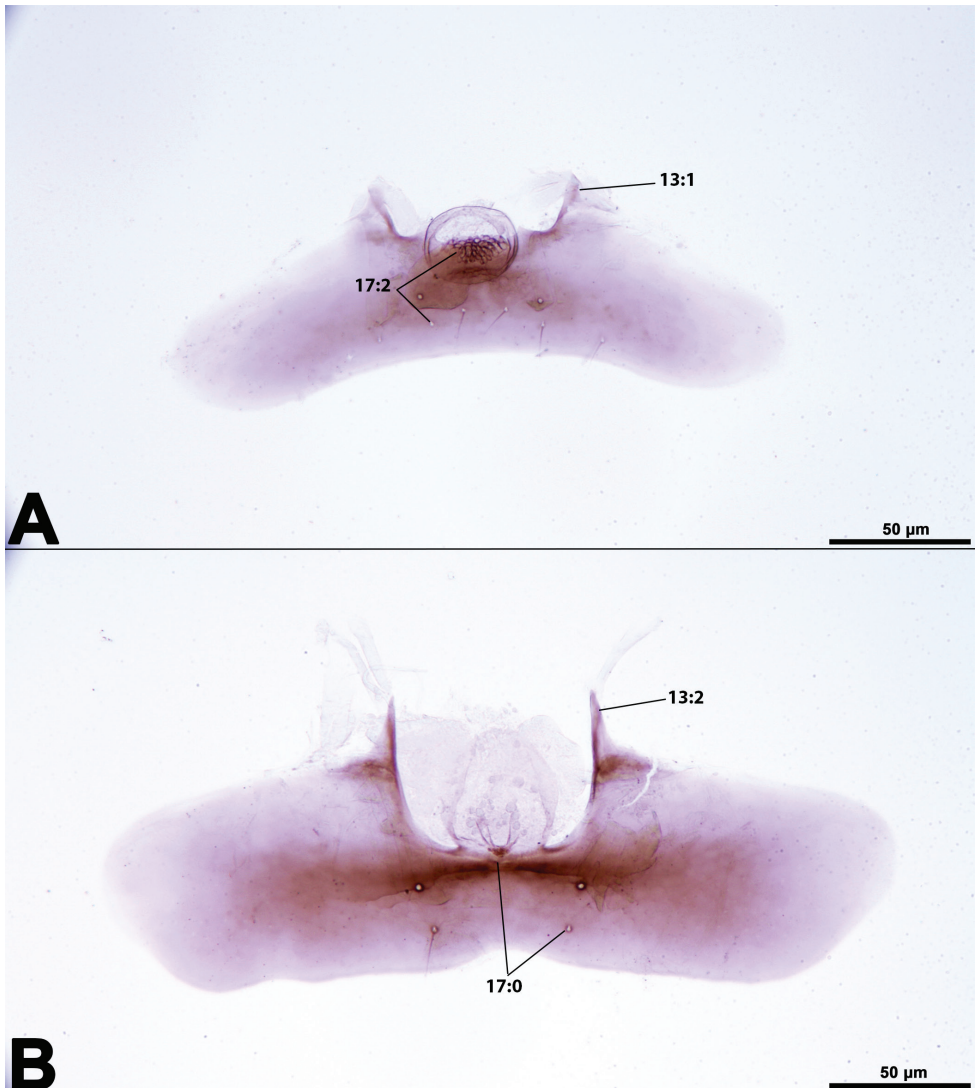


Figure 9. Variation of Waterston's evaporatorium between two major species complexes of *Aphanogmus* (brightfield) **A** *Aphanogmus fumipennis* **B** *Aphanogmus fasciipennis*. Character 13 = Tergal apodeme orientation. Character 17 = cell size in relation to setal base.

Taxonomic utility

Interspecific variation in the WE is focused primarily in the gestalt of the evaporatorium, with the relative size and sclerotized pattern of the reticulate network providing the clearest initial indicators of species variability (Fig. 12). Within *Ceraphron*, morphospecies based on male genitalia maintain the generic apomorphies (basomedial constriction, transverse sclerotization of the ta, smp), there is however, distinct

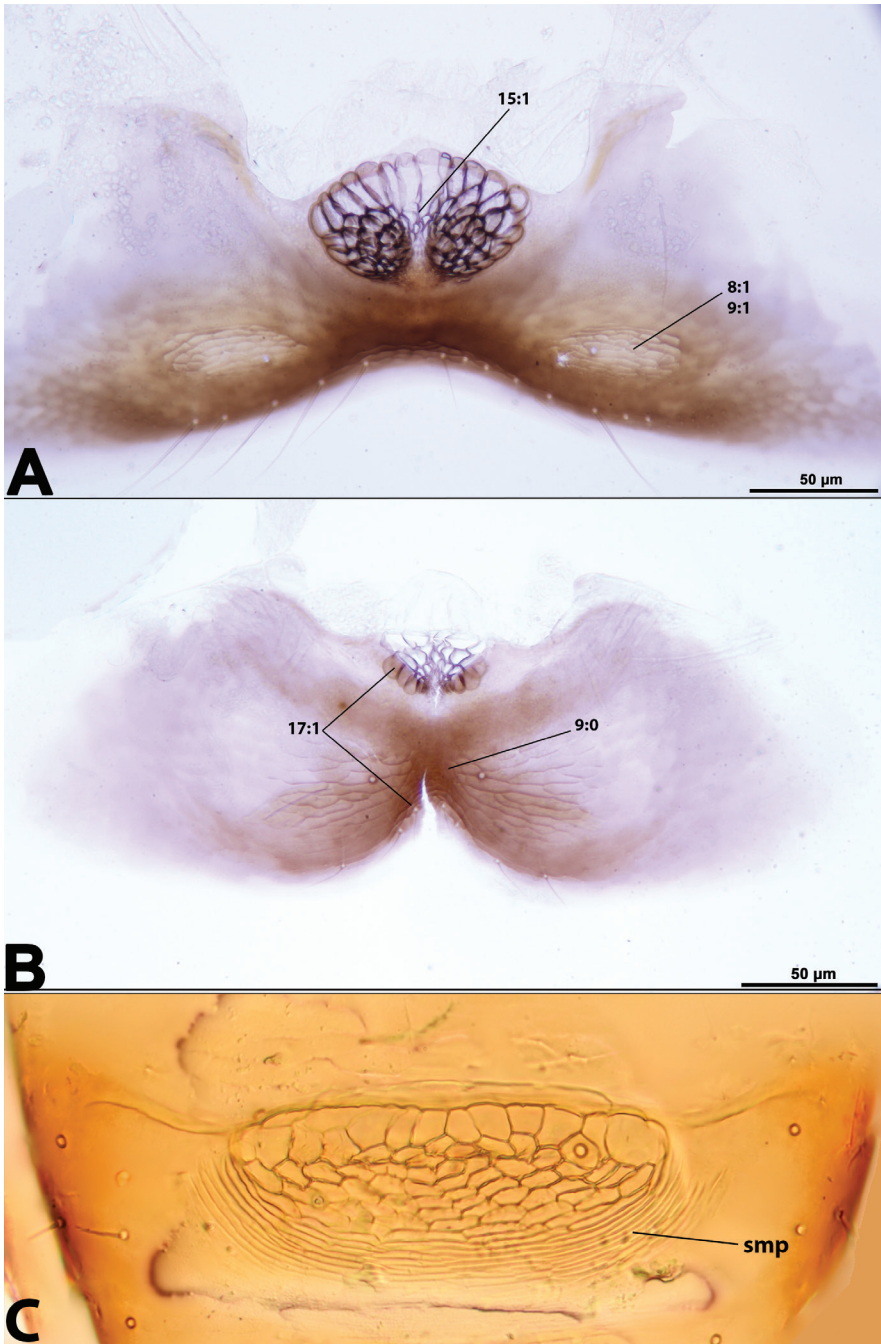


Figure 10. Variation in submedial patches within subgenera of *Ceraphron* (brightfield) **A** *Ceraphron (Allomicrops)* sp. **B** *Ceraphron Eulagynodes* sp. **C** *Masner lubomirus*. Characters states associated with the presence of smp (character 8). Lighter medial melanization of the evaporatorium found in some species of *Ceraphron Allomicrops* (chr. 15). The three states of character 9 can be seen, medially separated in *C. Allomicrops*; and medially continuous, in *C. Eulagynodes* and *M. lubomirus*.

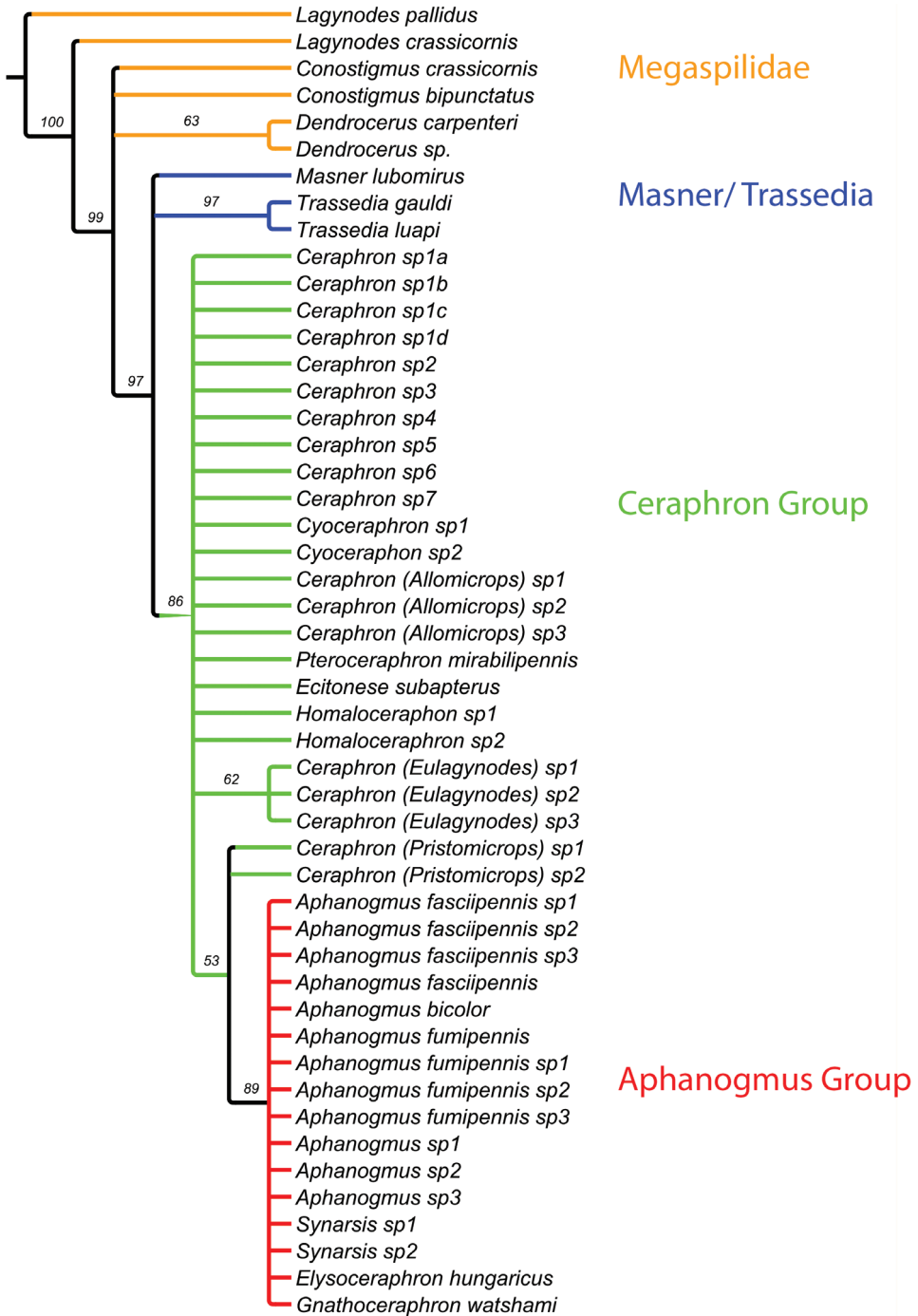


Figure 11. Phylogenetic relationships within Ceraphronoidea inferred by morphological characters from the Waterston's evaporatorium. Strict consensus tree with bootstrap support values higher than 50. Tree length = 136.

variation within these which as a combination of characters can be informative on the species level.

Within a single morphospecies the intraspecific variation results from a variation in the number of setae along the caudal margin, as well as the sclerotization of the evaporatorium with the darkness of the medial region being relatively variable (Fig. 13). Size variation in the tergite itself is the result of body size variability within a given species.

The structure is monomorphic between the sexes of a given species, with the intraspecific variation amongst males examined extending to the variation between conspecific males and females (Fig. 14). During the examination of males and females, it was noted that in many matched species the basomedial cells of the male tend to be strongly sclerotized relative to the corresponding female. Whether this is related to a function or a form of dimorphism in the structure is presently unknown.

Discussion

Modification of T5 and T6 and the presence of anterior tergal glands

Abdominal cuticular modifications corresponding to abdominal exocrine glands have been described in numerous other hymenopteran taxa, including Braconidae (Buckingham and Sharkey 1989; Quicke 1990), Platygastridae (*Xenomeres*, Mikó et al. 2010), and recently in one of the proposed sister taxa to Ceraphronoidea, Megalyridae (Mikó 2014). In the case of Braconidae, these structures have provided a useful character complex for both tribal and generic level classification (Buckingham and Sharkey 1989; Sharkey 1992). Emptying of these glands might be regulated by the telescopic movement of the tergites relative to each other (Mikó 2014) that is performed by the alternate contraction of the internal and external abdominal musculature.

Novel abdominal pulsatory organ in Apocrita

The dorsal vessel in Ceraphronidae terminates into an enlarged, multi-chambered accessory pulsatory organ that has never been reported in Apocrita (APO) (Fig. 5B, C). Within the sister family Megaspilidae, the dorsal vessel also terminates in a caudal chamber, however, it is not as large and is not divided into multiple chambers by septa. Pulsatory organs are usually developed to facilitate circulation in extremities like the insect appendages, antennae, wings and legs (Pass 2000).

In Ceraphronidae, where the WE and adjacent exocrine glands take up a considerable amount of internal space, the complex might represent a barrier between the anterior and posterior sections of the abdomen (Fig. 3B). A larger and more heavily muscled pulsatile organ may be necessary in order to provide appropriate hemolymph flow around the obstructive glands to more posterior organs including the sometimes disproportionately large and complex genitalia (Dessart 1995; Mikó et al. 2013; Ulmer et al. 2018).

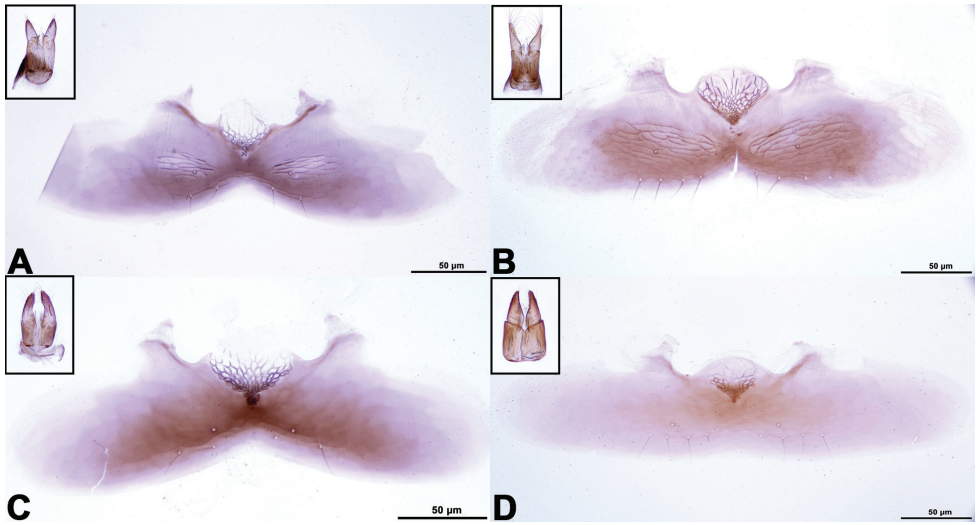


Figure 12. Species level variation of WE within morphospecies of *Ceraphron* (brightfield). Morphospecies based on male genitalia (inlays). Four distinct smp patterns and evaporatorium's.

The dorsal vessel is relatively short in both ceraphronoid families and potentially corresponds to the ability to telescope the entire abdomen into the syntergite. The presence of an enlarged caudal chamber of the dorsal vessel would provide circulation when the abdomen is fully extended.

The formation of a caudal chamber at the end of the dorsal vessel is a common trait found within wingless Hexapoda groups (*Diplura*, *Zygentoma*, and *Archaeognatha*). Some Pterygota, such as *Ephemeroptera* and *Plecoptera*, have a “pear-shaped” termination to the dorsal vessel, which functions as an accessory pulsatile organ for the abdominal appendages, including the cerci (Gerebren and Pass 2000; Pass 2000; Pass et al. 2006). A unique modification of the dorsal vessel into an enlarged lobed pulsatile organ has been described within *Acheta domesticus* (Linnaeus, 1758) (*Orthoptera*: *Gryllidae*), which allows for the backflow of hemolymph through its long ovipositor (Hustert et al. 2014). Unfortunately the study did not examine males to determine if this structure is found within both sexes with a redundancy in males, as could potentially be the case for the WE in *Ceraphronidae*.

Variations in the path of the dorsal vessel through the mesosoma and petiole have been examined across *Hymenoptera*, showing a remarkable range of diversity given the highly conserved nature of the structure (Matus and Pass 1999; Hillyer and Pass 2020). Amongst *Hymenoptera*, *Euglossini* (*Apidae*) have a unique shortening of the dorsal vessel into a caudal, enlarged chamber (Willie 1958). Functionally, the caudal chamber adaptations found within *Ceraphronoidea* and *Euglossini* are likely analogous to the enlarged “abdominal heart” and thin aorta found within several *Hemipteran* families, in which the heart is highly muscled via broad alary muscles and the aorta has little or no contraction power for circulation (Chiang et al. 1990; Hinks 1966; Pass pers.

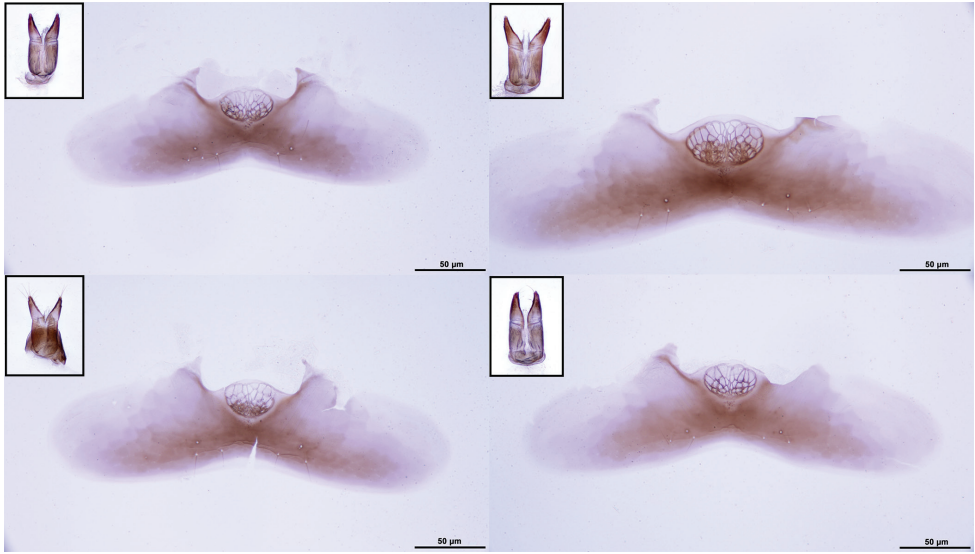


Figure 13. Intraspecific variation of WE within a single morphospecies of *Ceraphron* (brightfield). Morphospecies based on male genitalia (inlays).

comm.). We hypothesize that the presence of a caudal abdominal organ is not unique to Ceraphronoidea. Studies on the circulatory system in Hymenoptera are remarkably limited, especially for the minute parasitoid wasps (Quicke 1997) and future studies should explore the nature and phylogenetic significance of this complex anatomical system for Hymenoptera evolution.

Glandular function

The class III gland cells (Noirot and Quennedey 1974) along with the modification of the modified tergal apodemes strongly suggests an exocrine glandular function of the Waterston's evaporatorium (Mikó and Deans 2009). It is possible that these glands could be utilized in courtship rituals, as the glands are often monomorphic when present (Quicke 1997). Glands utilized in courtship allow for premating selection of compatible mates amongst cryptic species complexes or provide individual specificity in the case of lek mating to prevent repeated mating between two individuals (Assem 1994; Ayasse 2001). The tergal and sternal gland secretions of Opiinae (Braconidae: Ichneumonoidea) have been found to be species-specific in their chemical composition, with this specificity proposed as functioning in mating or courtship (Williams et al. 1988).

Another potential function is as a defensive gland against terrestrial predators or fungal parasites. Due to the diversity of hosts even within a single genus of Ceraphronidae (Peter and David 1990), the specialized adaptation of the structure to a specific habitat and its predatory fauna is unlikely, and its use as a deterrent to microbial infection is more probable if host-specificity is an assumed evolutionary driver. While

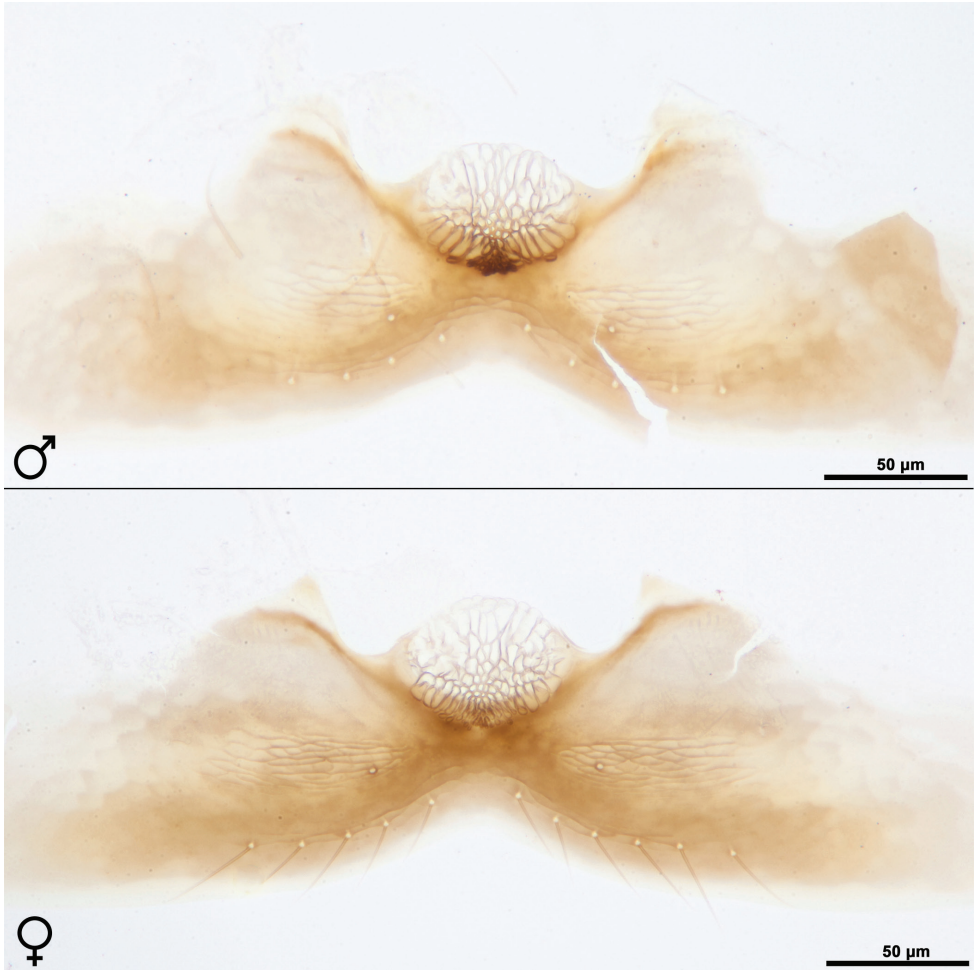


Figure 14. Morphological barcoding (brightfield). Matching male and female *Ceraphron* (*Allomicrops*) based on WE.

there are limited records of natural history, Ceraphronidae is often collected in pan traps or sweep netting which may indicate a ground-level or subterranean life history; this is in contrast to Megaspilidae, which is more commonly collected in flight intercept and Malaise traps (pers. obs.). Many arboreal ant genera have been found to have atrophied metapleural glands which may suggest a reason for the absence of the WE in Megaspilidae (Hölldobler et al. 1984). The putative defensive or antimicrobial function of the WE could be analogous to the metapleural glands of Formicidae. The metapleural gland excretion has been shown to be a weakly acidic compound that functions as an antimicrobial agent that is collected into a bulla structure and used in grooming (Beattie et al 1986; Fernández-Marín et al 2006). Further studies into the chemical makeup of the gland excretion of the Waterston's evaporatorium may further elucidate potential functions.

Phylogenetic implications

A limiting factor in resolving the generic and species level relationships within Ceraphronidae is the paucity of characters that are not sex specific. While family level separation is robust, based on ten two-state characters, one of which is the presence of a Waterston's evaporatorium, generic concepts lack the same degree of resolution (Mikó and Deans 2009). Dessart and Cancemi (1987) classified Ceraphronidae into "satellite" groups based upon compression of the mesosoma and male flagellomere shape. The WE character complex provides further evidence for this grouping (Fig. 11), particularly in those genera which are monotypic or only known from females.

The absence of an acrotergal calyx (ch.4:0) is implied to be the ground plan for the group in our analysis, lacking from the sister group Megaspilidae, *Masner* and *Trassedia* as well as from *Ceraphron*. Presence of an acrotergal calyx within *Pristomicrops*, *Homaloceraphron*, and *Pteroceraphron* in combination with the presence of evaporatorium cells extending along the lateral edges towards the anterior rim of T6 (ch.5:0) suggests a possible transformation series towards the presence of an acrotergal calyx and bulla found within all *Aphanogmus* and reduction of the evaporatorium cells to a small basomedial patch on the acrotergite.

Sclerotization of the inner margin of the tergal apodeme is also found to be plesiomorphic, (ch.11:0) being the state found in the Megaspilidae as well as in *Masner* and *Trassedia*, which are sister to Ceraphronidae s.s. Having the sclerotization traverse the base of the apodeme is a putative apomorphy for the *Ceraphron* group, with a reversal in *Aphanogmus*. Whether the state found in *Ceraphron* is associated with the tergal apodemes converging distally (ch.13:0) is uncertain. This transverse sclerotization however is not seen on the preceding tergal apodemes on T5, which in all ceraphronoids appear unmodified, being sclerotized along the inner margins and diverging distally (Fig.1C). In *Elysoeraphron hungaricus* (Szelényi 1936) and the *A. fasciipennis* complex, both inner margin sclerotization and sclerotization traversing the base of the apodeme are present, with the apodemes diverging distally or straight as in all other *Aphanogmus*-group genera.

Morphological barcoding

It has been notoriously difficult to obtain molecular barcodes for Ceraphronoidea (Ratnasingham and Hebert 2007; Bennett 2019). This has manifested itself taxonomically in a general inability to obtain species or even genus matches between specimens of opposite sex. However the taxonomic utility of barcoding cannot be overstated. While molecular barcoding is the standard medium within biology, the ultimate purpose of this tool is to develop discrete signatures efficiently which can be assigned to a taxon in order to differentiate it. Waterston's evaporatorium might offer an alternative to molecular barcoding for Ceraphronoidea, until the molecular impediment has been resolved within the group.

As one reaches lower taxonomic levels, characters naturally become more subtle and limited, as evolutionary distance is shortened. This is a problem which plagues both morphological and molecular taxonomy (Song et al 2008). In order to most effectively utilize the WE character complex to species level, inter- and intraspecific variation must be quantified (Fig. 12; 13). This issue has been partly resolved in molecular taxonomy through the use of large reference libraries. Pattern recognition software such as I3S, has proven capable of differentiating species and even single specimens (Sannolo et al 2016) with increasing accuracy as a reference library grows. While the reticulate cell structure of the evaporatorium is largely conserved within a given taxon, intraspecific variation is an inescapable aspect of evolution which may be accounted for through this method of reference library generation. Future studies should take care to preserve and image the WE in order to better understand its utility.

While male genital characters remain a far more robust system for diagnosing species, they are obviously limited by the sex of the specimen. Currently, the intraspecific characterization of the WE is the only way to confidently match sexes within Ceraphronoidea (Fig. 14). The WE would thus provide the ability to associate the sexes in these groups, which can then be diagnosed with male genitalia. We hope that use of this character set will only further bolster its application and utility within the family as more WE are described and defined.

Acknowledgements

We would like to thank Chuck Mooney (NCSU) for SEM, Missy Hazen (PSU) for assistance with CLSM, and Mark Townley (UNH) for assistance with CLSM. We would also like to thank Lars Vilhelmsen and an anonymous reviewer for constructive feedback on this manuscript. This material is based upon work supported by the National Science Foundation under Grant No. DEB-1353252. Any opinions, findings, and conclusions or recommendations expressed in this material are those of the authors and do not necessarily reflect the views of the National Science Foundation.

References

- Ayasse M, Paxton RJ, Tengö J (2001) Mating behavior and chemical communication in the order Hymenoptera. *Annual review of entomology* 46(1): 31–78. <https://doi.org/10.1146/annurev.ento.46.1.31>
- Beattie AJ, Turnbull CL, Hough T, Knox RB (1986) Antibiotic production: a possible function for the metapleural glands of ants (Hymenoptera: Formicidae). *Annals of the Entomological Society of America* 79(3): 448–450. <https://doi.org/10.1093/aesa/79.3.448>
- Bennett AM, Sheffield CS, de Waard JR (2019) Hymenoptera of Canada. *ZooKeys* (819): 311–360. <https://doi.org/10.3897/zookeys.819.28510>

- Brues CT (1902) New and little-known guests of the Texan legionary ants. *The American Naturalist* 36(425): 365–378. <https://doi.org/10.1086/278138>
- Buckingham GR, Sharkey MJ (1988) Abdominal exocrine glands in Braconidae (Hymenoptera). Reprints-US Department of Agriculture, Agricultural Research Service (USA).
- Chiang RG, Chiang JA, Davey KG (1990) Morphology of the dorsal vessel in the abdomen of the blood-feeding insect *Rhodnius prolixus*. *Journal of morphology* 204(1): 9–23. <https://doi.org/10.1002/jmor.1052040103>
- Dessart P (1963a) Contribution a l'étude des Hymenopteres Proctotrupoidea. (II) Revision des *Aphanogmus* décrits par CG Thomson. In: Bulletin et Annales de la Société Royale d'Entomologie de Belgique 99: 387–416.
- Dessart P (1963b) Contribution a l'étude Des Hymenopteres Proctotrupoidea. (III). Revision Du Genre *Allomicrops* Kieffer, 1914, et Description de *Ceraphron Masneri* sp. nov. (Ceraphronidae). Bulletin et Annales de La Société Royale d'Entomologie de Belgique 99: 513–39.
- Dessart P (1965) Contribution à l'étude des hyménoptères Proctotrupoidea. (VI). Les Ceraphroninae et quelques Megaspilinae (Ceraphronidae) du Musée Civique d'histoire Naturelle de Gênes. In: Bulletin et Annales de la Société Royale Entomologique de Belgique, Vol. 101: 105–192.
- Dessart P (1975) Material typical of myrmecophilic Microhymenoptera from the Wasmann collection deposited at the Wasmannianum Museum in Maastricht (Netherlands). *Naturhistorisch Genootschap*, Vol. 24, 1–94.
- Dessart P (1980) Description et redescription de quelques Ceraphronoidea (I). (Hymenoptera). In: Bulletin et Annales de la Société Royale Belge d'Entomologie, Vol. 116, 185–199.
- Dessart P (1984) *Retasus ater* gen. nov., sp. nov.: un ceraphronide de cauchemar! (Hymenoptera, Ceraphronoidea). In: Bulletin et Annales de la Société Royale Belge d'Entomologie, Vol. 120, 277–281.
- Dessart P, Cancemi P (1986) Dichotomous table of the genera of Ceraphronoidea (Hymenoptera) with comments and new species. *Frustula Entomologica* NS 7(20–21): 307–372.
- Dessart P (1991) Considerations sur le genre *Synarsis* Foerster, 1878 (Hym. Ceraphronoidea Ceraphronidae). In: Bulletin et Annales de la Société Royale Belge d'Entomologie, Vol. 127, 385–400.
- Dessart P (1992) L'organe Waterston des Ceraphronoidea (Hymenoptera Ceraphronoidea). In: Bulletin et Annales de la Société Royale Belge d'Entomologie, Vol. 128, 203–212.
- Duncan CD(1939) A contribution to the biology of North American Vespine wasps. Stanford University Publishing, Biological Sciences 8(1): 1–272.
- Fernández-Marín H, Zimmerman JK, Rehner SA, Wcislo WT (2006) Active use of the metapleural glands by ants in controlling fungal infection. *Proceedings of the Royal Society B: Biological Sciences* 273(1594): 1689–1695. <https://doi.org/10.1098/rspb.2006.3492>
- Gereben-Krenn BA, Pass G (2000) Circulatory organs of abdominal appendages in primitive insects (Hexapoda: Archaeognatha, Zygentoma and Ephemeroptera). *Acta Zoologica* 81(4): 285–292. <https://doi.org/10.1046/j.1463-6395.2000.00057.x>
- Hillyer JF, Pass G (2020) The insect circulatory system: Structure, function, and evolution. *Annual Review of Entomology* 65: 121–143. <https://doi.org/10.1146/annurev-ento-011019-025003>

- Hinks CF (1966) The dorsal vessel and associated structures in some Heteroptera. Transactions of the Royal Entomological Society of London 118(12): 375–392. <https://doi.org/10.1111/j.1365-2311.1966.tb00830.x>
- Hölldobler B, Engel-Siegel H (1984) On the metapleural gland of ants. Psyche 91(3–4): 201–224. <https://doi.org/10.1155/1984/70141>
- Hustert R, Frisch M, Böhm A, Pass G (2014) A new kind of auxiliary heart in insects: functional morphology and neuronal control of the accessory pulsatile organs of the cricket ovipositor. Frontiers in Zoology 11(1): e43. <https://doi.org/10.1186/1742-9994-11-43>
- Johnson NF, Musetti L (2004) Catalog of systematic literature of the superfamily Ceraphronoidea (Hymenoptera). Contributions of the American Entomological institute 33(2).
- Martínez de Murgía L, Angeles Vazquez M, Nieves-Aldrey JL (2001) The families of Hymenoptera (Insecta) in an heterogenous acidophilous forest in Artikutza (Navarra, Spain). Frustula Entomologica (Nuova Serie) 24: 81–98.
- Masner L, Dessart P (1967) La reclassification des categories taxonomiques superieures des Ceraphronoidea (Hymenoptera). Bulletin de l'Institut Royal des Sciences Naturelles de Belgique 43(22): 1–33.
- Matsuda R (1976) Morphology and evolution of the insect abdomen. International series in pure and applied biology, zoology division.
- Matus S, Pass G (1999) Antennal circulatory organ of *Apis mellifera* L. (Hymenoptera: Apidae) and other Hymenoptera: functional morphology and phylogenetic aspects. International Journal of Insect Morphology and Embryology 28(1–2): 97–109. [https://doi.org/10.1016/S0020-7322\(99\)00011-2](https://doi.org/10.1016/S0020-7322(99)00011-2)
- Mikó I, Deans AR (2009) *Masner*, a new genus of Ceraphronidae (Hymenoptera, Ceraphronoidea) described using controlled vocabularies. Advances in the systematics of Hymenoptera. Festschrift in honour of Lubomír Masner. ZooKeys 20: 127–153. <https://doi.org/10.3897/zookeys.20.119>
- Mikó I, AR Deans (2013) What is fluorescing? Hamuli 4: 19–22.
- Mikó I, Masner L, Deans AR (2010) World revision of *Xenomeres* Walker (Hymenoptera: Platygastroidea, Platygastriidae). Zootaxa, 2708(1): 1–73. <https://doi.org/10.11646/zootaxa.2708.1.1>
- Mikó I, Masner L, Johannes E, Yoder MJ, Deans AR (2013) Male terminalia of Ceraphronoidea: morphological diversity in an otherwise monotonous taxon. Insect Systematics & Evolution 44(3–4): 261–347. <https://doi.org/10.1163/1876312X-04402002>
- Mikó I (2014) Project top secret(ion): the sternal gland of *Megalyra fasciipennis*. <https://sites.psu.edu/frost/2014/03/27/project-top-secretion-the-sternal-gland-of-megalyra-fasciipennis/> [accessed 23 November 2018]
- Mikó I, Trietsch C, Sandall EL, Yoder MJ, Hines H, Deans AR (2016) Malagasy Conostigmus (Hymenoptera: Ceraphronoidea) and the secret of scutes. PeerJ 4: e2682. <https://doi.org/10.7717/peerj.2682>
- Mikó I, Trietsch C, van de Kamp T, Masner L, Ulmer JM, Yoder MJ, Deans AR (2018) Revision of *Trasedia* (Hymenoptera: Ceraphronidae), an evolutionary relict with an unusual distribution. Insect Systematics and Diversity 2(6): 1–4. <https://doi.org/10.1093/isd/ixy015>

- Nijhout HF, Emlen DJ (1998) Competition among body parts in the development and evolution of insect morphology. *Proceedings of the National Academy of Sciences* 95(7): 3685–3689. <https://doi.org/10.1073/pnas.95.7.3685>
- Noirot C, Quennedey A (1974) Fine structure of insect epidermal glands. *Annual review of entomology* 19(1): 61–80. <https://doi.org/10.1146/annurev.en.19.010174.000425>
- Packer L (2004) Morphological variation in the gastral sterna of female Apoidea (Insecta: Hymenoptera). *Canadian journal of zoology* 82(1): 130–152. <https://doi.org/10.1139/z03-196>
- Pass G (2000) Accessory pulsatile organs: evolutionary innovations in insects. *Annual review of entomology* 45(1): 495–518. <https://doi.org/10.1146/annurev.ento.45.1.495>
- Pass G, Gereben-Krenn BA, Merl M, Plant J, Szucsic NU, Tögel M (2006) Phylogenetic relationships of the orders of Hexapoda: contributions from the circulatory organs for a morphological data matrix. *Arthropod Systematics & Phylogeny* 64(2): 165–203.
- Peso M, Elgar MA, Barron AB (2015) Pheromonal control: reconciling physiological mechanism with signalling theory. *Biological Reviews* 90(2): 542–559. <https://doi.org/10.1111/brv.12123>
- Peter C, David BV (1990) Biology of *Aphanogmus fijiensis* (Fernere)(Hymenoptera: Ceraphronidae) a hyperparasite of *Diaphania indica* (Saunders)(Lepidoptera: Pyralidae) through *Apanteles taragamae* Viereck (Hymenoptera: Braconidae). *Proceedings: Animal Sciences* 99(2): 131–135. <https://doi.org/10.1007/BF03186382>
- Quicke DL (1990) Tergal and inter-tergal metasomal glands of male braconine wasps (Insecta, Hymenoptera, Braconidae). *Zoologica scripta* 19(4): 413–423. <https://doi.org/10.1111/j.1463-6409.1990.tb00268.x>
- Quicke DL (1997) Parasitic wasps. Chapman & Hall Ltd.
- Ratnasingham S, Hebert PDN (2007) Barcoding. BOLD: The barcode of life data system (www.barcodinglife.org). *Molecular Ecology Notes* 7(3): 355–364. <https://doi.org/10.1111/j.1471-8286.2007.01678.x>
- Sannolo M, Gatti F, Mangiacotti M, Scali S, Sacchi R (2016) Photo-identification in amphibian studies: a test of I3S Pattern. *Acta Herpetologica* 11(1): 63–68.
- Sharkey MJ (1992) Cladistics and tribal classification of the Agathidinae (Hymenoptera: Braconidae). *Journal of Natural History* 26(2): 425–447. <https://doi.org/10.1080/00222939200770251>
- Schmitt G (2004) Parasitoid communities (Hymenoptera) in the agricultural landscape: effects of land use types and cultivation methods on structural parameters. PhD thesis. Technische Universität Dresden, Dresden.
- Snodgrass RE (1931) Morphology of the insect abdomen. *Smithsonian Miscellaneous Collections*.
- Song H, Buhay JE, Whiting MF, Crandall KA (2008) Many species in one: DNA barcoding overestimates the number of species when nuclear mitochondrial pseudogenes are coamplified. *Proceedings of the National Academy of Sciences* 105(36): 13486–13491. <https://doi.org/10.1073/pnas.0803076105>
- Szelényi G (1940) Die Paläarktische Arten Der Gattung *Aphanogmus* Thoms. (Hym. Proct.). *Annales Historico-Naturales Musei Nationalis Hungarici* 33: 122–136.
- Tang P, Zhu JC, Zheng BY, Wei SJ, Sharkey M, Chen XX, Vogler AP (2019) Mitochondrial phylogenomics of the Hymenoptera. *Molecular Phylogenetics and Evolution* 131: 8–18. <https://doi.org/10.1016/j.ympev.2018.10.040>

- Tang P, Zhu JC, Zheng BY, Wei SJ, Sharkey M, Chen XX, Vogler AP (2019) Mitochondrial phylogenomics of the Hymenoptera. *Molecular Phylogenetics and Evolution* 131: 8–18. <https://doi.org/10.1016/j.ympev.2018.10.040>
- Trietsch C, Miko I, Ulmer JM, Deans AR (2017) Translucent cuticle and setiferous patches in Megaspilidae (Hymenoptera, Ceraphronoidea). *Journal of Hymenoptera Research*, 60: 135–156. <https://doi.org/10.3897/jhr.60.13692>
- Ulmer JM, Miko I, Deans AR (2018) *Ceraphron krogmanni* (Hymenoptera: Ceraphronidae), a new species from Lower Saxony with unusual male genitalia. *Biodiversity Data Journal* (6): e24173. <https://doi.org/10.3897/BDJ.6.e24173>
- Van den Assem J, Werren JH (1994) A comparison of the courtship and mating behavior of three species of *Nasonia* (Hymenoptera: Pteromalidae). *Journal of Insect Behavior* 7(1): 53–66. <https://doi.org/10.1007/BF01989827>
- Vilhelmsen L, Miko I, Krogmann L (2010) Beyond the wasp-waist: structural diversity and phylogenetic significance of the mesosoma in apocritan wasps (Insecta: Hymenoptera). *Zoological Journal of the Linnean Society* 159(1): 22–194. <https://doi.org/10.1111/j.1096-3642.2009.00576.x>
- von Esenbeck CGN (1834) *Hymenopterorum ichneumonibus affinium monographiae, genera europaea et species illustrantes* (Vol. 1). sumptibus JG Cottæ.
- Waterston J (1923) Notes on parasitic Hymenoptera. *Bulletin of Entomological Research* 14(1): 103–118. <https://doi.org/10.1017/S0007485300028248>
- Williams HJ, Wong M, Wharton RA, Vinson SB (1988) Hagen's gland morphology and chemical content analysis for three species of parasitic wasps (Hymenoptera: Braconidae). *Journal of Chemical Ecology* 14(9): 1727–1736. <https://doi.org/10.1007/BF01014640>

Appendix I

List of abbreviations for structures:

WE = Waterston's evaporatorium = (Waterston's organ)

ta = tergal apodeme

ev = evaporatorium

at = acrotergite

at cx = acrotergal calyx

bu = bulla

sr ta = sclerotized ridge of tergal apodeme

cs = campaniform sensilla

dcc = distal crenulate carina

csr = caudal setal row

smp = submedial patches

pml = proximomedial lamella

apo = abdominal pulsatile organ

dv = dorsal vessel

cc = caudal chamber

os = ostia

msv = median ventral concavity of T5

Ditr = dorsal intertergal retractor muscle = dorsal internal muscles = 133, 144, 155

Ite = intertergal extensor muscle = external dorsal muscles = 135, 146, 157

Litr = lateral intertergal retractor muscle = lateral internal dorsal muscles = 134, 145, 156.

Supplementary material 1

Data matrix for phylogenetic analysis

Author: Jonah M. Ulmer

Data type: phylogenetic

Explanation note: Character states for the examined taxa used in the phylogenetic analysis of the Waterston's evaporatorium.

Copyright notice: This dataset is made available under the Open Database License (<http://opendatacommons.org/licenses/odbl/1.0/>). The Open Database License (ODbL) is a license agreement intended to allow users to freely share, modify, and use this Dataset while maintaining this same freedom for others, provided that the original source and author(s) are credited.

Link: <https://doi.org/10.3897/jhr.85.67165.suppl1>

Supplementary material 2

URI Table of anatomical terms

Author: Jonah M. Ulmer

Data type: morphological

Explanation note: Controlled terminology used within this study referenceable to HAO.

Copyright notice: This dataset is made available under the Open Database License (<http://opendatacommons.org/licenses/odbl/1.0/>). The Open Database License (ODbL) is a license agreement intended to allow users to freely share, modify, and use this Dataset while maintaining this same freedom for others, provided that the original source and author(s) are credited.

Link: <https://doi.org/10.3897/jhr.85.67165.suppl2>

Revision of Nearctic *Heterischnus* Wesmael, 1859 (Hymenoptera, Ichneumonidae, Ichneumoninae, Phaeogenini)

Brandon Claridge¹

¹ Department of Biology, Utah State University, 5305 Old Main Hill, Logan, UT, 84322, USA

Corresponding author: Brandon Claridge (brandonclaridge1@gmail.com)

Academic editor: Gavin Broad | Received 29 April 2021 | Accepted 6 June 2021 | Published 31 August 2021

<http://zoobank.org/17378F99-93CF-4C53-8513-9879A9BCA2DE>

Citation: Claridge B (2021) Revision of Nearctic *Heterischnus* Wesmael, 1859 (Hymenoptera, Ichneumonidae, Ichneumoninae, Phaeogenini). Journal of Hymenoptera Research 85: 57–79. <https://doi.org/10.3897/jhr.85.67792>

Abstract

The Nearctic species of *Heterischnus* Wesmael are revised. Redescriptions are provided of the three known species, *H. bicolorator*, *H. huardi* and *H. coloradensis*. *Heterischnus mexicanus* **sp. nov.** is newly described and *H. bicolorator* is recorded for the first time from the Nearctic region. The first key to the Nearctic species is provided along with species images and distribution maps.

Keywords

Ichneumoninae, Phaeogenini, new species, taxonomy

Introduction

Heterischnus Wesmael (Hymenoptera: Ichneumonidae: Ichneumoninae) is a morphologically well-defined genus in the tribe Phaeogenini and is comprised of 30 described species in the Holarctic and Afrotropical regions (Yu et al. 2016). *Heterischnus* was formerly placed in the subtribe Heterischina (Diller 1981; Selfa and Diller 1994). However, Santos et al. (2021) found that the majority of the Phaeogenini subtribes were non-monophyletic and are therefore not recognized here. *Heterischnus* species are parasitoids of microlepidoptera, especially Pterophoridae (Bragg 1970; Sedivy 1986; Diller and Shaw 2014). Rearing records from other groups, such as noctuids (Rudow

1917; Meyer 1934) or even bark beetles (Scolytinae) (Uchida 1956), are suspect. Females of at least some species overwinter as adults (Diller and Shaw 2014; Longu-Constantineanu and Constantineanu 2014), and as in nearly all ichneumonines, adults emerge from the host pupa (Diller and Shaw 2014).

Species richness for *Heterischnus* is concentrated in the Palearctic with only five described species known from the Afrotropical region and three from the Nearctic (Yu et al. 2016). Unlike the Palearctic and Afrotropical regions, which have been the subject of more recent taxonomic works (Perkins 1959; Aubert 1965; Diller 1995; Selfa and Diller 1997; Rousse et al. 2013; Valemberg 2014), research on the Nearctic *Heterischnus* ended in the early twentieth century (Cushman 1927). The purpose of the current paper is to revise the Nearctic species. One new species is described and *Heterischnus bicolorator* (Aubert) is newly recorded from the Nearctic region. A species key is provided, along with images and distribution maps to aid in identification.

Materials and methods

Morphological terminology follows Bennett et al. (2019). “MS1” refers to the first metasomal segment and “T2”, “T3”, ect. refer to the corresponding metasomal tergites. Females are described in full, while only deviations in structure and color are noted for males. Specimen images were taken with a Canon EF-S 60mm macro lens for habitus images and a Venus Optics Laowa 25mm Ultra-Macro lens for higher magnification images mounted on a Canon 1200D camera body. Image stacking was performed with Helicon Focus and further processed in the web-based photo editor Photopea (photopea.com). Figures were assembled in LibreOffice Draw 5.4.4.2. Distribution maps were generated in the open-source software QGIS 3.6.2.

Specimens examined are deposited in the following collections:

- CNCI** Canadian National Collection of Insects, Arachnids and Nematodes Agriculture Canada: Ottawa, Ontario, Canada;
- EMUS** Entomology Museum, Utah State University: Logan, Utah, USA;
- UCDC** Bohart Museum of Entomology: University of California, Davis: Davis, California, USA;
- USNM** National Museum of Natural History, Smithsonian Institution: Washington D.C., USA;

Results

Heterischnus Wesmael, 1859

Heterischnus Wesmael, 1859: 83. Type species: *Ichneumon pulex* Müller. Monotypic.
Rhexidermus Förster, 1869: 192. Type species: *Rhexidermus japonicus* Ashmead. Monotypy by inclusion in Ashmead (1906).

Posocentrus Provancher, 1875: 273. Type species: *Posocentrus huardi* Provancher.

Monotypic.

Ischnopsidea Viereck, 1914: 77. Type species: *Ichneumon thoracicus* Gravenhorst.

Monotypic and original designation.

Aethiopsischnus Heinrich, 1938: 127. Type species: *Aethiopsischnus olsoufieffi* Heinrich.

Monotypic and original designation.

Generic diagnosis. Among Phaeogenini genera, *Heterischnus* is easily recognized by a combination of the following: unidentate, falciform mandible; epistomal suture distinct; basal flagellomeres slender and elongate (Fig. 1); scutellum moderately narrow, convex, and distinctly elevated above metanotum; areolet (cell 1-2Rs) of the fore wing is closed (Fig. 1); hind coxa simple; thyridium wide. In some species, notably *Heterischnus huardi* (Provancher), the clypeus is medially truncate with acute sublateral projections making such species instantly recognizable as *Heterischnus*. However, the ventral clypeal margin varies between the aforementioned morphology and being medially straight without acute sublateral projections. The majority of species tend toward the latter condition. Additionally, the tarsal claws of *Heterischnus pulex* (Müller) are pectinate which is unique among Phaeogenini, although the tarsal claws are simple in the remaining species.

Key to the Nearctic species of *Heterischnus*

- 1 Coxae black (Fig. 2A). No trace of white markings on head or mesosoma (Fig. 2A–C). Gena rugulose-punctate, sculpture becoming denser ventrally ***H. bicolorator***
- Coxae light brownish-red or yellowish-white (e.g. Fig. 7A). Yellowish-white markings on mesosoma or head (e.g. Figs 7A, 8B). Gena punctate without rugosity..... **2**
- 2 Propodeum densely and coarsely punctate (Fig. 10E). Propodeum with longitudinal carinae reduced or obsolete and at least lateral longitudinal carina obsolete posteriorly (Fig. 10E). Female with flagellomeres 7–8 to 11–12 white dorsally (Fig. 10A)..... ***H. mexicanus* sp. nov.**
- Propodeum smooth (Fig. 7E) or rugulose-punctate (Fig. 4E). Propodeal longitudinal carinae well-developed (Figs 4E, 7E). Female with flagellomeres 10–12 dorsally white (Fig. 4A) or antennae entirely dark-brown (Fig. 7A)..... **3**
- 3 Supra-antennal area densely rugulose-punctate (Fig. 4D). Supraclypeal area densely rugulose-punctate (Fig. 4C). Females with flagellomeres 10–12 dorsally white. Male clypeus black or dark reddish-brown (Fig. 5B) ***H. coloradensis***
- Supra-antennal area smooth with fine and sparse punctation (Fig. 7D). Supraclypeal area punctate or moderately rugulose-punctate (Fig. 7C). Females with no trace of white markings on flagellomeres (Fig. 7A). Male clypeus primarily white with ventral margin black to dark reddish brown (Fig. 8B) ***H. huardi***

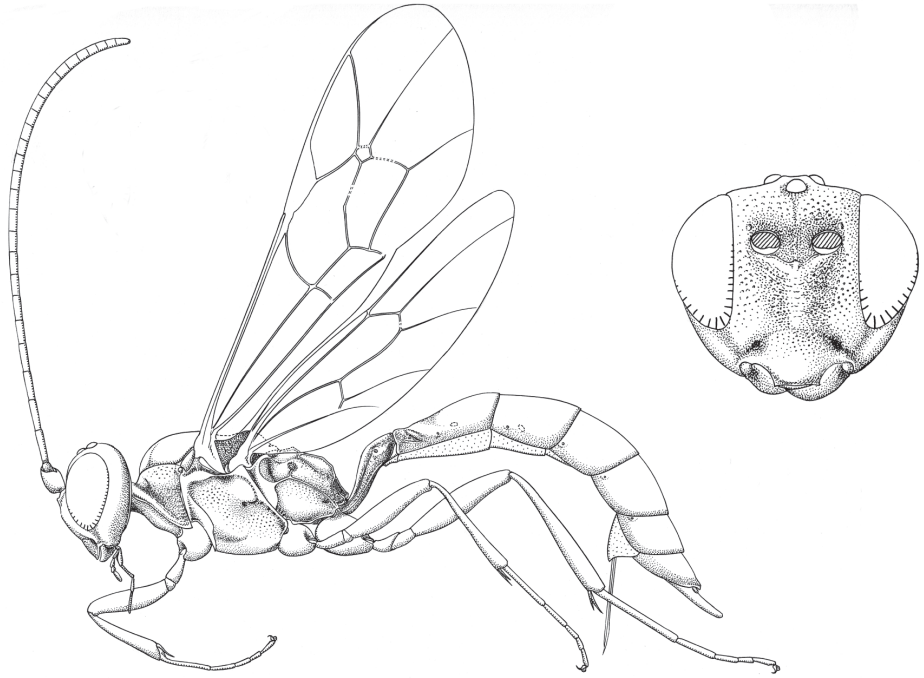


Figure 1. Unpublished illustration of *Heterischnus huardi* (Provancher) lateral habitus and frontal view of head by Professor Masaaki Tokunaga or his assistants, commissioned by Dr. Henry Townes.

***Heterischnus bicolorator* (Aubert)**

Figs 2, 3

Rhexidermis bicolorator Aubert, 1965: 16. Syntype series of 14 specimens [Musée de Zoologie, Lausanne, Switzerland]. Images of syntype (GBIFCH00759357) examined.

Diagnosis. *Heterischnus bicolorator* can be distinguished from other Nearctic *Heterischnus* species by a combination of the following: 1) flagellum, clypeus, and mesosoma without white markings; 2) coxae black to dark brown; 3) gena rugulose-punctate; and 4) T2–3 brownish-red.

Description. Female (Fig. 2). Body length: 7.7–8.2 mm. Fore wing length: 5.0–5.4 mm.

Color. Head black, except brownish-red mandibular apex. Antenna brown. Mesosoma black. Legs brownish-red with coxae and trochanters varying from black to dark brown, except for brown tarsomere 5. MS1 varying from 0.5 anterior black to dark brown with 0.5 posterior brownish-red, to entirely black; T2 varying from entirely brownish-red, to brownish-red with 0.1 posterior brown; T3 brownish-red with posterior 0.1 brown to dark brown; T4–7 dark brown to black. Wing membrane clear; veins light brown.

Head. Clypeus smooth with dorsal 0.6 punctate with punctures separated by 0.5–1.0× their diameter becoming less dense apically; apical margin medially concave

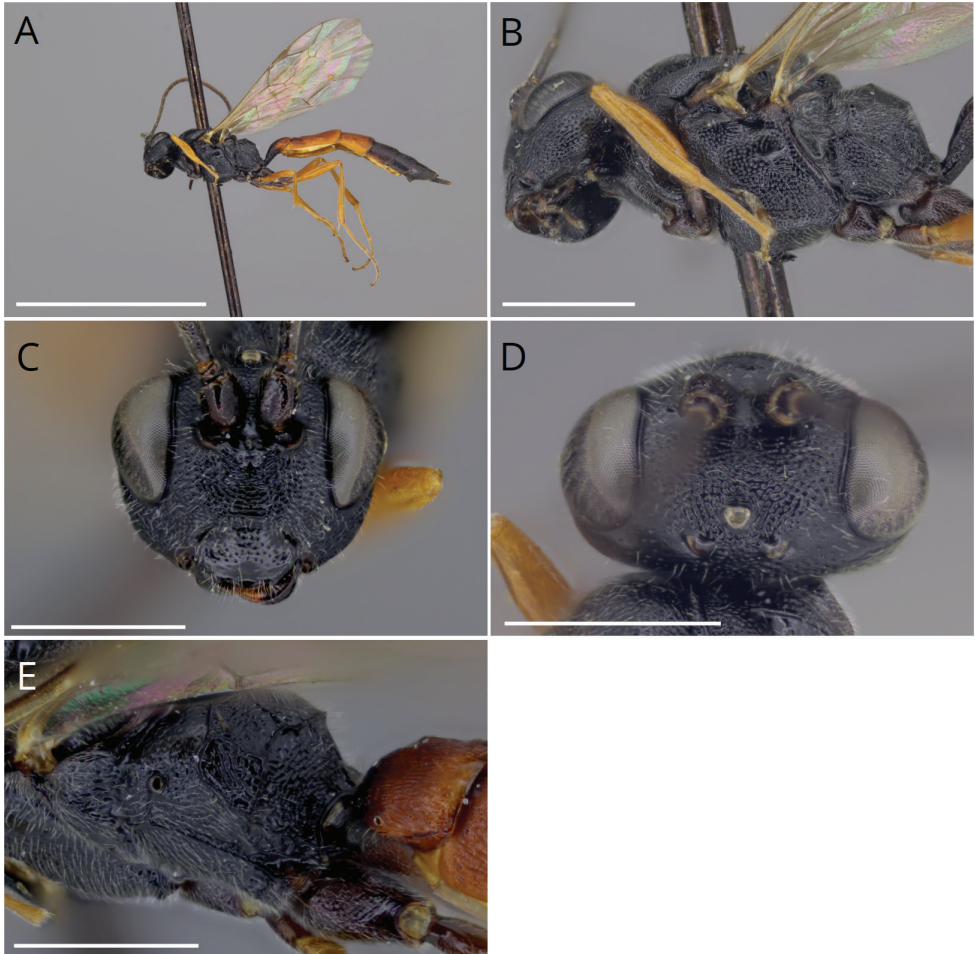


Figure 2. *Heterischnus bicolorator* (Aubert), female **A** habitus **B** mesosoma, lateral view **C** head, frontal view **D** head, dorsal view **E** propodeum, dorsolateral view. Scale bars: 5.0 mm (**A**); 1.0 mm (**B–E**).

to nearly straight with blunted sublateral apices. Supraclypeal area rugulose-punctate. Gena rugulose-punctate ventrally, dorsally smooth with coarse punctures $0.5\text{--}1.0\times$ their diameter. Malar space $1.5\text{--}1.8\times$ basal mandibular width. Supraclypeal area rugulose-punctate. Vertex smooth with coarse punctures separated by $0.5\text{--}1.0\times$ their diameter. Antenna with 34 flagellomeres.

Mesosoma. Mesonotum smooth with coarse punctures separated by $0.1\text{--}0.5\times$ their diameter. Scutellum smooth with dense, coarse punctures separated by $0.2\text{--}1.0\times$ their diameter. Mesopleuron varying from densely, coarsely punctate to rugulose-punctate. Speculum coarsely punctate dorsally. Ventral division of metapleuron densely, coarsely punctate to rugulose-punctate. Dorsal division of metapleuron finely punctate. Propodeum rugulose. Propodeal carination complete, except lateral longitudinal carina obsolete anteriorly. Tarsal claws simple.



Figure 3. Nearctic distribution of *Heterischnus bicolorator* (Aubert).

Metasoma. Postpetiole varying from granulate to rugulose. T2 length 1.4–1.5× posterior width. T2–7 granulate with dense, shallow, punctation becoming sparser and indistinct posteriorly. Gastrocoelus longitudinally rugulose. Thyridium distant from T2 anterior margin by 2.0–3.0× thyridial length.

Male. Not examined (not known from Nearctic region).

Material examined. Non-type material: CANADA • 1♀; British Columbia, Stone Mountain Park; 5500 ft; 20.vii.1973; H. & M. Townes; EMUSENT00000302 • 1♀; same collection data as preceding; 22.viii.1973; H. & M. Townes; EMUS00000151. USA • 1♀; Alaska, Umiat; 20.vii.1947; C. Schultz; USNM.

Distribution and biology. *Heterischnus bicolorator* is known from western Europe and as far east as Chita Oblast in Russia (Yu et al. 2016). In the Nearctic, it is known only from two localities in Alaska and British Columbia (Fig. 3), but is likely present throughout the intervening areas, including the Yukon Territory. No host information is known.

Comments. The three Nearctic specimens examined agree with both the original description (Aubert 1965) and images of a syntype specimen. No significant color or morphological differences could be found that would indicate that the examined Nearctic specimens are not conspecific with Palearctic specimens of *H. bicolorator*.

***Heterischnus coloradensis* (Cushman)**

Figs 4–6

Ischnopsidea coloradensis Cushman, 1920: 253. Holotype: ♀ [USNM]. Not examined.

Diagnosis. *Heterischnus coloradensis* (Cushman) is chromatically and morphologically similar to *H. huardi* but can be distinguished from the latter and other Nearctic species

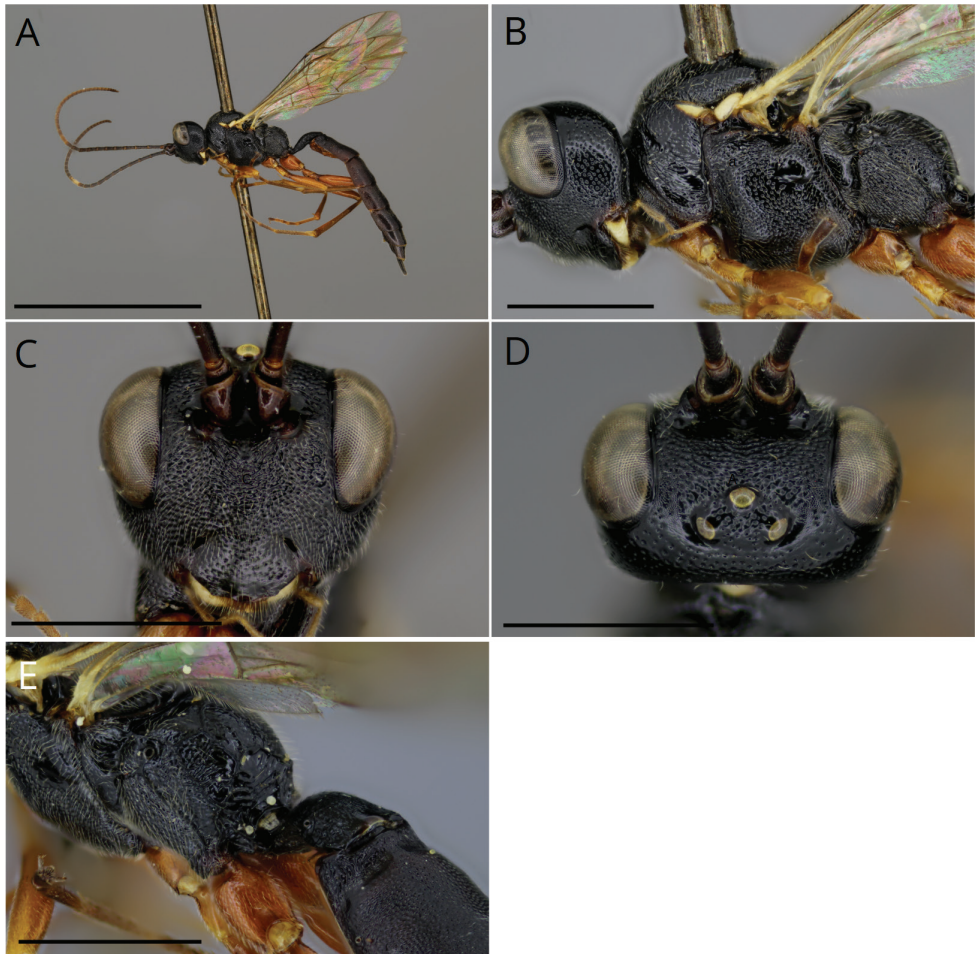


Figure 4. *Heterischmus coloradensis* (Cushman) female **A** habitus **B** mesosoma, lateral view **C** head, frontal view **D** head, dorsal view **E** propodeum, dorsolateral view. Scale bars: 5.0 mm (**A**); 1.0 mm (**B–E**).

by a combination of the following: 1) male clypeus dark reddish-brown to black; 2) flagellomeres 10/11–12/13 dorsally white in female; 3) supra-antennal area rugulose-punctate; and 4) first lateral area of propodeum rugulose-punctate.

Description. Female (Fig. 4). Body length: 6.8–8.7 mm. Fore wing length: 4.2–5.1 mm.

Color. Head black. Mandible yellowish-white with brown apex. Antenna dark brown with flagellomeres 10/11–12/13 dorsally white. Mesosoma black with following areas white: occasionally anterior margin of pronotum (25% of specimens), posterior 0.2 of dorsal margin of pronotum, usually subalar prominence (60% of specimens), and tegula. Fore and middle legs light brownish-red except for tarsomere 5 brown. Hind leg brownish-red except for basal 0.1 of tibia white, apical 0.2 of tibia brown, tarsomeres brown. Metasoma black to dark brown. Wing membrane clear; basal 0.1–0.2 of wing with veins white, remaining sections brown.

Head. Clypeus smooth, basally with fine punctures separated by 0.5–1.0× their diameter becoming less dense apically; ventral margin with sublateral apical projections subobsolete to obsolete. Malar space 1.5–2.0× basal mandibular width. Supraclypeal area rugulose-punctate. Gena smooth, coarsely punctate with punctures separated by 0.2–1.5× their diameter. Supra-antennal area rugulose-punctate. Vertex smooth, finely punctate with punctures separated by 0.5–2.0× their diameter. Antenna with 32–34 flagellomeres.

Mesosoma. Mesonotum smooth, with punctures separated by 0.5–2.0× their diameter. Scutellum smooth, finely punctate with punctures separated by 1.0–2.0× their diameter. Mesopleuron densely, coarsely punctate with punctures confluent to separated by about 0.5× their diameter becoming more sparse dorsally; tendency in some specimens to form lateral rugulae. Speculum coarsely punctate dorsally, smooth ventrally. Ventral division of metapleuron rugulose-punctate. Dorsal division of metapleuron with a few scattered punctures. Propodeum overall rugulose-punctate with areola and posterodorsal face rugulose; carination complete. Tarsal claws simple.

Metasoma. Postpetiole rugulose-punctate. T2 length 1.0–1.2× posterior width. T2–7 granulate with dense, shallow punctures; punctation becoming sparser and indistinct posteriorly. Gastrocoelus rugulose-granulate. Thyridium distant from T2 anterior margin by 0.5–2.0× thyridial length.

Male (Fig. 5). Body length 6.8–9.1 mm. Fore wing length: 4.3–5.6 mm. As in female except for: yellowish-white markings on mesosoma more extensive.

Material examined. Paratype: USA • 1♀; Colorado, Larimer Co., Forrester's; 19.vii.1895; C. F. & N. E. Baker; USNM paratype 22850.

Non-type material: USA • 1♀; California, Modoc Co. 1 mile N of Stough Reservoir; [41.5767, -120.2538], 15.vi.1963; UCDC • 1♀; California, Modoc Co., Cedar Pass; [41.5623, -120.2688]; 29.vi.1955; D. L. Dahlsten; UCDC • 1♀; California, Nevada Co., Sagehen Cr. near Hobart Mills; [39.4342, -120.2048]; 15.vii.1964; M. E. Irwin; UCRCENT529785 • 1♀; Colorado, Grand Co., Phantom Valley, Rocky Mountain National Park; 9400 ft; [40.2833, -105.8505]; 16.vi.1948; H., M., G., D. & J. Townes; EMUSENT00000417 • 1♀, 3♂♂; Colorado, Routt Co., Steamboat Springs; [40.4857, -106.8309]; 6.viii.1948; H., M., G., D. & J. Townes; EMUSENT00000722, EMUSENT00000132, EMUSENT00000207, EMUSENT00000073 • 1♂; same collection data as preceding; 5.viii.1948; EMUSENT00000345 • 1♂; Idaho, Oneida Co., 3 mi. S of Roy Summit; [42.2635, -112.7653]; 6.vii.1972; G. F. Knowlton; EMUSENT00000137 • 1♂; Idaho, Blaine Co., 9 mi. SW Bellevue; [43.3353, -114.2901]; 28.viii.1965; J. S. Buckett; UCDC • 1♀; Idaho, Boise Co., Idaho City; [43.82813, -115.8341]; 9.vi.1978; H. & M. Townes; EMUSENT00000777 • 3♀♀; same collection data as preceding; 13.vi.1978; EMUSENT00000258, EMUSENT00000317, EMUSENT00000225 • 1♀♀; same collection data as preceding; 14.vi.1978; EMUSENT00000192 • 2♂♂; Idaho, Custer Co., nr. Stanley; [44.2161, -114.9353]; 2.viii.1978; H. & M. Townes; EMUSENT00000253, EMUSENT00000206 • 1♂; same collection data as preceding; 7.viii.1978; EMUSENT00000288 • 2♂♂; same collection data as preceding; 8.viii.1978; EMUSENT00000719, EMUSENT00000297 • 1♀; Idaho, Oneida Co., Rock Creek; [42.4320, -114.3054]; 17.vii.1972; G. F.



Figure 5. *Heterischnus coloradensis* (Cushman) male **A** habitus **B** head, frontal view. Scale bars: 5.0 mm (**A**); 1.0 mm (**B**).

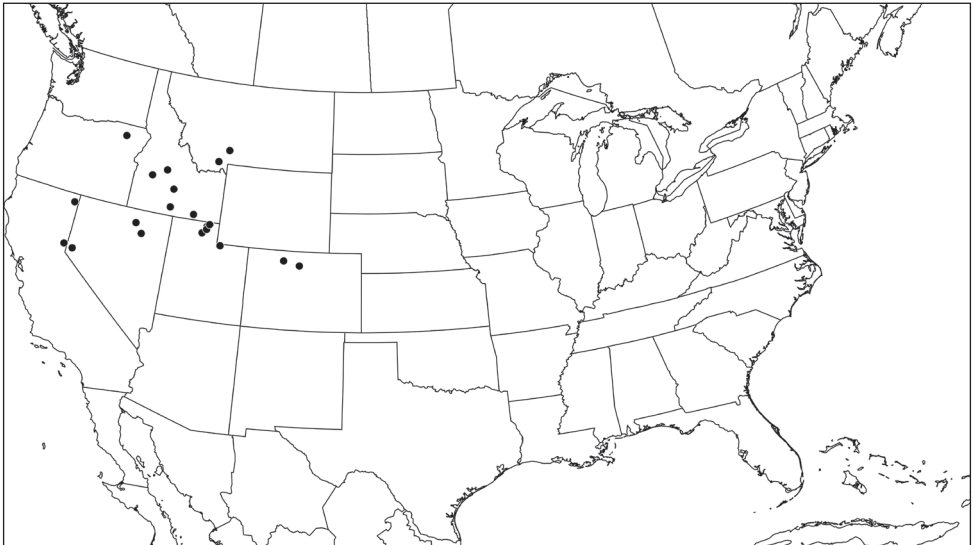


Figure 6. Distribution of *Heterischnus coloradensis* (Cushman).

Knowlton; EMUSENT00000138 • 1♂; same collection data as preceding; 6.vii.1972; EMUSENT00000224 • 1♂; Montana, Madison Co., 16 miles S. of Cameron; [45.0604, -111.6656]; 18.vii.1971; UCDC • 3♀♀; Montana, Gallatin Co., Bozeman; [45.6771, -111.0428]; 30.vi.1978; R., B. & C. Dasch; EMUSENT00000629, EMUSENT00000056, EMUSENT00000194 • 4♀♀; same collection data as preceding; 7.vii.1978; EMUSENT00000193, EMUSENT00000077, EMUSENT00000566, EMUSENT00000357 • 1♂; Nevada, Elko Co., Elko; [40.8385, -115.7628]; 21.viii.1964; F. S. Buckett; UCDC • 1♀; Nevada, Elko Co., Tuscarora; [41.3146 -116.2233]; 5.vi.1978; H. & M. Townes; EMUSENT00000393 • 1♀; Nevada, Storey Co., Virginia City; [39.3093, -119.6499]; 14.vi.1951; W. J. Wall; UCDC • 1♀; Oregon, Union Co., Mt. Emily; [45.4379, -118.0913]; 03–11.vi.1987; T. R.

Torgersen, EMUSENT00000420 • 1♀; Utah, Box Elder Co. Willard Peak.; 9000 ft; [41.4210, -112.0561]; 25.vii.1960; G. E. Bohart; EMUSENT00000347 • 2♀♀; Utah, Cache Co., Black Smith Fork Canyon; [41.6278, -111.8040]; 1–6.vii.1964; W. J. Hanson; EMUSENT00000391, EMUSENT00000108 • 1♀; Utah, Cache Co., North Logan; [41.7706, -111.8045]; 25–31.v.1983; C. R. Nelson; EMUSENT00000030 • 1♂; Utah, Cache Co., Tony Grove; 2290 m; 41.8884, -111.6571; 18.v.–1.vi.2019; B. Claridge; Malaise trap; EMUSENT00000547 • 1♀; Utah, Cache Co., Tony Grove Canyon; [41.8902, -111.6371]; 25.viii.–2.ix.1976; W. J. Hanson; EMUSENT00000026 • 1♂; Wyoming, Albany Co., Pole Mountain; 41.22, -105.45; 13–20.vii.2013; Malaise trap, ungrazed short grass prairie; L. Haimowitz, H, Aguirre; EMUSENT00004739.

Distribution and biology. Collecting dates span mid-May to early September, although the greatest number of records are from July and August. *Heterischnus coloradensis* occurs from the Rocky Mountains west to the eastern slopes of the Sierra Nevada Range (Fig. 6). Throughout its range, *H. coloradensis* is sympatric with *H. huardi*. No host information is known.

Comments. In addition to the examined paratype, a specimen that was compared with the holotype by Henry Townes was examined.

Heterischnus huardi (Provancher)

Figs 7–9

Posocentrus huardi Provancher, 1875: 273. Lectotype: ♀ [University of Laval Entomology Collection, Quebec, Canada]: designated by Townes (1939). Not examined.

Phaeogenes recticaudus Provancher, 1886: 42. Holotype: ♀ [University of Laval Entomology Collection, Quebec, Canada]: Synonymized by Townes (1944). Not examined.

Ischnopsidea alberta Cushman, 1927: 1. Holotype: ♀ [USNM]: Synonymized by Townes (1944). Not examined.

Diagnosis. *Heterischnus huardi* can be distinguished from other Nearctic species by the combination of the following: 1) clypeus yellowish-white in males; 2) female flagellum without any trace of yellowish-white banding; 3) supra-antennal area smooth with fine, shallow punctures; 4) and first lateral area of propodeum varying from entirely smooth to smooth and rugulose, but never rugulose-punctate as in *H. coloradensis*.

Description. Female (Fig. 7). Body length: 5.5–8.8 mm; fore wing length: 3.8–5.6 mm.

Color. Head usually black, infrequently varying from dark reddish-brown to dark brown. Mandible yellowish-white except for dark brown apex. Antenna brown. Mesosoma overall black to dark brown, with the following areas yellowish-white: dorsal margin of pronotum, subalar prominence, and tegula; specimens from California and Oregon usually with mesonotum, scutellum, mesopleuron, and ventral division of metapleuron brownish-red to varying extents. Fore and middle legs with coxae,

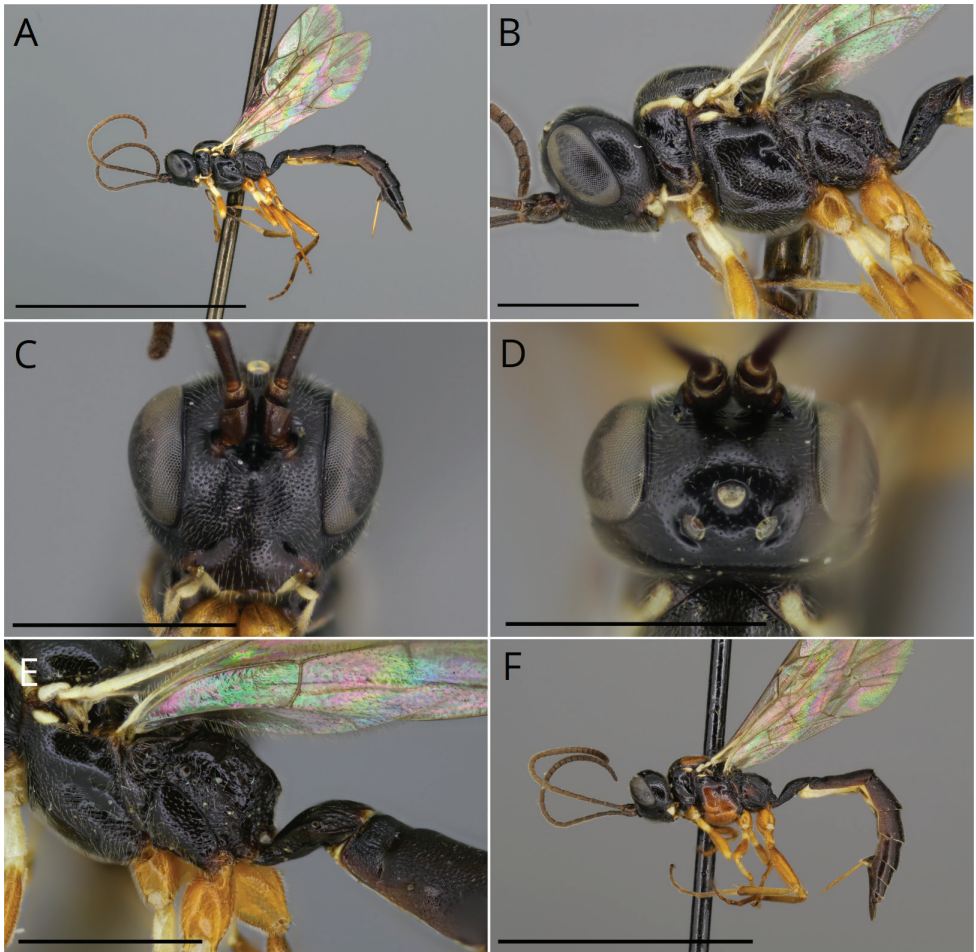


Figure 7. *Heterischmus huardi* (Provancher) female. Eastern and western Nearctic dark phase (A–E) **A** habitus **B** mesosoma, lateral view **C** head, frontal view **D** head, dorsal view **E** propodeum, dorsolateral view **F** western Nearctic reddish phase *H. huardi* female habitus. Scale bars: 5.0 mm (A, F); 1.0 mm (B–E).

trochanters and trochantelli white to light reddish-brown; tibiae and femora light reddish-brown; tarsomeres 1–4 light reddish-brown; tarsomere 5 brown. Hind leg with coxa and trochanter light reddish-brown; trochantellus white to light reddish-brown; femur light reddish-brown; tibia light reddish brown with apical 0.5 dorsally brown; tarsomere 1 brown with basal 0.3 varying from light reddish-brown to brown; tarsomeres 2–5 brown. Metasoma varying from dark brown to black; one specimen from Nojoqui Falls Park, California with T1 medially brownish-red. Wing: membrane clear; basal 0.2 of wing with veins white, remaining vein sections brown.

Head. Clypeus smooth, dorsally with fine punctures separated by 0.5–1.0× their diameter becoming less dense ventrally; ventral margin truncate medially and with sublateral projections varying from blunt to sharp. Supraclypeal area rugulose-punc-

tate with punctures separated by 0.5–1.5× their diameter, becoming less dense laterally. Gena smooth, finely punctate with punctures separated by 3.0–5.0× their diameter. Malar space 1.0–1.2× basal mandibular width. Supra-antennal area smooth and finely punctate with punctures separated by 1.0–3.0× their diameter. Vertex smooth and finely punctate with punctures separated by 1.0–3.0× their diameter. Antenna with 25–29 flagellomeres.

Mesosoma. Mesonotum smooth and finely punctate with punctures separated by 0.5–2.0× their diameter. Scutellum smooth and finely punctate with punctures separated by 2.0–3.0× their diameter. Mesopleuron punctate with punctures separated by 0.2–1.0× their diameter, tendency in some specimens to form lateral rugulae. Speculum smooth with several scattered punctures. Ventral division of metapleuron punctate with punctures separated by 0.2–1.0× their diameter. Dorsal division of metapleuron finely punctate separated by 0.4–1.0× their diameter. Propodeum overall smooth, pleural area rugulose-punctate; carination complete, except lateral longitudinal carina absent anteriorly. Tarsal claws simple.

Metasoma. MS1 with postpetiole smooth anteriorly, posteriorly longitudinally rugulose laterally. T2 length 1.3–1.4× posterior width. T2–7 granulate with dense shallow punctation becoming sparser and indistinct posteriorly. Gastrocoelus longitudinally rugulose. Thyridium distant from T2 anterior margin by 2.5–4.0× thyridial length.

Male (Fig. 8). Body length: 5.4–8.9 mm; fore wing length: 3.8–5.6 mm. As in female except for: clypeus usually (90% of specimens) white except for dark brown to black apical margin and medial mark extending from apical 0.1 up to 0.3; infrequently most of clypeus dark brown to black with white area only present medially or as dorso-lateral markings; very rarely clypeus entirely dark brown. Malar space shorter (0.8–1.0 basal mandibular width.)

Material examined. Non-type material: CANADA • 1♀; Alberta, Edmonton; [53.5487, -113.4927]; 1.iv.1924; Owen Bryant; USNM • 1♀; Alberta, Seebe, K.F.E.S; 29.viii.1958; “ex Pterophoridae willow”; 57-A-1575-047; 314; CNCI • 3♀♀; Alberta, Sturgeon, L. Rt. 34; [53.6316, -113.6161]; 26.vi.1977; B. & C. Dasch; EMUSENT00000163, EMUSENT00000567, EMUSENT00000254 • 1♂; British Columbia, Craigallachie, 22 km E Sicamous; 350 m; [50.8397, -118.9738]; 28.vi.–14.viii.1988; S. & J. Peck; EMUSENT00000453 • 5♂♂; British Columbia, Dome Creek; [53.7503, -121.1034]; 27.viii.1973; H. & M. Townes; EMUSENT00000092, EMUSENT00000178, EMUSENT00000088, EMUSENT00000268, EMUSENT00000718 • 1♂; British Columbia, Fort Nelson; [58.8040, -122.6981]; 25.viii.1973; H. & M. Townes; EMUSENT00000538 • 11♀♀; British Columbia, Mt. Robson Provincial Park; [53.0352, -119.2310]; 23.vii.1977; B. & C. Dasch; EMUSENT00000477, EMUSENT00000195, EMUSENT00000568, EMUSENT00000213, EMUSENT00000479, EMUSENT00000027, EMUSENT00000343, EMUSENT00000447, EMUSENT00000358, EMUSENT00000122, EMUSENT00000536 • 1♂; British Columbia, Stone Mountain Peak; 3800 ft; [58.5862, -124.7642]; 13.vii.1973; H. & M. Townes; EMUSENT00000628 • 1♀; same collection data as preceding; 17.vii.1973, EMUSENT00000241 • 1♀; British Columbia, Y.N.P, “End of



Figure 8. *Heterischmus huardi* (Provancher) male **A** habitus **B** head, frontal view. Scale bars: 5.0 mm (**A**); 1.0 mm (**B**).

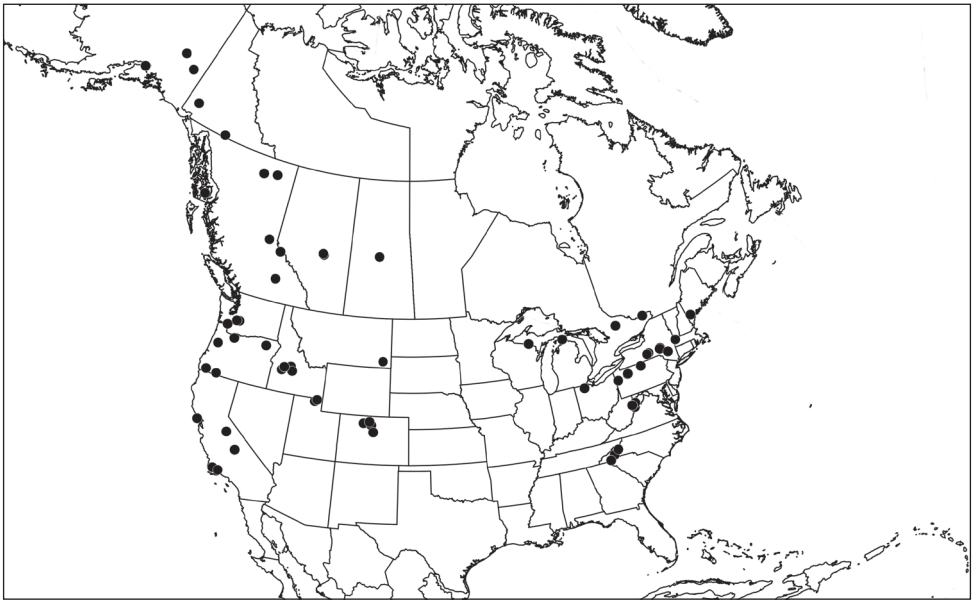


Figure 9. Distribution of *Heterischmus huardi* (Provancher).

Ire River Road”; 10.viii.1956; “ex. *Platyptilia* sp. A. fir.”; 56-18-1148-01; 406; CNCI • 2♀♀; Ontario, Algonquin Provincial Park; [45.5539, -78.5965]; 08.viii.1983; B. & C. Dasch; EMUSENT00000344, EMUSENT00000328 • 1♀; Ontario, Cumberland; [45.5163, -75.4060]; 3.v.1975; L. Ling; EMUSENT00000752 • 1♀; same collection data as preceding; 8.v.1975; EMUSENT00000541 • 1♀; same collection data as preceding; 10.v.1975; EMUSENT00000661 • 1♀; same collection data as preceding; 11.v.1975; EMUSENT00000032 • 1♀; same collection data as preceding; 6. vi.1975; EMUSENT00000033 • 1♀; same collection data as preceding; 8.vi.1975; EMUSENT00000063 • 1♂; same collection data as preceding; 9.vii.1975; EMUSENT00000631 • 2♂♂; same collection data as preceding; 13.vii.1975; EMUSE-

NT00000482, EMUSENT00000061 • 2♂♂; same collection data as preceding; 18.vii.–10.viii.1975; EMUSENT00000121, EMUSENT00000512 • 1♀; Saskatchewan, Prince Albert National Park; [53.9143, -75.4060]; 19.vii.1941; J. G. Rempel; EMUSENT00000508 • 1♀; same collecting data as preceding; 20.vii.1941; EMUSENT00000418 • 1♀; Yukon Territory, Burwash Flats Mi. 1105 Alcan Hwy.; [61.3536, -138.9976]; 4.vii.1977; B. & C. Dasch; EMUSENT00000506 • 1♀; Yukon Territory, Teslin L. Mi. 820 Alcan Hwy.; [60.1745, -132.7143]; 30.vi.1977; B. & C. Dasch; EMUSENT00000603 • 1♀; same collecting data as preceding; 1.vii.1977; EMUSENT00000167. USA • 4♀♀; Alaska, Municipality of Anchorage, Anchorage; [61.1993; 149.8533]; 6–12.vii Peter A. Rush; EMUSENT00000028, EMUSENT00000720, EMUSENT00000058, EMUSENT00000690 • 2♀♀; same collection data as preceding; 16–20.vii.1976; EMUSENT00000089, EMUSENT00000118 • 1♀; same collection data as preceding; 20–23.vii.1976; EMUSENT00000390 • 3♀♀; Alaska, Delta Junction; [64.0377; -145.7301]; 7.vii.1977; B. & C. Dasch; EMUSENT00000228, EMUSENT00000136, EMUSENT00000633 • 1♂; Alaska, Ketchikan Gateway Borough, Ketchikan; [55.3465; -131.643] 16.viii.1959; R. H. Washburn • 1♀; Alaska, Tok; [63.3361; -142.9855]; 5.vii.1977; B. & C. Dasch; EMUSENT00000717 • 1♀; California, Big Oak Flat Road, nr. Crane Crk., Yosemite National Park; [37.7517; -119.8004]; 28.vi.1959; D. W. Price; UCDC • 2♂♂; California, Marin County, Inverness; [38.0998; -122.8619]; 6.x.1946; H. K. Townes; EMUSENT00000287, EMUSENT00000389 • 1♀; California, Tulare County, Mineral King Road; [36.4500; -118.5945]; 16.v.1970; B. Knapp; EMUSENT00000449 • 1♀; California, Santa Barbara County, Montecito; [34.4368; -119.6321]; 08.iv.1997–13.iv.1997; A. Calderwood, R. Doust; EMUSENT00000078 • 1♀; California, Santa Barbara County, Nojoeui Falls Park; [34.5344; -120.1776]; 3.vii.1959; R. M. Bohart; UCDC • 1♀; Colorado; Doolittle Ranch, Mt. Evans; [39.6752; -105.6011]; 9800 ft; 20.vii.1964; B. & C. Dasch; EMUSENT00000688 • 1♀; same collection data as preceding; 12.vii.1973; EMUSENT00000753 • 2♀; Colorado, Jackson County, Gould; [40.5271; -106.0300]; 6.viii.1974; H. & M. Townes; EMUSENT00000212, EMUSENT00000062 • 1♀; Colorado, Grand County, Grand Lake; [40.2518; -105.8301]; 2.viii.1948; H. & M. Townes; EMUSENT00000510 • 1♀; same collecting data as preceding; H., M., G., D. & J. Townes; EMUSENT00000658 • 1♀; Colorado, Rabbit Ears Pass; [40.3847; -106.6117]; 9500 ft; 7.viii.1948; H., M., G. & D. Townes; EMUSENT00000422 • 1♀; Idaho, Galena Summit, nr. Stanely; [43.8702; -114.7134]; 8700 ft; 4.viii.1978; H. & M. Townes; EMUSENT00000778 • 2♀♀; Idaho; Boise County; Idaho City; [43.82813; -115.8341]; 13.vi.1978; H. & M. Townes; EMUSENT00000299, EMUSENT00000269 • 1♀; Idaho; Boise County, Lowman; [44.0807; -115.6202]; 4000 ft; 11.vi.1978; H. & M. Townes; EMUSENT00000723 • 2♀♀; same collection data as preceding; 12.vi.1978; EMUSENT00000331, EMUSENT00000211 • 3♀♀; same collection data as preceding; 6000 ft; 13.vi.1978; EMUSENT00000180, EMUSENT00000242, EMUSENT00000751 • 1♀; same collection data as preceding; 4000 ft; 14.vi.1978; EMUSENT00000090 • 1♂, 2♀♀; Idaho, Boise County, Lowman; [44.0807; -115.6202]; 6.viii.1978; H. & M. Townes; EMUSENT00000478, EMUSENT00000450, EMUSENT00000029 •

1♂; same collection data as preceding; 3.viii.1978 • 1♀; Idaho, nr. Stanley; [44.2159; -114.9352]; 5.viii.1978; H. & M. Townes; EMUSENT00000570 • 1♀; Maine, 4.5 mi. W Bangor; [44.7994; -688326]; 12.viii.1986; B. & C. Dasch; EMUSENT00000416 • 1♀; same collection data as preceding; 13.viii.1986; EMUSENT00000086 • 2♀♀; Maine, Cumberland County, Sebado Lake; [43.9303; -70.5678]; 12.v.1919; B. W. Hall; EMUSENT00000093, EMUSENT00000183 • 2♀♀; Massachusetts; Mt. Greylock; [42.6375; -73.1663]; 02.viii.1958; B. & C. Dasch; EMUSENT00000283, EMUSENT00000282 • 1♀; Michigan, Emmet County, Mackinaw City; [45.7776; -84.7283]; 04.viii.1980; B. & C. Dasch; EMUSENT00000313 • 1♂, 1♀; Michigan, Iron County, Pentoga Park; [46.0387; -88.5105]; 01.viii.1980; B. & C. Dasch; EMUSENT00000689, EMUSENT00000749 • 1♀; New York, Ithaca; [42.4443; -76.5017]; 12.vi.1952; C. Dasch; EMUSENT00000107 • 1♀; same collection data as preceding; 15.vii.1950; EMUSENT00000315 • 1♀; same collection data as preceding; 22.vii.1950; EMUSENT00000256 • 2♂♂; same collection data as preceding; 7.vii.1951; EMUSENT00000597, EMUSENT00000569 • 1♀; New York, McLean Bogs; [42.4911; -76.2971]; 22.v.1953; B. & C. Dasch; EMUSENT00000476 • 2♂♂; New York, Otsego County, Milford Center; [42.5241; -74.9887]; 13.vii.1935; H. K. Townes; EMUSENT00000662, EMUSENT00000452 • 1♀; New York, Oneonta County, Oneonta; [42.4584; -75.0602]; 1900 ft; 18.viii.1935; H. K. Townes; EMUSENT00000183, EMUSENT00000721 • 1♀; New York, Ulster County, Slide Mountain, [41.9996; -74.3854]; 2800–4000 ft; 25.viii.1936; H. & C. Townes; EMUSENT00000481 • 2♂♂, 2♀♀; North Carolina, Macon County, Highlands; [35.0536; -83.1969]; 21.vi.1977; H & M Townes; EMUSENT00000359, EMUSENT00000573, EMUSENT00000660, EMUSENT00000148 • 1♂, 2♀; same collection data as preceding; 22.vi.1977; EMUSENT00000208, EMUSENT00000633, EMUSENT00000240 • 3♀♀; same collection data as preceding; 23.vi.1977; EMUSENT00000119, EMUSENT00000633 • 1♀; same collection data as preceding; 24.vi.1977; EMUSENT00000210 • 1♂; same collection data as preceding; 26.vi.1977; EMUSENT00000598 • 1♀; North Carolina, Mt. Mitchell; [35.7668; -82.2653]; 5500 ft; 25.vii.1968; C. Dasch; EMUSENT00000542 • 1♀; North Carolina, Buncombe County, Pisgah Mountain; [35.4197; -82.7484]; 4800–5300 ft; 21.vi.1940; H & M Townes; EMUSENT00000513 • 1♂; Ohio, McAllister Biological Station; [41.4478; -83.7789]; 18–21.vi.1986; B. & C. Dasch; EMUSENT00000198 • 1♀; Oregon, Benton County, Corvallis; [44.5630; -123.2644]; 02.vi.1978; H. & M. Townes; EMUSENT00000043 • 1♀; same collection data as preceding; 11.v.1987; EMUSENT00000045 • 1♀; same collection data as preceding; 19–20.vi.1965; C. Dasch; EMUSENT00000329 • 1♀; Oregon; Jackson County, Hyatt Reservoir; [42.1683; -122.4634]; 29.vi.1978; H. & M. Townes; EMUSENT00000252 • 1♂; Oregon, Pierce County, Hyatt Reservoir; [42.1683; -122.4634]; 29.vi.1978; H. & M. Townes; EMUSENT00000356 • 1♂; Oregon, Union County, Mt. Emily; [45.4379; -118.0913]; 06–21.viii.1987; T. R. Torgersen; EMUSENT00000166 • 4♀♀; Oregon, Mt. Hood; [45.3269; -121.7136]; 3500 ft; 19.vii.1978; H. & M. Townes; EMUSENT00000177, EMUSENT00000342, EMUSENT00000296, EMUSENT00000327 • 1♀; same collection data as preceding; 20.vii.1978; EMUSENT00000165 • 1♀;

same collection data as preceding; 24.vii.1978; EMUSENT00000223 • 1♀; same collection data as preceding; 26.vii.1978; EMUSENT00000227 • 3♀♀; same collection data as preceding; 30.vii.1978; EMUSENT00000386, EMUSENT000000386, EMUSENT00000133, EMUSENT000000226 • 1♀; Oregon, Josephine County, Selma; [42.2787; -123.6152] 20.v.1978; H. & M. Townes; EMUSENT00000480 • 2♀♀; same collection data as preceding; 27.v.1978; EMUSENT00000075, EMUSENT00000656 • 1♀; Pennsylvania, Forest County, 1 mi. N Marienville; [41.4794; -79.1101]; ; 3.vii.1980; C. Dasch; EMUSENT00000236 • 1♀; Pennsylvania, Forest County, 4 mi. N Marienville; [41.5104; -79.0688]; 03.vii.1980; C. Dasch; EMUSENT00000419 • 2♀♀; Pennsylvania, Tioga County, Gaines; [41.7520; -77.5572]; 23–26.vii.1994; B. & C. Dasch; EMUSENT00000059, EMUSENT00000179 • 1♀; same collection data as preceding; 26.vii.1994; EMUSENT00000239 • 1♂; same collection data as preceding; 30.vi.1980; EMUSENT00000338 • 1♀; Pennsylvania, Mercer County, Mercer; [41.2265; -80.2393]; 12–15.vi.1995; B. & C. Dasch; EMUSENT00000149 • 1♂; Utah, Cache County, Logan, USU campus; 41.74194; -111.81183; 1460 m; 8.vii.2019; B. Claridge; EMUSENT00000021 • 2♀♀; Utah, Cache County, Uinta-Wasatch-Cache National Forest, Tony Grove; 41.8876; -111.6009; 2290 m; 03–17.viii.2019; B. Claridge; EMUSENT00000202, EMUSENT00000232 • 1♀; Utah, Cache County, UWC National Forest, Tony Grove; 41.8884; -111.6299; 17–31.viii.2019; B. Claridge; EMUSENT000003712 • 1♂, 1♀; Washington, Pierce County, Ashford; [46.7579; -122.0304]; 6.vii.1940; H. & M. Townes; EMUSENT00000483, EMUSENT00000630 • 1♀; same collection data as preceding; 11.vii.1940; EMUSENT00000360 • 1♀; same collection data as preceding; 20.vii.1940; EMUSENT00000540 • 1♀; Washington, Barnes State Park; [46.2724; -122.909]; 12.viii.1940; H. & M. Townes; EMUSENT00000060 • ♀; Washington, Mt. Rainier; 2900 ft; 12.vii.1940; H. & M. Townes; EMUSENT00000750 • 1♀; same collecting data as preceding; 7.vii.1940; EMUSENT00000693 • 1♀; same collecting data as preceding; 4200 ft; 15.vii.1940; EMUSENT00000301 • 1♀; same collecting data as preceding; 4700 ft; 21.vii.1940; EMUSENT00000330 • 1♀; same data as preceding; 5000 ft; 14.vii.1940; EMUSENT00000543 • 1♀; same data as preceding; 9.vii.1940; EMUSENT00000120 • 1♀; same data as preceding; 5300 ft; 16.viii.1940; EMUSENT00000332 • 1♀; same data as preceding; 17.viii.1940; EMUSENT00000571 • 1♀; same data as preceding; 5700 ft; 8.vii.1940; EMUSENT00000362 • 1♀; Washington, Mt. Rainier National Park, Paradise; [46.7853; -121.7349]; ; 26–27.vi.1987; B. V. Brown; EMUSENT00000600 • 2♂♂, 2♀♀; West Virginia, Bickle Knob; [38.9343; -79.7314]; 4020 ft; 15.vii.1979; B. & C. Dasch; EMUSENT00000691, EMUSENT00000103, EMUSENT00000314, EMUSENT00000687 • 5♂♂, 1♀; same data as preceding; 17.vii.1979; EMUSENT00000316, EMUSENT00000599, EMUSENT00000284, EMUSENT00000057, EMUSENT00000042, EMUSENT00000147 • 1♀; West Virginia; Randolph County, Bowden; [38.9088; -79.7098]; 14–17.vii.1992; B. & C. Dasch; EMUSENT00000146 • 1♀; same collection data as preceding; 21–22.vii.1982; EMUSENT00000104 • 1♀; same collection data as preceding; 23–24.vii.1982; EMUSE-

NT00000044 • 1♂, 1♀; same collection data as preceding; 25.vii.1982; EMUSENT000000387, EMUSENT000000776 • 1♀; same collection data as preceding; 7-9.v.1993; EMUSENT00000238 • 1♀; same collection data as preceding; 16.vii.1979; C. Dasch; EMUSENT00000117 • 2♂♂, 1♀; West Virginia, Dolly Sods Area; [39.0447; -79.3438]; 26.vii.1982; B. & C. Dasch; EMUSENT00000255, EMUSENT00000392, EMUSENT00000627 • 1♂; West Virginia, Pendleton County, Spruce Knob; [38.7001; -79.5328]; 4862 ft; 18.vii.1979; B. & C. Dasch; EMUSENT00000209 • 4♀♀; same collection data as preceding; 19.vii.1979; B. & C. Dasch; EMUSENT00000537, EMUSENT00000747, EMUSENT00000659, EMUSENT00000074

Distribution and biology. *Heterischnus huardi* is the most widely distributed North American *Heterischnus* species. It ranges from the eastern US and throughout Canada to western North America, where it extends north to Alaska, centrally south through the Rocky Mountains, and south along the Pacific Coast through the Sierra Nevada and outer California Coast Ranges. In the California Coast Ranges, it is associated with mixed hardwood forests in the north near Inverness and coastal woodland near Nojoqui Falls Park and Montecito in the south (Küchler 1978).

Bragg (1970) reared five *H. huardi* specimens from the plume moth, *Amblyptilia pica* (Walsingham) (Pterophoridae) on *Pelargonium* (Geraniaceae). Females oviposited into fourth instar prepupae (Bragg 1970). Additionally, two specimens from the CNCI were reared from pterophorids. The first was reared from a *Platyptilia* pupa collected from *Abies* (Pinaceae) in British Columbia. The second record was from an unidentified pterophorid pupa collected from *Salix* (Salicaceae) in Seebe, Alberta.

Comments. The color pattern of *H. huardi* varies throughout its range. The usual color pattern consists of a dark brown to black head, mesosoma, and metasoma, excluding white markings. Along the Pacific coast in Oregon and California, specimens exhibit varying degrees of brownish-red color on the mesonotum, scutellum, mesopleuron, and ventral division of the metapleuron.

Without stating any supporting evidence, Valemborg (2014) listed *Ischnopsidea alberta* Cushman and *Phaeogenes recticaudus* Provancher as subspecies of *H. huardi*. The elevation of these names from synonymy to subspecific status is unwarranted. There is no indication from the material examined in this study that any subspecies of *H. huardi* can be delimited.

The lectotype of *H. huardi* was not examined, although a specimen that was compared with the lectotype by Townes was examined.

***Heterischnus mexicanus* sp. nov.**

<http://zoobank.org/C665E98C-D2E7-4EDB-A6AF-181C26B1DB50>

Figs 10–12

Diagnosis. *Heterischnus mexicanus* sp. nov. can be distinguished from all congeners by a combination of the following: 1) flagellomeres 7/8–11/12 dorsally white in female;

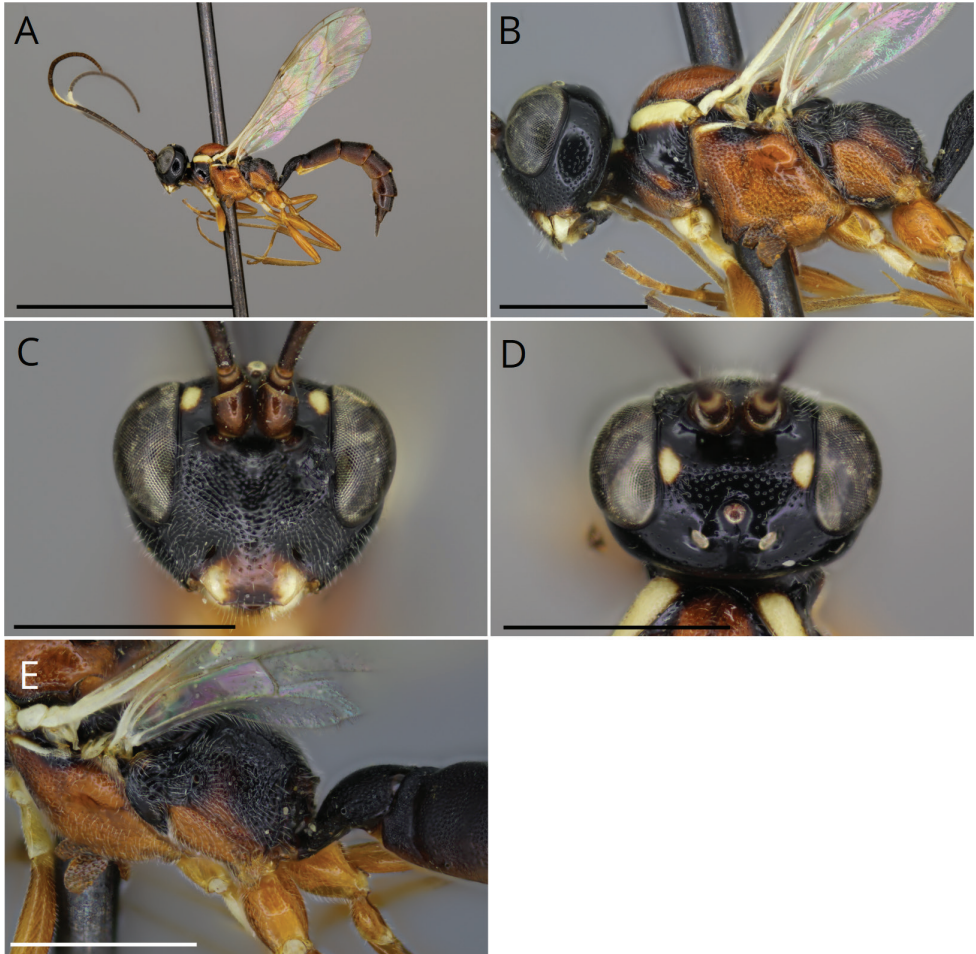


Figure 10. *Heterischmus mexicanus* sp. nov., holotype female **A** habitus **B** mesosoma, lateral view **C** head, frontal view **D** head, dorsal view **E** propodeum, dorsolateral view. Scale bars: 5.0 mm (**A**); 1.0 mm (**B–E**).

2) propodeum densely and coarsely punctate; and 3) longitudinal carinae of propodeum reduced or obsolete with at least lateral longitudinal carina posteriorly obsolete.

Description. Female (Fig. 10). Body length: 7.7–8.4mm; fore wing length: 4.4–4.5 mm.

Color. Head black, except following areas white: mandible except for brown apex, venterolateral corners of clypeus, and small ovoid adjacent to eye in supra-antennal area; clypeus varying from black to brownish-red; supraclypeal area brown in one specimen; flagellum brown, flagellomeres 7/8–11/12 with ventral surfaces white. Mesosoma overall brownish-red; anterior margin of pronotal collar, dorsal margin of lateral area of pronotum, subalar prominence, and tegula, white; following areas can be dark brown to fuscous: dorsal 0.5 of propleuron, more or less all of remaining non-white areas of pronotum, dorsal region of mesopleuron immediately below tegula, posterior margin of mesoscutum, metanotum, dorsal division of metapleuron, and propodeum.

Fore and middle legs with coxae, trochanters, and trochantelli white except for: basal 0.5–0.7 of coxae brownish-red ventrally; femora and tibia brownish-red; tarsomeres light brown to brown. Hind leg brownish-red except for: narrow white apical margin of trochanter; tibia dorsally with irregular light brown maculations; and brown tarsomeres. Metasoma varying from completely brown to dark brown, to having median section of T1, and lateral margins of remaining tergites, brownish-red and remaining areas dark brown. Wing: membrane clear; basal 0.2 of wing with veins white, remaining vein sections brown.

Head. Clypeus smooth, dorsally with fine punctures separated by 1.0–1.5× their diameter becoming less dense ventrally; ventral margin medially straight and with blunted or obsolete sublateral apices. Supraclypeal area rugulose-punctate with punctures separated by 0.5–1.2× their diameter becoming sparser laterally. Gena smooth, finely punctate with punctures separated by 0.5–1.5× their diameter. Malar space 1.5–1.8× basal mandibular width. Supra-antennal area smooth, coarsely punctate with punctures separated by 0.2–0.5× their diameter. Vertex smooth, with coarse punctures separated by 0.5–2.0× their diameter. Antenna with 31–33 flagellomeres.

Mesosoma. Mesonotum smooth with coarse punctures separated by 0.5–1.0× their diameter. Scutellum smooth, coarsely punctate with punctures separated by 0.5–1.0× their diameter. Mesopleuron coarsely punctate with punctures separated by 0.2–0.5× their diameter. Speculum smooth, punctation varying between impunctate to coarsely punctate dorsally. Ventral division of metapleuron coarsely punctate with punctures separated by 0.1–0.3× their diameter. Dorsal division of metapleuron varying from smooth to sparsely and finely punctate. Propodeum coarsely punctate with punctures separated by 0.1–0.3× their diameter. Posterior transverse carina and pleural carina present; lateral longitudinal carina absent; remainder of carinae reduced and varying from obsolete to subobsolete medially. Tarsal claws simple.

Metasoma. Postpetiole varying from punctate to granulate. T2 length 1.3–1.4× posterior width. T2–7 granulate with dense shallow, punctures becoming sparser and indistinct posteriorly. Gastrocoelus granulate. Thyridium distant from T2 anterior margin by 0.8–1.2× thyridial length.

Male (Fig. 11). Body length 7.0–7.3 mm; fore wing length: 3.9–4.4 mm. As in female, except for: UCDC specimen with small yellowish-white triangular mark between clypeus and ventral corner of eye; clypeus yellowish-white except dark brown ventral margin; apical 0.3 of hind tibia brown. In the Big Bend, Texas specimen hind tibia entirely brown.

Material examined. *Holotype*: MEXICO • ♀; Coahuila, 6 mi. west of Saltillo; 21.vii.1972; B. & C. Dasch; EMUSENT00000197.

Paratypes: MEXICO • 4♂; same collection data as holotype; 20–22.vii.1972; B. & C. Dasch; EMUSENT00000162, EMUSENT000000346, EMUSENT000000326, EMUSENT00000509 • 1♀; Puebla, 30 mi. SW of Tehuacán; 6800 ft; 12.x.1968; R. H., E. M. Painter; EMUSENT00000692. USA • 1♀; Arizona; Portal, 28.viii.1974; H. & M. Townes; EMUS0000273 • 1♀; same data as preceding; 6.ix.1987; EMUSENT00000272 • 1♂; Texas Big Bend; 5000 ft.; 10.viii.1975; S. & J. Peck; EMUSENT00000361 • 1♂, 1♀; Texas, Government Springs, Grapevine Hills, Big Bend Na-

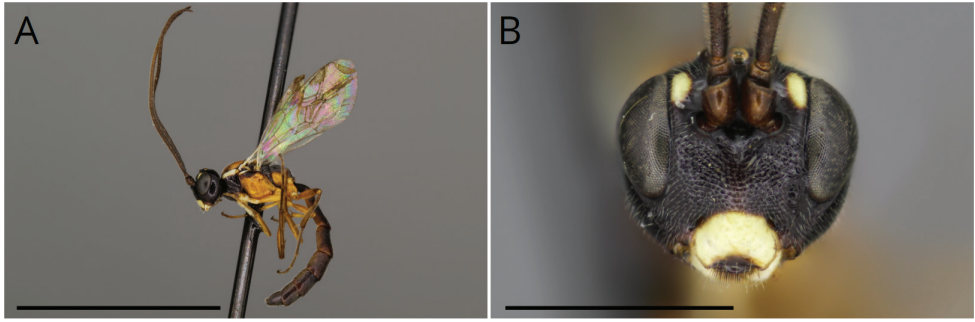


Figure 11. *Heterischnus mexicanus* sp. nov., paratype male (Mexico: Saltillo) **A** habitus **B** head, frontal view. Scale bars: 5.0 mm (**A**); 1.0 mm (**B**).



Figure 12. Distribution of *Heterischnus mexicanus* sp. nov.

tional Park; 5000 ft.; 1.ix.1971; E. E. Grissell & R. F. Denno; UCDC • 1♀; “Ex-chrysanthemum cut flws. fr. Mexico at El Paso”; 1.xi.1963; C. Overmiller; USNM.

Distribution and biology. *Heterischnus mexicanus* sp. nov. is the southernmost ranging *Heterischnus* species in the New World. Its range spans from the southern border of the USA in Arizona and Texas south to central Mexico in Tehuacán (Fig. 11). Records indicate that adults are active from late July to October and are likely active later in the year in the southern portion of its range as the latter date is from Tehuacán, Mexico. No host records are known for *H. mexicanus*.

Comments. As in *H. coloradensis* and *H. huardi*, a few specimens of *H. mexicanus* sp. nov. show an overall lighter coloration.

Etymology. This species epithet refers to its distribution, the majority of which is in Mexico.

Acknowledgments

I am thankful to Dr. Andrew Bennett (CNCI), Dr. Robert Kula (USNM), and Dr. Lynn Kimsey (UCDC) for providing valuable specimens and Dr. Michael Ivie for his assistance searching for specimens at the Montana State University insect collection. I'm also thankful to Dr. Gavin Broad, Dr. Andrew Bennett, and Davide Dal Pos for their helpful comments that greatly improved the manuscript. Finally, I am grateful to Dr. David Wahl for his encouragement and guidance throughout this research.

This research was supported by the Utah Agricultural Experiment Station, Utah State University, and approved as journal paper number 9466.

References

- Ashmead WH (1906) Descriptions of new Hymenoptera from Japan. *Proceedings of the United States National Museum* 30: 169–201. <https://doi.org/10.5479/si.00963801.30-1448.169>
- Aubert JF (1965) Ichneumonides d'Europe appartenant a dix espèces nouvelles et plusieurs genres nouveaux. *Bulletin de la Sociét Entomologique de Mulhouse*: 15–23.
- Bennett AMR, Cardinal S, Gauld ID, Wahl DB (2019) Phylogeny of the subfamilies of Ichneumonidae (Hymenoptera). *Journal of Hymenoptera Research* 71: 1–156. <https://doi.org/10.3897/jhr.71.32375>
- Bragg, DE (1970) Host records for the parasites *Diadegma acuta* and *Rhexidermus huardi* (Hymenoptera: Ichneumonidae). *Annals of the Entomological Society of America* 62(1): e339. <https://doi.org/10.1093/aesa/63.1.339>
- Cushman RA (1920) North American Ichneumon-flies, New and Described, with Taxonomic and Nomenclatorial Notes. *Proceedings of the United States National Museum* 58: 251–292. <https://doi.org/10.5479/si.00963801.58-2334.251>
- Cushman RA (1927) Miscellaneous notes and descriptions of ichneumon-flies. *Proceedings of the United States National Museum* 72: 1–22. <https://doi.org/10.5479/si.00963801.72-2709.1>
- Diller E (1981) Bemerkungen zur systematik der Phaeogenini mit einem vorläufigen catalog der gattungen (Hymenoptera, Ichneumonidae). *Entmofauna* 2: 93–111.
- Diller E (1995) Neues über Arten aus der Gattung *Heterischmus* Wesmael 1859 (Hymenoptera, Ichneumonidae, Ichneumoninae, Phaeogenini). *Linzer Biologische Beiträge* 27: 785–794.
- Diller E, Shaw MR (2014) Western Palaearctic Oedicephalini and Phaeogenini (Hymenoptera: Ichneumonidae, Ichneumoninae) in the National Museums of Scotland, with distributional data including 28 species new to Britain, rearing records, and descriptions of two new species of *Aethecerus* Wesmael and one of *Diadromus* Wesmael. *Entomologists's Gazette* 65: 109–129.
- Förster A (1869) Synopsis der Familien und Gattungen der Ichneumonien. *Verhandlungen des Naturhistorischen Vereins der Preussischen Rheinlande und Westfalens* 25: 135–221.
- Heinrich GH (1938) Les Ichneumonides de Madagascar. 3. Ichneumonidae–Ichneumoninae. *Mémoires l'Academie Malgache* 25: 1–138.

- Küchler AW (1978) The map of the natural vegetation of California. Department of Geography, University of Kansas, Lawrence, Kansas.
- Lungu-Constantineanu CS, Constantineanu R (2014) New data on ichneumonid hibernation (Hymenoptera: Ichneumonidae) in the Barnova forest massif (Iasi county, Romania). Romanian Journal of Biology 59(1): 11–16.
- Meyer NF (1934) Schlupfwespen die in Russland in den letzten Jahren aus Schädlingen gezogen sind. Zeitschrift für Angewandte Entomologie 20: 611–618. <https://doi.org/10.1111/j.1439-0418.1934.tb00385.x>
- Perkins JF (1959) Hymenoptera. Ichneumonoidea. Ichneumonidae, key to subfamilies and Ichneumoninae–I. Handbook for the Identification of British Insects 7(2a): 1–116.
- Provancher L (1875) Les Ichneumonides de Québec. Naturaliste Canadien 7: 263–274.
- Provancher L (1886) Additions et corrections au Volume II de la Faune Entomologique du Canada. Traitant des Hyménoptères. Québec, 495 pp.
- QGIS Development Team (2020) QGIS geographic information system. Open Source Geospatial Foundation Project. <http://qgis.osgeo.org>
- Rousse P, van Noort S, Diller E (2013) Revision of the Afrotropical Phaeogenini (Ichneumonidae, Ichneumoninae), with description of a new genus and twelve new species. ZooKeys 354: 1–85. <https://doi.org/10.3897/zookeys.354.5968>
- Rudow F (1917) Ichneumoniden und ihre Wirte. Entomologische Zeitschrift 31: 66–67.
- Santos BF, Wahl DB, Rousse P, Bennett AMR, Kula R, Brady S (2021) Phylogenomics of Ichneumoninae (Hymenoptera, Ichneumonidae) reveals pervasive morphological convergence and the shortcomings of previous classifications. Systematic Entomology 46: 704–724. <https://doi.org/10.1111/syen.12484>
- Sedivy J (1986) The hosts of Ichneumon flies in Europe (Hymenoptera, Ichneumonidae). Acta Entomologica Bohemoslovaca 83(1): 10–23.
- Selfa J, Diller E (1994) Illustrated key to the Western Palearctic genera of Phaeogenini (Hymenoptera, Ichneumonidae, Ichneumoninae). Entomofauna 15(20): 237–251.
- Selfa J, Diller E (1997) A new species of *Heterischmus* Wesm., 1859, from the Western Palearctic Region (Hymenoptera, Ichneumonidae, Ichneumoninae). Entomofauna 18: 469–476.
- Townes HK (1939) Corrections to the Gahan and Rohwer lectotypes of Provancher's Ichneumonidae (Hymenoptera). Canadian Entomologist 71: 91–95. <https://doi.org/10.4039/Ent7191-4>
- Townes HK (1944) A catalogue and reclassification of the Nearctic Ichneumonidae (Hymenoptera). Part 1. The subfamilies Ichneumoninae, Tryphoninae, Cryptinae, Phaeogeninae and Lissonotinae. Memoirs of the American Entomological Society 11: 1–477.
- Uchida T (1956) Neue oder bisher unbekannte Ichneumoniden aus Japan und seinen Umgebenden (I). Insecta Matsumurana 20: 57–76.
- Valemborg J (2014) Les *Heterischmus* Palearctiques (Hymenoptera: Ichneumonidae: Ichneumoninae: Phaeogenini: Heterischina). Clefs dichotomiques. Supplément au Bulletin de la Société Entomologique du Nord de la France 351: 1–44.
- Viereck HL (1914) Type species of the genera of Ichneumon flies. United State National Museum Bulletin No. 83, 186 pp. <https://doi.org/10.5479/si.03629236.83.1>

Wesmael C (1859) Remarques critiques sur diverses espèces d'Ichneumons de la collection de feu le Professor J.L.C. Gravenhorst, d'un court appendice Ichneumonologique. Memoires Couronnes Académie Royale Sciences Belgique 8: 1–99. <https://www.biodiversitylibrary.org/page/42580283>

Yu DSK, Achterberg C van, Horstmann K (2016) Taxapad 2016, Ichneumonoidea 2015. Database on flash-drive, Nepean. <http://www.taxapad.com>

Supplementary material I

Nearctic *Heterischmus* material examined

Author: Brandon Claridge

Data type: occurrences

Explanation note: The .csv file contains the material examined section in table format and follows the Darwin Core guidelines. This file is intended to help readers better use the material examined section and for uploading the occurrence data to GBIF.

Copyright notice: This dataset is made available under the Open Database License (<http://opendatacommons.org/licenses/odbl/1.0/>). The Open Database License (ODbL) is a license agreement intended to allow users to freely share, modify, and use this Dataset while maintaining this same freedom for others, provided that the original source and author(s) are credited.

Link: <https://doi.org/10.3897/jhr.85.67792.suppl1>

A Revision of *Cresson* Pate (Hymenoptera, Apoidea, Bembicidae) with the description of two new species

Laurence Packer¹

¹ *Department of Biology, York University, Toronto, Ontario, Canada*

Corresponding author: Laurence Packer (geodiscelis@mail.com)

Academic editor: Michael Ohl | Received 28 April 2021 | Accepted 16 June 2021 | Published 31 August 2021

<http://zoobank.org/17E5042F-F2F4-47F9-AC1A-6B5D54DF688F>

Citation: Packer L (2021) A Revision of *Cresson* Pate (Hymenoptera, Apoidea, Bembicidae) with the description of two new species. *Journal of Hymenoptera Research* 85: 81–117. <https://doi.org/10.3897/jhr.85.68023>

Abstract

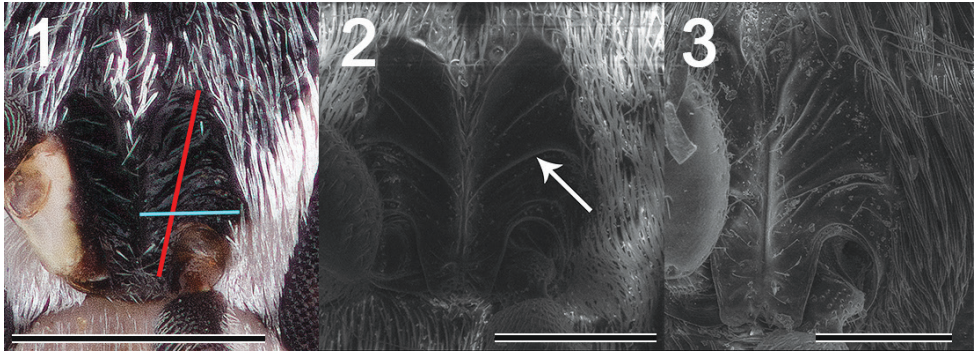
I describe two new species of the previously monotypic, Chilean endemic nyssonine genus *Cresson*: *C. mariastea* Packer, **sp. nov.** and *C. salitrera* Packer, **sp. nov.**, redescribe the type species *C. parvispinosus* (Reed) and provide an identification key for the three species. I clear up the confusion associated with the original type material of the latter species by designating a specimen from the type locality as the **lecto-type**. The new species extend the range of the genus northwards, one by over 1000 km. I suggest putative hosts for all three species, all of which are in the genera *Tachysphex* or *Parapiagetia*.

Keywords

Apoiid wasp, Chile, cleptoparasite, host association, identification key, taxonomy

Introduction

The nyssonine genera *Cresson* Pate, 1938, *Perisson* Pate, 1938 and *Antomartinezius* Fritz, 1955 contain one, one and three described species, respectively (Fritz 1973; Bohart and Menke 1976). Amarante (1993) noted a fourth, still undescribed, species of the latter genus. The last two of these genera were originally described as subgenera of *Cresson* but were raised to generic level by Fritz (1955) and Bohart and Menke (1976), respectively. Bohart and Menke (1976) noted both the superficial similar-



Figures 1–3. Supra-antennal areas of *C. parvispinosus* **1** standard light photomicrograph of male, red line indicates measurement of length of the area, the blue line indicates its width. Scale bar: 0.5 mm. **2** ESEM of female, the white arrow indicates the lamella. Scale bar: 300 μ m. **3** ESEM of another female showing different number of carinae to that in figure 2. Scale bar: 200 μ m.

ity among the five species of the three genera as well as putatively more substantive shared features such as the Y-shaped frontal crest (Figs 1–3) and double-edged posterior margins to the metasomal terga in both sexes (Fig. 4, yellow curly bracket) and the sternal setal fringes in males (Fig. 5). They (Bohart and Menke 1976) also noted the differences among these three taxa which they considered sufficient to support generic level status for all of them. These differences include *Cresson* and *Perisson* having arolia that are lacking in *Antomartinezzius*; *Perisson* and *Antomartinezzius* with lateral lobes to the sterna in both sexes (see Bohart and Menke, 1976, fig. 154) and two midtibial spurs in males, whereas *Cresson* has no lateral sternal lobes (Fig. 5) and but one midtibial spur in the male.

Antomartinezzius and *Perisson* are restricted to Argentina, although Amarante's (1993) undescribed species of the former was from NE of Brasilia. In contrast, *Cresson* is endemic to Chile, known from the central region of the country. Extensive trapping and net collecting of aculeate Hymenoptera by members of my laboratory in Chile over the past two decades has resulted in the discovery of two new species of *Cresson* and the purpose of this paper is to describe them, redescribe the type species: *C. parvispinosus* (Reed), designate a lectotype for the latter, provide an identification key and updated diagnosis and description for the genus and suggest likely hosts for all three.

Methods

Classification

I use the generic level classification of apoid wasps of Pulawski (2020), while considering the family level status of nyssonines as being in some flux: they would have been Crabronidae for most recent authors, but Sann et al. (2018) suggest that this family

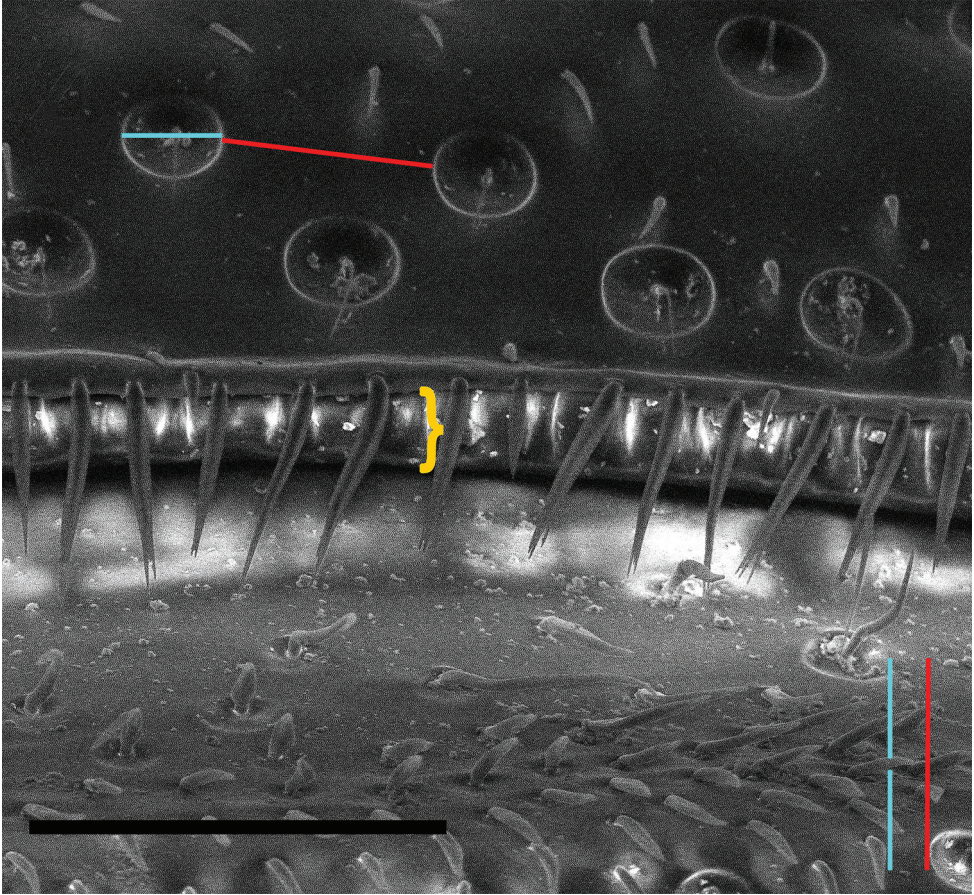


Figure 4. Apex of T1 and base of T2 of female *C. parvispinosus* to show measurement of puncture spacing (diameter (**d**) – blue line, interspace length (**i**) red line (here $i-2d$ as indicated to the bottom right) and the double-edged nature of the apex of the tergum, indicated by the yellow curly bracket. Scale bar: 100 μ m.

should be divided into additional families among which the nyssonines belong to the Bembicidae. The latter classification is followed here.

Collecting

Wasps were collected mostly in pan traps or deep cup traps (a deeper version of the standard pan trap – see Packer and Darla-West 2021; fig. 3.1d). The dimensions of the most commonly used of the latter are 84 mm in diameter at the mouth, 52 mm at the base and 110 mm in depth. They were partially dug into the ground (for -half their depth) and left out for varying durations, often for weeks. Blue vane traps (Stephen and Rao 2005; Kimoto et al. 2012; Packer and Darla-West 2021, fig. 3.1f) were employed at some sites, particularly in areas with very limited rainfall and difficult to access. Both trap types permit chronologically extensive sampling in areas where daily

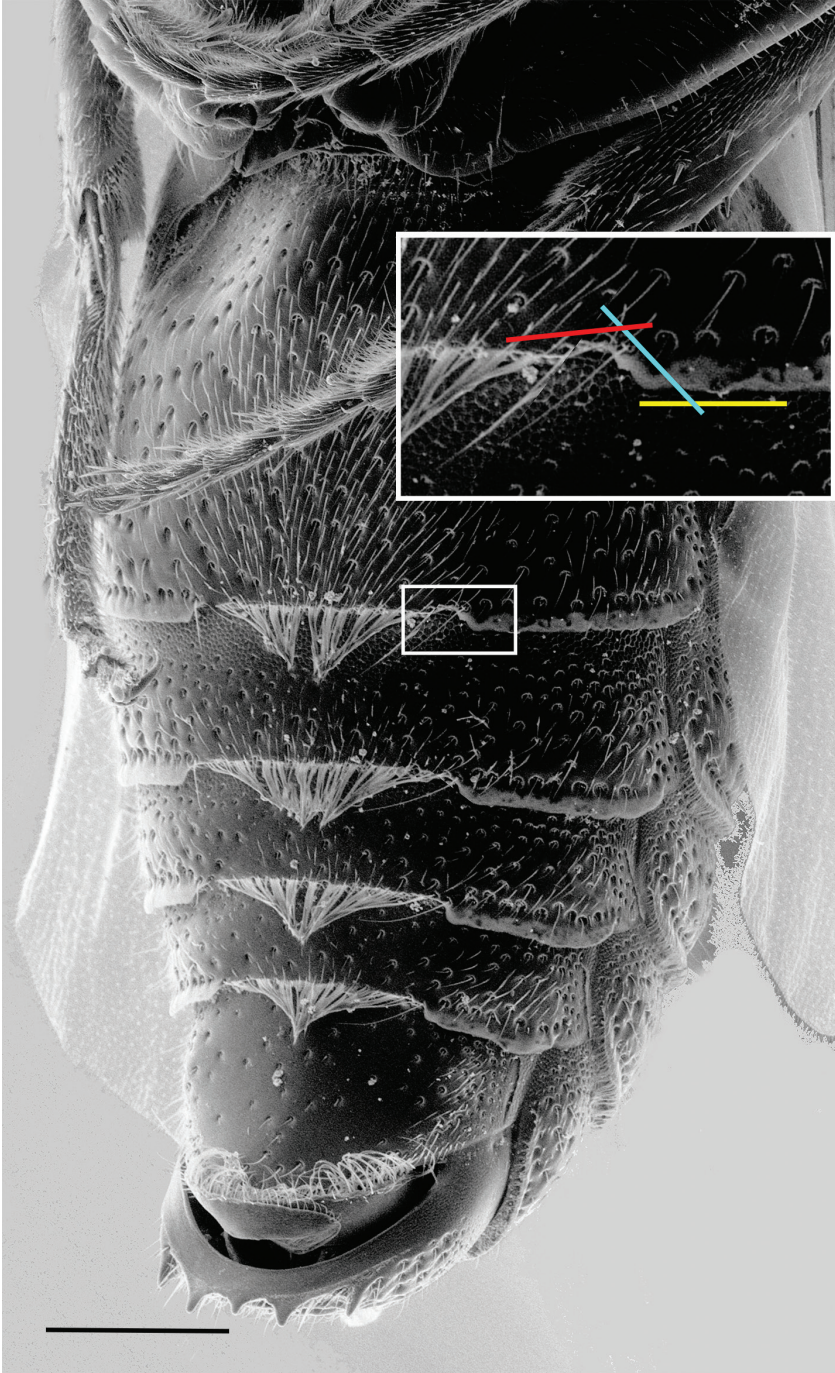


Figure 5. Oblique ventral view of metasoma of male *C. parvispinosus* to show apicomedial setal fringes situated within the medial gap in apical sternal depressions along with the angles formed at the margin of the gap (inset). The angle formed by the red and blue lines indicates the anterior angle, that formed by the blue and yellow lines the posterior angle. Scale bar: 0.5 mm.

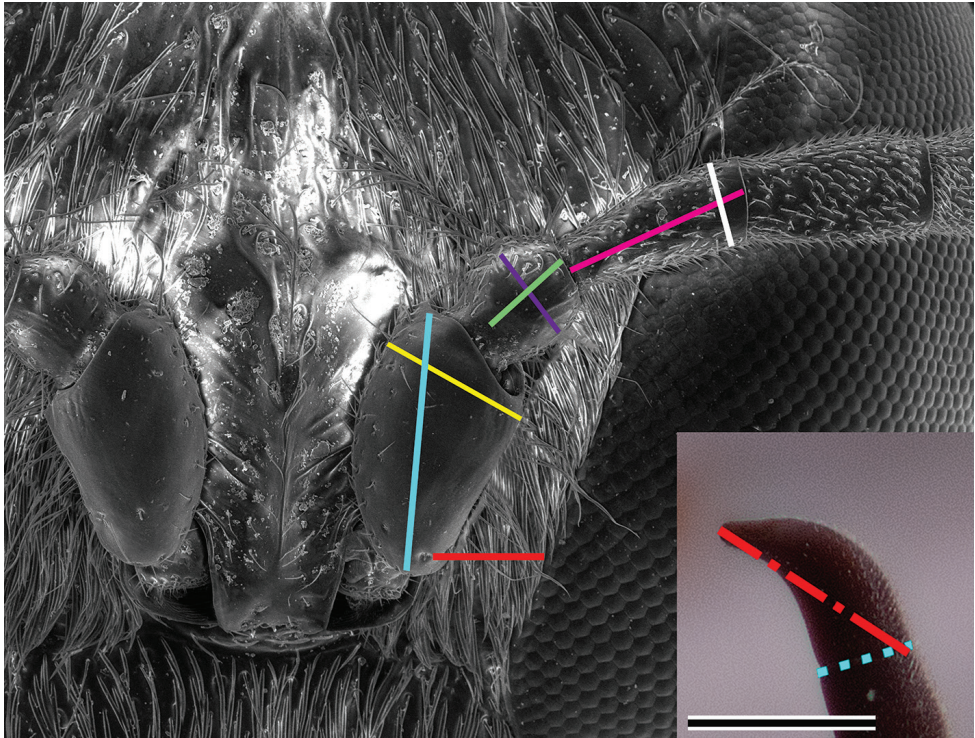


Figure 6. Part of face and parts of antenna of male *C. parvispinosus* to show landmarks used in some measurements. Red line: AOD; blue line: scape length; yellow line: scape width; green line: pedicel length (note only the swollen part contributes to this measurement); purple line: pedicel width; pink line: F1 length; white line: F1 width; inset red dashed line: F11 length; blue dashed line: F11 width. Scale bars: 0.25 mm.

catch rates are likely to be very low. Propylene glycol was used as the collecting fluid in both trap types due to its slow evaporation rate even under hot arid conditions.

Descriptions

Observations were made with a Leica MZ 12.5 microscope with 16× Leitz Wetzlar eyepiece lenses. Measurements were taken with an eyepiece graticule of unknown provenance. Lighting was from an AmScope LED-80-AM light source, except for surface sculpture features for which a Luminus PLY1223 energy saving bulb was used because of its superior ability to avoid bright reflection and to cast the light more evenly over the specimen.

I use a descriptive format and the morphological terminology that is consistent with our recent work (albeit on bees; e.g. Mir Sharifi and Packer 2018; Packer and Graham 2020) which incorporates some terms from Prentice's (1998) work on apoid wasps (such as vertexal area, apical sternal and tergal depressions) while otherwise largely agreeing with Michener (2007). Following the first three of those citations,

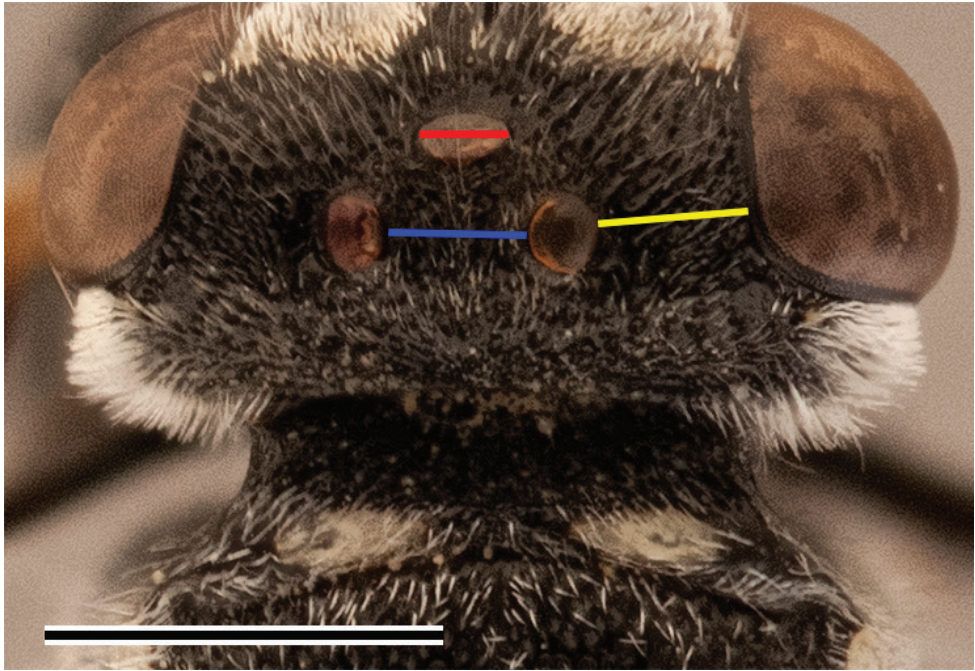


Figure 7. Top of head of female *C. salitreira*. Red line: MOD; blue line IOD; yellow line OOD. Scale bar: 1.0 mm.

based upon the findings of Brothers (1976), the term metapostnotum is used. Its dorsal surface is what has often been termed the propodeal triangle or propodeal enclosure in studies of apoïd wasps. On either side of the metapostnotum there is a densely setose area above the almost vertical lateral surface of the propodeum. I call this densely setose area the dorsolateral area of the propodeum. Surface sculpture terminology follows Harris (1976) except that stria and associated terms (striae, striate etc.) are taken to mean raised, rather than depressed linear features. For the newly designated lectotype of *C. parvispinosus*, some features could not be observed, being hidden behind other structures or damaged; such parts were described from a different specimen [Valparaiso, MCZ-ENT 00731886] and such data are given in square brackets.

The following acronyms are used: F, S and T followed by a number for flagellomeres, sterna and terga; AOD: transverse distance between outer margin of antennal socket and inner margin of compound eye (Fig. 6, red line); IOD: shortest distance between lateral ocelli (Fig. 7, blue line); LOD: distance between inner margin of compound eyes at posterior mandibular articulation in frontal view (Fig. 8, pale blue line); MINOD: minimum distance between compound eyes (Fig. 8, purple line); MOD: transverse diameter of median ocellus Fig. 7, red line); OOD: minimum distance between outer margin of lateral ocellus and compound eye (Fig. 7, yellow line); UOD: distance between inner margins of compound above in frontal view (Fig. 8, yellow line). Puncture spacing is given in terms of the distance between punctures (interspaces) and the diameter of nearby

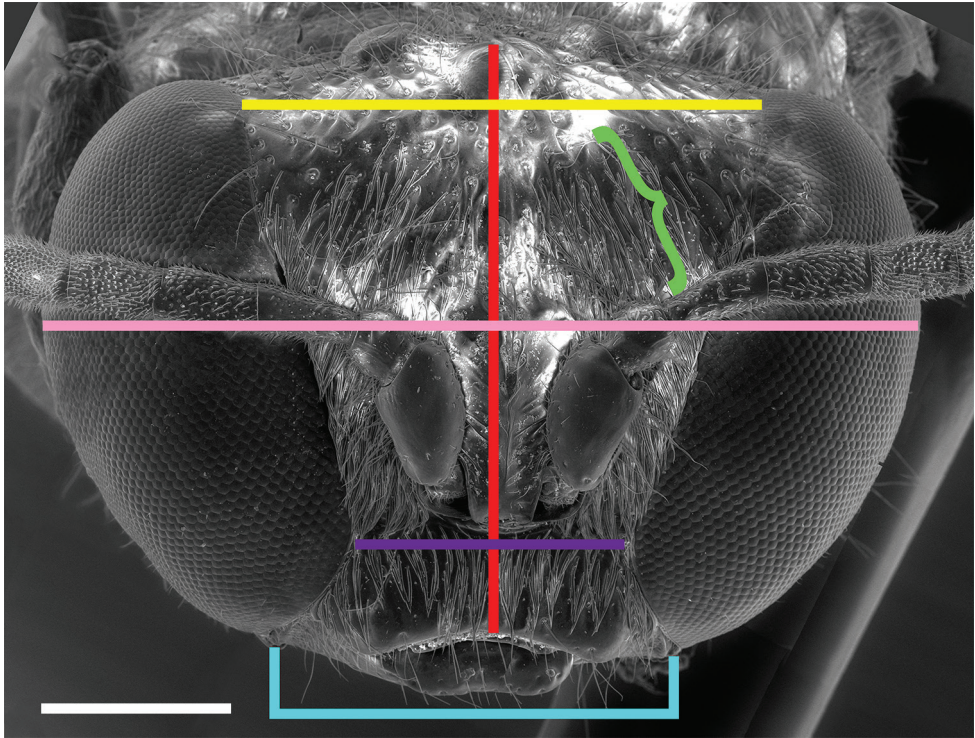


Figure 8. Face of *C. parvispinosus* to show landmarks used in some measurements. Red line: head length; pink line: head width; yellow line: UOD; purple line: MINOD; blue line: LOD; green curly bracket shows extent of frontal depression. Scale bar: 0.5 mm.

punctures, such that $i-2d$ indicates the interspaces (Fig. 4, red line) approximately two puncture diameters apart (Fig. 4, blue line), $i = 1-5d$ indicates irregular spacing of equal to one to five times the puncture diameters. Additional landmarks used in the definitions of some other head parameters are indicated in Figs 1, 6–8. Some measurement and other observations are made of the head “in frontal view”, this is defined as having both the apex of the clypeal lip and the top of the head in focus simultaneously. Two morphological terms are defined: 1) the supra-antennal area, which is defined by the medial and dorsolateral arms of the frontal crest, it is slightly concave, bears oblique carinae (usually with one developed into a lamella) and lacks setae (Figs 1–3); 2) the frontal depression a slightly concave area between the recurved arm of the frontal crest and the compound eye (Fig. 8, green curly bracket). Mesosomal measurement landmarks are shown in Fig. 9. Terminology for leg surfaces follows Aguiar and Gibson (2010).

Light microscopy images used a Visionary Digital BK Plus imaging system with a Canon EOS 5D digital SLR camera. Environmental scanning electron micrographs (ESEMs) were taken with a Thermofisher Quanta 3D FEG DualBeam microscope, no coating and both Low Vacuum and Gaseous Sensory Electron Detectors. Images were processed with Adobe Photoshop CS6.

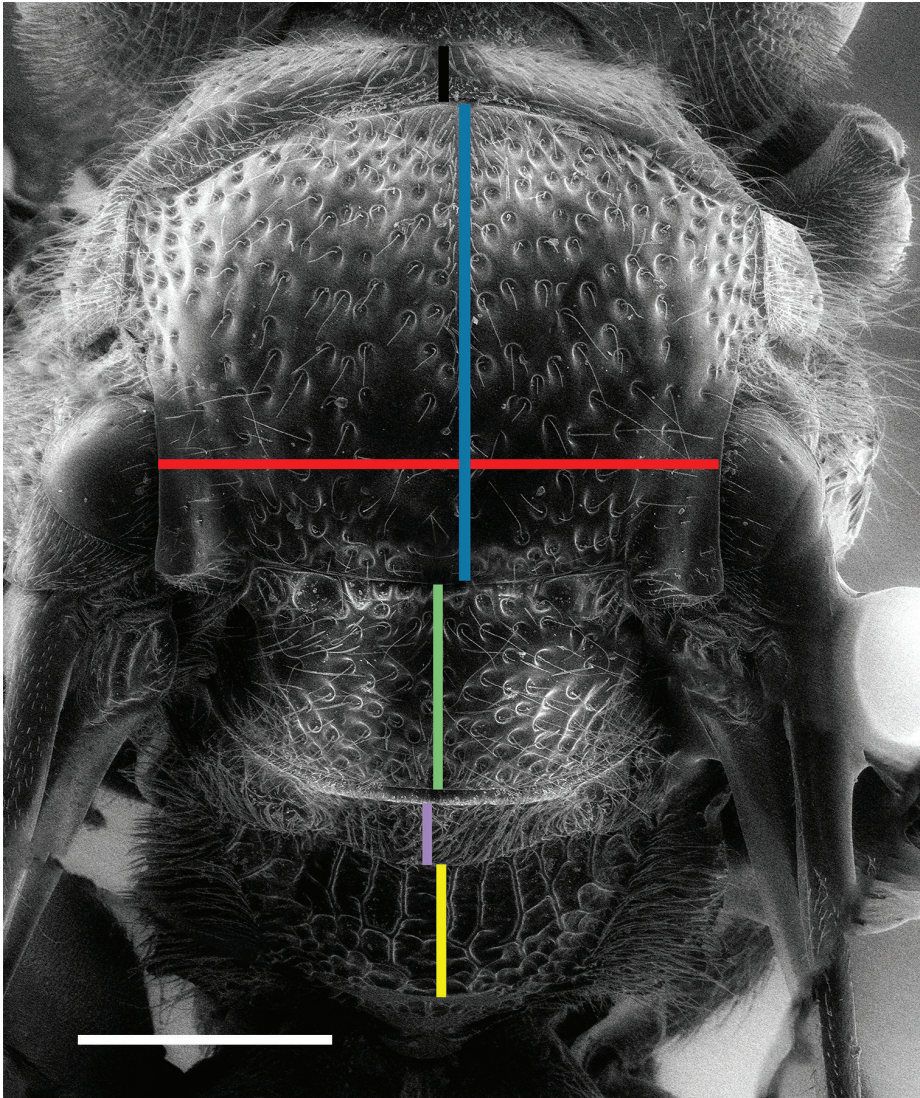


Figure 9. Dorsal view of mesosoma of *C. parvispinosus* to show landmarks for some measurements. Black line: length of pronotal collar; blue line: length of mesoscutum; red line: ITW; green line: length of scutellum; purple line length of metanotum; yellow line: length of dorsal surface of metapostnotum (note that the latter is taken from the metanotal-metapostnotal suture to the transverse carina closest to the change in angulation from approximately horizontal to approximately vertical surfaces of the metapostnotum). Scale bar: 0.5 mm.

Geography

Chile is divided into Regions which receive both a Roman numeral (except for the area around Santiago – Region Metropolitana) as well as a name. We use the Roman numerals for regions where we have collected and when such data can be gleaned from

the information provided on labels affixed to material collected by others. In instances of the latter, the region is given in square brackets and the label data are as given but re-organized to follow a standardized format. Coordinates are given in decimal degrees to three decimal places when known with that level of precision. Coordinates estimated from collection locality names are given in square brackets at a lower level of accuracy. The map was prepared using SimpleMapp (Shorthouse 2010).

Institutional abbreviations

- AMNH** American Museum of Natural History, New York, New York, United States of America
CAS California Academy of Sciences, San Francisco, California, United States of America
CUIC Cornell University Insect Collection, Ithaca, New York, United States of America
MNHN Museo Nacional de Historia Natural, Santiago, Chile
MCZ Museum of Comparative Zoology, Harvard University, Cambridge, Massachusetts, United States of America
PCYU Packer Collection at York University, Toronto, Ontario, Canada
UCDC R.M. Bohart Museum of Entomology, Davis, California, United States of America
ZMHB Museum für Naturkunde der Humboldt-Universität, Berlin, Germany.

Results

Taxonomy

Cresson Pate, 1938

Cressonius Bradley, 1956: 257. Unnecessary emendation.

Type species. *Nysson parvispinosus* Reed, 1894: 641, by original designation and monotypy.

Diagnosis. *Cresson* can be separated from other South American nyssonine wasps by the combination of i) metatibia lacking teeth, with bristles that clearly arise from an articulation in a socket; ii) metasomal sterna lacking lateral lobes as opposed to lobes present (compare Fig. 5 herein with fig. 154 in Bohart and Menke 1976); iii) metasomal terga with posterior margins thickened and appearing double-edged (Fig. 4, yellow curly bracket) versus simple and iv) a Y-shaped crest on the lower frontal area with the apices of the paired arms recurved (Figs 1–3). Feature i) separates *Cresson* from *Idionysson* Pate, 1940, *Metanysson* Ashmead, 1899, *Neonysson* Bohart, 1968, and *Zanysson* Rohwer, 1914, ii) separates it from both *Antomartinezius* and *Perisson*, iii) separates it from *Losada* Pate, 1940 and *Nysson* and iv) from *Epinysson* Pate, 1935, *Foxia* Ashmead, 1898 and all aforementioned genera except *Antomartinezius* and *Perisson*.

Description. Colouration: Black with white to cream coloured markings on face, pronotal collar (rarely absent), pronotal lobe, scutellum (rarely absent), legs, subapical bands on most terga, sometimes on sterna; red markings on metasoma absent to extensive. Both sexes with labrum and base of mandible pale, female with clypeus pale laterally, black medially, male clypeus entirely pale except lip orange-brown.

Pubescence: Silvery appressed to subappressed setae extensive on face, genal area, dorsal surface of pronotum, most of mesopleuron (sparser anteriorly and ventrally, absent posteriorly), posterolaterally on scutellum, metanotum, dorsolateral area of propodeum and sometimes on T1, setae of scutellum and metanotum anteriorly or anterolaterally oriented; fine erect setae longer on upper part of face, shorter on mesoscutum and mesopleuron, vertically oriented dense row of short setae occupying space between extreme apical margin of terga and base of succeeding tergum, metasomal sterna with scattered longer erect setae; male with median setal fringes on S2–S5 situated in a gap in the apical sternal depressions, lateralmost fringe setae longest, posteromedially oriented but sparser than more posteriorly oriented remaining fringe setae.

Surface sculpture: Microsculpture largely absent, integument shiny, punctures bimodal in size on face and mesoscutum, minute punctures sparsely scattered among interspaces between larger mostly dense punctures; larger punctures especially on face and mesoscutum with minute punctures at their bottoms and often with several punctures aggregated in groups with edges raised, sometimes giving somewhat striate appearance; minute punctures more numerous on metasomal terga and sterna among distinct larger punctures; junctions between mesoscutum and scutellum and between meso- and metapleuron foveate, the latter finely so; lateral surface of pronotum and posterodorsal part of lateral surface of propodeum obliquely costate; posterior portion of mesopleuron, metapleuron and rest of lateral surface of propodeum generally lacking sculpture, glassy smooth; posterior surface of propodeum coarsely sculptured; metapostnotum rugoso-striate dorsally. Portion of metasomal terga posterior to graduli (usually hidden beneath preceding tergum) imbricate, dull; sterna with similar imbricate areas more extensive. Metasomal terga and sterna with most punctures separated by distance greater than their diameters, except last metasomal tergum with coarse, irregularly shaped, almost crowded punctures; last visible sternum with small, scattered punctures; apical impressed tergal and sternal depressions with row of punctures at their base.

Structure: Head 1.3–1.5 × wider than long; labrum short, transverse, apical margin slightly concave to transverse medially; clypeus short, apicomediaally concave with pronounced bevelled edge, lip approximately half as wide as clypeus; supraclypeal area small, sometimes hidden beneath ventral expansion of frontal crest, crest Y-shaped, ventral margin of crest swollen with angulate ventral incision, in frontal view crest obscures the medial margin of the antennal socket lateroventrally, medially the crest is conspicuously developed, almost lamellate, dorsal arms less developed, recurved, space between median lamella and entire recurved arm with one dorsolaterally oriented lamella and varying number of subparallel carinae; space between lateral margin of supra-antennal area and compound eye with frontal depression extending upwards for a variable distance below lower tangent of median ocellus, dorsal margin of depres-

sion often ill defined; inner margin of compound eyes markedly convergent below, shortest distance between them at base of clypeus; occipital and hypostomal carinae complete, lamellate. Scape longer than wide, slightly produced basoventrally, integument somewhat translucent for apicoventral one-third of length; pedicel with medial surface globose, conspicuously narrowed towards base, lateral surface straighter; male apical flagellomere falcate, concave below narrowing to acute apex. Pronotum with vertical carina that in dorsal view appears as a tooth, pronotal collar in dorsal view transverse anteromedially, convex anterolaterally; in profile gradually rounded onto anterior declivitous surface except abruptly and angulately so medially. Mesoscutum posterolaterally markedly reflexed upward, projecting over medial margin of tegula. Lateral propodeal spine conspicuous, acute. Mesotibia of male with one apical spine, mesobasitarsus of male with ventral setal fringe; female lacking rake spines on protarsus; metatibia slightly concave apicodorsally, extreme apex angulate dorsally, lacking robust spines or teeth; arolia in both sexes small. Three submarginal cells, second cell petiolate; stigma subequal in size to prestigma; hindwing media diverging beyond cu-a by more than twice the length of the latter; jugal lobe somewhat larger than tegula. Metasomal terga posterior margins double-edged. T2 transversely depressed anteriorly. Apical tergum of both sexes with apicolateral margin spinose; in females, the medial pair longer than others, in males the single median spine is short. S2 swollen anteromedially and depressed anterolaterally. Metasomal sterna not extended laterally as lobes, male S2–S5 with apical sternal depression abruptly absent medially, this area in female sometimes slightly concave.

Cresson parvispinosus (Reed)

Figures 1–6, 8–21, 34

Nysson parvispinosus Reed, 1894:641, ♀ Lectotype (here designated): ♀, Chile, Colchagua Province; no specific locality (MCZ); Dalla Torre 1897: 573, catalog; Pate 1938: 155, description of genus; Maidl and Klima 1939: 149, catalog; Fritz 1955: 14, redefinition of genus; Bohart and Menke 1976: 476, generic key, diagnosis, range, systematic position, checklist; Sielfeld 1980: 74, catalog; Amarante 2002: 20, catalog; Chiappa 2012: 9, catalog.

Material examined. 55 ♀, 47 ♂: **Lectotype** ♀; CHILE, Colchagua Province [Region VI]; 1890; E.C. Reed; MCZ-ENT-17200; Additional material: 1 ♂; • CHILE [Region IX], 20 km E. of Temuco; [-38.7 – 72.35]; 7.i.1951; Ross and Michelbacher; CAS; • 1 ♀; [Region VII] Curicó Prov., Fundo La Montaña, Estero La Palma at Rio Teno, 6 km E. of Los Queñes; [-35.00 – 70.75]; 4.i.1967; M.E. Irwin; CAS; • 1 ♀; Valparaiso Province [Region V], Valparaiso; [-33 – 71.5]; 26.xi.1919; P. Herbst; MCZ; MCZ-ENT 00731885; • 1 ♀; identical data as previous; CAS; • 1 ♀; identical data as previous; 12.i.1921; MCZ (MCZ-ENT 00731886); • 2 ♀, 3 ♂; identical data to MCZ-ENT 00721886; CAS; • 1 ♀; Valparaiso [Region V], Concon; [-32.9 – 71.5];

74.xii.1910; P. Herbst; MCZ; MCZ-ENT 00731884; • 1 ♂; identical data to MCZ-ENT 00731884; CAS; • 1 ♂; [Region V], Rio Blanco; 7.xii.1917; P. Herbst; CAS; • 1 ♀; Valparaiso Province, [Region V] Olmué; [-33.0 – 71.2]; 4.ii.1920; P. Herbst; MCZ; MCZ-ENT 00731883; • 1 ♂ (dissection code 65-xi-250); [Region V] Perales, Quilpué; [-33.05 – 71.4]; 4.ii.1925; P. Herbst; CAS; • 1 ♀; Valparaiso Province [Region V]; Marga-Marga; 9.i.1919; P. Herbst; MCZ; MCZ-ENT 00731880; • 1 ♂; Santiago Province [Region Metropolitana], Cerros de Tiltil; [-33.1 – 70.9]; 18.i.1919; P. Herbst; MCZ; MCZ-ENT 00731881; • 1 ♂ identical data as previous; 2000m; i.1920; MCZ; MCZ-ENT 00731882; • 1 ♂ (“homotype” A.R. Menke); [Region V], Valparaiso; 19.i.1921; P. Herbst; UCDC; • 1 ♀; [Region V], Altos de Lliu Lliu; [-33.1 – 70.9]; 20.i.1919; P. Herbst; UCDC; • 1 ♂; [Region Metropolitana], Santiago; 1922; F. Jaffuel; UCDC; • 1 ♀; [Region Metropolitana], Santiago, Maipu, Quebrada de La Plata; 26.xii.1966; L. Stange; UCDC; • 1 ♀; [Region IV], 10 km E. of Fray Jorge Nat[ional] P[ark]; [-30.6 -71.6]; 28.xii.1966; dry wash; M.E. Irwin; CAS; • 2 ♂, 1 ♀; Region IV, El Pangue; -30.164 -70.664; 1700m; A Ugarte; PCYU; • 33 ♂, 40 ♀; Region III, 13.5 km W. of Los Sapos; -28.019 -70.554; 500m; 22–25.x.2010; pan traps; L. Packer; CAS, MNHN, PCYU, UCDC and ZMBH; • 1♂; Region III, Rd. to Pastos Largos; -28.164 -69.791; 2100m; 6.xi.–11.xii.2013; S. Monckton and J. Postlethwaite; pan trap; PCYU; • 1 ♀; CHILE; UCDC.

Diagnosis. The type species of the genus can be differentiated from the new species most easily by the more extensive red colouration of the metasoma in both sexes with T1–T2 entirely red (except for the extreme anterior margin and one male has a small posteromedial dark mark on T2) (Figs 12–14). Females usually also have T3 entirely red. The other species have T1 and T2 black at least medially, although T1 is usually almost entirely black (see Figs 24, 31). The pronotal collar is relatively longer, at least two-thirds as long as MOD, whereas in the two other species it is approximately ½ as long as MOD (compare Figs 34 and 35).

Redescription. Lectotype Female (Fig. 10)

Dimensions: Body length 6.1 mm, head width 2.05 mm, forewing length 4.4 mm, ITW 1.15 mm.

Colouration: Black except as follows: cream to pale yellow on labrum, basal half of mandible (rest orange to red-brown), clypeus lateral one-third (entire apical bevelled region and lip orange-brown), small semicircular-triangular mark on upper paraocular area adjacent to compound eye, small spot on genal area above adjacent to compound eye; large lateral marks on pronotal collar almost twice as wide as the space that separates them, pronotal lobe, lateral spot on scutellum, narrow oblique mark in front of mesocoxa, small apicolateral mark on meso- and metacoxae, apicoventral two-thirds of profemur, narrow stripe on anterior surface of pro- and mesotibiae (suffused with orange on protibia), narrow dorsal stripe on metatibia (rest of legs dark brown, except metatibia posterior surface and all tarsi orange to orange-brown), medially interrupted narrow subapical bands on T1–T5. Most of ventral surface of scape yellow brown. Following parts orange-red: T1 and T2, T3 laterally; S1 and S2 (both suffused with red-brown medially), S3 narrowly subapically, S4 narrowly apicolaterally. Apical tergal and sternal depressions pale translucent brown to straw; T6 teeth pale brown.



Figures 10–11. *Cresson parvispinosus* specimens used in the redescription of the species **10** lectotype female **11** male from Cerros de Tiltit (MCZ–ENT 00731881). Scale bars: 1.0 mm.

Pubescence: [described from female from Valparaiso, MCZ–ENT 00731886]: Silver, appressed, obscuring integument only on lower paraocular area, genal area close to compound eye, most of mesopleuron and dorsolateral area of propodeum; sparser



Figures 12–14. Metasomas of *C. parvispinosus* to show variation in colour **12** male with T1–T2 red **13** female with T1–T3 and sides of T4 red **14** female with T1–T2 and sides of T3 red. Scale bars: 1.0 mm.

on clypeus, sparser and suberect on genal area posteriorly. Face with erect to suberect pale setae < 1.2 MOD, those of lower frontal area curved ventrally; pronotal collar and mesoscutum anteriorly with sparse, posteriorly oriented appressed setae; mesoscutum, scutellum, metanotum and mesopleuron with sparse erect setae $< \text{MOD}$. Metasomal terga and sterna with sparse short subappressed posteriorly oriented setae ≤ 0.4 MOD; suberect setae intermixed on terga < 0.5 MOD, these longer and denser on more posterior sterna, $< \text{MOD}$ on S6.]

Surface sculpture [described from female from Valparaiso MCZ-ENT 00731886: Head, mesoscutum and mesoscutellum with minute punctures scattered in interspaces among large dense (mostly $i \leq d$) areolate-punctate background; frontal area punctures denser, in rows with interspaces almost absent; upper paraocular area punctures smaller, irregularly spaced $i < d$; vertexal area punctate-reticulate; genal area with small punctures dense $i < d$ sparser below, larger punctures scattered. Mesoscutum densely punctate $i \leq d$ except for a few larger interspaces posteriorly on disc, scutellum densely punctate $i < d$ except punctures sparse on pale lateral portion. Mesopleural punctures coarse $i < d$ except posterior glabrous portion with few scattered punctures restricted to ventral half and a subvertical row anterior to meso-metapleural suture; metapleuron with few short horizontal carinae posterodorsally; side of propodeum posterodorsally with irregularly sized shallow punctures among costae; metapostnotum horizontal portion longitudinally carinate-rugose with numerous faint transverse striae between carinae, areolate posterodorsally. Metasomal terga doubly punctate, minute punctures abundant; large coarse punctures dense $i \leq 2d$ on T1, $i \leq 4d$ on T2; T3–T6 punctures increasingly dense, $i < 1.5d$ on T5, T6 areolate-punctate; S2 minute punctures sparse and obscure, larger punctures $i = 0.5\text{--}2d$; S3–S5 minute punctures distinct, larger punctures mostly $i \leq 1.5d$; S6 $i < d$ somewhat sparser along midline.]

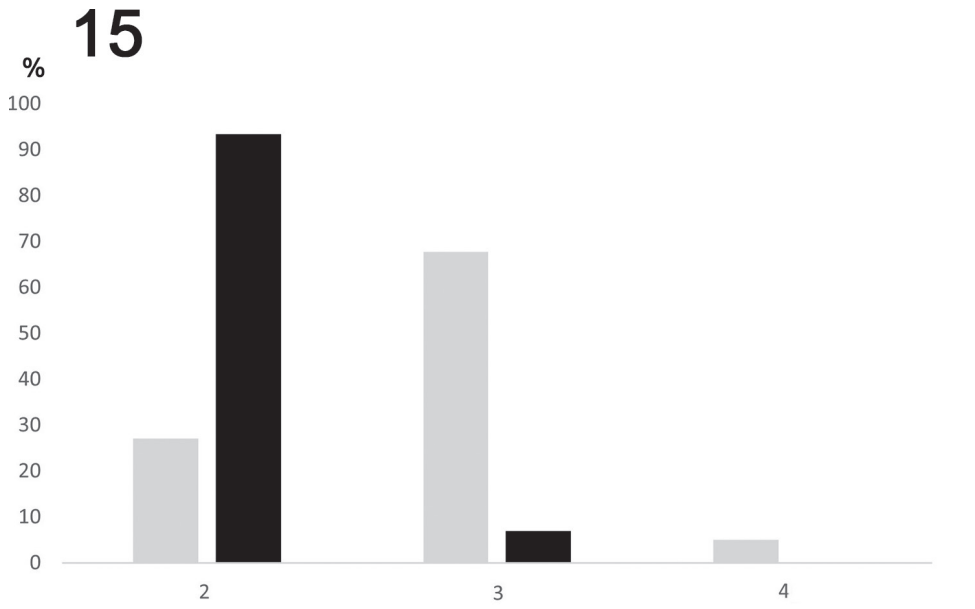
Structure. Head $\sim 1.3 \times$ as wide as long, 83:60; [labrum transverse, narrowly oval, $\sim 3 \times$ as wide as medial length, W:L 41:14, aboral surface somewhat and apical margin conspicuously concave;] clypeus more than $2.5 \times$ as wide as medial length, 63:24, lip \sim half as wide as maximum width of clypeus 32:64; supraclypeal area median length one-quarter that of clypeus, 6; AOD $1.5 \times$ maximum width of F1 (18:12); supra-antennal area with a complete somewhat dorsolaterally oriented lamella at lower third and several similarly oriented carinae above it and a few smaller ones below, area longer than maximum width 35:26, shorter than scape 37; frontal depression continuing above to somewhat below lower tangent of median ocellus; inner margin of compound eyes markedly convergent below UOD:LOD:MINOD 64:45:33; IOD = OOD; scape less than twice as long as greatest width (37:20); pedicel length = width; F1 $\sim 2 \times$ as long as greatest width 25:12; F2 $\sim 1.5 \times$ as long as greatest width 24:14, [remaining flagellomeres longer than wide, decreasing in length from F3 to F9, F10 longer L:W 22:16]; pronotal collar shorter medially than MOD, 15:19; [admedian line more than half medial length of mesoscutum], scutellum not depressed medially but with large posteromedial pit; length of scutellum:metanotum:metapostnotum 40:18:23. T6 somewhat triangular, sides slightly less than right angular to each other, with five teeth on each side, two apicomedial teeth the longest with length and basal width subequal, separated by somewhat more than their length. S2–S4 apical sternal depressions < 0.25 MOD, narrower medially, absent medially on S5.

Male: based upon the specimen from Cerros de Tiltit (MCZ-ENT 00731881), this specimen bears a minute red label devoid of script. (Fig. 11).

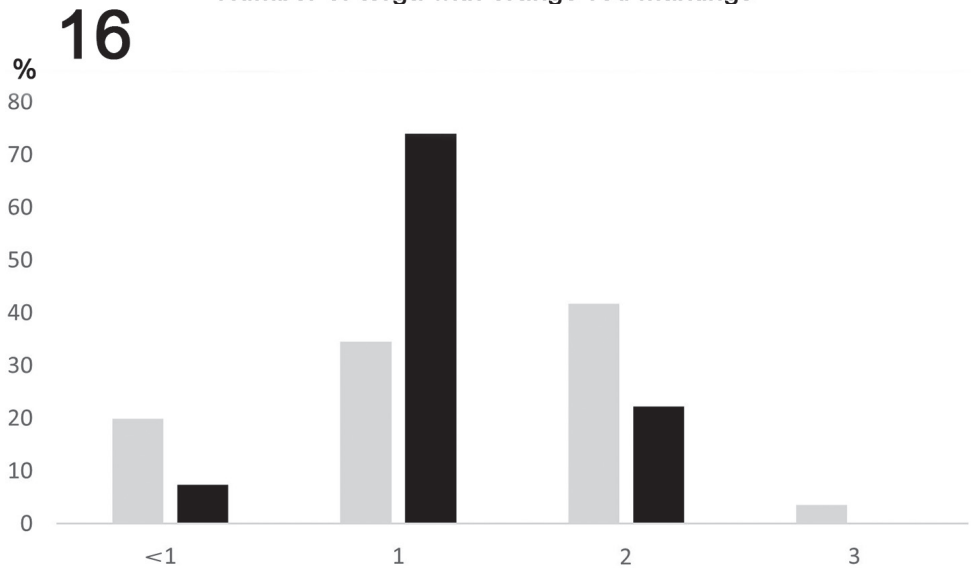
Dimensions Body length 4.93 mm, head width 1.47 mm, forewing length 3.45 mm, ITW 0.8 mm.

Colouration: Black except as follows: cream to pale yellow on basal two-thirds of mandible (rest orange to red-brown), clypeus (except lip orange-brown), supra-clypeal area, lower paraocular area mark narrowly extending along inner eye margin to 1 MOD below lower tangent of median ocellus, small spot on genal area above adjacent to compound eye, ventral half of scape, small spot on pedicel, large lateral marks on pronotal collar twice as wide as space that separates them, pronotal lobe (margined with orange-brown dorsally), large lateral spot on scutellum, most of propodeal spine, mark in front of mesocoxa as large as ventral surface of mesocoxa, most of ventral surfaces of all coxae, most of ventral surface of profemur, dorsal surface of pro- and mesotibiae extending onto posterior surfaces apically, narrow ventral stripe on apical half of mesofemur, most of anterior surface of metatibia, anterior surfaces of all basitarsi (rest of metatibia and maining tarsomeres orange to pale orange-brown), medially interrupted narrow subapical bands on T1–T6, most widely separated on T2 and most narrowly on T6. Following parts orange-red: T1 and T2, T3 apicolaterally; S2 (suffused with red-brown medially), S3–S5 subapical markings increasingly narrow on more apical sterna. Apical tergal and sternal depressions pale translucent orange-brown.

Pubescence: As in female except for S2–S5 with dense apicomedial setal fringes, setae long, medially 0.75 MOD.



Number of terga with orange-red markings



Number of sterna with extensive orange-red markings

Figure 15–16. Frequency histograms of different colour patterns of *C. parvispinosus* **15** for metasomal terga **16** for metasomal sterna. Females in grey, males in black.

Surface sculpture: As in female except as follows: micropunctures almost absent on face and mesoscutum; upper paraocular area more sparsely punctate i > d; vertexal area punctures variable in size; lateral surface of propodeum punctures among carinae deeper.

Structure. Head $\sim 1.3 \times$ as wide as long, 81:60; labrum transverse, narrowly oval, less than $2.5 \times$ as wide as medial length, W:L 37:16, apical margin somewhat concave medially; clypeus $\sim 2.5 \times$ as wide as medial length, 69:27, lip almost half as wide as whole clypeus, 33:69; supraclypeal area minute, median length one-quarter as long as clypeus 7:27; AOD equal to maximum width of F1; supra-antennal area much longer than maximum width 31:18, shorter than scape 34; frontal depression poorly demarcated above; UOD:LOD:MINOD 60:40: 29; IOD greater than OOD 28:23; scape almost twice as long as greatest width 34:18; pedicel length subequal to width; F1 more than twice as long as greatest width 23:10; F2 less than twice as long as greatest width 20:12, remaining flagellomeres longer than wide, increasingly shorter from F3 to F10, F11 L:W 18:11, F11 somewhat falcate, ventral surface markedly concave. Pronotal collar shorter medially than MOD, 13:19; [admedian line more than half medial length of mesoscutum], scutellum narrowly impressed medially, with large posteromedial pit; length of scutellum:metanotum:metapostnotum 35:14:18. T7 somewhat semicircular with five apical teeth, median one shortest, submedian ones longest. Apical sternal depressions short; anterior angle of all medial interruptions of apical sternal depressions acute, posterior angles obtuse, less markedly so on more posterior sterna.

Variation. In both sexes there is variation in the colour of the propodeal spine, ranging from mostly semi-translucent white through cream to partially or entirely black. The extent of the pale subapical cream bands on the metasomal terga also varies: on T1 and T4 in females, T1 and T5 in males, the band may be interrupted medially or entire, it is always interrupted on T2–T3 in females and T2–T4 in males but may also be entire on T5 in females and T6 in males. The number of metasomal terga and sterna that are orange-red varies (Figs 12–16). For terga, both sexes always have T1 and T2 orange, both sexes sometimes have T3 entirely orange, but only in females does this sometimes extend to the entirety of T4. For the sterna, S2 is sometimes not entirely orange in both sexes, females sometimes have S2–S4 entirely orange, though in males only S2–S3 may be entirely orange (Fig. 16). Figures 15 and 16 show the relative frequency of the number of terga or sterna that are red separately for males and females. Clearly females, on average, have more extensive orange markings.

The frontal depressions are often almost obscured by silvery setae and vary somewhat in extent sometimes reduced such that their dorsal margin is 1 MOD below the lower tangent of the medial ocellus. The mesoscutal punctation varies from being fairly uniformly dense $i < 0.5d$, to having quite a few interspaces at least as wide as the adjacent punctures especially on the posterior third.

In males: 1) The supraclypeal area varies from entirely whitish to entirely black with intermediate conditions of brown or dappled pale and dark (Figs 17–19). 2) There is variation in the extent of pale colouration on the antenna, pronotum and scutellum. Some individuals have pale spots on the ventral surface of the pedicel and F1 and F2, while others have these lacking or restricted to the pedicel. The colour of these markings also varies from pale cream to orange-brown. The markings on the pronotum and scutellum, while always present, vary somewhat in size.



Figures 17–19. Heads of male *C. parvispinosus* to show variation in colour of supraclypeal area **17** area entirely white **18** area entirely black **19** area dappled with asymmetrical white mark (white arrow). Scale bars: 1.0 mm.

In females the extent of the pale marking along the inner margin of the compound eye is variable: it is subequal in length to MOD in the lectotype but may extend more narrowly to below the upper tangent of the supra-antennal area. There is minor variation in the extent of yellow-brown on the scape and of pale colouration on the clypeus, pronotum and scutellum.

Two males (MCZ-ENT 00731882) have an additional cross-vein towards the apex of the second discoidal cell. This can be seen in figure 11 as forming a wishbone shaped outline that is almost a mirror image of the second submarginal cell on either side of the median vein. In the second specimen the additional cell is much smaller. There is variation in the size of the second submarginal cell such that the petiole can be almost absent to extending for more than two-thirds the distance between the marginal and second discoidal cells. One female has the right forewing with an additional vein that separates off a small quadrate cell towards the distal extremity of the second submarginal cell. Another has this additional vein incomplete, and on the left wing. One male from El Pangue has the second submarginal cell sufficiently reduced it is almost circular with a diameter of less than three vein widths.

The two sexes average sizes are very similar; for the head width for the large sample from Region III females average 2.32 mm, SD. 0.215, n = 33, maximum 2.77 mm, minimum 1.82 mm; males average 2.33 mm, SD 0.16, n = 28, maximum 2.65 mm, minimum 2.03 mm. The series from the MCZ contains some smaller specimens: the smallest male has a head width of 1.45 mm, and the smallest female 1.48 mm. The smallest of all males available, the individual from El Pangue noted above, has a head width of 1.3mm.

Comments. There has been confusion over the nature of the type material of this species. Reed (1894) described a female specimen: his description starts with the female symbol. This is confirmed by the statement that the clypeus is pale marked on either side “una punta en cada lado del marjin anterior del cípeo amarillo blanquizco”; the male, in contrast, has an entirely pale clypeus. However, at the end of the description he implies that he has seen only two males, both from Colchagua “[H]e encontrado dos ejemplares, machos, de esta especie en Colchagua”. This is the only statement made about the provenance of any material of this species he studied. In the material from MCZ there is a single specimen from Colchagua and it is the only specimen bearing a red “type” label



Figure 20. Labels from the lectotype of *C. parvispinosus*.

(Fig. 20). Seemingly confirming Reed's confusion over the gender of the material he described, it bears a label stating that it is a male (Fig. 20). Consequently, I designate this specimen, which is a female, as the lectotype. As no other specimen from Colchagua is among the MCZ material, no paralectotype is designated at this time. Indeed, as none of the remaining MCZ material was available to Reed at the time of his publication (1894), they cannot be considered as syntypes. Pate (1938) was correct in noting that the "type" was a female, but implied that Reed had also described a male even though none of the males he listed had been collected prior to 1919, 25 years after Reed's publication.

The lectotype female (Fig. 10) is in reasonably good condition, albeit with some apparent damage from mould with dried mycelia obscuring some features and it is missing the following parts: left antenna, right antenna beyond F4, left tegula, left mesotarsus beyond the 3rd tarsomere, entire left metatarsus, right metatarsus beyond 2nd tarsomere. Its condition necessitated some parts of the redescription to be made from a different specimen; the MCZ specimen from Valparaíso: MCZ-ENT 00731885 being chosen for this purpose.

Additional records for specimens not examined in this study but cited by Pate (1938) are as follows: CHILE • 1 ♂; Valparaiso Province [Region V], Valparaiso; 25.xii.1919; P. Herbst; • 1 ♂, 1 ♀; Limache; [-33.0 -71.3]; 31.i.[no year]; A. Faz; AMNH; • 2 ♂ same collector as previous; CUIC.

Pate (1938) listed a female specimen from the MCZ with the locality "VALPARAISO PROVINCE, Concepcion, 4. Dec. 1910", I believe that Pate misread the label, as it actually states "Concon", with the gender of the specimen and date of its collection being the same, this specimen is listed in the material examined section above. Concon is just north of Valparaiso, there is no location known as "Concepcion" in Chile's Region V (Ugarte, pers. comm.). The well known Chilean Concepción [Concepción de la Madre Santissima de la Luz] is the capital of Region VIII.

The type species of the genus is known from low altitudes in Central Chile, from 28°S in Region III in the north to ~38.7°S in Region IX in the south, Santiago to the

east and Valparaiso and near Temuco to the west (Fig. 21). Despite our having collected extensively around Santiago and in the area between Santiago and Valparaiso, we have found no specimens of *C. parvispinosus* here. This area has been severely impacted by agricultural intensification since the time of the earlier collections of this species, but there remain large areas of good quality habitat especially in the more rugged areas, such as around Til-til (where we have collected frequently). Instead, most of our material comes from the southern Atacama Desert, over 500 km further north than the previous most northerly record for the species. Despite the distance and more arid habitat, it seems clear that the populations are conspecific, in that extensive study failed to reveal any consistent morphological differences among specimens from Region III and those from Regions V, VI, VII, IX and Metropolitana.

The Los Sapos locality where large numbers of *C. parvispinosus* were collected was a small, vegetated patch situated within a large area that was very dry and otherwise devoid of greenery over the time the samples were collected. It seems that roadwork immediately adjacent to the site had resulted in concentration of runoff in a small area (see fig. 30 in Mir Sharifi et al. 2018). Considerable numbers of bees and wasps were collected in traps (mostly bright blue) left out here for a few days and these included putative hosts for this cleptoparasitic nyssonine. The most likely hosts are among the following species for which large numbers of individuals were collected in the same traps as *C. parvispinosus*: two species of *Tachysphex*, identified using Pulawski (1974) as *T. rufitarsis* (Spinola) and a species perhaps allied to *T. reedi* Menke and two undescribed species of *Parapiagetia* Kohl.

***Cresson mariastea* Packer, sp.nov.**

<http://zoobank.org/053F859C-30DD-4FFD-8479-7998CEB8EAB7>

Figs 21–25, 27, 29

Material examined. 9 ♀, 9 ♂ (several males missing apical metasomal segments):

Holotype: ♀; CHILE, Region I, 73 km E. Pozo Almonte; -20.312 -69.129; 3150m; 16.–21.iv.2012; pan trap; L. Packer; MNHN. **Paratypes:** • 6 ♂, 7 ♀ paratypes identical data to previous; CAS, MNHN, PCYU, UCDC; • 1 ♂, 1 ♀ paratype; identical data to previous; 10.v.2012; net; PCYU; • 1 ♂ paratype; identical data to previous; 21.iv.–10.v.2012; PCYU.

Diagnosis. This species, as well as the following new species, is most readily distinguished from *C. parvispinosus* by the reduced areas of red on the metasomal terga (Figs. 22–24); T2 with at least a broad medial black band for the entire length of the tergum (Figs 23–24) and usually mostly black, sometimes entirely so other than for the subapical cream band, most of T1 is also black whereas *C. parvispinosus* has T1 and T2 entirely red (Figs 12–14), with at most the extreme base of the anterior declivitous surface of T1 black and T2 with at most a small apicomedial dark mark (in one male). Females can be differentiated from those of *C. salitrera* Packer sp.nov described below by the structure of T6. In *C. mariastea* the apicomedial spines are relatively long, sub-

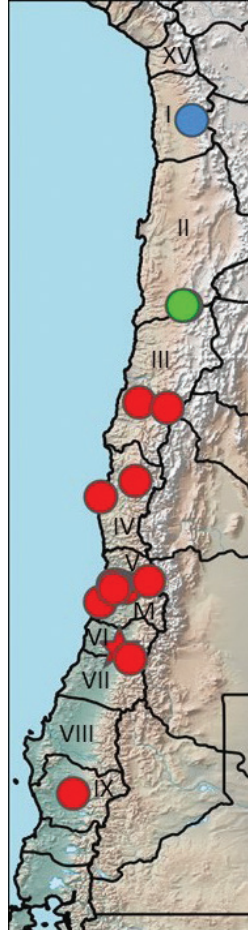


Figure 21. Distribution map of all records of *Cresson* spp. Red symbols: *C. parvispinosus*, star: the type locality for *C. parvispinosus*; blue: *C. mariastea*; green: *C. salitrera*. Scale bar: 500 km.

equal to, to longer than, the space that separates them (compare Figs 25 and 26), the lateral spines are usually less numerous, most commonly with 4 in *C. mariastea* (range 2 to 6) and 6 in *C. salitrera* (range 4 to 7) and they are also relatively shorter, less sharp and extend less than half the way up the side of the postgradular portion of the tergum as opposed to \sim three-fifths the distance in *C. salitrera*. In males, the easiest distinguishing feature is the degree of curvature of the apical flagellomere. In *C. mariastea* the ventral surface towards the apex is at an angle of \sim 40° to the long axis of the flagellum, while this is \sim 80° in *C. salitrera* (compare Figs 27 and 28). There are also differences in surface sculpture between the two species, most clearly shown in the basal depressed area of T2 in both sexes which has large, distinct, deep and dense ($i < d$) punctures in *C. mariastea* (Fig. 29) but minute, sparse ($i > 5d$) punctures in *C. salitrera* (Fig. 30) which are largely imperceptible with the light microscope.

Description. Holotype Female (Fig. 22)

Dimensions: Body length 7.3 mm, forewing length 5.1 mm, head width 2.15 mm, ITW 1.3 mm.

Colouration: Black, following parts white to pale yellowish: mandible (except apical half increasingly dark towards apex, yellowish at midlength, red-brown at apex), labrum, lateral one-quarter of clypeus, narrow club-shaped mark on upper paraocular area adjacent to inner margin of compound eye extending from above upper tangent of antennal socket to below level of lower tangent of median ocellus, small mark on genal area above adjacent to posterior margin of compound eye, small mark towards side of pronotal collar separated by more than twice the width of the mark, pronotal lobe (margined with black above), small anterolateral mark on scutellum, triangular mark on mesopleuron anterior to mesocoxa, apical mark on all coxae (most extensive on mesocoxa where it occupies the outer third of the ventral surface), apicoventral less than two-thirds of profemur, anterodorsal surface of all tibiae (mostly pale yellow on pro- and mesotibiae, mostly white on metatibiae), transverse subapical bands on T1–T5, entire only on T5, most broadly interrupted on T2, the interruptions are orange to orange-brown and narrower than the adjacent white bands. Scape yellow-orange apicoventrally. Following parts orange to orange-brown: torulus, all tarsi (probasitarsus suffused with yellowish, successive tarsomeres increasingly darker), posterior surface of metatibia entirely towards base, narrowing apically to absent at extreme apex; T1 and T3 narrow anterior margin to subapical pale transverse band, substantially broadened laterally on T1; T2 broadly towards side. Apical tergal and sternal depressions translucent straw laterally, orange-brown medially; T6 spines translucent orange-brown. S2 red brown, orange-brown towards margins; S3–S5 dark brown except red-brown towards apices.

Pubescence: Silver appressed and obscuring, or almost obscuring, underlying integument on lower paraocular area, genal area adjacent to compound eye, mesopleuron (sparser anteriorly and ventrally, absent posteriorly), scutellum posteriorly and dorsolateral portion of propodeum; somewhat less dense on clypeus, pronotal collar, anterior half of horizontal portion of T1; suberect longer setae ~ 0.7 MOD on most of genal area; sparse erect long whitish setae \leq MOD on upper face, posterolaterally on pronotum, mesopleuron; similar setae somewhat shorter on mesoscutum and scutellum. Metasomal terga with short subappressed posteriorly oriented setae with sparse suberect setae intermixed, longest on T6, 0.3 MOD; short setae

Surface sculpture: Micropunctures very sparse on head and thorax except on vertexal and genal areas, abundant on metasomal terga and sterna; punctation mostly coarse and dense, almost crowded on face with interspaces raised among linear groups of punctures; genal area with dense small punctures $i < d$ among irregularly spaced large ones, surface uneven somewhat rugose posteriorly. Mesoscutum densely punctate $i < d$ except posteriorly on disc $i \leq 2d$; punctures of scutellum as on upper face except sparser laterally; metapostnotum longitudinally rugoso-striate on horizontal portion,



Figures 22–24. *Cresson mariastea* **22** a paratype female, lateral view **23** holotype female, dorsal metasoma **24** male, dorsal metasoma. Scale bars: 1.0 mm.

areolate posteriorly. Larger punctures of terga mostly dense $i < d$ with some sparser areas laterally on T1 and towards apex of T2 and T3; basal depressed area of T2 deeply, coarsely and densely punctate $i < d$; sculpture of T6 similar to that of face; sterna punctures dense towards sides $i < d$, less regularly spaced medially, $i = 1-4d$ on S2, mostly $i < 2d$ on S3–S5, $i < d$ on S6 except midline largely impunctate.

Structure: Head almost $1.5 \times$ as wide as long, 89:61; [labrum transverse, narrowly oval, three times as wide as medial length, W:L 36:12 apical margin transverse]; clypeus almost $3 \times$ as wide as medial length, 61:21, lip almost half as wide as clypeus, 28; supra-clypeal area minute, median length third as long as clypeus; AOD $1.7 \times$ maximum width of F1 (17:10); supra-antennal area longer than maximum width 27:20, shorter than scape 32; frontal depression poorly defined dorsally; UOD:LOD:MINOD 66:47:35; IOD:OOD 27:25; scape twice as long as greatest width 32:16; pedicel shorter than wide 11:13; F1 more than twice as long as greatest width 22:10; F2 less than twice as long as greatest width 22:12, remaining flagellomeres decreasing in length from F3 to F9 (F9 L = W), F10 18:12; pronotal collar approximately 0.5 MOD medially, 10:19; [admedian line distinct anteriorly for less than half medial length of mesoscutum], scutellum with faint medial line with large shallow depression postero-medially; length of scutellum:metanotum:metapostnotum 39:15:30. T6 triangular, sides forming an angle of $\sim 60^\circ$, with three acute teeth on each side, restricted to less than apical one-third of side of tergum, two apicomedial teeth longer than their basal width 7:5, separated by a distance subequal to their basal width. S2–S5 apical depressions ~ 0.3 MOD, narrowed medially, abruptly so on S4–S5.

Male. Dimensions: Body length 6.6 mm; forewing length 4.1 mm; head width 1.75 mm; intertegular width 1.1 mm.

Colouration: Black, following parts white to pale yellowish: mandible basal third (mid third orange, apical third red-brown), labrum, clypeus, supra-clypeal area, par-ocular area completely filling space between antennal socket and compound eye below, extending narrowly along eye margin above to just below lower tangent of median ocellus, small oval mark on genal area above behind compound eye, ventral surface of scape, ventral spot on pedicel, pair of small spots on pronotal collar separated by more than 2 MOD and $< 0.2 \times$ the space that separates them, pronotal lobe (margined with black), large mark anterior to mesocoxa approximately equal in area to ventral surface of mesocoxa, ventral surface of all coxae except at base, ventral surface of profemur except basal fifth, apicodorsal mark on pro- and mesofemora, dorsal and most of posterior surfaces of pro- and mesotibiae, most of anterior surface of metatibia (posterior surface orange basally, orange-brown apically, blackish ventrally), anterior surface of all basitarsi and most of anterior surface of all second tarsomeres (remaining tarsomeres red brown), transverse subapical bands on T1–T6, very narrowly interrupted medially on T1, T4 and T5, more broadly interrupted on T2 and T3, complete on T6; S2 sub-apical band broad, S3 band narrow, S4 with small faint pale subapical mark. Pale marking on T1 narrowly margined with orange-brown, T2 with lateral orange brown spot anterior to pale band. Apical tergal; depressions translucent, largely colourless except orange-brown medially, apical sternal depressions pale straw except on S5 yellowish.

Pubescence: Silver appressed and obscuring, or almost obscuring, underlying integument on clypeus, lower paraocular area, frontal depressions, mesopleuron, metanotum posterolaterally, dorsolateral area of propodeum; somewhat sparser on genal area, pronotal collar, laterally on pronotum, anteromedially on mesoscutum, posterolaterally on scutellum, metanotum, most of horizontal surface of T1, anterior depressed area of T2. Longer, $< 1.5 \text{ MOD}$, erect whitish setae on frontal and vertexal areas, mesoscutum and scutellum; similar setae somewhat shorter and sparser on mesopleuron; metasomal terga with sparse suberect setae posteriorly on T4–T7, longest on T7 $< 0.5 \text{ MOD}$. Mesobasitarsal fringe setae $< 1.3 \times$ as long as greatest width of mesobasitarsus. S2–S5 apicomedial setal fringe $\sim 0.7 \text{ MOD}$ in length medially.

Surface sculpture: As in female except as follows: Micropunctures absent on head and thorax, abundant on metasomal terga and sterna; genal area densely punctate, vertexal area and scutellum rugoso-punctate, mesoscutum more sparsely punctate posteriorly on disc, $i \leq 3d$; lateral surface of propodeum somewhat rugulose below propodeal spine. Larger punctures of S2 denser $i \leq 2d$; S6 sparsely punctate except anterolaterally $i \leq d$.

Structure: Head $\sim 1.4 \times$ as wide as long, 86:62; labrum transverse, narrowly oval, almost $3 \times$ as wide as medial length, W:L 35:13, apical margin transverse; clypeus less than $3 \times$ as wide as medial length, 61:22, supraclypeal area almost entirely obscured by frontal crest in frontal view, only extreme lower margin visible medially; AOD slightly greater than maximum width of F1, 12:10; supra-antennal area longer than maximum width 28:20, shorter than scape 31; frontal depression extending to $< 0.5 \text{ MOD}$ below lower tangent of median ocellus; UOD:LOD:MINOD 55:38:26; IOD greater than OOD 23:16; scape more than $1.5 \times$ as long as greatest width (31:18); pedicel length subequal to width; F1 twice as long as greatest width 20:10; F2 $\sim 1.5 \times$ as long as greatest width 19:12, remaining flagellomeres longer than wide, increasingly shorter from F3 to F10, F11 L:W 23:11, F11 somewhat falcate, ventral surface concave, apicoventral surface at $\sim 40^\circ$ to longitudinal axis of flagellum; pronotal collar approximately 0.5 MOD , 11:20; admedian line distinct anteriorly, obscure posteriorly, posteromedial scutellar pit obscure; length of scutellum:metanotum:metapostnotum 33:13:23. T7 somewhat semicircular with five narrow apical teeth, the median one shortest, the others subequal in length. Apical sternal depressions long, on S2 longer than the diameter of the largest punctures on the sternum; anterior and posterior medial angles of apical sternal depressions acute and obtuse, respectively on S2–S3, both approximately right angular on S4–S5.

Variation. The extent of red colouration on the metasoma varies, four males have the red restricted to a narrow line immediately anterior to the apical whitish tergal bands on T1 and T2 (as in Fig. 24), four have the mark on T2 expanded into a lateral patch and one has even more extensive red marks quite similar to the male imaged for the following species (Fig. 33). Five females have an expanded lateral red mark on T2 and the anterior edge of the white mark on T1 margined with red while four have large lateral marks on T1 and T2 (as in Fig. 23). Some specimens have more broadly interrupted tergal bands on T2–T4. Two female paratypes have whitish subapical transverse bands on S2 and one has such marks also on S3. Females vary in the size of the lateral pale mark on the scutellum from absent to extending for approximately half the length of the

lateral margin. One male paratype has the pale spots on the pronotal collar extensive, almost as wide as the space that separates them, while three of them have these marks entirely absent. One male has a small pale lateral mark on the scutellum. One male lacks the pale mark on the pedicel while two also have pale marks ventrally on F1 and F2. The larger males have the lateral surface of the propodeum with dorsolaterally oriented carinae above as in the female. One male has the petiole of the second submarginal cell duplicated on one side, forming an additional, small, quadrate cell anterior to the normal second submarginal cell. One female has the petiole on the right forewing second submarginal cell almost absent.

Males vary in size from a head with of 1.6 to 2.02 mm; females vary in head width from 1.65 to 2.15 mm.

Etymology. This species is named in honour of the late Maria Stea. During her too-short time at York University she was tireless in her efforts to assist the hymenopterists in the Biology Department.

Comments. All specimens of *Cresson mariastea* are from the mountainous area Northeast of the oasis town of Pica, and almost due South of Mamiña (less than 30 km from either) in an area known as the Pica Highlands (Fig. 21). This area has yielded many interesting species of Apoidea in recent years, including a new genus of fideliiine (Praz and Packer 2017) and a new species of *Colletes* (Ferrari 2017) as well as its presumptive cleptoparasite, a recently described species of *Isepeolus* (Packer and Graham 2020).

An undescribed species of *Parapiagetia* and a species of *Tachysphex* I have not been able to identify were found simultaneously with *C. mariastea* and are its potential hosts.

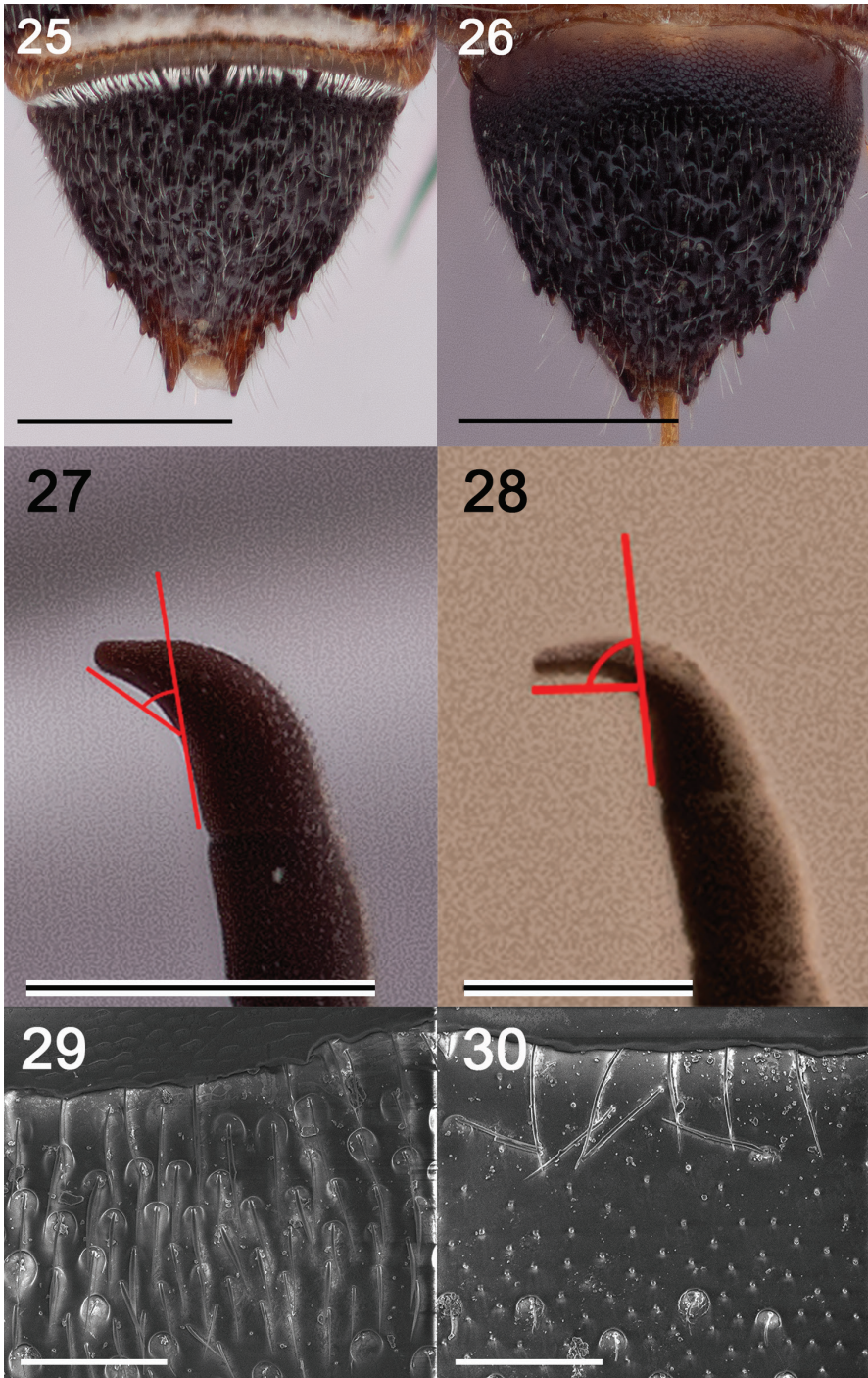
***Cresson salitrera* Packer, sp.nov.**

<http://zoobank.org/D9159A6E-2CBE-4271-BF0B-58FEAA37DA9C>

Figs 7, 21, 26, 28, 30–33, 35

Material Examined. 7 ♀, 7♂. • **Holotype:** ♀; CHILE, Region II, km 26.7, Rd. to Aguas Calientes (N. of Mina Vaquillas); -25.375 -69.288; 3350m; 31.x.2015–6.ii.2016; L. Packer, blue vane trap; MNHN. **Paratypes:** CHILE • 1 ♀, 2 ♂ paratypes identical data as holotype; PCYU; • 1 ♂; Region II, Rd to Plato de Sopa, km 51.2; -25.379 -69.388; 3040m; 31.x.2015–6.ii.2016; L. Packer; yellow pan trap; PCYU; • 3 ♀, 1 ♂; CAS, PCYU; Region II, W. of Mina Vaquillas; -25.370 -69.372; 3130m; 31.x.2015–3.ii.2016; L. Packer; white pan trap; PCYU; • 1 ♂; Region II, S. of Cerro dos Hermanos; -25.404 -69.040; 4020m; 17.xi.–7.xii.2013; S. Monckton; PCYU.

Diagnosis. Most readily distinguished from *C. parvispinosus* by the reduced areas of red on the metasomal terga (Figs 31–33), although usually not as reduced as in *C. mariastea*; T1 and T2 are at least black medially, although in one male only narrowly so. In contrast, *C. parvispinosus* has T1 and T2 entirely red, with at most the extreme base of the anterior declivitous surface of T1 black and T2 with a small apicomedial dark mark. Compared to *C. mariastea*, the apicomedial spines of T6 in the females are shorter, at most as long as their basal width, but the lateral spines are relatively longer



Figures 25–30. Characters used to differentiate *C. mariastea* and *C. salitrella* **25** T6 of female *C. mariastea*, **26** T6 of female *C. salitrella*. Scale bars: 0.5 mm. **27** F11 of male *C. mariastea* **28** F11 of male *C. salitrella*. Scale bars: 0.25 mm. **29** base of T2 *C. mariastea* **30** base of T2 of *C. salitrella*. Scale bars: 100 μ m.

and sharper (compare Figs 26 and 25). In both sexes the basal depressed area of T2 is minutely, sparsely punctate in *C. salitrera* (Fig. 30) but more coarsely and densely, $i < d$, punctate in *C. mariastea* (Fig. 29). The degree of curvature of F11 differs, in *C. salitrera* the ventral surface is at an angle of $\sim 80^\circ$ to the longitudinal axis of the flagellum (Fig. 28) while this is $\sim 40^\circ$ in *C. mariastea* (Fig. 27).

Description. Holotype female (Figs 31–32)

Dimensions: Body length 7.1 mm, forewing length 5.1 mm, head width 2.18 mm, ITW 1.35 mm.

Colouration: Black, following parts white to pale yellowish: mandible basal one-third (rest red brown), labrum, lateral $\frac{1}{4}$ of clypeus, narrow club-shaped mark on upper paraocular area adjacent to inner margin of compound eye extending from upper tangent of supra-antennal area almost to dorsal tangent of frontal depression, small spot on genal area above adjacent to posterior margin of compound eye, transverse mark towards side of pronotal collar separated by slightly less than width of the mark, pronotal lobe (margined with black above, red–brown below), mark on scutellum occupying less than lateral one-quarter, posterior extremity of axilla, broadly divided transverse mark on mesopleuron anterior to mesocoxae, outer half of ventral surface of procoxa, outer half of mesocoxa, extreme apex of metacoxa, apicoventral and posterior two-thirds of profemur, anterodorsal surface of all tibiae (mostly pale yellow on pro- and mesotibiae, mostly white on metatibia), probasitarsus anteriorly, mesobasitarsus basal half; transverse subapical bands on T1–T5, entire on T1, T4 and T5, medial interruptions of T2–T3 blackish; narrow subapical bands on S2–S4 interrupted medially and incomplete laterally (replaced by orange-brown). Following parts orange to orange-brown: torulus, scape apicoventrally, most of posterior surface of metatibia (blackish ventrally), all remaining tarsomeres, T1 triangular marking anterior to subapical cream band broadest laterally, T2 lateral three-tenths red except anterior depression; apical tergal depressions pale straw to transparent.

Pubescence: Silver appressed and obscuring, or almost obscuring, underlying integument on lower paraocular area, frontal depressions, genal area adjacent to compound eye, mesopleuron, scutellum posterolaterally, metanotum except anteromedially and dorsolateral portion of propodeum; somewhat less dense on clypeus, pronotal collar, anterior one eighth of mesoscutum, most of horizontal portion of T1; suberect longer whitish setae ~ 1.2 MOD on most of genal area and mesepisternum; erect long whitish setae < 1.7 MOD on upper face; short < 0.5 MOD erect pale setae on dorsal surface of mesoscutum and T4–T6, similar setae shorter on T1–T3 and metasomal sterna with a few longer setae subapically ≤ 0.7 MOD.

Surface sculpture: Micropunctures absent on face except on vertex, sparse on mesoscutum and scutellum, abundant on metasomal terga, sparse on sterna and dense, $i < d$ on genal area; punctation mostly coarse and dense, almost crowded on face with interspaces raised among linear groups of punctures, appearing almost striate, striae radiating from ocellar area; genal area larger punctures irregularly spaced $i = 0.2\text{--}4d$. Mesoscutum densely punctate $i < d$ except posteriorly on disc $i \leq 2d$; scutellum punc-



Figures 31–33. *Cresson salitrea* **31** male, lateral view **32** holotype female, dorsal metasoma **33** male, dorsal metasoma. Scale bars: 1.0 mm.

tures $i < d$; mesopleuron large punctures $i < 2d$, posteriorly almost impunctate, metapleuron lacking sculpture except for a few short longitudinal carinae posterodorsally; lateral surface of propodeum carinate for posterodorsal two-thirds. Larger punctures

of T1 irregularly spaced $i < 3d$, on T2 $i < 4d$ except with areas lacking large punctures posteromedially; basal depressed area of T2 with shallow, sparse minute punctures $i > 5d$; T3 $i < 3d$, T4–T5 $i > 2d$, T6 $i < 0.5d$; S2 $i < 2d$, S3 $i < 1.5d$, S4 $i \leq d$, S5 $i < 2d$, S6 $i < d$ except midline largely impunctate.

Structure: Head almost $1.5 \times$ as wide as long, 89:61; labrum W:L 36:13 apical margin somewhat concave medially; clypeus W:L 62:23, lip less than half as wide as clypeus, 28, distinctly narrower medially than towards sides; supraclypeal area median length approximately one sixth as long as clypeus; AOD almost $1.5 \times$ maximum width of F1 (15:11); supra-antennal area longer than maximum width 30:18, as long as scape; frontal depression extending to ~ 0.5 MOD below lower tangent of median ocellus above; UOD:LOD:MINOD 71:45:35; IOD = OOD; scape less than twice as long as greatest width (30:17); pedicel shorter than wide 11:13; F1 $2.5 \times$ as long as greatest width 25:10; F2 less than twice as long as greatest width 20:11, remaining flagellomeres increasingly shorter from F3 to F9 except F10 16:12; pronotal collar almost half as long medially as MOD, 10:18; admedian line complete, more distinct for anterior half, scutellum with irregular medial line and large shallow depression posteromedially; length of scutellum:metanotum:metapostnotum 41:15:23. T6 triangular, sides forming an angle of $\sim 80^\circ$, with four (left) to five acute teeth (right) extending to midlength of side of tergum, two apical teeth short, equal in length to their basal width, 4:4, separated by a distance clearly greater than their length, 7.5. S2–S5 apical depressions ~ 0.5 MOD, somewhat narrower medially but not abruptly so.

Male (Fig. 33)

Dimensions: Body length 7.8 mm, forewing length 5.2 mm, head width 2.25 mm, ITW 1.42 mm.

Colouration: Black, following parts white to pale yellowish: mandible basal half (rest red-brown), labrum, clypeus, supraclypeal area, paraocular area completely filling space between antennal socket and eye below, extending narrowly along eye margin above to approximately 1 MOD below lower tangent of medial ocellus, tiny spot on genal area above behind compound eye, ventral surface of scape, ventral spot on pedicel, pair of small spots on pronotal collar separated by $2 \times$ MOD, pronotal lobe (margined with black), large mark anterior to mesocoxa approximately equal in area to ventral surface of mesocoxa, ventral surface of procoxa, mesocoxa except base, apical two-thirds of ventral surface of metacoxa, ventral and much of posterior surface of profemur except basal one-quarter, apicodorsal mark on pro- and mesofemora, dorsal surface and apical one-third of anterior surface of pro- and mesotibiae, anterior surface of metatibia (posterior surface orange basally, orange-brown apically, blackish ventrally), anterior surface of all basitarsi, transverse subapical bands on T1–T6, narrowly interrupted medially on T1, T4 and T5, more broadly interrupted on T2 and T3, complete on T6; irregularly-shaped subapical mark on S2, S3 band narrow and interrupted medially, junction of disc and apical sternal depressions narrowly orange brown. Second tarsomere on all legs yellowish, increasingly dark on more apical tarsomeres to red brown on pretarsus. Posterior surface of metatibia orange. Pale marking on T1 margined with orange anteriorly, marking broad laterally, restricted to narrow line medially; T2 orange for more than

lateral one-third width of tergum. S2 with large orange spot on each side. Apical tergal depressions translucent, somewhat orange medially, on T1, T2 and T6 pale straw, on T3–T5 colourless all somewhat orange medially, apical sternal depressions straw yellow except of S5 yellowish.

Pubescence: As in female except as follows: suberect longer whitish setae \sim MOD on genal area above and sides of mesopleuron; \sim 1.7 MOD on genal area below and scutellum; shorter \sim MOD erect pale setae on mesoscutum, short 0.5 MOD suberect setae on T2–T6 and metasomal sterna, similar setae shorter on T1.

Surface sculpture: As in female except as follows: micropunctures abundant on S2; lateral surface of propodeum carinate for dorsal $\frac{1}{2}$. Larger punctures of T1–T3 $i \leq 4d$, T4 $i \leq 3d$, T5–T6 $< 2d$, T7 $i < d$, crowded towards apex. S2 and S5 $i < 6d$, S3–S4 $i < 2d$, S6 with scattered punctures $i = 1-6d$.

Structure: Head almost $1.5 \times$ as wide as long, 93:64; [labrum W:L 32:14, apical margin shallowly concave;] clypeus more than $2.7 \times$ as wide as medial length, 66:24, lip less than half clypeal width 29, slightly shorter medially than towards side; supra-clypeal area entirely obscured by frontal crest in frontal view; supra-antennal area L:W 27:18, shorter than scape 31; AOD greater than maximum width of F1 13:11; frontal depression almost reaching lower tangent of median ocellus; UOD:LOD:MINOD 73:49:33; IOD:OOD 19:17; scape $\sim 1.5 \times$ as long as greatest width, 31:20; pedicel almost as long as maximum width 13:12; F1 $2.5 \times$ as long as greatest width 32:13; F2 shorter than F1, $> 1.5 \times$ as long as greatest width 28:16, remaining flagellomeres $\sim 1.5 \times$ as long as wide except F11 26:10, somewhat falcate, downcurved and narrowing from base to apex, apicoventral surface at $\sim 80^\circ$ to longitudinal axis of flagellum; pronotal collar more than 0.5 MOD medially, 12:20; admedian line impressed for anterior two-thirds; length of scutellum:metanotum:metapostnotum 42:16:29; scutellum posteromedial pit absent. T7 semicircular with five teeth, medial tooth the shortest and broadest, submedial teeth as long as lateral ones but broader. S2–S5 apical depressions broad submedially > 0.3 MOD on S2, longer than largest punctures on sternum, impunctate apical portion clearly longer than diameters of basal punctures. Apical sternal depressions long, on S2 longer than diameter of largest punctures on sternum; anterior and posterior angles of medial interruption of apical sternal depressions slightly acute and slightly obtuse, respectively on S2, both approximately right angular on S3–S5.

Variation. There is minor variation in the extent of pale marking in females, some lack the medial interruption to the pale marking in front of each mesocoxa or have the metacoxa narrowly pale medially on the ventral surface. All have the red markings on T1 and T2 completely interrupted by black medially although in one male the dark marks are narrowed to < 0.5 MOD on T2 and are dark brown.

Etymology. The species is known only from moderate to high altitude in an area of the Atacama Desert that is famous for its sodium nitrate (chile saltpeter) mines. These “salitreras” give the species its name, which is a noun in apposition. These mines dotted the landscape, especially in the late 1890s and early 1900s; but are now abandoned, mostly indicated by ruins and/or just their cemeteries. The

known localities for the species are all from the sides of roads that form networks among these abandoned mines in a part of the country that would otherwise be almost inaccessible.

Comments. Two unidentified species of *Tachysphex* and an undescribed species of *Parapiagetia* were found in association with this species; none of them seem to be the same as those found associated with the other species of *Cresson* treated above.

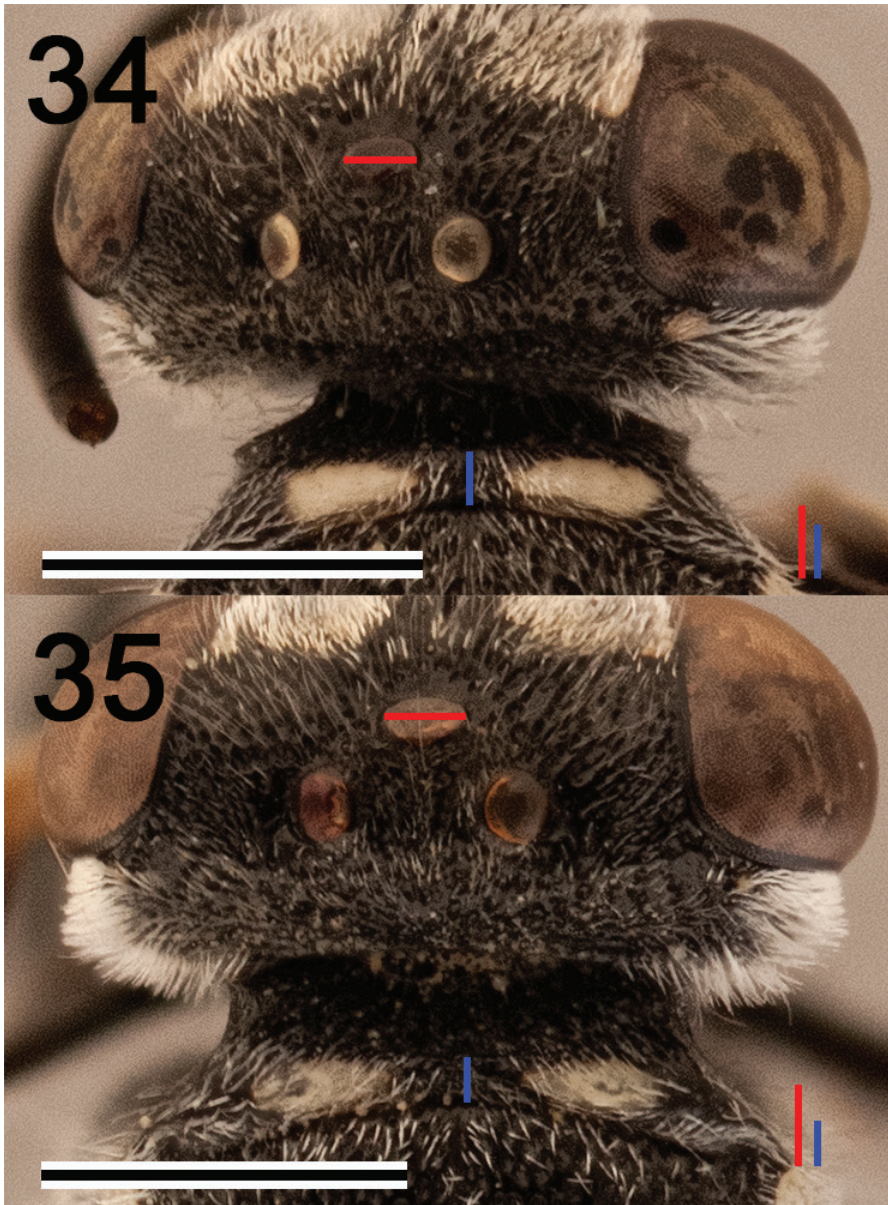
This species comes from the part of the Atacama Desert where the absolute desert (rainfall less than 10 mm/yr) gets furthest inland, almost to the border with Argentina. Other species of interest from this area include the wasps just mentioned and a recently described cuckoo bee, *Melectoides desiccata* Packer and Graham. The type locality was imaged by Packer and Graham (2020; Fig. 9). The Cerro dos Hermanos locality is even drier and inhospitable.

Identification key

- 1 T1 and T2 entirely red except sometimes T1 with extreme base of anterior declivitous surface and a small apicomedial spot dark (Figs 10–14); pronotal collar medial length clearly more than $0.5 \times \text{MOD}$ (Fig. 34) ***C. parvispinosus* (Reed)**
- T1 and T2 broadly black medially to mostly black (Figs 23, 24) pronotal collar medial length approximately $0.5 \times \text{MOD}$ (Fig. 35) **2**
- 2 Both sexes with punctures of basal transverse depression of T2 large, coarse and dense, $i < d$ throughout (Fig. 29). Male: F11 shallowly curved, apicoventral surface $\sim 40^\circ$ from longitudinal axis of flagellum (Fig. 27). Female, T6 apicomedial spines long, subequal in length to the space that separates them; lateral spines extending at most halfway from apex of tergum to base, spines usually short and blunt (Fig. 25) ***C. mariastea* Packer sp.nov.**
- Both sexes with punctures of basal transverse depression of T2 minute and sparse, $i > 5d$, contrasting with the densely punctate posterodorsally sloping portion (Fig. 30). Male: F11 markedly curved, apicoventral surface $\sim 80^\circ$ from longitudinal axis of flagellum (Fig. 28); Female T6 apicomedial spines short, clearly shorter than the distance separating them; lateral spines extending more than halfway from apex of tergum to base, spines usually long and sharp (Fig. 26) ***C. salitreira* Packer sp.nov.**

Discussion

Nyssonini with known ecologies are cleptoparasitic on other apoid wasps (Bohart and Menke 1976, table 18). All specimens we have collected recently have been associated with *Tachysphex* Kohl, 1883 and/or *Parapiagetia* Kohl, 1897 and it is suspected that one or both genera include hosts for *Cresson*. The former genus has been revised for South America (Pulawski 1974) while the latter has no described species from Chile, although its presence there has been known for some time (e.g. Bohart and Menke 1976, p. 277).



Figures 34–35. Relative dimensions of MOD and pronotal collar medial length for couplet 1 of identification key of *Cresson* species **34** *C. parvispinosus* and **35** *C. salitrena*. Red lines MOD, blue lines medial length of pronotal collar. Scale bars: 1.0 mm.

At least six *Parapiagetia* species have been discovered as a result of our collecting in Chile and descriptions of these species (among others) are in progress. Of the various *Cresson*-associated *Tachysphex* species, I have been able to identify only one with any confidence, suggesting that new species of this genus also await description from Chile. Bohart

and Menke (1976) suggested Heliocausini as potential hosts for *Cresson* (also for *Antomartinezius* and *Perisson*). Our collections suggest that Heliocausini are unlikely to be hosts for *Cresson*. One species of *Heliocausus* Kohl, 1892 was quite common at the Los Sapos locality for *C. parvispinosus* but almost all individuals seem too small compared to the size of the cleptoparasite.

While I did find variation in some details of S8, the apex of the volsella and the apex of the penis valve among specimens of the species discussed herein, variation among specimens of the type species of *Cresson* suggested that intraspecific variation is too great for these structures to be of species-level taxonomic value.

Traps with propylene glycol as the preservative fluid can be left out in arid areas for weeks to months (Packer and Darla-West 2021). As noted previously (Packer and Graham 2020) this is a particularly useful strategy for sampling in remote areas with very low primary productivity and hence low abundances of insects and now can be said to be potentially as useful for sampling apoid wasps as they are for bees.

Conclusion

There are now three species in the genus *Cresson*, all from Chile. It seems probable that their hosts are Larrini of the genera *Parapiagetia* and/or *Tachysphex*. The new species would not have been discovered without the use of traps with propylene glycol left out for long periods in inhospitable habitat.

Acknowledgements

Completion of this work would have been impossible without the prompt response of Crystal Maier of the MCZ who sent me the series of *C. parvispinosus* from that museum just before both our institutions were locked down due to COVID19. I am also grateful to Lynn Kimsey, Steven Heydon, Robert Zuparko and Chris Grinter who sent me material from UCDC and CAS during the pandemic. The fieldwork that resulted in the new species being discovered was funded by a Natural Sciences and Engineering Research Council of Canada Discovery Grant to the author, some carried out by Spencer Monckton and James Postlethwaite, and facilitated by Alfredo Ugarte and Rolando Humire Coca. I am particularly grateful to Liam Graham for taking the images of wasps herein and amalgamating them into plates, his contribution was funded by a generous donation from Robert and Cecily Bradshaw for which I am extremely grateful and his use of the ESEM system was facilitated by Magdalena Jaklewicz. Both Wojciech Pulawski and Matthias Buck provided very useful comments that improved the manuscript and I am extremely grateful to both of them.

References

- Aguiar AP, Gibson GAP (2010) The spatial complexity in describing leg surfaces of Hymenoptera (Insecta), the problem and a proposed solution. *Zootaxa* 2415: 54–62. <https://doi.org/10.11646/zootaxa.2415.1.5>
- Amarante STP (1993) Collecting in Northeastern Brazil. *Sphecos* 25: 16–20.
- Amarante STP (2002) A synonymic catalog of the Neotropical Crabronidae and Sphecidae (Hymenoptera: Apoidea). *Arquivos de Zoologia* 37: 1–139. <https://doi.org/10.11606/issn.2176-7793.v37i1p1-139>
- Ashmead WH (1898) Two new genera of sand wasps. *Entomological News* 9: 187–189.
- Ashmead WH (1899) Classification of the entomophilous wasps, or the superfamily Sphegoidea. *The Canadian Entomologist* 31: 322–330. <https://doi.org/10.4039/Ent31322-11>
- Bohart RM (1968) New Nyssoninae from North and South America (Hymenoptera: Sphecidae). *Proceedings of the Entomological Society of Washington* 81: 431–437.
- Bohart RM, Menke AS (1976) *Sphecid Wasps of the World. A generic revision*. University of California Press, Berkeley, Los Angeles and London, 695 pp. <https://doi.org/10.1525/9780520309548>
- Brothers DJ (1976) Modifications of the metapostnotum and origin of the ‘propodeal triangle’ in Hymenoptera Aculeata. *Systematic Entomology*, 1: 177–182. <https://doi.org/10.1111/j.1365-3113.1976.tb00036.x>
- Bradley JC (1956) On the use of “*Cresson*” as a generic name (Hymenoptera: Sphegidae). *Entomological News* 67: e257.
- Chiappa E (2012) Especies de Vespidae y Sphecidae (Hymenoptera) de Valparaiso, Chile, diagnóstico de la distribución regional. *Revista Chilena de Entomología* 37: 5–16.
- Dalla Torre CG de (1897) *Catalogus Hymenopterorum hucusque descriptorum systematicus et synonymicus, Volumen VIII: Fossores (Sphegidae)*. Guilelmi Engelmann, Lipsiae, 749pp.
- Ferrari RR (2017) Taxonomic revision of the species of *Colletes* Latreille, 1802 (Hymenoptera: Colletidae: Colletinae) found in Chile. *Zootaxa* 4364: 1–137. <https://doi.org/10.11646/zootaxa.4364.1.1>
- Fritz MA (1955) Nyssonini neotropicales (Hym. Sphecidae). *Revista de la Sociedad Entomológica Argentina* 18: 11–16.
- Fritz MA (1973) Nyssonini neotropicales VI (Hym.: Sphecidae: Nyssoninae). *Anales del Museo de Historia Natural de Valparaiso* 6: 191–202.
- Harris RA (1979) A glossary of surface sculpturing. *Occasional papers in Entomology* 28: 1–31.
- Kimoto C, Deban SJ, Thorp RW, Rao S, Stephen WP (2012) Investigating temporal patterns of a native bee community in a remnant North American bunchgrass prairie using blue vane traps. *Journal of Insect Science* 12: e108. <https://doi.org/10.1673/031.012.10801>
- Kohl FF (1883) Über neue Grabwespen des Mediterrangebietes. *Deutsche Entomologische Zeitschrift (Berlin)* 27: 161–186. <https://doi.org/10.1002/mmnd.48018830125>
- Kohl FF (1892) Neue Hymenopterenformen. *Annalen des k.k. Naturhistorischen Hofmuseums* 7: 197–234.

- Kohl FF (1897) Die Gattungen der Sphegiden. *Annalen des k.k. Naturhistorischen Hofmuseums* 11: 233–516. <https://doi.org/10.5962/bhl.part.27397>
- Maidl F, Klima A (1939) Pars 8: Sphecidae I. (Astatinae – Nyssoninae) in H. Hedicke (Ed.). *Hymenopterorum Catalogus*. Dr. W. Junk, Verlag für Naturwissenschaften, 's-Gravenhage, 150pp.
- Michener CD (2007) *The Bees of the World* (2nd edn). The Johns Hopkins University Press, Baltimore, 953pp.
- Mir Sharifi N, Graham L, Packer L (2018) Fifteen new species of *Liphanthus* (Hymenoptera: Andrenidae) with two submarginal cells. *Zootaxa* 4645: 1–80. <https://doi.org/10.11646/zootaxa.4645.1.1>
- Packer L, Darla-West G (2021) Bees: How and why to sample them. In: Santos JC, Fernandes GW (Eds) *Measuring Arthropod Diversity*. Springer, 55–83. https://doi.org/10.1007/978-3-030-53226-0_3
- Packer L, Graham L (2020) Four new species of Isepeolini (Hymenoptera; Apidae) from northern Chile. *BMC Zoology* 5: e3 <https://doi.org/10.1186/s40850-020-00052-8>
- Pate VSL (1935) Synonymical notes on the fossorial wasps (Hymenoptera: Sphecidae, Pompilidae and Tiphidae). *Entomological News* 46: 244–267.
- Pate VSL (1938) Studies in the Nyssonine wasps. IV. New or redefined genera of the tribe Nyssonini, with descriptions of new species (Hymenoptera: Sphecidae). *Transactions of the American Entomological Society* 64: 117–190.
- Pate VSL (1940) On two new genera of nyssonine wasps from the Neotropical Region (Hymenoptera: Sphecidae). *Notulae Naturae of the Academy of Natural Sciences of Philadelphia* 55: 1–9.
- Praz CJ, Packer L (2017) Phylogenetic position of a remarkable new fideiine bee from northern Chile (Hymenoptera: Megachilidae) *Systematic Entomology* 42: 473–488. <https://doi.org/10.1111/syen.12229>
- Prentice MA (1998) The comparative morphology and phylogeny of apooid wasps (Hymenoptera: Apoidea). PhD Thesis, University of California, Berkeley, 1439pp.
- Pulawski WJ (1974) A revision of the Neotropical *Tachysphex* Kohl (*Hym.*, *Sphecidae*). *Polskie Pismo Entomologiczne* 44: 3–102.
- Pulawski WJ (2020) Catalogue of Sphecidae *sensu lato*. <https://www.calacademy.org/scientists/projects/catalog-of-sphécidae> [accessed 29.iii.2020 and 17.ii.2021]
- Reed EC (1894) Los fosores o avispa cavadoras. *Anales de la Universidad de Chile* 85: 599–653.
- Rohwer SA (1921) Some notes on wasps of the subfamily Nyssoninae, with descriptions of new species. *Proceedings of the United States National Museum* 59: 403–413. <https://doi.org/10.5479/si.00963801.2374.403>
- Sann M, Niehuis O, Peters RS, Mayer RS, Kozlov A, Podsiadlowski L, Bank S, Meusemann K, Misof B, Bleidorn C, Ohl M (2018) Phylogenomic analysis of Apoidea sheds new light on the sister group of bees. *BMC Evolutionary Biology* 1: e71. <https://doi.org/10.1186/s12862-018-1155-8> [accessed 19.v.2019]
- Shorthouse (2010) SimpleMapp, an online tool to produce publication-quality point maps. <https://www.simplemapp.net> [accessed 24.viii.2020]

- Sielfeld K. WH (1980) Las especies de Sphecidae (Hymenoptera) conocidas para territorio Chileno. *Revista Chilena de Entomología* 10: 7–76.
- Stephen WP, Rao S (2005) Unscented color traps for non-*Apis* bees (Hymenoptera: Apiformes). *Journal of the Kansas Entomological Society* 78: 373–380. <https://doi.org/10.2317/0410.03.1>

A new genus and species of Pristocerinae (Hymenoptera, Bethylidae) from upper Eocene Baltic amber with a review of conspecific association from insect fossils

Carly Melissa Tribull¹, Madeline V. Pankowski², Wesley Dondoni Colombo³

1 Farmingdale State College (State University of New York), Biology Department, Farmingdale NY, USA
2 Rockville, Maryland, USA **3** Universidade Federal do Espírito Santo, Departamento de Ciências Biológicas, Vitória ES, Brazil

Corresponding author: Carly Melissa Tribull (cmtribull@gmail.com)

Academic editor: Michael Ohl | Received 14 May 2021 | Accepted 15 June 2021 | Published 31 August 2021

<http://zoobank.org/9D5B00CA-75F0-4E1F-B847-11D490F769CD>

Citation: Tribull CM, Pankowski MV, Colombo WD (2021) A new genus and species of Pristocerinae (Hymenoptera, Bethylidae) from upper Eocene Baltic amber with a review of conspecific association from insect fossils. *Journal of Hymenoptera Research* 85: 119–133. <https://doi.org/10.3897/jhr.85.68658>

Abstract

A new extinct genus and species of Pristocerinae, †*Archeonesia eocena* Tribull, Pankowski & Colombo, **gen. et. sp. nov.**, are described from upper Eocene Baltic amber from the Yantary amber mine in the Kaliningrad region, Russia. Descriptions, remarks, illustrations, and comparisons to all extinct and extant Pristocerinae are provided. †*Archeonesia* is described as a new genus because neither the male nor the female can be placed in any previously described genera, although the female is most similar to *Acrenesia* and the male is most similar to *Cleistopyris*. Rare for Bethylidae, and Hymenoptera in general, this fossil contains both a male and female specimen that we are describing as conspecifics. A brief review from the paleoentomological literature is provided to describe how insect fossils containing evidence of reproductive behavior have been used to associate conspecifics in extinct species.

Keywords

Amber, Bethylidae, Eocene, fossil, Pristocerinae

Introduction

Bethylidae are a family of parasitoid wasps within the aculeate superfamily Chrysi-doidea that have a cosmopolitan distribution and are known for attacking lepidopteran and coleopteran hosts, including agricultural pests like the navel orangeworm, pink bollworm, and coffee berry borer (Gordh et al. 1983; Abraham et al. 1990; Azevedo et al. 2018). Currently, the family contains nearly 3,000 species in about 100 genera within five extant subfamilies (Bethylinae, Epyrinae, Mesitiinae, Pristocerinae, and Scleroderminae) and four extinct subfamilies (†Elektroepyrinae, †Lancepyrinae, †Holopsenellinae, and †Protopristocerinae) (Azevedo et al. 2018; Colombo et al. 2020a, b). There are about 90 flat wasps fossil species described, with the oldest known extinct Bethylidae coming from early Cretaceous amber deposits (Engel et al. 2016). However, the greatest number of fossil bethylids comes from the Eocene, specifically Oise, Rovno, and Baltic amber deposits (Colombo et al. 2020a, 2021).

With over 1,000 species in 26 genera, Pristocerinae are the most speciose subfamily within Bethylidae and are found worldwide (Azevedo et al. 2018; Colombo et al. 2020a, 2021). The subfamily is known for its remarkable sexual dimorphism, with males possessing robust bodies, wings, and conspicuous eyes and ocelli while females are wingless, lack ocelli, and have eyes that are extremely reduced or missing (Alencar et al. 2018). The vast majority of Pristocerinae species are known from ‘males-only’ or ‘females-only’ and conspecific associations between males and females are rare, typically the result of collecting specimens copulating or rearing them from the same host (Azevedo et al. 2016; Alencar et al. 2018; Chen and Azevedo 2020).

There are 15 extinct species of Pristocerinae in 10 genera, with the oldest species, †*Foenobethylus electriphilus* (Cockerell) known from mid-Cretaceous Burmese amber (Cockerell 1920; Falières and Nel 2019, 2020; Colombo et al. 2020a). Of these species, 11 are known from males only, three are known from females only, and only one species, *Pristocera skwarrae* (Brues), was described from a fossil that contained both a male and female. Additionally, Brues (1933) does not include any illustrations of the species and it was presumed to be lost during World War II (Colombo et al. 2021).

About 50% of extinct Bethylidae come from Baltic amber deposits dated to the late Eocene, including four of the 15 extinct Pristocerinae from the genera *Pseudisobrachium* Kieffer, *Cleistepyris* Kieffer, and *Pristocera* Klug (Colombo and Azevedo 2019; Colombo et al. 2021). Here we present a new extinct genus of Pristocerinae from Baltic amber, †*Archeonesia* Tribull, Pankowski & Colombo, gen. nov. with the type species †*A. eocena* Tribull, Pankowski & Colombo, sp. nov. Like the lost *Pristocera skwarrae*, this amber fossil shows both a male and female together, granting us the rare opportunity to describe both sexes for a new extinct bethylid genus.

Materials and methods

The specimens are embedded in Baltic amber sourced from the Yantarny mine in the Kaliningrad region. The piece was acquired from, trimmed, and polished by Marius

Veta and has clear dorsal and ventral views, although the lateral views are obscured by bubbles. The type material is deposited in the American Museum of Natural History, USA (AMNH, curator: David Grimaldi) with the specimen catalogue number AMNH_IZC 00361788.

The specimens were studied with an Olympus SZX-10 stereomicroscope and photomicrographs were acquired with a DP27 digital camera, using Olympus's Cellsens software. Multiple Z-stacks were compiled using Helicon Focus. The drawings were scanned and vectorized into Adobe Illustrator CS6 version 23.0.3, and images were edited and combined into a single plate using Adobe Photoshop CC.

Terminology for the integument and sculpturing follows Harris (1979) and general terms follow Lanes et al. (2020).

Systematic palaeontology

Family Bethylidae Haliday, 1839

Subfamily *Pristocerinae* Mocsáry, 1881

Genus †*Archeonesia* Tribull, Pankowski & Colombo, gen. nov.

<http://zoobank.org/6764DE3C-095F-4067-B96D-79706FF609C5>

Type-species. †*A. eocena* Tribull, Pankowski & Colombo, sp. nov. by original designation.

Description. Male (Figs 1–4). Head, pronotum, mesoscutum, metapectal-propodeal complex, petiole, antenna, and metasoma dark castaneous to black; wings hyaline. Head as long as wide and subquadrate, not globoid in lateral view. Clypeus with triangular median lobe, visible dorsally, lateral lobe reduced. Median clypeal carina delimited, lower than frons. Flagellomere longer than wide, with first flagellomeres larger than distal ones; flagellar pubescence erected; pedicel shorter than flagellomere I, apex dilated. Eye located touching mandibular base, glabrous, bulging. Frons weakly coriaceous, punctures large and sparse. Frontal line not visible. Ocellus large, salient. Frontal angle of ocellar triangle in obtuse angle. Anterior ocellus posterior to supraocular line. Occipital carina present. Dorsal pronotal area wider than long, weakly coriaceous, punctures small and sparse. Metafurcal pit oval. Posterior mesofurcal pit crown-shaped. Notaulus present, large, converging posteriorly, smooth. Parapsidal signum shorter than notauli. Forewing with three cells closed (C, R, 1Cu), distal flexion line visible, 2r-rs&Rs vein tubular, long, well pigmented, angled, not converging posteriorly to anterior margin, R1 vein tubular, long. Pterostigma enlarged, lanceolate. Mesoscutum-mesoscutellar sulcus present, posterior margin strongly incurved medially. Metanotum well-developed medially. Metapectal-propodeal disc not visible. Mesotibia without spines. Metasoma polished. Ninth abdominal segment with margin weakly incurved, undivided.

Female (Figs 1–3, 5). Head, pronotum, mesoscutum, metapectal-propodeal complex, petiole, antenna, and metasoma light to dark brown. Head longer than wide and rectangular, not globoid in lateral view. Clypeus with median lobe trapezoidal,

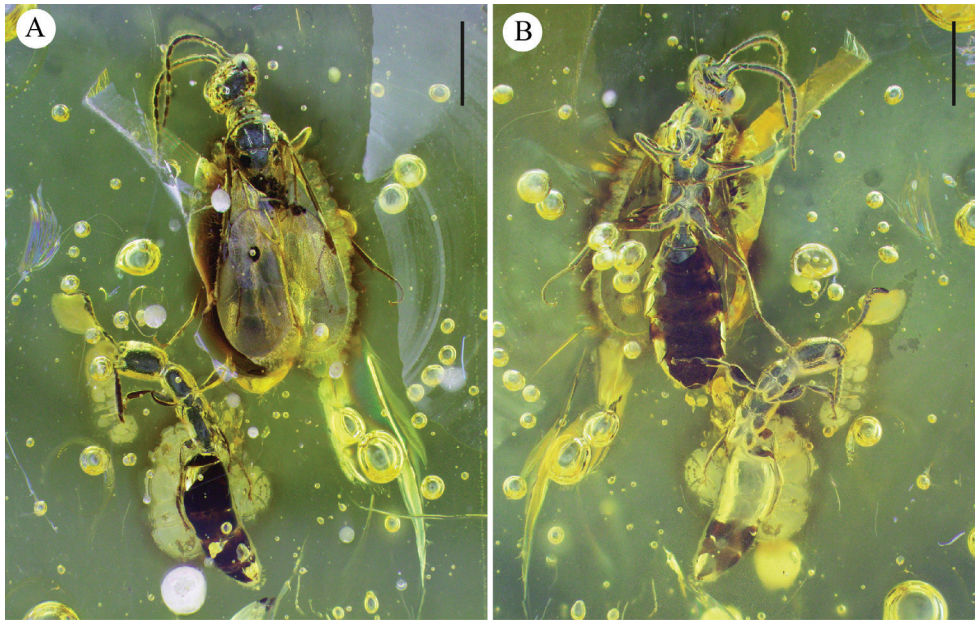


Figure 1. †*Archeonesia eocena* Tribull, Pankowski & Colombo, gen. et. sp. nov. **A** dorsal habitus of male holotype and female allotype **B** ventral habitus of male holotype and female allotype. Scale bars: 1 mm (**A,B**).

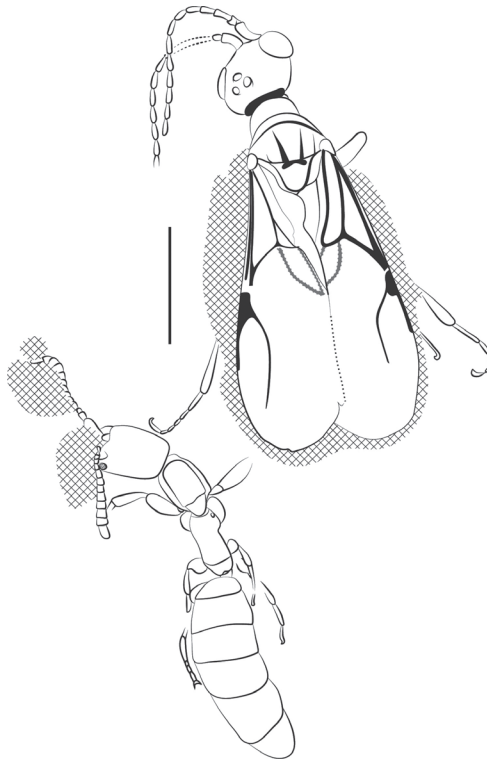


Figure 2. †*Archeonesia eocena* Tribull, Pankowski & Colombo, gen. et. sp. nov. Illustration of dorsal habitus of male holotype and female allotype. Scale bar: 1 mm.



Figure 3. †*Archeonesia eocena* Tribull, Pankowski & Colombo, gen. et. sp. nov. Illustration of ventral habitus of male holotype and female allotype. Scale bar: 1 mm.

visible dorsally, lateral lobe reduced. Median clypeal carina not visible. Flagellomere as long as wide, with first flagellomeres wider than distal ones; flagellar pubescence appressed; pedicel barrel shaped, as long as flagellomere I. Eye located almost touching mandibular base, glabrous, reduced, flat. Frons weakly coriaceous, punctures small and sparse. Frontal line not visible. Ocelli absent. Dorsal pronotal area smooth, longer than mesoscutellum medially. Metafurcal pit oval. Posterior mesofurcal pit oval. Anteromesoscutum with anterior margin straight. Notaulus absent. Parapsidal signum absent. Mesoscutum-mesoscutellar sulcus absent. Mesopleuron visible dorsally, broad. Apterous. Mesotibia spinose. Metapectal-propodeal disc long, broadly in contact with anteromesoscutum, anterior margin wider than posterior one, lateral margin almost parallel in dorsal view, weak constriction at spiracles present. Second abdominal segment without flap expanded laterally.

Etymology. The name †*Archeonesia* comes from the genus *Acrenesia*, which the female is closest to. The prefix 'Archeo' represents the extinct nature of the genus. Gender feminine.

Included species. †*A. eocena* sp. nov.

Distribution. Baltic amber, Russian Federation.

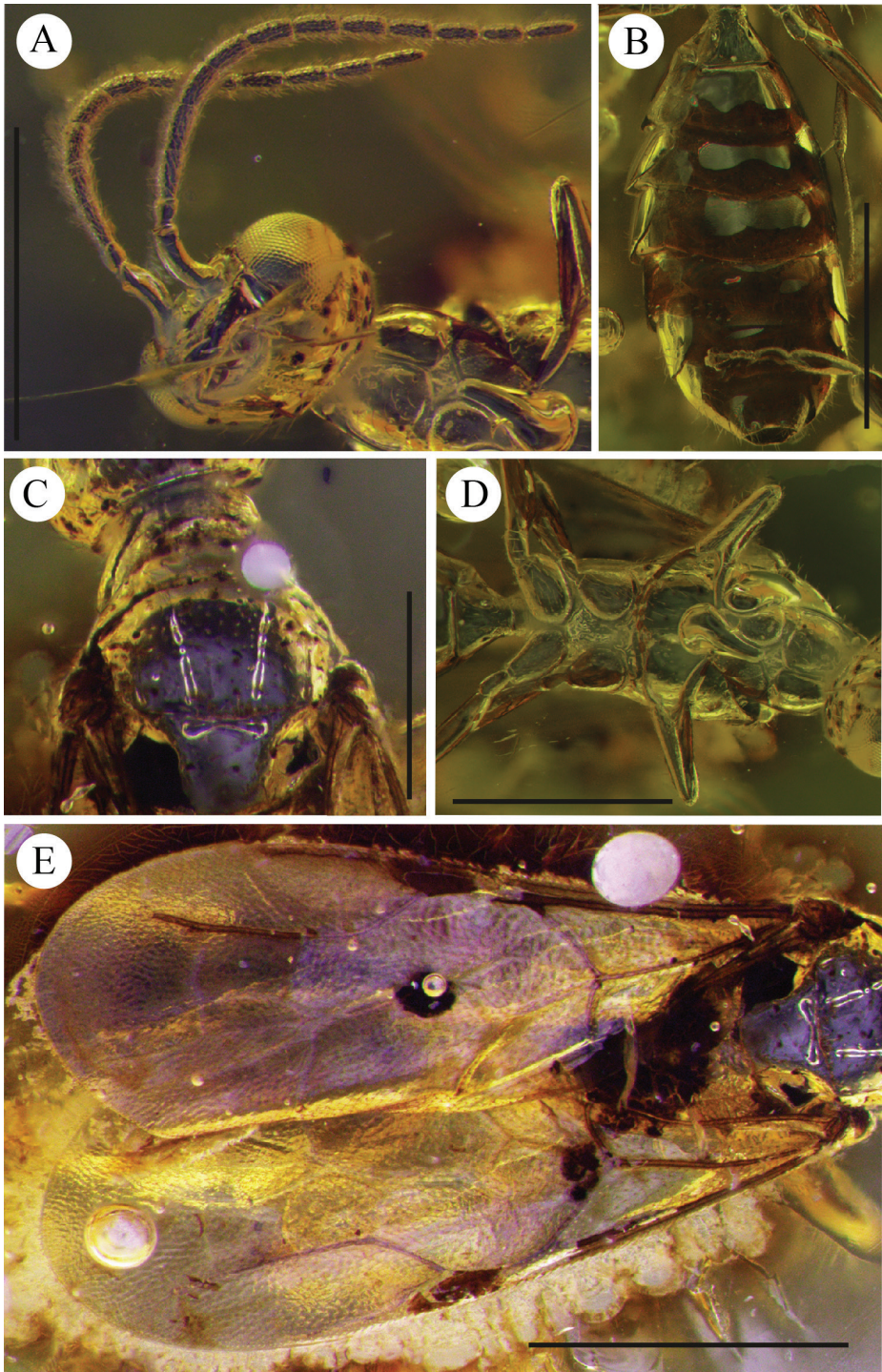


Figure 4. †*Archeonesia eocena* Tribull, Pankowski & Colombo, gen. et. sp. nov., male holotype **A** head, ventro-frontal view **B** metasoma, ventral view **C** prothorax and mesothorax, dorsal view **D** mesosoma, ventral view **E** wings, dorsal view. Scale bars: 500 μ m (**C**); 1 mm (**A**, **B**, **D**, **E**).



Figure 5. †*Archeonesia eocena* Tribull, Pankowski & Colombo, gen. et. sp. nov., female allotype **A** habitus, dorsal view **B** habitus, ventral view **C** head, ventro-lateral view **D** eye, with red arrow pointing to lower margin. Scale bars: 650 μ m (**D**), 1 mm (**A–C**).

†*Archeonesia eocena* Tribull, Pankowski & Colombo, sp. nov.

<http://zoobank.org/DD4A55F3-1F38-4415-A91D-C9FD28E8B287>

Description. Male holotype (Figs 1–4). Same as the genus, except for the following features: body length 4.0 mm. Mandible pentadentate. Palpal formula 5:3. Genitalia not visible.

Female allotype (Figs 1–3, 5). Same as the genus, except for the following features: body length 3.30 mm. Mandible not unidentate, either bidentate or tridentate, but obscured by bubbles in resin. Palps obscured. Metasoma polished.

Type material. Holotype, deposited at the AMNH Invertebrate Zoology Collection (specimen catalogue number AMNH_IZC 00361788). Two complete flat wasps are embedded in amber measuring about 21 mm × 11 mm. There are numerous bubbles, but no other syninclusions.

Etymology. The species epithet *eocena* represents the geological epoch the species is known from.

Stratigraphic horizon. Priabonian, 33.9 to 37.7 million years ago (Cohen et al. 2020), upper Eocene.

Discussion

The specimens considered here were assigned to the subfamily Pristocerinae based on the following character states, in the key from Azevedo et al. (2018), for males: (1) the forewings without Rs+M veins, (2) the metanotum is well-developed medially; and for females: (1) the wings are absent, (2) the eyes are very reduced, and (3) the ocelli are absent.

The male specimen studied here does not have visible important morphological characters, mainly from the genitalia, which does not allow the correct identification of the genus. We performed comparisons with males of all 23 known pristocerine genera, excluding *Anisobrachium* Kieffer, †*Ekaterina* Colombo & Azevedo (in Colombo et al. 2020a) and *Scaphepyris* Kieffer, because these genera are known only from females.

The male of this species has the ninth abdominal segment undivided and with the posterior margin weakly concave. For this reason, this species does not belong to †*Eopristocera* Falières & Nel, *Pristocera* Klug, *Prosapenesia* Kieffer, *Propristocera* Kieffer and *Pristonesia* Alencar & Azevedo (in Alencar et al. 2018), because the males of *Pristocera* have the ninth abdominal segment divided into two lobes and the males of †*Eopristocera*, *Prosapenesia*, *Propristocera* and *Pristonesia* have the ninth abdominal segment with the posterior margin strongly concave.

The male of this species does not belong to *Dissomphalus* Ashmead, *Protisobrachium* Benoit and *Trichiscus* Benoit, because those males have the clypeus with median and lateral lobes not well outlined, whereas †*A. eocena* sp. nov. has the clypeus with median lobe clearly defined and lateral lobes reduced.

Additionally, the median clypeal lobe of †*A. eocena* sp. nov. is projected forward, triangular, and the median clypeal carina is lower than frons, and for this reason, this

species does not belong to *Acrenesia* Alencar & Azevedo (in Alencar et al. 2018), *Dracunesia* Alencar & Azevedo (in Alencar et al. 2018), *Eleganesia* Alencar & Azevedo (in Alencar et al. 2018), *Epynesia* Alencar & Azevedo (in Alencar et al. 2018), *Pristepyris* Kieffer and †*Uniceratops* Colombo & Azevedo (in Colombo et al. 2020), because the males of *Pristepyris* have the median clypeal lobe short and truncate; the males of *Eleganesia* also have the median clypeal lobe short and with apical margin outcurved; males of *Acrenesia* and *Dracunesia* have the median clypeal lobe trapezoidal; males of *Epynesia* have the median clypeal lobe very projected and sharply angulated, and the male of †*Uniceratops* has the median clypeal carina higher than frons, horn-shaped.

†*A. eocena* sp. nov. has the dorsal pronotal area with the lateral and anterior margins distinct and for this reason, this species does not belong to *Apenesia* Westwood, *Afgoiogfa* Argaman, *Foenobethylus* Kieffer and *Parascleroderma* Kieffer, because the males of these genera have the dorsal pronotal area with the lateral and anterior margins barely distinct. Additionally, the males of the last three genera, together with *Austranesia* Alencar & Azevedo (in Alencar et al. 2018), have the prepectus very large, about 0.25× mesopectus length, whereas the male of this species has the prepectus reduced, about -0.15× mesopectus length.

The male of this species does not belong to *Caloapenesia* Terayama, *Calobrachium* Gobbi & Azevedo and *Pseudisobrachium* Kieffer, because these males have the eyes very setose, and the median clypeal lobe is usually trapezoidal, whereas †*A. eocena* sp. nov. has the eyes glabrous and the median clypeal lobe triangular, as aforementioned.

The last possible genus is *Cleistepyris* Kieffer. However, males of *Cleistepyris* have the forewings with the junction of 2r-rs and Rs veins almost indistinct, pterostigma triangular, and the R cell as wide as 1Cu cell, and for this reason, this species does not belong to *Cleistepyris*, because the male of this species has the forewings with the junction of 2r-rs and Rs veins distinct, pterostigma lanceolate, and the R cell wider than 1Cu cell. Finally, due to the male morphological differences aforementioned, we are allocating this species to a new genus.

We concluded that the female is the same species as the male (see below), and we studied the female morphology to support the allocation of this species in a new genus. The female specimen studied here does have important morphological characters visible and because of this, we used the key proposed by Azevedo et al. (2018, p. 57–58). Following the key, it would go to the genus *Acrenesia*, because of the following characters: (1) the head is longer than wide; (2) the clypeus with the median lobe trapezoidal; (3) the eyes with more than one facet; (4) the mesonotum is triangular, short, transverse, and much wider than long; (5) the mesopleuron is quite large and is reaching at least the anterior third of metapectal-propodeal complex, in dorsal view; (6) the anterior portion of the metapectal-propodeal complex is slightly narrower than posterior one; (7) the metapectal-propodeal complex with inconspicuous constriction near the spiracles; and (8) the second abdominal segment without flap expanded laterally. However, †*A. eocena* sp. nov. has the pronotum as wide as the metapectal-propodeal complex, in dorsal view; and anteromesoscutum with anterior margin straight; whereas *Acrenesia* has the pronotum wider than the metapectal-propodeal complex, in

dorsal view; and anteromesoscutum with anterior margin incurved. Only †*Ekaterina* is not included in the pristocerine key of Azevedo et al. (2018, p. 57–58), because this genus was published later by Colombo et al. (2020a). †*Ekaterina* has the mesonotum somewhat diamond-shaped and metapectal-propodeal disc with strongly evident constriction; however, †*A. eocena* sp. nov. has the mesonotum triangular and metapectal-propodeal disc with weakly evident constriction. So, this female does not belong to any known pristocerine genera, and we are describing it as a new genus.

The amber fossil contains both a male and female specimen of Pristocerinae, an occurrence of conspecifics in the subfamily that has only previously been recovered in *Pristocera skwarrae*, which was never photographed or drawn, and was lost in World War II (see Colombo et al. 2021). While the two specimens were not preserved copulating, we have chosen to assign them to the same species as conspecifics. To justify this decision, we reviewed the paleoentomological literature concerning the association of conspecifics in fossils and found three main reasons why authors choose to associate specimens in the same fossil as conspecifics: 1) The specimens were preserved during copulation, 2) the specimens present evidence that copulation just occurred or was about to occur, and 3) knowledge of reproductive and/or social behavior of extant relatives was used to justify the association.

When previously undescribed insects are preserved during copulation, authors describe them as the same species – examples have been found in both rock impressions and amber fossils from a variety of different terrestrial arthropods. For example, in Li et al. (2013), a rock compression fossil from the middle Jurassic of China shows two froghoppers copulating with the male's aedeagus inserted into the female. In Klimov and Sidorchuk (2011) and Sidorchuk and Klimov (2011), a pair of copulating mites were redescribed from upper Eocene Baltic amber. Although there are other records of insects (especially Diptera) being preserved while mating in amber or as rock compressions, these publications broadly focus on describing behavior instead of acting as new species records (Grimaldi and Engel 2005; Takahashi et al. 2017).

Taxonomic records written from insects preserved while unequivocally copulating are rare, and more common are examples in which specimens are presumed to have already mated or were engaged in mating behavior. Evidence provided by the authors typically relies on the close proximity of supposed conspecifics, evidence of reproductive behaviors (like grasping), or evidence of exposed genitalia. For example, in Fischer and Hörnig (2019), the authors describe a new species of Tineidae from a male and female preserved in Baltic amber, arguing that the orientation of abdomens and genitalia, plus the rarity of moths in Baltic amber (less than 1% of all inclusions), means that it is unlikely the fossil represents a random co-occurrence. In Andersen and Poinar (1998), a new species of water strider was described from a Dominican amber piece that contained a male grasping a female, a position that suggests that they were trapped just before, during, or after mating. From Burmese amber, Chen and Su (2019) described a new species of Zoraptera in which copulation was suspected based on the identification of the male's intromittent organ.

Finally, authors also rely on knowledge of extant relatives' behavior to suggest that male and female conspecifics were preserved before, during, or just after mating. From

Mexican amber, Macadam and Ross (2016) describe two mayfly imagos (a male and female) as the same species, suggesting that it's unlikely the pair would have been caught in the same amber if not during a mating swarm given the short lifespan of extant adult Ephemeroptera. From mid-Cretaceous Burmese amber, a new species of dance fly was described from possible conspecifics with the justification that extant dance flies only form aggregations during courtship and mating. The authors also rely on possible evidence of the consumption of a nuptial meal by the female and sexual dimorphism in the inflated antennae of the male (Zhang et al. 2021). Gregarious mating behavior is also used as a justification for conspecific association of a whitefly species, especially given that all previous extinct Aleyrodidae were only known from individual specimens (Szwedo and Drohojowska 2016). From Upper Cretaceous Burmese amber, Cockx and Mckellar (2018) described a new genus and species of Crabronidae from two males and a female, noting that the co-occurrence of the three could be due to either social behavior (as seen in extant relatives) or evidence of mating. It should also be noted that there are examples in the taxonomic literature in which no justification is given to support the association of conspecifics beyond the preservation of a male and female together (Szadziewski and Grogan 1998; Fanti and Kupryjanowicz 2017). Similarly, there are instances where authors do not assign potential conspecifics to the same species, but instead place them in the same genus (Wichard et al. 2020). Within Bethylidae, there have only been two other instances of sexual association entirely from fossils – the aforementioned †*Pristocera skwarrae* and †*Lytopsenella maritima* Ramos and Azevedo (from the subfamily Bethylinae). Beyond being found in the same amber piece, Brues (1933) does not provide justification for the former, and Ramos et al. (2014) cite shared anatomical features (sexual dimorphism is low in the species) and preservation in the same piece.

Herein, we associate the male and female syninclusions as conspecifics based on our knowledge of the reproductive behavior of extant *Pristocerinae*. Female *Pristocerinae* are apterous and rarely collected by the same methods that commonly capture winged males. Occasionally, males and females will be captured attached (in copula) from Malaise traps and yellow pan traps as a result of phoretic copulation, in which the male transports the female while mating (Azevedo et al. 2016; Chen and Azevedo 2020). Phoretic copulation is observed in several Hymenopteran families with extreme sexual dimorphism, such as Tiphiidae, Mutillidae and Bethylidae, and is hypothesized as a method to aid in the dispersal of apterous females in need of hosts or food sources (Azevedo et al. 2016; Vivallo 2021). The male and female described here might have been trapped in resin millions of years ago, much in the same way that an extant male *Pristocerinae* occasionally transports his mate to her demise.

In addition to †*A. eocena* sp. nov., four other species of *Pristocerinae* are known from Baltic amber deposits – †*Pristocera skwarrae*, †*Cleistopyris baryonyx* Colombo, Gobbi & Azevedo, †*Pseudisobrachium elatus* (Brues), and †*Pseudisobrachium inhabilis* (Brues) (Colombo et al. 2020a, 2021). Besides Baltic amber, Rovno amber deposits are also linked to the upper Eocene and contain extinct *Pristocerinae* – †*Pseudisobrachium megalosaurus* Colombo, Gobbi & Azevedo, †*Pseudisobrachium stegosaurus* Colombo, Gobbi & Azevedo, and †*Cleistopyris allosaurus* Colombo, Gobbi & Azevedo (Colombo

et al. 2020a). Given that Baltic amber from the Kaliningrad region has been extracted for more than a century and averages much greater yields than Rovno amber from Ukrainian mines in recent years, it's possible that †*A. eocena* sp. nov., might also be recovered from Rovno amber (Colombo et al. 2021). This possibility is reinforced by the finding that 50% of Rovno amber Hymenoptera fauna are also found in Baltic amber (Perkovsky 2018).

Of the upper Eocene Pristocerinae, *Cleistepyris*, *Pristocera*, and *Pseudisobrachium* are known from both extant and extinct species, while †*Archeonesia* is only known from the extinct species described here. From lower Eocene Oise amber, there is also the extinct monotypic genus *Eopristocera*. While extant *Pristocera* are known from the Palearctic (as well as other parts of the world), extant *Cleistepyris* are known only from Nearctic and Neotropical regions, and extant *Pseudisobrachium* are primarily found in southern distributions and common in the neotropics, which demonstrates how the biogeography of Pristocerinae has changed since the Eocene (Azevedo et al. 2018; Colombo et al. 2020a). The end of the Eocene marked the start of a cooling period, which likely drove the extinction of thermophile bethylids like †*Archeonesia* and †*Eopristocera*, as well as the local extinction of *Cleistepyris* in Europe (Bogri et al. 2017).

Conclusion

Compared to other Bethyridae families like Epyrinae (30 species) and Bethylinae (20 species), there are fewer records of extinct Pristocerinae (Ramos et al. 2014; Azevedo et al. 2018; Colombo et al. 2021). With the description of †*Archeonesia eocena*, there are now 16 extinct species of Pristocerinae. Given that Pristocerinae are the most speciose and abundant subfamily of Bethyridae, it is interesting that it would rank third in extinct diversity. However, this could be due to the extreme sexual dimorphism within the subfamily reducing the number of individuals that were captured in resin – unlike Pristocerinae, most females of Bethylinae and Epyrinae can fly. In Epyrinae and Bethylinae, more than 65% of fossil records are from females, but in Pristocerinae, the opposite is seen with more than 70% of fossil records from males, suggesting that when the female is winged in Bethyridae, the chances are greater that a specimen will be preserved as a fossil.

Finally, extinct Bethyridae known from both sexes are extremely rare. In addition to †*Pristocera skwarrae*, one other extinct species of Bethyridae is known from both sexes. In Bethylinae, one species (representing 5% of extinct bethylines), †*Lytopenella maritima*, is known and the association was justified by the weak sexual dimorphism and proximity of the specimens in the amber. In Epyrinae, one species (representing 3% of all extinct epyrines), *Epyris staphylinoides* (Hope), is known for only one extinct male and other extant males and females, so the association was not performed by representatives in the same fossil. While we hope for the discovery of more fossils that have preserved both sexes of a species together, it is likely that their occurrence will continue to be rare in Bethyridae.

Acknowledgements

We thank the subject editor Dr. Michael Ohl, Dr. Evgeny Perkovsky and one anonymous reviewer for their valuable suggestions. The authors are thankful for the resources and support from their home institutions and research departments. CMT thanks the biology department and office of the provost at Farmingdale State College (State University of New York), as well as the American Museum of Natural History for accessioning the fossil. WDC thanks CAPES – Demanda Social for its Ph.D. scholarship. Additionally, we are thankful for the generosity of the Pankowski family in supporting paleontological research through their donation of fossils to research institutions.

References

- Abraham YJ, Moore D, Godwin G (1990) Rearing and aspects of biology of *Cephalonomia stephanoderis* and *Prorops nasuta* (Hymenoptera: Bethyridae) parasitoids of the coffee berry borer, *Hypothenemus hampei* (Coleoptera: Scolytidae). *Bulletin of Entomological Research* 80: 121–128. <https://doi.org/10.1017/S000748530001333X>
- Andersen NM, Poinar GO (1998) A marine water strider (Hemiptera: Veliidae) from Dominican amber. *Insect Systematics & Evolution* 29: 1–9. <https://doi.org/10.1163/187631298X00131>
- Alencar IDCC, Waichert C, Azevedo CO (2018) Opening Pandora's box of Pristocerinae: molecular and morphological phylogenies of *Apenesia* (Hymenoptera, Bethyridae) reveal several hidden genera. *Systematic Entomology* 43: 481–509. <https://doi.org/10.1111/syen.12295>
- Azevedo CO, Alencar IDCC, Ramos MS, Barbosa DN, Colombo WD, Vargas JMR, Lim J (2018) Global guide of the flat wasps (Hymenoptera, Bethyridae). *Zootaxa* 4489: 1–1. <https://doi.org/10.11646/zootaxa.4489.1.1>
- Azevedo CO, Colombo WD, Alencar IDCC, Brito CD de, Waichert C (2016) Couples in phoretic copulation, a tool for male-female association in highly dimorphic insects of the wasp genus *Dissomphalus* Ashmead (Hymenoptera: Bethyridae). *Zoologia (Curitiba)* 33: e20160076. <https://doi.org/10.1590/s1984-4689zool-20160076>
- Bogri A, Solodovnikov A, Żyła D (2018) Baltic amber impact on historical biogeography and palaeoclimate research: oriental rove beetle *Dysanabatium* found in the Eocene of Europe (Coleoptera, Staphylinidae, Paederinae). In: Smith A (Ed.) *Papers in Palaeontology* 4: 433–452. <https://doi.org/10.1002/spp2.1113>
- Brues, CT (1933) The parasitic hymenoptera of the Baltic amber Part I. *Bernstein-forschungen* 3: 4–172.
- Chen H, Azevedo CO (2020) Discovery of a couple of *Foenobethylus* (Hymenoptera, Bethyridae) in copulation suggests a synonym under *Parascleroderma*. *Journal of Asia-Pacific Entomology* 23: 1241–1247. <https://doi.org/10.1016/j.aspen.2020.10.001>
- Chen X, Su G (2019) A new species of *Zorotypus* (Insecta, Zoraptera, Zorotypidae) and the earliest known suspicious mating behavior of Zorapterans from the mid-cretaceous amber

- of northern Myanmar. *Journal of Zoological Systematics and Evolutionary Research* 57: 555–560. <https://doi.org/10.1111/jzs.12283>
- Cockerell TDA (1920) XXXVI. Fossil arthropods in the British Museum. I. *Annals and magazine of Natural History* 5: 273–279. <https://doi.org/10.1080/00222932008632376>
- Cockx PFD, McKellar RC (2018) A new genus and species of the subfamily Pempredoninae (Hymenoptera: Crabronidae) in Upper Cretaceous amber from Myanmar. *Comptes Rendus Palevol* 17: 153–157. <https://doi.org/10.1016/j.crpv.2017.10.004>
- Cohen, KM, Harper DAT, Gibbard PL (2020) ICS international chronostratigraphic chart 2020/03. International Commission on Stratigraphy, IUGS. www.stratigraphy.org [accessed 10 May 2021.]
- Colombo WD, Azevedo CO (2019) Synopsis of the fossil Scleroderminae (Hymenoptera, Bethyridae) with description of a new genus and four new species from Baltic amber. *Historical Biology* 33: 630–638. <https://doi.org/10.1080/08912963.2019.1650275>
- Colombo WD, Gobbi FT, Perkovsky EE, Azevedo CO (2020a) Synopsis of the fossil Pristocerinae (Hymenoptera, Bethyridae), with description of two new genera and six species from Burmese, Taimyr, Baltic and Rovno ambers. *Historical Biology*: 1–17. <https://doi.org/10.1080/08912963.2020.1733551>
- Colombo WD, Perkovsky EE, Azevedo CO (2020b) Phylogenetic overview of flat wasps (Hymenoptera, Bethyridae) reveals Elektroepyrinae, a new fossil subfamily. *Palaeoentomology* 3: 269–283. <https://doi.org/10.11646/palaeoentomology.3.3.8>
- Colombo WD, Perkovsky EE, Waichert C, Azevedo CO (2021) Synopsis of the fossil flat wasps Epyrinae (Hymenoptera, Bethyridae), with description of three new genera and 10 new species. *Journal of Systematic Palaeontology* 19: 39–89. <https://doi.org/10.1080/14772019.2021.1882593>
- Engel MS, Ortega-Blanco J, Azevedo CO (2016) A new bethylid wasp in Lebanese Early Cretaceous amber (Hymenoptera: Chrysidoidea), with comments on other Mesozoic taxa. *American Museum Novitates* 2016: 1–14. <https://doi.org/10.1206/3855.1>
- Falières E, Nel A (2019) A new bethylid wasp from the Lowermost Eocene Oise amber, France (Insecta: Hymenoptera). *Palaeoentomology* 2: 211–214. <https://doi.org/10.11646/palaeoentomology.2.3.2>
- Falières E, Nel A (2020) First fossil of the extant flat wasp genus *Dissomphalus* Ashmead, 1893 (Hymenoptera: Bethyridae: Pristocerinae). *Zoosystema* 42: e207. <https://doi.org/10.5252/zoosystema2020v42a15>
- Fanti F, Kupryjanowicz J (2017) A new genus of soldier beetles from Baltic amber. *Acta Palaeontologica Polonica* 62. <https://doi.org/10.4202/app.00388.2017>
- Fischer T, Hörnig M (2019) Mating moths (Tineidae, Ditrysia, Lepidoptera) preserved as frozen behavior inclusion in Baltic Amber (Eocene). *Palaeontologia Electronica*. <https://doi.org/10.26879/829>
- Gordh G, Woolley JB, Medved RA (1983) Biological studies on *Goniozus legneri* Gordh (Hymenoptera: Bethyridae) a primary external parasite of the navel orangeworm *Amyelois transitella* and pink bollworm *Pectinophora gossypiella* (Lepidoptera: Pyralidae, Gelechiidae). *Contributions of the American Entomological Institute* 20: 433–468.
- Grimaldi D, Engel MS (2005) *Evolution of the Insects*. Cambridge University Press.

- Harris RA (1979) A glossary of surface sculpturing. Occasional papers in Entomology 28: 1–31.
- Klimov PB, Sidorchuk EA (2011) An enigmatic lineage of mites from Baltic amber shows a unique, possibly female-controlled, mating: ENIGMATIC MITE FROM BALTIC AMBER. *Biological Journal of the Linnean Society* 102: 661–668. <https://doi.org/10.1111/j.1095-8312.2010.01595.x>
- Lanes GO, Kawada R, Azevedo CO, Brothers DJ (2020) Revisited morphology applied for Systematics of flat wasps (Hymenoptera, Bethyridae). *Zootaxa* 4752: 1–127. <https://doi.org/10.11646/zootaxa.4752.1.1>
- Li S, Shih C, Wang C, Pang H, Ren D (2013) Forever Love: The Hitherto Earliest Record of Copulating Insects from the Middle Jurassic of China. *PLoS ONE* 8: e78188. <https://doi.org/10.1371/journal.pone.0078188>
- Macadam CR, Ross AJ (2016) A New Species of Mayfly, *Maccaffertium annae* sp. nov. (Ephemeroptera: Heptageniidae) from Mexican Amber (Miocene). *Boletín de la Sociedad Geológica Mexicana* 68: 1–5. <https://doi.org/10.18268/BSGM2016v68n1a1>
- Perkovsky EE (2018) Only a half of Species of Hymenoptera in Rovno Amber Fauna is Common with Baltic Amber. *Vestnik Zoologii* 52: 353–360. <https://doi.org/10.2478/vzoo-2018-0037>
- Ramos MS, Perkovsky EE, Rasnitsyn AP, Azevedo CO (2014) Revision of Bethyridae fossils (Hymenoptera: Bethyridae) from Baltic, Rovno and Oise amber, with comments on the Tertiary fauna of the subfamily. *Neues Jahrbuch für Geologie und Paläontologie – Abhandlungen* 271: 203–228. <https://doi.org/10.1127/0077-7749/2014/0385>
- Sidorchuk EA, Klimov PB (2011) Redescription of the mite *Glaesacarus rhombeus* (Koch & Berendt, 1854) from Baltic amber (Upper Eocene): evidence for female-controlled mating. *Journal of Systematic Palaeontology* 9: 183–196. <https://doi.org/10.1080/14772019.2011.566585>
- Szadziewski R, Grogan Jr, William L (1998) Biting midges from Dominican amber. III. Species of the tribes Culicoidini and Ceratopogonini (Diptera: Ceratopogonidae). 12: 1–15.
- Szwedo J, Drohojowska J (2016) A swarm of whiteflies—the first record of gregarious behavior from Eocene Baltic amber. *The Science of Nature* 103: 1–35. <https://doi.org/10.1007/s00114-016-1359-y>
- Takahashi Y, Sutou M, Yamamoto S (2017) The Compression Mating Fossil of Sciarid Fly (Diptera: Sciaridae) from Shiobara, Tochigi Prefecture, Japan. *Paleontological Research* 21: 288–292. <https://doi.org/10.2517/2016PR031>
- Vivallo, F (2021) Phoretic copulation in Aculeate (Insecta: Hymenoptera) a review. *Zoological Journal of the Linnean Society* 191: 627–636. <https://doi.org/10.1093/zoolinnean/zlaa069>
- Wichard W, Espeland M, Müller P, Wang B (2020) New species of caddisflies with bipectinate antennae from Cretaceous Burmese amber (Insecta, Trichoptera: Odontoceratidae, Calamoceratidae). *European Journal of Taxonomy*: 17. <https://doi.org/10.5852/ejt.2020.653>
- Zhang S, Xie S, Zhang Y, Wang B, Zhang P, Zeng X, Yu Y (2021) A new species of dance fly (Diptera, Empidoidea, Atelestidae) from mid-Cretaceous Burmese amber. *Cretaceous Research* 118: e104660. <https://doi.org/10.1016/j.cretres.2020.104660>

Red wood ants in Bulgaria: distribution and density related to habitat characteristics

Vera Antonova¹, Martin P. Marinov¹

¹ Department of Animal Diversity and Resources, Institute of Biodiversity and Ecosystem Research, Bulgarian Academy of Sciences, 2 Gagarin Street, 1113 Sofia, Bulgaria

Corresponding author: Vera Antonova (vera_antonova@yahoo.com)

Academic editor: F. Hita Garcia | Received 6 December 2020 | Accepted 15 June 2021 | Published 31 August 2021

<http://zoobank.org/20891081-AF4D-4C4E-8277-FF103168927B>

Citation: Antonova V, Marinov MP (2021) Red wood ants in Bulgaria: distribution and density related to habitat characteristics. Journal of Hymenoptera Research 85: 135–159. <https://doi.org/10.3897/jhr.85.61431>

Abstract

The only National Inventory of red wood ants in Bulgaria was carried out about 50 years ago (1970–1973). *Formica rufa* Linnaeus, 1761, *F. pratensis* Retzius, 1783, *F. lugubris* Zetterstedt, 1838 and *F. polycytena* (as *F. polycytena* × *rufa* hybrid) were found in a current monitoring programme. This study presents data on their current distribution and nest density, and provides more details about the habitat requirements for conservation purposes. Field studies were carried out by the transect method along the main mountainous areas in Bulgaria. We found 256 nests of red wood ants along 172 transects. The most abundant species was *F. lugubris*, followed by *F. rufa* and *F. pratensis*. Among the environmental variables, the elevation, exposure, ecological groups of plants, stone cover, grass cover, canopy cover and forest age appeared as significantly related to the presence and nest density of red wood ants.

Keywords

Balkans, conservation, *Formica rufa* group, habitat preferences, monitoring method

Introduction

Being territorial species, the *Formica rufa* species group, known as red wood ants (RWA), plays a keystone role in the forest ecosystems (Gösswald 1990). Out of thirteen Palearctic species of *Formica rufa* group, ten are present in Europe: *Formica* (*Formica*) *rufa* Linnaeus, 1761, *F.* (*F.*) *lugubris* Zetterstedt, 1838, *F.* (*F.*) *paralugubris* Seifert,

1996, *F. (F.) helvetica* Seifert, 2021, *F. (F.) polycytena* Foerster, 1850, *F. (F.) pratensis* Retzius, 1783, *F. (F.) aquilonia* Yarrow, 1955, *F. (F.) truncorum* Fabricius, 1804, *F. (F.) dusmeti* Emery, 1909 and *F. (F.) frontalis* Santschi, 1919 (Seifert 2021). Despite the comprehensive studies of this group (Otto 1960, 1968; Dlussky 1967; Pavan and Ronchetti 1972; Cherix 1977; Gösswald 1989, 1990; Czechowski 1996; Stockan and Robinson 2016), its taxonomy remains unclear (Maeder et al. 2005; Bernasconi et al. 2010, 2011; Korczynska et al. 2010; Seifert 2018, 2021). Detailed information about the distribution and habitat preferences of RWA is much needed to evaluate population changes and to develop conservation and management strategies (Sorvari and Hakkarainen 2007; Freitag et al. 2008, 2016a, b; Dekoninck et al. 2010, 2014; Breen 2014; Chen and Robinson 2014; Vandegehuchte et al. 2017). Research on habitat features in respect of RWA presence and density typically addresses particular species only, and such studies from the Balkans are rather descriptive and scarce (Tsikas et al. 2016; Çamlitepe and Aksoy 2019).

Nest density estimation of RWA varies among different regions. Risch et al. (2016) summarized data, collected from different European countries and Russia, and reported a maximum of 20 nests/ha, as usually the density is under 5 nests/ha. Nest destruction, air and heavy metal pollution, collection of ant pupae for food for cage birds were reported as the main reasons for low nest densities in Central Europe (Domisch et al. 2005). Additional reasons could also be the variation in climate and differences in habitat characteristics in each country, the different methods of counting the nests and their density, interspecies interactions, etc. RWA often establish their colonies through social parasitism, i.e. the founder-queen uses ready nests of *Formica fusca* (Czechowski et al. 2012), therefore, RWA nest density depends also on the density of their host. Another factor is the presence of their competitors (Savolainen and Vepsäläinen 1988).

Climate, light conditions, productivity and food resource availability seem to be key factors determining the distribution of ant mounds in Finland (Kilpeläinen et al. 2005). According to Vandegehuchte et al. (2017), the RWA abundance in Switzerland depends mainly on the slope aspect, climate, forest structure and conifer abundance but not on the forest fragment size, distance to forest edges, or woody vegetation diversity. Serttaş et al. (2020) reported altitude, aspect, canopy closure, landform, nest substrate and slope as significant habitat variables for *F. rufa* translocation success in Turkey. RWA avoid north-facing slopes and prefer south-, south-west- or west-facing exposure of the slopes (Risch et al. 2016). In the temperate zone, the subalpine *F. lugubris* commonly occurs at a higher elevation of mountainous areas, whereas *Formica rufa* prefers their lower parts (Seifert 2018).

For the UK forest region, Chen and Robinson (2014) reported that in shadier areas the nest size of *F. lugubris* is bigger but the canopy cover had no relation with the number of nests. In Finland *F. rufa* and *F. polycytena* have similar frequencies in an open and closed canopy, while the other RWA prefer mostly open spaces (Punntila and Kilpeläinen 2009).

The presence of conifers is a key factor for RWA existence (Vandegehuchte et al. 2017) but they prefer mixed forests to pure coniferous ones (Rosengren et al. 1979). Domisch et al. (2005) reported a statistically significant difference between nest density in a mature and young boreal forest in Finland.

RWA in Bulgaria have been under protection since 1959 (Izvestiya 1959). The first summarised records about RWA in Bulgaria were published by Otto et al. (1962). A National Inventory of RWA in Bulgaria was carried out in 1970–1973 and the results are given by Bobev (1972, 1973) and Vatov and Bobev (1976). Though these results are currently outdated, they represent a basis for an assessment of the long-term trends in the dynamics of RWA populations in Bulgaria. There is scarce information about the field methodology of the inventory: “Detailed visit of all plantations and discovery of available ant nests” (Bulgarian State Archives). Only a few Forestries keep archive details for registering the nests, fencing, marking and numbering them, filling the field form and collecting samples. In Smolyan Forestry 91 nests had been fenced with wooden cross-beams. It is not clear how exactly the nests have been counted (quadrates, transects or other methods). Detailed, quantitative data about habitat characteristics were not reported.

The last summarized literature data about the findings of RWA in Bulgaria are given by Lapeva-Gjonova et al. (2010). Later, occasional localities were published by Lapeva-Gjonova (2011, 2013), Lapeva-Gjonova and Rucker (2011), Lapeva-Gjonova and Santamaria (2011), Lapeva-Gjonova and Kiran (2012), Lapeva-Gjonova and Ilieff (2012), Antonova et al. (2016) and Lapeva-Gjonova et al. (2021).

The RWA species from Bulgaria – *Formica lugubris*, *F. polyctena*, *F. pratensis*, *F. rufa*, *F. aquilonia* and *F. truncorum* – are considered species of special conservation measures in Europe (IUCN 2021). Except for *F. truncorum*, they all are recognized as Lower Risk /Near Threatened species. All of them are included in CORINE biotopes checklist (Annex 4). In addition, *F. rufa* is protected by the Bulgarian Biodiversity Act (2002), Annex 2 and 3. However, the conservation needs of RWA are underestimated (Sorvari 2016). RWA need proper breeding habitats to support their huge colonies with feeding territory up to a few tens of square kilometres (Savolainen and Vepsäläinen 1988). We need detailed information about their habitats that could advance the conservation policy and management of territories occupied by RWA, thus protecting them more effectively. In monitoring programs, nest density should be used as a dependent variable to assess the population dynamics by quantitative analyses (Delabie et al. 2000). Predictive models describe the relationship between species’ distribution and their environment allowing researchers to assess habitat quality by monitoring nests of RWA species (Freitag et al. 2016a).

The present study aims to assess the present distribution, nest density of the red wood ants in Bulgaria, as well as to examine their relationships with environmental variables and to assess the most appropriate habitat characteristics for conservation purposes.

Material and methods

Study area

The study was carried out during a monitoring project between May 2013 and September 2014 in the mountainous areas in Bulgaria. The field studies were conducted in 11 sampling sites in the following mountains: Rila, Pirin, Belasitsa, Vitosha, Osogovo, Western Stara Planina, Central Stara Planina, Eastern Stara Planina, Western Rhodopes, Eastern Rhodopes and Strandza (Fig. 1). In the fieldwork of the recent monitoring project, the efforts were concentrated on the most suitable habitats of RWA in places with registrations of literature data.

Sampling method

For the four ant species, sampling transects were set in areas with appropriate homogeneous biotopes. For a homogeneous biotope, a continuous polygon was taken from

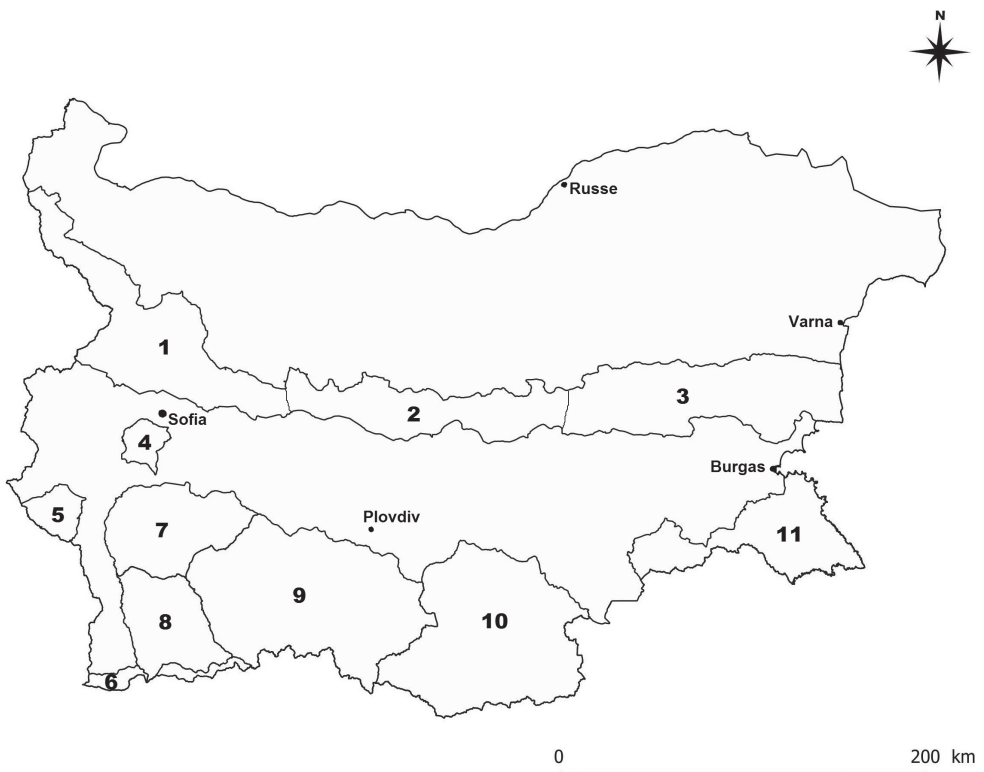


Figure 1. The eleven sampling monitoring sites (mountains): **1** Western Stara Planina, **2** Central Stara Planina, **3** Eastern Stara Planina, **4** Vitosha, **5** Osogovo, **6** Belasitsa, **7** Rila, **8** Pirin, **9** Western Rhodopes, **10** Eastern Rhodopes, **11** Strandza.

the potential habitat of each species, which was falling within a single monitoring area characterised by similar environmental features. Potential habitats are predetermined by mapping patterns or on the terrain. Potential habitat GIS models for each target RWA were made using the “intersect” tool of ArcGIS 10 with polygon vector layers of Bulgarian Forest GIS database: Dominant tree type, Canopy cover <80%, Forest age: young (<50 years), middle (50–100), old (>100 years) and Elevation according to the ecological preferences of each species by literature data for Bulgarian populations (Atanassov and Dlusskij 1992).

According to the Bulgarian landscape characteristics and specifics, we used a combination of sampling methods from other countries in the temperate climatic zone (Cherix 1977; Domisch et al. 2005; Cherix et al. 2007, 2012; Hughes and Broome 2007; Gotelli et al. 2011; Borkin et al. 2012; Zakharov et al. 2013, and Breen 2014).

In each selected monitoring area, a minimum of 8 sampling transects of 250 m and a width of 5 m were examined (i.e. 2 km length in total and 1250 m² per transect) across a homogeneous biotope (Borkin et al. 2012). In total, 172 sampling transects (21.5 ha) were selected. Eight to 29 transects were sampled per site (i.e. at least 10 000 m²) (Peřtal and Pisarski 1966). Transects were separated by at least 10 meters to avoid counting nests twice (Leponce et al. 2004). Each transect was visited once per year during the daylight from May to the end of September. In each transect, one GPS point was taken at the beginning of it, one at its end and one point per each localised nest inside the transect (by Garmin MAP 60CS). Thus, the same transects could be used for future monitoring studies.

The separate nests (active and abandoned) were counted, with a diameter greater than 20 cm (Domisch et al. 2005; Zakharov et al. 2013). Each nest was digitally photographed, including the surrounding vegetation within a radius of up to 30 m (Cherix et al. 2007, 2012). At least 10 ant specimens were taken from each nest in 95% ethanol (Bestelmeyer et al. 2000). All the samples were preserved in the collection of V. Antonova at the IBER, Bulgarian Academy of Sciences, Sofia.

The nests’ description and environmental variables were filled in a field form (see Suppl. material 1). One field form was completed for each transect.

Nests’ description:

1. Nest number: number of nests of each species within one sampling transect (1250 m²)

2. Nest measurements and identification:

- * Diameter of the nest (± 5 cm) (for further monitoring);
- * Height of the nest (± 5 cm) (vertically from the ground level to the top of the nest, for further monitoring);

* Active/abandoned: Binary variable (abandoned: for further monitoring) (Domisch et al. 2005); A mound with workers only passing on it was not considered as an active.

* Species. The determination of the species was done in a laboratory using the identification keys of Atanassov and Dlusskij (1992); Czechowski et al. (2012) and Seifert (2018).

* Cluster of colonies (more than one mound per colony): Binary variable (yes/no). It was noted whether the nest was isolated or there was a cluster formed (Hughes and Broome 2007) by observing the workers' behaviour by „transplant experiments”: when a worker from one nest being placed near another nest is aggressively attacked by the others, the nests belong to different colonies (Kaspari 2000).

Predictor variables recorded were related to the topography and habitat characteristics of each sampling transect. Data for the first 10 variables were taken in situ as approximate assessment, based on the whole transect range:

1. Elevation: based on GPS current data.
2. Exposure of the slope (based on a compass) 8 variables: N, NW, W, SW, S, SE, E, NE.
3. Slope as degrees in 4 classes: 0–5, 6–15, 16–30, >30 degrees.
4. Ecological groups of plants (adapted for Bulgaria, Lyubenova 2004), defined by dominant plants species in respect of their adaptations to soil and air humidity in 5 categories: xerophytes (low humidity – succulents, *Euphorbia falcata*, *Dianthus petraeus*, *Poa bulbosa*, etc.); meso-xerophytes (drought-tolerant – *Hypericum perforatum*, *Adonis vernalis*, *Potentilla argentea*, *Quercus pubescens*, etc.); mesophytes (moderate humidity – *Bellis perennis*, *Festuca pratensis*, *Medicago arabica*, *Alcea rosea*, etc.); meso-hygrophytes (increased moisture affinity – *Ranunculus sceleratus*, *Carex distans*, *Juncus bufonis*, etc.); hygrophytes (high moisture – mosses, *Caltha palustris*, *Epilobium hirsutum*, *Oxalis acetosella*, etc.).
5. Stone cover as percentage in 5 classes: 0–5%, 6–25%, 26–50%, 51–75%, 76–100%.
6. Habitat type in 7 categories by EUNIS habitat classification (<https://www.eea.europa.eu/data-and-maps/data/eunis-habitat-classification>, Level 1 and 2; ecotones added): coniferous forest, ecotone of coniferous forest, broadleaved deciduous forest, ecotone of deciduous forest, mixed forest, ecotone of mixed forest, grasslands.
7. Grass cover as a percentage in 4 classes: <25%, 25–49%, 50–74%, 75–100%.
8. Canopy cover as a percentage in 5 classes: <20%, 20–40%, 41–60%, 61–80%, >80%.
9. Undergrowth (shrub) density as a percentage in 4 classes: <5%, 6–25%, 26–50%, 51–100%.
10. Dominant tree species of the forest in 12 categories: *Picea abies*, *Pinus sylvestris*, *Pinus nigra*, *Pinus mugo*, *Pinus peuceledreichii*, *Pinus* spp. with *Fagus* spp., *Juniperus* spp., *Fagus* spp., *Quercus* spp., *Castanea sativa*, single trees (fruit trees), grass (open habitat). Identification keys according to Delipavlov et al. (2003) were used.
11. Forest mean age as years in 4 classes: 0–50, 51–100, 101–150, >150. The data were taken from the Bulgarian Forest GIS database (www.agrolesproject.com/cgi-bin/agrol?m=med6).

Data analyses

Nest density calculations for each monitoring site were based on the total number of nests of the particular species and the total area of its sampling transects. For each monitoring site, the study surface area (the number of transects) increased proportionally to the area of the appropriate forest habitats for RWA.

Non-parametric statistics were used as our data have not normal distribution and could not be normalised by a transformation. The species represented by < 5 mounds were not included in the statistical analyses as they were too rare. Binomial logistic regression with a logit link function was used for a detailed study of the predictive significance of all independent variables (elevation, exposure, slope, ecological groups of plants, stone cover, grass cover, canopy cover, undergrowth and forest age) for the likelihood of the presence of each species. For all models, we started with a full model and followed a backward stepwise selection procedure to eliminate the effects that were furthest from statistical significance. Only the final models were presented. The categorical variables Habitat and Dominant tree were excluded from the statistical analysis because they consisted of too many levels while there were too few cases relative to the number of levels.

Spearman rank order correlation test was used for searching correlations among nest density of each species and the predictor variables used in the logistic regression analysis (missing data were pairwise deleted). All statistical analyses, except circular-linear correlation tests between exposure and ant species nest density, were performed using JASP 0.14.1. The circular-linear correlation tests and graphs were conducted with ORIANA 3.21.

Results

Distribution and nest density of RWA in Bulgaria

A total of 256 mounds (active and abandoned) were found in 10 of the 11 studied sites and 104 (61%) of the 172 sampling transects (see Suppl. material 2: Table S1). The 229 active nests (89%) belonged to four RWA species: *F. lugubris*, *F. rufa*, *F. pratensis* and *F. polycтена x rufa* (Table 1). Abandoned nests were 27 (11%).

The most abundant species was *Formica lugubris* with 100 nests (44%), followed by *F. rufa* with 91 nests (40%), *F. pratensis* with 35 nests (15%) and the hybrid *F. polycтена x rufa* with 3 nests (1%). The average nest density of the four species was 11.1 nests/ha. The distribution of the nests is presented on the potential habitats' maps for *F. pratensis* (Fig. 2A), *F. rufa* (Fig. 2B) and *F. lugubris* (Fig. 2C).

The number of the recorded ant nests varied across the studied mountain ranges (Table 1). In Pirin Mt the greatest number of nests (63) was found, followed by Western Rhodopes (47) and Rila (35). In the remaining regions, between 0 and 18 nests were registered in each.

The most abundant population of *F. lugubris* was found in Pirin (43 nests, 14 nests/ha) and Western Rhodope Mts (35 nests, 12 nests/ha); *F. rufa* was most

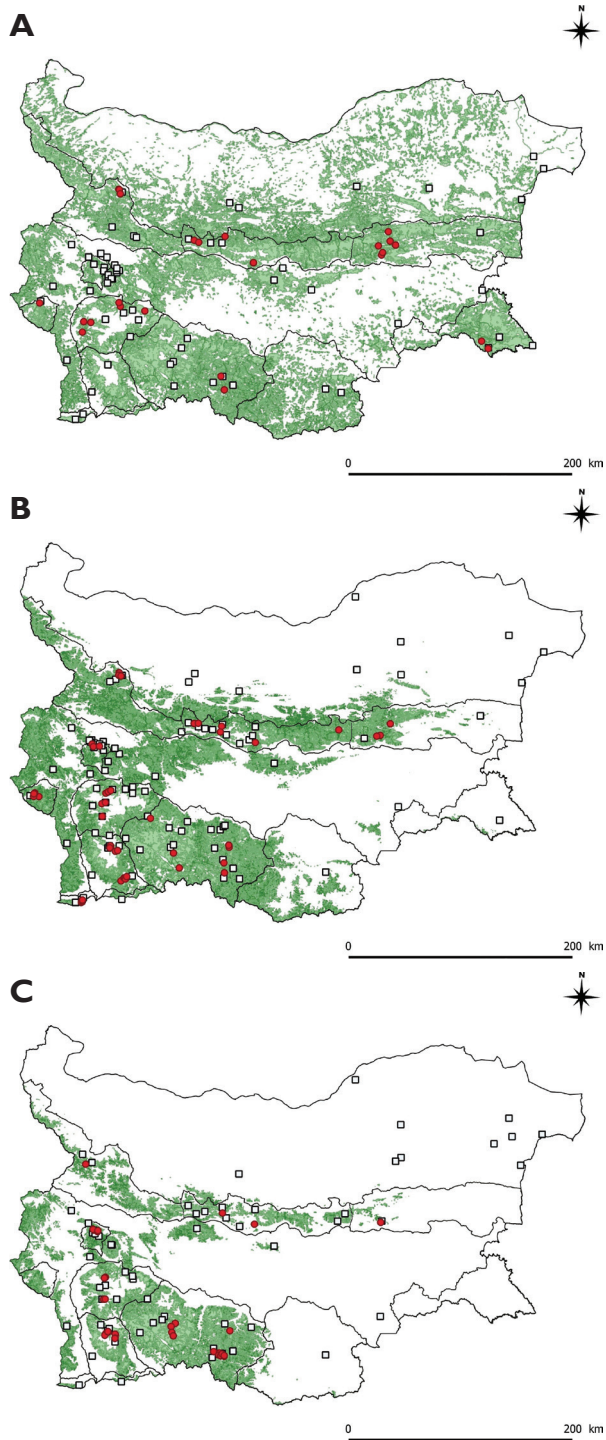


Figure 2. Potential habitats of RWA in Bulgaria. Localities (transects) recorded in the course of the present study are designated (red dots), previous literature data (squares) **A** *Formica pratensis* **B** *Formica rufa* **C** *Formica lugubris*.

Table 1. Number of red wood ants' active nests by monitoring territories in mountainous areas of Bulgaria.

Mountain range	Nest numbers					Activity %	Transects number	Hectares	Nest number/ ha
	<i>Formica rufa</i>	<i>Formica polyctena</i> x <i>rufa</i>	<i>Formica pratensis</i>	<i>Formica lugubris</i>	Total				
Western Rhodopes	11	0	1	35	47	92	24	3	16.3
Eastern Rhodopes	0	0	0	0	0	-	8	1	0
Vitosha	4	0	0	7	11	92	10	1.3	10.8
Osogovo	15	0	1	0	16	100	9	1	16
Belasitsa	13	0	0	0	13	63	9	1	13
Pirin	17	1	0	43	61	87	25	3	21
Rila	15	2	9	9	35	94	29	4	8.75
Western Stara Planina	5	0	5	1	11	87	9	1	11
Central Stara Planina	8	0	7	3	18	95	25	3	6
Eastern Stara Planina	3	0	10	2	15	88	16	2	7.5
Strandza	0	0	2	0	2	100	8	1	2
Total number	91	3	35	100	229	-	172	-	-
Average						90		21.3	11.1

abundant in Belasitsa (13 nests and 13 nests/ha), Pirin (17 nests, about 5.5 nests/ha), Western Rhodope Mts (11 nests and 3.7 nests/ha), Rila and Osogovo (15 nests and about 3 nests/ha per each); *F. pratensis* – in Eastern Stara Planina (10 nests, about 5 nests/ha) and Rila (9 nests, about 2 nests/ha). Four of the 91 fenced nests of *F. lugubris* in Smolyan Forestry (Western Rhodope Mts) were found (Fig. 3).

**Figure 3.** One of the four active *Formica lugubris* nests fenced 50 years ago.

Table 2. Results from binomial logistic regression for *F. pratensis*. Only independent variables selected by the backward stepwise procedure are listed. Marked coefficients are significant at $p < 0.05$ level. $N = 172$.

Parameter	Estimate	Standard Error	Odds Ratio	z	Wald Test		
					Wald Statistic	df	p
(Intercept)	-10.735	4.377	2.176e-5	-2.453	6.016	1	0.014
Elevation	-0.002	0.001	0.998	-2.728	7.440	1	0.006
Slope	0.735	0.376	2.085	1.956	3.826	1	0.050
Grass cover	2.333	1.041	10.308	2.240	5.019	1	0.025

Note: *F. pratensis* presence coded as class 1.

Table 3. Results from binomial logistic regression for *F. rufa*. Only independent variables selected by the backward stepwise procedure are listed. Marked coefficients are significant at $p < 0.05$ level. $N = 172$.

Parameter	Estimate	Standard Error	Odds Ratio	z	Wald Test		
					Wald Statistic	df	p
(Intercept)	-1.878	0.790	0.153	-2.377	5.651	1	0.017
Elevation	0.001	0.001	1.001	2.444	5.973	1	0.015
Stone cover	-0.476	0.208	0.621	-2.295	5.267	1	0.022
Forest age	0.007	0.005	1.007	1.473	2.171	1	0.141

Note: *F. rufa* presence coded as class 1.

Table 4. Results from binomial logistic regression for *F. lugubris*. Only independent variables selected by the backward stepwise procedure are listed. Marked coefficients are significant at $p < 0.05$ level. $N = 172$.

Parameter	Estimate	Standard Error	Odds Ratio	z	Wald Test		
					Wald Statistic	df	p
(Intercept)	-32.514	9.220	7.572e-15	-3.526	12.436	1	< .001
Elevation	0.019	0.006	1.019	3.313	10.974	1	< .001
Slope	1.137	0.613	3.117	1.854	3.439	1	0.064
Ecological groups of plants	1.345	0.842	3.839	1.598	2.555	1	0.110
Stone cover	0.658	0.428	1.931	1.538	2.364	1	0.124
Canopy cover	-1.649	0.696	0.192	-2.370	5.618	1	0.018

Note: *F. lugubris* presence coded as class 1.

Formica aquilonia and *F. truncorum* were not found in our samplings during the survey. Similar to RWA *Formica (Coptoformica) exsecta* and *Formica (Raptiformica) sanguinea* were recorded in samples from the same monitoring sites.

Factors influencing the presence and density of RWA

The studied species had specific altitudinal distribution, though partly overlapping. *Formica pratensis* was found between 320 and 1173 m, *F. rufa* between 537 and 1650 m, and *F. lugubris* between 1040 and 2240 m. The elevation was a statistically significant predictor of the presence of the three RWA, with a higher probability for *F. pratensis* to be found at a lower elevation, and for *F. rufa* and *F. lugubris* to be present at higher elevations (Table 2–4; Fig. 4A).

Exposure was significantly correlated with the nest density of *F. lugubris* (Table 5) and showed a bidirectional (axial) distribution. The highest nest density corresponded to either NE-E or SW-W nest exposure (Fig. 5). Since the exposure of *F. lugubris* nests

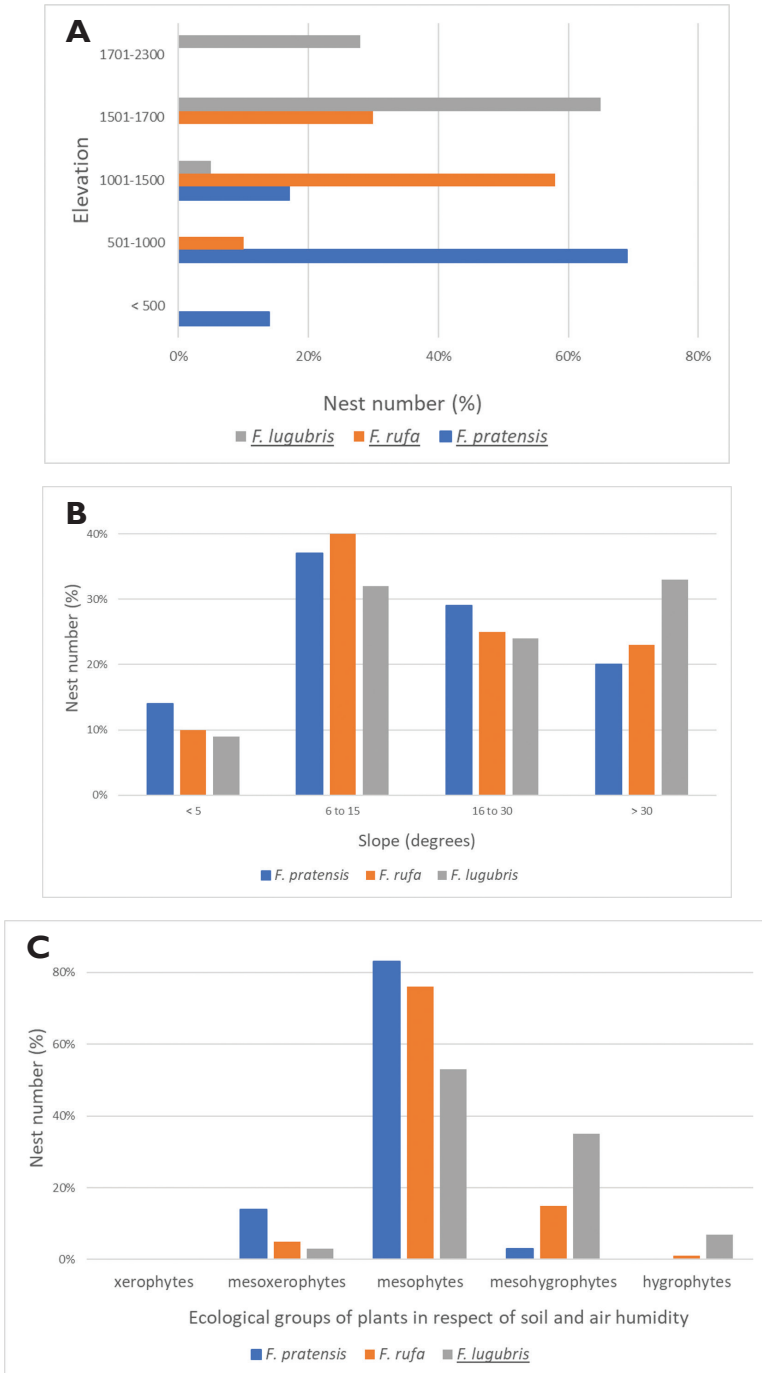


Figure 4. Distribution of RWA by studied variables in percentage by species (*F. pratensis*: N = 35, *F. rufa*: N = 91, *F. lugubris*: N = 100) **A** elevation **B** slope **C** ecological groups of plants **D** stone cover **E** grass cover **F** canopy cover **G** dominant tree **H** forest age (transects with unknown values are excluded). For underlined species the impact is statistically significant.

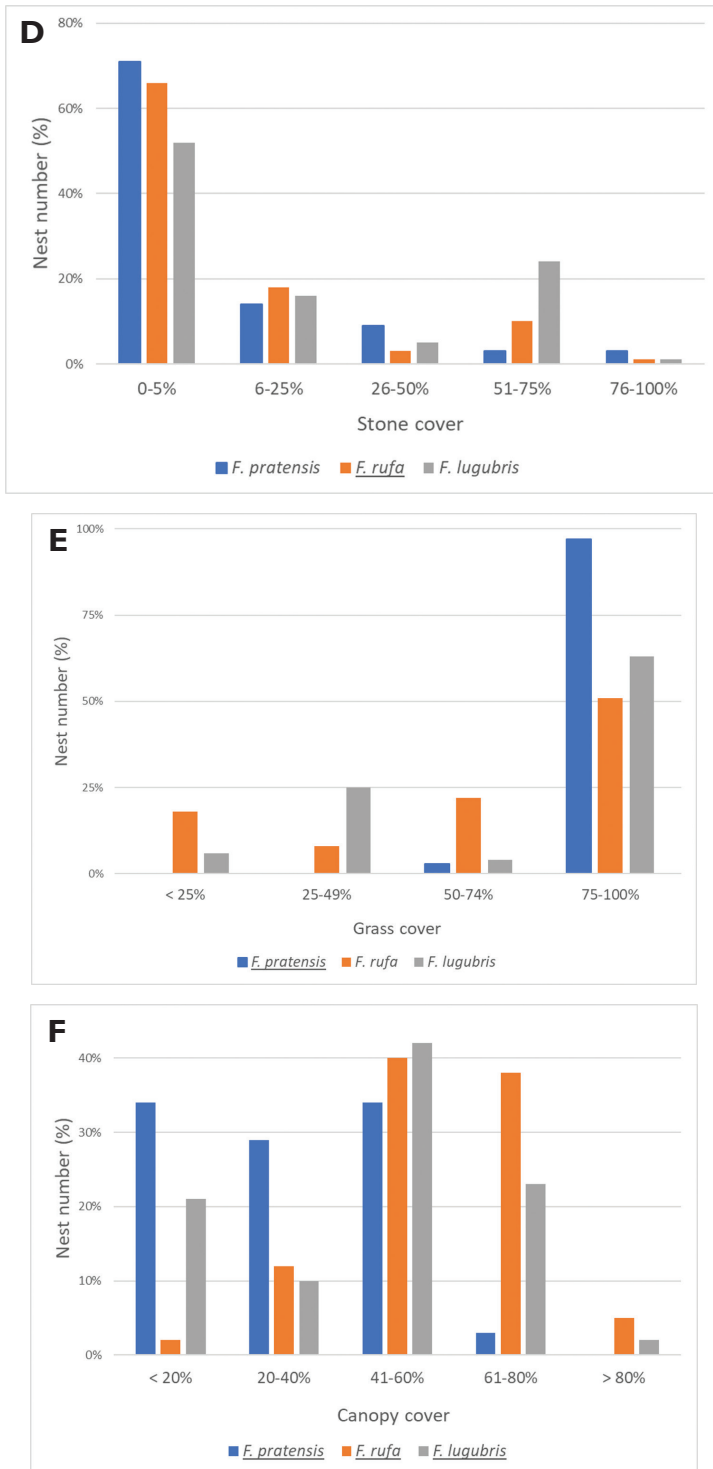


Figure 4. Continued.

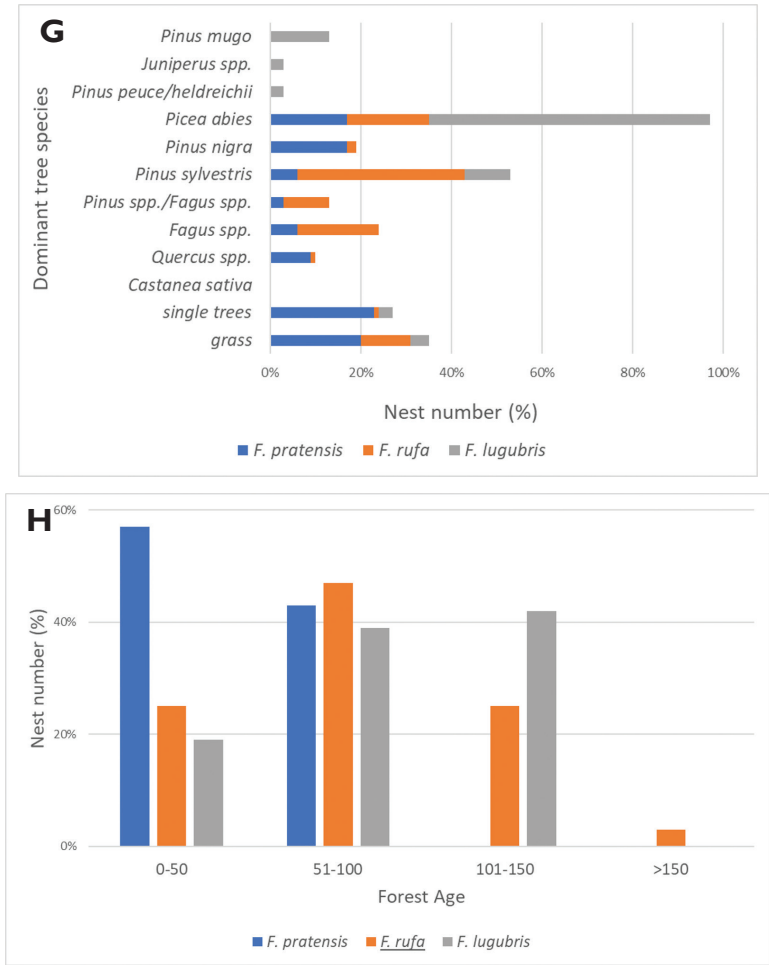


Figure 4. Continued.

was also significantly correlated with elevation, with NE-E exposure corresponding to higher elevations and SW-W exposure to lower elevations ($r = 0.401$, $p = 0.006$, $n = 34$), we suppose that our results reflect rather an interrelationship of exposure with elevation and, perhaps, some other environmental parameters than exposure by itself.

The slope was a marginally significant predictor of *F. pratensis* and *F. lugubris* presence (Table 2, 4; Fig. 4B).

Along a moisture gradient, the ecological groups of plants were significantly correlated with the nest density of *F. lugubris* (Table 5). Most of its nests were found where mesophytes (53%) and meso-hygrophytes (35%) were dominant plants, and nests were rarely recorded in places where meso-xerophytes and xerophytes dominated (Fig. 4C).

All RWA species were most common at the lowest (0–5%) level of stone cover, however, this variable was a significant negative predictor of *F. rufa* presence only, and was negatively correlated with its nest density (Tables 3, 5; Fig. 4D).

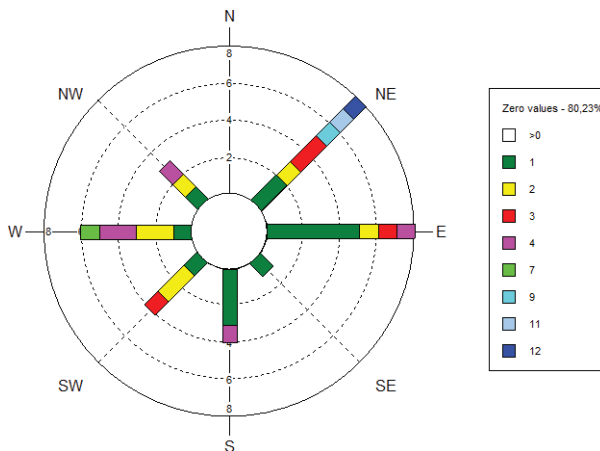


Figure 5. A histogram of *F. lugubris* nest density and exposure. The frequency distribution of the nest number recorded at any particular direction is represented by different colours. For better visualisation, zero values are excluded.

Table 5. Spearman rank order correlations between a number of nests of each ant species and environmental variables. Marked correlations are significant at $p < 0.05$.

Variable	n	<i>F. pratensis</i>		<i>F. rufa</i>		<i>F. lugubris</i>	
		r(s)	p	r(s)	p	r(s)	p
Elevation	172	-0.290	< .001	0.222	0.003	0.628	< .001
Exposure *	172	0.016	0.955	0.113	0.115	0.173	0.007
Slope	172	-0.053	0.493	-0.053	0.494	0.011	0.885
Ecological groups of plants	172	-0.077	0.317	0.104	0.173	0.313	< .001
Stone cover	172	-0.136	0.075	-0.196	0.010	-0.030	0.700
Grass cover	172	0.289	< .001	-0.002	0.980	0.135	0.078
Canopy cover	172	-0.281	< .001	0.199	0.009	-0.101	0.189
Underwood	172	-0.111	0.146	0.075	0.329	-0.016	0.839
Forest age	128	-0.142	0.110	0.209	0.018	0.134	0.131

*Circular-linear correlation coefficient, range from 0 to 1.

Most of the nests of examined RWA species were found in habitats with 75–100% grass cover. This variable significantly predicted the presence of *F. pratensis* only and correlated positively with its nest density (Tables 2, 5; Fig. 4E).

Canopy cover negatively predicted the presence of *F. lugubris* (Table 4). Additionally, canopy cover was negatively correlated with the nest density of *F. pratensis* and positively correlated with the nest density of *F. rufa* (Table 5; Fig. 4F). *Formica pratensis* preferred habitats with canopy cover from 0 up to 60% and was lacking in habitats with canopy cover over 80%. *Formica rufa* had peaks of nest numbers between 40 and 80% of the canopy cover as the nests were situated on light spots in forests’ interiors. The majority of nests of *F. lugubris* (42%) were found at 40–60% and 21% of them at 0–20% canopy cover.

A great percentage (37%) of the nests of all studied species were found in the habitats of *Picea abies* (Fig. 4G). No RWA were found in *Castanea sativa* forests. In habitats with *Juniperus* sp., *Pinus peuce*, *P. heldreichii* and *P. mugo* we met only *F. lugubris*. In

total, 65% of the nests of *F. rufa* were found within or in the vicinity of *P. sylvestris* forests, mixed forests with *Fagus* spp. or deciduous forests of *Fagus* spp.

Concerning the forest age, there was a significant positive correlation with the nest density of *F. rufa* (Table 5). This species was met even in forests older than 160 years, but the highest density was recorded in forests between 70 and 100 years old (Fig. 4H).

None of the species showed a statistically significant correlation with undergrowth density.

Discussion

Species diversity of RWA in Bulgaria at present

Most of the known localities of the particular RWA species (*F. lugubris*, *F. pratensis* and *F. rufa*) were confirmed in our study. The new findings are marked in the Suppl. material 2: Table S1. In all monitoring sites (except Eastern Rhodope Mts), at least one RWA species has been found. *Formica lugubris* was expected (Lapeva-Gjonova et al. 2010) but not found in the transects of Belasitsa and Osogovska Mts. It should be searched at a higher elevation. *Formica rufa* was also expected in Eastern Rhodope Mts and Strandza Mt. In Eastern Rhodope Mts the species should be searched for in the southern parts of the mountain. For Strandza Mt, it has been reported by Bobev (1972); Vatov and Bobev (1976); Wesselinoff (1979) and Vesselinov (1981) and should be searched also at a higher elevation. *Formica pratensis* was not found in our sampling transects on Pirin, Vitosha and Belasitsa Mt but mounds were found in all these mountains out of the transects.

Formica polyctena was not recorded in the course of the present study. Bobev (1972), Keremidchiev et al. (1972) and Vatov and Bobev (1976) reported also that *F. polyctena* is absent from the samples collected during the National Inventory of RWA (1970–1973). According to Bernhard Seifert (pers. comm. 2015), old data reported for *F. polyctena* from Bulgaria (Seifert 2008) are “a misplacement”. The three nests similar to *F. polyctena*, found in this research, were identified as *F. polyctena* x *rufa* and later confirmed by B. Seifert. Stable *F. polyctena* x *rufa* hybrid populations in Europe are known (Seifert 2018, 2021). There is no other recently published record on *F. polyctena* from Bulgaria either. So, we could accept Seifert’s opinion about the old findings: “The earlier findings of *F. polyctena* in Bulgaria, some 50 years ago, I suppose more likely to represent a misidentification rather than indicating a dying out process”.

Formica aquilonia was not found during our survey. If this species occurs in the country as reported for Rila Mt. at Zavrachitsa hut (Wesselinoff 1973) and Western Predbalkan at Belogradchik (Atanassov and Dlusskij 1992), its presence is probably very scarce. The samples identified as “*F. aquilonia*”, collected in 1982 from Bulgaria and preserved in the Senckenberg Museum of Natural History Görlitz, were kindly checked by B. Seifert in 2015 with modern taxonomic methods and were found to be seta-reduced *F. lugubris* (Pirin Mt) and seta-reduced *F. pratensis* (Rhodope Mts).

Table 6. Average nest density of RWA according to the National Inventory (1970–1973) and the recent survey (2013–2014). The non-target species *F. exsecta* and *F. sanguinea* were included in the percentage calculations for the sake of comparability with the National Inventory (1970–73) where these species have been initially included.

Regions grouped by RWA richness and abundance	Data from the National Inventory (1970–1973): Bobev (1972, 1973); Vatov and Bobev (1976): nest density and proportions	This study (2013–2014): nest density and proportions
Rich region	Central and Western Rhodopes: 0.3–0.6 nests/ha;	Pirin, Western Rhodopes (previous Central+Western Rhodopes), Osogovo: 16–21 nests/ha.
	<i>F. rufa</i> 47%; <i>F. lugubris</i> 42%; <i>F. pratensis</i> 10% and <i>F. exsecta</i> 0.5%.	<i>F. lugubris</i> 63%; <i>F. rufa</i> 35%; <i>F. pratensis</i> 1.6%; others (<i>F. polycytena x rufa</i> and non-target species) 0.4%.
Middle rich region	Rila and Pirin: 0.06 nests/ha.	Belasitsa, Western Stara Planina, Vitoshka: 10–13 nests/ha.
	<i>F. rufa</i> 37%; <i>F. lugubris</i> 37%; <i>F. pratensis</i> 22%; and <i>F. exsecta</i> 4%.	<i>F. rufa</i> 63%; <i>F. lugubris</i> 23%; <i>F. pratensis</i> 13.9%; non-target species 0.1%.
Middle poor region	Western and Central Stara Planina, Sredna Gora, Eastern Rhodopes and the mountains in West-SouthWest Bulgaria (Kraishte, Malashevska, Ograzden, Belasitsa): 0.01 nests/ha.	Rila, Central and Eastern Stara Planina: from 6 to 9 nests/ha.
	<i>F. pratensis</i> 49%; <i>F. rufa</i> 45%; <i>F. lugubris</i> 3% and <i>F. sanguinea</i> 3%	<i>F. pratensis</i> 38%; <i>F. rufa</i> 38%; <i>F. lugubris</i> 20%; others (<i>F. polycytena x rufa</i> and non-target species) 1%.
Poor region	Danube plain, Strandza and Eastern Stara Planina: 0.006/ha.	Strandza, Eastern Rhodopes: up to 2 nests/ha.
	Dominant species: <i>F. pratensis</i> 79%; <i>F. rufa</i> 20% and non-target species 1%.	Dominant species: <i>F. pratensis</i>

Nest densities and habitat requirements

The average nest density (11.1 nests/ha) is greatly increased compared to that calculated at the National Inventory 1970–1973 (0.1 nests/ha) given by Bobev (1972, 1973) and Vatov and Bobev (1976) (see Table 6). The reasons are the different sampling methodology, the difference in the calculation of the nest density, and the concentration of efforts for the studied species in the most suitable habitats during the fieldwork of this project.

Regarding the field's methodology of the Inventory, there is scarce information in the Bulgarian State Archives and it is difficult to compare the results with confidence. Nevertheless, the confirmation of the localities and the new findings are extremely valuable from the conservation viewpoint.

As seen from the comparative Table 6, Western Rhodope Mts were the richest of the RWA region in 1970 and still, they are. The majority of the nests in the 1970s and nowadays are of *F. lugubris* and *F. rufa*. In our study, *F. lugubris* was the dominant species in Pirin Mt. Middle rich/poor regions in both projects remain Western and Central Stara Planina, Rila and Belasitsa Mts. There the species' proportions remained approximately the same, although *F. lugubris* decreased at the expense of *F. rufa* and *F. pratensis*. In the poor regions (Strandza and Eastern Rhodope Mts) the dominance of *F. pratensis* was confirmed again in our study.

The nest density of *F. rufa* and *F. lugubris* in our survey is many times larger in the forest boundary area (in a strip with a width of up to 10 m) or small-size forest

fragments with respectively higher solar radiation. Similar are the observations made by Punttila et al. (1994), Punttila (1996), Underwood and Fisher (2006), Babik et al. (2009), Crist (2009) and Chen and Robinson (2014) for RWA in the cool temperate forests in Europe. The density of the *Formica rufa* group is higher in deforested strips as they prefer nesting in sun-warmed places and use the forest interior as foraging area (Babik et al. 2009). In Western Poland, the nest density decreases towards the centre of clear-cuts although the influencing factors are not clear (Żmihorski 2010). The mounds in young forests and clear-cuttings are smaller and flatter, caused by the splitting of the large mounds into smaller colonies (Rosengren and Pamilo 1978; Domisch et al. 2005). During our survey, nests of *Formica fusca* (the host species of RWA) were often found in grassy runs or shrubs at the forest edges.

In our study, *F. lugubris*, *F. rufa* and *F. pratensis* were found at altitudes corresponding to the previously reported altitude from Bulgaria by Atanassov and Dlusskij (1992). In Switzerland, the great abundance of *F. lugubris* was at about 1000 m (Cherix et al. 2012) while in Bulgaria was higher, between 1500 and 1800 m. In Switzerland, *F. rufa* and *F. polyctena* were found at lower elevations up to 800 m (Vandegehuchte et al. 2017) similar to their optimal range in Bulgaria. *Formica polyctena* x *rufa* hybrid was found between 1200 and 1410 m, as the elevation preference for *F. polyctena* was up to 1200 m (Atanassov and Dlusskij 1992). In other European countries, almost every species of RWA occurs at lower altitudes than in Bulgarian mountains, which is the expected phenomenon of shifting up of altitudinal preferences of mountainous species in the southern part of their ranges.

In the present study, the nest density of *F. pratensis* and *F. rufa* was significantly influenced by the canopy cover. There was an example of shading effect: Wesselinov (1968) published an article about the high diversity of RWA for Parangalitza Biosphere Reserve in the Rila National Park. As a reserve since 1933 (Darzhaven vestnik 1933) with about 300–400 years old trees of *Picea abies*, the wood clearance, removing the old fallen woods and felling had been strongly forbidden. The consequences nowadays are that as the forest interior is almost closed (over 80% canopy cover), the RWA are only to be found in the vicinity of the forest, around the roads and the alpine meadows at present. A similar situation was observed in other old reserves and RWA populations there were decreasing. Our observations confirmed the conclusions of other authors (Collingwood 1979; Punttila et al. 1994; Dekoninck et al. 2010; Tsikas et al. 2016; Serttaş 2020) that RWA populations decline with increasing the canopy closure and a little intervention as forest thinning for light spots would be a support for the RWA existence.

In Bulgaria, the mounds of *F. lugubris* were mostly located on north-east-facing slopes, similarly to the same species in Switzerland, found mainly at an eastern aspect (Freitag et al. 2016b; Vandegehuchte et al. 2017). In southern Norway, it was strongly orientated to the South (Hill et al. 2018).

The positive correlation of grass cover to both *F. pratensis* presence and nest density was expected because this species is an open habitat specialist (Seifert 2018). This

variable did not show a statistically significant impact on the abundance of other RWA as well as in West Poland for *F. rufa* and *F. polycтена* (Žmihorski 2010). According to Sorvari (2016), the higher ground vegetation benefits RWA as it plays a protection and feeding role.

The dominant tree species associations, where the RWA species occur, were *Picea abies*, *Pinus sylvestris*, *Abies alba*, young *Juniperus* spp. communities (according to Atanasov and Dlusskji 1992) and also *Pinus mugo*, *P. heldreichii* and *P. peuce* communities (according to our study).

The conservation needs of the RWA are underestimated (Sorvari 2016). For a viable colony, these territorial species need at least a few hectares of stable habitat with enough food resources to maintain sexual forms for reproduction. The loss, shading, drying/flooding, disturbance or destruction of their habitat are their major threats (Dekoninck 2010). Not only human activities but changes in climatic conditions and natural enemies (as pathogens) may cause a decline of a colony. As RWA play a keystone role in the ecosystems (Dlussky 1967), the reduction or extinction of their populations may have a huge effect on the local and even global ecosystems. Therefore, studying the most suitable habitat characteristics in detail, and conducting regular monitoring studies on RWA populations are of primary importance.

Conclusions

- The recent proportions of RWA species in Bulgaria remain similar to those in the National Inventory of RWA (1970–1973): most abundant is *F. lugubris* followed by *F. rufa*, *F. pratensis* and the hybrid *Formica polycтена x rufa*. The existence of *F. polycтена* and *F. aquilonia* in Bulgaria is probably doubtful and should be a matter of further investigation.

- Western Rhodope Mts were the richest of the RWA region in 1970–1973 and still are at present, with successful examples of nests that have survived over 50 years.

- The GIS predictive models of RWAs' potential habitats are useful for optimising their area for conservation purposes.

- As habitat characteristics of primary importance for the distribution and density of the three RWA, we identified elevation and canopy cover; exposure and ecological groups of plants were important for *F. lugubris*, stone cover and forest age – for *F. rufa*, and grass cover – for *F. pratensis*. However, the slope was marginally significant for the presence of *F. pratensis* and *F. lugubris* only, and undergrowth density was not related to the ecological demands of neither of the three RWA species.

- The optimal habitat conditions for the distribution of the four RWA species in Bulgaria are: elevation between 500–2000 m (lower parts occupied by *F. pratensis*, middle – by *F. rufa* and upper – by *F. lugubris*); mesophyte coniferous, mixed and deciduous forests with canopy cover between 30 and 80% and their ecotones; lack of stone cover on the surface; the presence of forest meadows and clearings/rides.

Acknowledgements

The study was supported by the Executive Environment Agency (Ministry of Environment and Water), Bulgaria, and carried out by consortium Fortis Facility-National Museum of Natural History-Institute of Biodiversity and Ecosystem Research (2013–2015) in the frame of the project Grant: DIR 5113024-1-48.

The fieldwork was possible due to the help of Dimitar Kyonev. Deep thanks to Prof. Dr. Wojciech Czechowski (MIIZ-PAS, Warsaw) for his valuable advice about the field methods at the beginning of the project. We are grateful to Dr. Bernhard Seifert (Senckenberg Museum of Natural History, Görlitz) for the confirmation of the identification of the hybrid species. Great thanks to Elena Ivanova for the elaboration of the GIS models. Deep thanks also to Prof. Dr. Lyubomir Penev, Prof. DSc Boyko Georgiev (IBER-BAS), and both referees for the constructive remarks on the previous version of the manuscript.

References

- Antonova V, Lapeva-Gjonova A, Gradinarov D (2016) Ants (Hymenoptera: Formicidae) from Vrachanska Planina Mountains. In: Bechev D, Georgiev D (Eds) Faunistic diversity of Vrachanski Balkan Nature Park. ZooNotes, Supplement 3: 155–161. http://www.zo-onotes.bio.uni-plovdiv.bg/Suppl%203_Vrachanski%20balkan.html
- Atanassov N, Dlusskij G (1992) Fauna Bulgarica 22. Hymenoptera, Formicidae. Bulgarian Academy of Sciences (Ed.), Sofia, 310 pp. [in Bulgarian]
- Babik H, Czechowski W, Włodarczyk T, Sterzyńska M (2009) How does a strip of clearing affect the forest community of ants (Hymenoptera: Formicidae). *Fragmenta Faunistica* 52(2): 125–141. <https://doi.org/10.3161/00159301FF2009.52.2.125>
- Bernasconi C, Maeder A, Cherix D, Pamilo P (2005) Diversity and genetic structure of the wood ant *Formica lugubris* in unmanaged forests. *Annales Zoologici Fennici* 42: 189–199.
- Bernasconi C, Pamilo P, Cherix D (2010) Molecular markers allow sibling species identification in red wood ants (*Formica rufa* group). *Systematic Entomology* 35(2): 243–249. <https://doi.org/10.1111/j.1365-3113.2009.00503.x>
- Bernasconi C, Cherix D, Seifert B, Pamilo P (2011) Molecular taxonomy of the *Formica rufa* group (red wood ants) (Hymenoptera: Formicidae): a new cryptic species in the Swiss Alps? *Myrmecological News* 14: 37–47.
- Bestelmeyer BT, Agosti D, Alonso LE, Brandão CRF, Brown Jr WL, Delabie JHC, Silvestr R (2000) Field Techniques for Study of Ground-Dwelling Ants: An overview, Description and Evaluation. Chapter 9. In: Agosti D, Majer JD, Alonso LE, Schultz T (Eds) *Ants: standard methods for measuring and monitoring biodiversity*. Smithsonian Institution Press, 122–144.
- Bobev R (1972) Red wood ants – a main part of the biological insect pest control. *Rastitelna zashtita* 11: 9–13. [In Bulgarian]

- Bobev R (1973) Ecological and systematic features in the distribution of few wood ants. Gorskostopanstvo 2: 38–41. [In Bulgarian]
- Borkin KM, Summers RW, Thomas L (2012) Surveying abundance and stand type associations of *Formica aquilonia* and *F. lugubris* (Hymenoptera: Formicidae) nest mounds over an extensive area: Trailing a novel method. European Journal of Entomology 109: 47–53. <https://doi.org/10.14411/eje.2012.007>
- Breen J (2014) Species dossier, range and distribution data for the Hairy Wood Ant, *Formica lugubris*, in Ireland. Irish Wildlife Manuals 68. National Parks and Wildlife Service, Ireland, 26 pp.
- Bulgarian Biodiversity Act (2002) Darzhaven Vestnik 77(9): 49–49. [In Bulgarian] [https://doi.org/10.1016/S1351-4210\(02\)00910-1](https://doi.org/10.1016/S1351-4210(02)00910-1)
- Chen YH, Robinson EJ (2014) The relationship between canopy cover and colony size of the wood ant *Formica lugubris* – Implications for the thermal effects on a keystone ant species. PLoS ONE 9(12): e116113. <https://doi.org/10.1371/journal.pone.0116113>
- Cherix D (1977) Les fourmis des bois et leur protection. Publication du WWF Suisse et du CSEE/SZU, 32 pp.
- Cherix D, Bernasconi C, Maeder A, Freitag A (2012) Fourmis des bois en Suisse: état de la situation et perspectives de monitoring. Schweizerische Zeitschrift für Forstwesen 163(6): 232–239. <https://doi.org/10.3188/szf.2012.0232>
- Cherix D, Devenoges A, Frietag A, Bernasconi C, Maedler A (2007) Premier recensement des fourmis des bois (groupe *Formica rufa*) au Parc National Suisse. In: Cherix D, Gonthier Y, Pasche A (Eds) Faunistique et écologie des invertébrés au PNS, Nationalpark-Forschung in der Schweiz 94: 69–79.
- Collingwood CA (1979) The Formicidae (Hymenoptera) of Fennoscandia and Denmark. Scandinavian Science Press. Fauna entomologica scandinavica 8: 1–174.
- CORINE biotopes (2000) The Corine biotopes (Version 2000) database is an inventory of major nature sites. <https://www.eea.europa.eu/data-and-maps/data/corine-biotopes>
- Crist TO (2009) Biodiversity, species interactions, and functional roles of ants (Hymenoptera: Formicidae) in fragmented landscapes: a review. Myrmecological News 12: 3–13.
- Czechowski W (1996) Colonies of hybrids and mixed colonies; interspecific nest takeover in wood ants (Hymenoptera, Formicidae). Memorabilia Zoologica 50: 1–116. [+20]
- Czechowski W, Radchenko A, Czechowska W, Vepsäläinen K (2012) The ants of Poland with reference to the myrmecofauna of Europe. Natura optima dux Foundation, Warszawa, 496 pp.
- Çamlıtepe Y, Aksoy V (2019) Distribution and Conservation Status of the European Red Wood Ant Species *Formica pratensis* Retzius, 1783 (Hymenoptera, Formicidae) in (European) Turkey. Journal of the Entomological Research Society 21(2): 199–211. <http://www.entomol.org/journal/index.php/JERS/article/view/1589>
- Darzhaven vestnik (1933) No 77. [In Bulgarian]
- Dekoninck W, Hendrickx F, Grootaert P, Maelfait J-P (2010) Present conservation status of red wood ants in north-western Belgium: Worse than previously, but not a lost cause. European Journal of Entomology 107: 209–218. <https://doi.org/10.14411/eje.2010.028>
- Dekoninck W, Maebe K, Breyne P, Hendrickx F (2014) Polygyny and strong genetic structuring within an isolated population of the wood ant *Formica rufa*. Journal of Hymenoptera Research 41: 95–111. <https://doi.org/10.3897/JHR.41.8191>

- Delabie JH, Fisher BL, Majer JD, Wright IW (2000) Sampling effort and choice of methods. In: Agosti D, Majer JD, Alonso LE, Schultz T (Eds) *Ants: standard methods for measuring and monitoring biodiversity*. Smithsonian Institution Press, 145–154. <https://doi.org/10.5281/zenodo.11736>
- Delipavlov D, Cheshmedzhiev I, Popova M, Terzijski D, Kovatchev I (2003) Key to the Plants in Bulgaria. Agricultural University Press, Plovdiv, 788 pp. [In Bulgarian]
- Dlussky GM (1967) *Ants of the genus Formica* (Hymenoptera: Formicidae g. *Formica*). Akademiya Nauk SSSR, Moscow, 236 pp. [In Russian]
- Domisch T, Finér L, Jurgensen MF (2005) Red wood ant mound densities in managed boreal forests. *Annales Zoologici Fennici* 42: 277–282. <https://www.jstor.org/stable/23735915>
- Freitag A, Dischinger C, Cherix D (2008) *Formica pratensis* (Hyménoptères: Formicidae) dans le canton de Vaud: état des peuplements et importance des talus de routes comme milieu de substitution. *Bulletin de la Société vaudoise des sciences naturelles* 91: 47–68.
- Freitag A, Stockan JA, Bernasconi C, Maeder A, Cherix D (2016a) Sampling and Monitoring Wood Ants. In: Stockan JA, Robinson EJH (Eds) *Wood Ant Ecology and Conservation*, 238–263. <https://doi.org/10.1017/CBO9781107261402>
- Freitag A, Kaiser-Benz M, Bernasconi C, Cherix D, Duggelin C, Risch A, Wermelinger B (2016b) Vielfalt und Verbreitung der Waldameisen in Graubünden (Hymenoptera, Formicidae, *Formica* rufa-Gruppe): erste Ergebnisse. *Jahresbericht der Naturforschenden Gesellschaft Graubünden* 119: 161–176. <https://www.dora.lib4ri.ch/wsl/islandora/object/wsl%3A9666>
- Gösswald K (1989) Die Waldameise I: Biologische Grundlagen, Ökologie und Verhalten. – AULA-Verlag Wiesbaden, 660 pp.
- Gösswald K (1990) Die Waldameise II: Die Waldameise im Ökosystem Wald, ihr Nutzen und ihre Hege. AULA-Verlag Wiesbaden, 510 pp.
- Gotelli NJ, Ellison AM, Dunn RR, Sanders NJ (2011) Counting ants (Hymenoptera: Formicidae): Biodiversity sampling and statistical analysis for myrmecologists. *Myrmecological News* 15: 13–19.
- Hill JL, Vater AE, Geary AP, Matthews JA (2018) Chronosequences of ant nest mounds from glacier forelands of Jostedalbreen, southern Norway: Insights into the distribution, succession and geo-ecology of red wood ants (*Formica lugubris* and *F. aquilonia*). *The Holocene* 28(7): 1113–1130. <https://doi.org/10.1177/0959683618761551>
- Hughes J, Broome A (2007) *Forests and Wood Ants in Scotland*. Information note, Forestry Commission, Crown copyright, 8 pp.
- IUCN (2021) *The IUCN Red List of Threatened Species*. Version 2021-1. <https://www.iucn-redlist.org> [Downloaded on 03 June 2021]
- Izvestiya (1959) Order No. 1626 of Ministry of Agriculture and Forestry. No. 101: 2. [In Bulgarian]
- Kaspari M (2000) A primer on ant ecology. In: Agosti D, Majer JD, Alonso LE, Schultz T (Eds) *Ants: standard methods for measuring and monitoring biodiversity*. Smithsonian Institution Press, 9–24. <https://doi.org/10.5281/zenodo.11736>
- Keremidchiev M, Vatov V, Ganchev G, Bobev R (1972) Distribution results from the Red Wood ants of genus *Formica*. *Gorsko stopanstvo* 12: 13–18. [In Bulgarian]

- Kilpeläinen J, Puntila P, Sundström L, Niemelä P, Finér L (2005) Forest stand structure, site type and distribution of ant mounds in boreal forests in Finland in the 1950s. *Annales Zoologici Fennici* 42: 243–258. <http://www.sekj.org/PDF/anzf42/anzf42-243.pdf>
- Korczynska J, Gajewska M, Pilot M, Czechowski W, Radchenko A (2010) Genetic polymorphism in “mixed” colonies of wood ants (Hymenoptera: Formicidae) in southern Finland and its possible origin. *European Journal of Entomology* 107(2): 157–167. <https://doi.org/10.14411/eje.2010.021>
- Lapeva-Gjonova A, Antonova V, Radchenko A, Atanasova M (2010) Catalogue of the ants (Hymenoptera: Formicidae) of Bulgaria. *ZooKeys* 62: 1–124. <https://doi.org/10.3897/zookeys.62.430>
- Lapeva-Gjonova A (2011) Ants (Hymenoptera, Formicidae) from Western Rhodope Mountains (Bulgaria). In: Beron P (Ed.) *Biodiversity of Bulgaria*. 4 Biodiversity of Western Rhodopes (Bulgaria and Greece). Part II. Pensoft & Natural Museum Natural History, Sofia, 287–298.
- Lapeva-Gjonova A, Rücker WH (2011). Latridiidae and Endomychidae beetles (Coleoptera) from ant nests in Bulgaria. *Latridiidae* 8: 5–8.
- Lapeva-Gjonova A, Santamaria S (2011) First record of Laboulbeniales (Ascomycota) on ants (Hymenoptera: Formicidae) in Bulgaria. *Zoonotes* 22: 1–6. http://www.zoonotes.bio.uniplovdiv.bg/all%20articles_pdf_2.html
- Lapeva-Gjonova A (2013) Ant-associated beetle fauna in Bulgaria: a review and new data. *Psyche: A Journal of Entomology* 2013: e242037. [14 pp.] <https://doi.org/10.1155/2013/242037>
- Lapeva-Gjonova A, Ilieff O (2012) Ant-associated rove beetles (Coleoptera: Staphylinidae) in Bulgaria. *Acta entomologica slovenica* 20(1): 73–84. <http://www.dlib.si/?URN=URN:NBN:SI:doc-K2ILFUKX>
- Lapeva-Gjonova A, Kiran K (2012) Ant fauna (Hymenoptera, Formicidae) of Strandzha (Istranca) Mountain and adjacent Black Sea coast. *North-Western Journal of Zoology* 8(1): 72–84. <http://biozoojournals.3x.ro/nwzj/index.html>
- Lapeva-Gjonova A, Antonova V, Ljubomirov T (2021) Ants (Hymenoptera, Formicidae) of Sarnena Sredna Gora Mountains (Bulgaria). In: Georgiev D, Bechev D, Yancheva V (Eds) *Fauna of Sarnena Sredna Gora Mts, Part 2, Zoonotes, Supplement 10*: 18–27.
- Leponce M, Theunis L, Delabie JHC, Roisin Y (2004) Scale dependence of diversity measures in a leaf-litter ant assemblage. *Ecography* 27: 253–267. <https://doi.org/10.1111/j.0906-7590.2004.03715.x>
- Lyubenova M (2004) *Phytoecology*. Academic Publisher M. Drinov, Sofia, 574 pp. [In Bulgarian]
- Maeder A, Freitag A, Cherix D (2005) Species- and nestmate brood discrimination in the sibling wood ant species *Formica paralugubris* and *Formica lugubris*. *Annales Zoologici Fennici* 42: 201–212. <http://www.sekj.org/PDF/anz42-free/anz42-201.pdf>
- Otto D (1960) Statistische Untersuchungen über die Beziehungen zwischen Königinnenzahl und Arbeiterinnengröße bei den Roten Waldameisen (“engere *Formica rufa* L.-Gruppe”). *Biologisches Zentralblatt* 79(6): 719–739.
- Otto D (1968) Zur Verbreitung der Arten der *Formica rufa* Linnaeus-Gruppe. *Beiträge zur Entomologie* 18(5/6): 671–692.
- Otto D, Keremidchiev M, Vatov V (1962) The wood ants in Bulgaria and trends of their use in biological insect pest control in the forests. *Gorsko Stopanstvo* 12: 24–28. [In Bulgarian]

- Pavan M, Ronchetti G (1972) Le Formiche del gruppo *Formica rufa* in Italia nell'asestamento ecologico forestale. *Waldhygiene* 9(5–8): 223–238.
- Pełal J, Pisarski B (1966) Metody ilościowe stosowane w badaniach myrmekologicznych. *Ekologia Polska* 12: 363–376.
- Punntila P (1996) Succession, forest fragmentation, and the distribution of wood ants. *Oikos* 75: 291–298. <https://doi.org/10.2307/3546252>
- Punntila P, Haila Y, Niemelä J, Pajunen T (1994) Ant communities in fragments of old-growth taiga and managed surroundings. *Annales Zoologici Fennici* 31: 131–144. <https://www.jstor.org/stable/23735506>
- Punntila P, Kilpeläinen J (2009) Distribution of mound-building ant species (*Formica* spp., Hymenoptera) in Finland: preliminary results of a national survey. *Annales Zoologici Fennici* 46(1): 1–15. <https://doi.org/10.5735/086.046.0101>
- Risch AC, Ellis S, Wiswell H (2016) Where and Why? Red Wood ant Population Ecology. In: Stockan JA, Robinson EJH (Eds) *Wood Ant Ecology and Conservation*, Cambridge, 81–105. <https://doi.org/10.1017/CBO9781107261402.005>
- Rosengren R, Vepsäläinen K, Wuorenrinne H (1979) Distribution, nest densities, and ecological significance of wood ants (the *Formica rufa* group) in Finland. *OILB Bull SROP* 3: 181–213.
- Rosengren R, Pamilo P (1978) Effect of winter timber felling on behaviour of foraging red wood ants (*Formica rufa* group) in early spring. *Memorabilia Zoologica* 29: 143–155.
- Savolainen R, Vepsäläinen K (1988) A competition hierarchy among boreal ants: impact on resource partitioning and community structure. *Oikos* 51: 135–155. <https://doi.org/10.2307/3565636>
- Seifert B (2008) Removal of allometric variance improves species separation in multi-character discriminant functions when species are strongly allometric and exposes diagnostic characters. *Myrmecological News* 11: 91–105. https://myrmecologicalnews.org/cms/index.php?option=com_download&view=download&filename=volume11/mn11_91-105_printable.pdf&format=raw
- Seifert B (2018) *The ants of central and north Europe*. Lutra Verlags-und Vertriebsgesellschaft, 407 pp.
- Seifert B (2021) A taxonomic revision of the Palaearctic members of the *Formica rufa* group (Hymenoptera: Formicidae) – the famous mound-building red wood ants. *Myrmecological News* 31: 133–179. https://doi.org/10.25849/myrmecol.news_031:133
- Serttaş A, Bakar Ö, Alkan UM, Yılmaz A, Yolcu HI, Ipekdal K (2020) Nest Survival and Transplantation Success of *Formica rufa* (Hymenoptera: Formicidae) Ants in Southern Turkey: A Predictive Approach. *Forests* 11(533): 1–15. <https://doi.org/10.3390/f11050533>
- Sorvari J (2016) Threats, Conservation and Management. In: Stockan JA, Robinson EJH (Eds) *Wood Ant Ecology and Conservation*. Cambridge, 264–286. <https://doi.org/10.1017/CBO9781107261402.013>
- Sorvari J, Hakkarainen H (2007) Wood ants are wood ants: deforestation causes population declines in the poly domous wood ant *Formica aquilonia*. *Ecological Entomology* 32(6): 707–711. <https://doi.org/10.1111/j.1365-2311.2007.00921.x>
- Stockan JA, Robinson EJ (2016) *Wood ant ecology and conservation*. Cambridge University Press, 304 pp. <https://doi.org/10.1017/CBO9781107261402>

- Stockan JA, Robinson EJH, Trager JC, Yao I, Seifert B (2016) Introducing wood ants: evolution, phylogeny, identification and distribution. In: Stockan JA, Robinson EJH (Eds) Wood ant ecology and conservation. Cambridge University Press, Cambridge, 1–36. <https://doi.org/10.1017/CBO9781107261402.002>
- Tsikias A, Karanikola P, Papageorgiou AC (2016) Distribution and physical traits of red wood ant mounds in a managed Rhodope mountains forest. Environmental Monitoring and Assessment 188: e436. <https://doi.org/10.1007/s10661-016-5398-9>
- Underwood EC, Fisher BL (2006) The role of ants in conservation monitoring: if, when, and how. Biological conservation 132(2): 166–182. <https://doi.org/10.1016/j.biocon.2006.03.022>
- Vandegheuchte ML, Wermelinger B, Fraefel M, Baltensweiler A, Düggelin C, Brändli UB, Freitag A, Bernasconi C, Cherix D, Risch AC (2017) Distribution and habitat requirements of red wood ants in Switzerland: Implications for conservation. Biological Conservation 212: 366–375. <https://doi.org/10.1016/j.biocon.2017.06.008>
- Vatov V, Bobev R (1976) Distribution of the red wood ants in Bulgaria. Zashchita na prirodata 1: 10–11. [In Bulgarian]
- Vesselinov G (1981) Diffusione e protezione delle formiche del gruppo *Formica rufa* in Bulgaria. Collana Verde 59: 317–318.
- Wesselinoff GD (1973) Die hügelbauenden Waldameisen Bulgariens. Waldhygiene 10: 103–117.
- Wesselinoff GD (1979) Verbreitung und Schutz der Waldameisen in Bulgarien. Comptes rendus de la reunion des groupes de travail “*Formica rufa*” et “Vertebres prédateurs des insectes” de l’olib, Bulletin srop, II-3: 495–498.
- Wesselinov GD (1968) The ants from Parangalitsa Reserve. Priroda i znanie 6: 20–22. [In Bulgarian]
- Zakharov AA, Dlusskiy GM, Goryunov DN, Gilev AV, Zryanin VA, Fedoseeva EB, Gorokhovskaya E, Radchenko AG (2013) Monitoring of *Formica* ants. Moscow, 99 pp. [In Russian]
- Żmihorski M (2010) Distribution of red wood ants (Hymenoptera: Formicidae) in the clear-cut areas of a managed forest in Western Poland. Journal of forest research 15(2): 145–148. <https://doi.org/10.1007/s10310-009-0161-5>

Supplementary material I

Supplementary Field Form

Authors: Vera Antonova

Data type: Empty field form (excel file)

Explanation note: Field form for each transect with lines for General information of the locality, Habitat data, Threats, Nests' description, GPS points.

Copyright notice: This dataset is made available under the Open Database License (<http://opendatacommons.org/licenses/odbl/1.0/>). The Open Database License (ODbL) is a license agreement intended to allow users to freely share, modify, and use this Dataset while maintaining this same freedom for others, provided that the original source and author(s) are credited.

Link: <https://doi.org/10.3897/jhr.85.61431.suppl1>

Supplementary material 2

Table S1

Authors: Vera Antonova, Martin P. Marinov

Data type: Sample transects, localities, environmental variables, number of nests (excel file)

Explanation note: The locality, environmental variables and number of red wood ants nests are given per each sample transect (172). The new localities per each species are marked.

Copyright notice: This dataset is made available under the Open Database License (<http://opendatacommons.org/licenses/odbl/1.0/>). The Open Database License (ODbL) is a license agreement intended to allow users to freely share, modify, and use this Dataset while maintaining this same freedom for others, provided that the original source and author(s) are credited.

Link: <https://doi.org/10.3897/jhr.85.61431.suppl2>

Update on the invasion status of the Argentine ant, *Linepithema humile* (Mayr, 1868), in Madrid, a large city in the interior of the Iberian Peninsula

Diego López-Collar¹, Francisco J. Cabrero-Sañudo¹

¹ Department of Biodiversity, Ecology and Evolution, Faculty of Biological Sciences, Complutense University of Madrid, C/ José Antonio Novais, 12, 28040, Madrid, Spain

Corresponding author: Diego López-Collar (dlopezcollar@gmail.com)

Academic editor: Francisco Hita García | Received 10 March 2021 | Accepted 15 June 2021 | Published 31 August 2021

<http://zoobank.org/344F3B32-F469-419B-B0F6-3E4241BEDD08>

Citation: López-Collar D, Cabrero-Sañudo FJ (2021) Update on the invasion status of the Argentine ant, *Linepithema humile* (Mayr, 1868), in Madrid, a large city in the interior of the Iberian Peninsula. Journal of Hymenoptera Research 85: 161–177. <https://doi.org/10.3897/jhr.85.65725>

Abstract

New geolocated records of the invasive ant *Linepithema humile* (Mayr, 1868) are added to the previous references for the city of Madrid and its surroundings, and the possible causes of the occurrence and permanence of this species in urban areas are discussed. The data collection corresponds to a series of samplings carried out for the last three years in green areas of the city, bibliographic searches, citizen science platforms and personal communications. To date, eleven locations in the urban area of Madrid and four points outside the city have been registered. The city of Madrid is undergoing a colonisation by the Argentine ant, although it is not widespread yet, since observations over time and space are isolated and apparently unrelated. However, this species has a great capacity to disperse and establish new colonies, mainly human-mediated through the transport of goods, plants, gardening tools, etc. Considering the numerous colonizable urban green areas in the city that can provide the necessary conditions for its expansion, the Argentine ant should not be underestimated, and immediate action is strongly recommended.

Keywords

Formicidae, green areas, introduced species, invasive species, new records, Spain, urban environment

Introduction

The Argentine ant, *Linepithema humile* (Mayr, 1868), is a well-known and widely studied organism due to its highly potential as an invasive species (Wetterer et al. 2009; GISD 2015). This ant presents a wide range of strategies, such as its characteristic interspecific aggressiveness, polygynic and polydomic colonies and a large number of individuals per nest, which gives it a greater capacity to establish new settlements, indirectly and profusely aided by humans (Suarez et al. 2001; Carpintero et al. 2004; Ward et al. 2005). The cosmopolitan and dominant behaviour of this ant (McGlynn 1999) allows it to displace other native species, both in naturalised environments (Kennedy 1998; Carpintero et al. 2014) and urban areas (Touyama et al. 2003; Holway and Suarez 2006; Stringer et al. 2009). In this context, and due to the potential damage that this species can cause in new environments, it is important to monitor the spatial distribution of the Argentine ant.

In the Iberian Peninsula, *L. humile* has a predominant coastal distribution (Espadaler and Collinwood 2001; Espadaler and Gómez 2003), but there are several records of its presence in inland provinces: Badajoz, Córdoba, Madrid, Orense, Salamanca, Sevilla, Soria and Zaragoza in Spain, (Obregón and Reyes-López 2016; <http://mirmecologia.jimdo.com>), and other references including Penalva do Castelo, the most inland locality of Portugal according to Silva Dias (1955). These locations attract our attention when, in terms of biogeography, they correspond to inland regions that may pose a challenge to the survival of this species by presenting unfavourable conditions for its activity, such as cold winters or lack of humidity when they are far from a coastal Mediterranean climate (Espadaler and Gómez 2003). This climatic unsuitability could be a limiting factor for the expansion of the Argentine ant in inner regions of the Iberian Peninsula, as shown by the potential distribution modelling work by Roura-Pascual et al. (2006, 2009), but it may not have a plausible effect in cities, where most of the inner recorded evidence occurs.

In this way, green areas, parks, and botanical and private gardens located in urban environments provide microhabitat scale conditions, in terms of humidity, food and shelter resources, which not only allow but also favour the development of Argentine ant colonies (Martínez et al. 1997). These locations often have in common the presence of irrigation systems and nutritious plants for Hemiptera Sternorrhyncha (aphids, whiteflies and scale insects) (Greenberg et al. 2006; Mgocheki et al. 2009; Powell et al. 2010), where ants can easily supply the colony by acquiring sugary substances and water. On a landscape scale, the Urban Heat Island effect could be another driver for the permanence of the Argentine ant in cities along with other characteristics corresponding to a finer scale (e.g.: green areas features). This effect is a valuable factor to explain the insect community structure (McGlynn et al. 2019) since the temperature increase associated with it has been shown to be beneficial for the subsistence of native thermophilic species (Menke et al. 2011; Kaiser et al. 2016) as well as for the maintenance of invasive species (Borden and Flory 2021).

The present article compiles all the records of the Argentine ant, *L. humile*, obtained from various samplings across the city of Madrid and its surrounding areas between 2018 and 2020, including previous information from the bibliography, citizen science web platforms and personal communications. The aim of this study was to update the available information on the Argentine ant in the city of Madrid and nearby locations.

Methods

Records of the Argentine ant, *L. humile*, were searched and catalogued from different sources, involving mostly green areas in the city of Madrid and its surroundings. These references were obtained from: (i) the bibliography (B, Table 1), (ii) consultations with the citizen science platform 'Biodiversidad Virtual' (BV; <https://www.biodiversidadvirtual.org>), where it was possible to request georeferenced data associated to photographs of *L. humile*, (iii) personal communications (P), and (iv) survey data (S).

The survey data correspond to a series of samplings in green areas of the city carried out from 2018 to 2020, between May and September of each year. Three locations do not correspond to green areas but to streets, where the same sampling protocol was applied (S, Streets, Table 1). Due to the large number of parks within the city limits (nearly 200), a representative sample of them was obtained through a cluster analysis following Hair et al. (1999). For this purpose, a series of factors was obtained from different types of variables (Table 2), through a principal component analysis. A dendrogram which grouped sets of the 200 parks in the city of Madrid was built (matrix based on Euclidean distances, Group average amalgamation) and a threshold was set to establish a reasonable number of parks to sample. During 2018, a total of 13 green areas were chosen to be surveyed. Samplings were then carried out in another 7 green areas as well as in some of the previous parks during 2019 and 2020 in order to continue monitoring the ant fauna of the parks and gardens of Madrid, selecting them randomly from the cluster groups or because the presence of the Argentine ant was known. Each green area was visited at least 2 times and ants were collected from a variety of habitats (ground surface, under stones and stumps, walls, trees, etc.) over a period of time proportional to the size of the parks. A logarithmic curve was established to achieve the sampling effort in the largest parks (approximately, a minimum of 25 minutes for an area of 1 hectare or less and a maximum of 180 minutes for parks of more than 140 hectares). The logarithmic curve had been previously tested in the *urban Butterfly Monitoring Scheme project* (uBMS, 2018), as suggested by Constanti Stefanescu (personal communication). The formula was $t = (\text{LN}(\text{hec}) + 0.75) * 30$, where t is the search time and hec the hectares that the park occupies.

Ants were directly sampled with an aspirator, and pitfall traps were used to maximise the sampling effort whenever they could be set due to impracticable ground conditions or when permits could not be obtained (Agosti and Alonso 2000). Ants were

Table 1. Localities where samplings have been carried out and/or the Argentine ant has been registered. Classification of localities (city of Madrid and surroundings): B, the species has been registered according to bibliographic references (Collingwood and Yarrow 1969; Martínez et al. 1997; Ruiz-Heras et al. 2011); BV, the species has been registered, according to the citizen science platform ‘Biodiversidad Virtual’; P, the species has been registered through personal communication, according to information given by a pest control company (N. Trotta leg.), by J. Reyes, J. Arcos, K. Gómez and M. Sierra or by other citizens; S, survey data from exhaustive ant sampling. Presence/Colony extension: the confirmed presence of the species in each locality and the area occupied by ants in squared metres if known. ✓: confirmed presence; no presence: no Argentine ants have been found after an exhaustive sampling. Pitfall traps: whether pitfall traps could be set. Time spent: minutes of sampling effort. N° of visits: number of times each area was surveyed.

Sampling areas	Location	Classification	Presence/Colony extension	Date of sampling	Pitfall traps	Time spent (min)	N° of visits
City of Madrid: green areas							
Casa de Campo Park (east side)	40°25.020'N, 3°44.040'W	B	✓	2011	–	–	–
		S	✓ / 11816 m ²	2018–2019	Yes	184	3
Madrid Río Park (Central part)	40°25.133'N, 3°43.340'W	P	✓	Prior to 2019	–	–	–
		S	✓ / 54494 m ²	2019–2020	Not practicable	122	2
Real Jardín Botánico de Madrid	40°24.660'N, 3°41.460'W	BV	✓	2016	–	–	–
		S	✓ / 2857 m ²	2018–2019	Not practicable	91	2
del Norte–Carmen Tagle Park	40°28.843'N, 3°41.734'W	S	✓ / 377 m ²	2018	Yes	121	3
Enrique Tierno Galván Park	40°23.312'N, 3°40.961'W	S	✓ / 1974 m ²	2018	Yes	143	3
Sorolla Museum Gardens	40°26.120'N, 3°41.540'W	S	✓ / 830 m ²	2020	Not practicable	25	2
Campus Moncloa, North side	40°26.930'N, 3°43.688'W	S	No presence	2010–2019	Yes	Continuous monitoring	3+
Bellas Artes Gardens	40°26.410'N, 3°41.425'W	S	No presence	2018	Yes	25	3
Campo del Moro Gardens	40°25.068'N, 3°43.089'W	S	No presence	2018	Yes	119	3
Berlín Park	40°27.026'N, 3°40.547'W	S	No presence	2019	No	76	2
Cuña Verde de la Latina Park	40°24.048'N, 3°44.620'W	S	No presence	2018	Yes	158	3
Pradolongo Park	40°22.545'N, 3°42.384'W	S	No presence	2019	No	156	2
Roma Park	40°24.988'N, 3°39.762'W	S	No presence	2018	Yes	101	3
Emperatriz María de Austria Park	40°22.741'N, 3°43.422'W	S	No presence	2018	Yes	156	3
Entrevías Urban Park	40°22.224'N, 3°40.107'W	S	No presence	2018	Yes	104	3
Eugenia de Montijo Park (part 2)	40°23.032'N, 3°45.014'W	S	No presence	2018	Yes	69	3
Forestal de Valdebebas Park	40°29.466'N, 3°37.994'W	S	No presence	2019	No	184	2
Forestal de Vicalvaro Park	40°24.476'N, 3°35.894'W	S	No presence	2018–2019	Yes	135	3
Juan Carlos I Park	40°27.642'N, 3°36.324'W	S	No presence	2018	Yes	184	3
Quinta de Torre Arias	40°26.688'N, 3°37.190'W	S	No presence	2018	Yes	115	3
City of Madrid: Streets							
Campus Moncloa, east side, Rector Royo–Villanova Street	40°27.120'N, 3°42.960'W	B	✓ / Unknown	1991–1992	–	–	–
		P	Unknown	2019	Not practicable	–	–
Valmojado Street, Aluche Neighbourhood	40°23.220'N, 3°45.540'W	P	✓ / Unknown	24/01/2004	Not practicable	–	–
Alfonso XII Street, Jerónimos Neighbourhood	40°24.660'N, 3°41.333'W	S	✓ / 2440 m ²	2018–2019	Not practicable	25	2
Príncipe de Vergara Street	40°25.382'N, 3°40.826'W	S	✓ / 225 m ²	2020	Not practicable	25	2
Nueva España Neighbourhood (various streets)	40°27.560'N, 3°40.358'W	BV	✓	2011	–	–	–
		S	✓ / 93290 m ²	2019–2020	Not practicable	157	3
Outside the city of Madrid							
Aranjuez	40°2.220'N, 3°36.300'W	B	✓	1952–1968	–	–	–
		P	✓ / Unknown	2019	–	–	–
Pozuelo de Alarcón	40°27.50'N, 3°48.28'W	B	✓	1952–1968	–	–	–
Pozuelo de Alarcón, Vereda de las Columnas Street, El Paular Neighbourhood	40°27.50'N, 3°48.28'W	P	✓ / Unknown	2020	Not practicable	–	–
Rivas–Vaciamadrid	40°21.540'N, 3°32.820'W	B	✓	2011	–	–	–
		P	✓ / Unknown	2010	–	–	–
Villanueva de la Cañada, Villagolf residential area	40°26.700'N, 3°59.880'W	P	✓ / Unknown	2019	Not practicable	–	–

Table 2. Variables used in the park selection process sorted by type, with a brief description.

Type	Variable	Description
Geographical	Latitude and longitude	Georeferences of the park centroid
Spatial	Area and perimeter	Surface spatial attributes
	Orientation	Ratio between longitude and latitude differences.
	Shape	Ratio between perimeter and area. It gives an idea of the edge effect.
Management	Timetable	Opening hours
	Type of management	'Naturalised' or 'garden' type of management
Urban matrix	Distance between parks	Distance between park centroids
	Distance to city centre	Distance from park centroids to centre of the city (centroid of all parks)
	Distance to wildlife sources	Corresponding to large naturalised areas*.
	Surrounding green areas	Surface of other green areas in buffers of 100 m, 250 m, 500 m, 1000 m, 1500 m, 2000 m, 2500 m and 5000 m

*'Monte de El Pardo' and the main Protected Natural Spaces surrounding the city of Madrid: Middle Course of the Guadarrama River and its surroundings, Axes of the Lower Courses of the Manzanares and Jarama Rivers, and the Upper Basin of the Manzanares.

identified to genus or species level whenever possible, following Gómez and Espadaler (2007) and Lebas et al. (2017). All the specimens were placed in vials containing 70% ethanol and were deposited in the 'Colección de Entomología UCM' (UCME).

Those sites where *L. humile* was found were properly surveyed to measure the surface area covered by each colony. To assess the expansion limits of the colony, workers of Argentine ant were searched and mapped until they were no longer seen after having walked through the area in concentric circles, moving 50 to 100 metres away from the ant trails. The extent of the colony reflected in QGIS software (QGIS 2021) means that no Argentine ants were found beyond the boundaries of the polygon (see Fig. 3).

Results

The presence of the Argentine ant was recorded in a total of eleven points within the urban area of the city of Madrid and four peripheral locations (Fig. 1), which shows the historical and geographical background of this invasive ant in Madrid (Table 1).

The bibliographic search resulted in three documents that located the presence of the Argentine ant in five locations (B, Table 1). Data from the citizen science platform resulted in two locations (BV). We obtained six records from personal communications from the following persons: J. Reyes, J. Arcos, K. Gómez, M. Sierra, or anonymous citizens and a pest control company (N. Trotta leg.) (P). While three of them can be considered new records, the other three confirm bibliographic data. Finally, we can point out six new locations from the survey data (S), not previously recorded by other methods.

Nine of the 23 localities exhaustively sampled in the city of Madrid during the last three years showed the presence of *L. humile* (39.1% of the locations sampled;

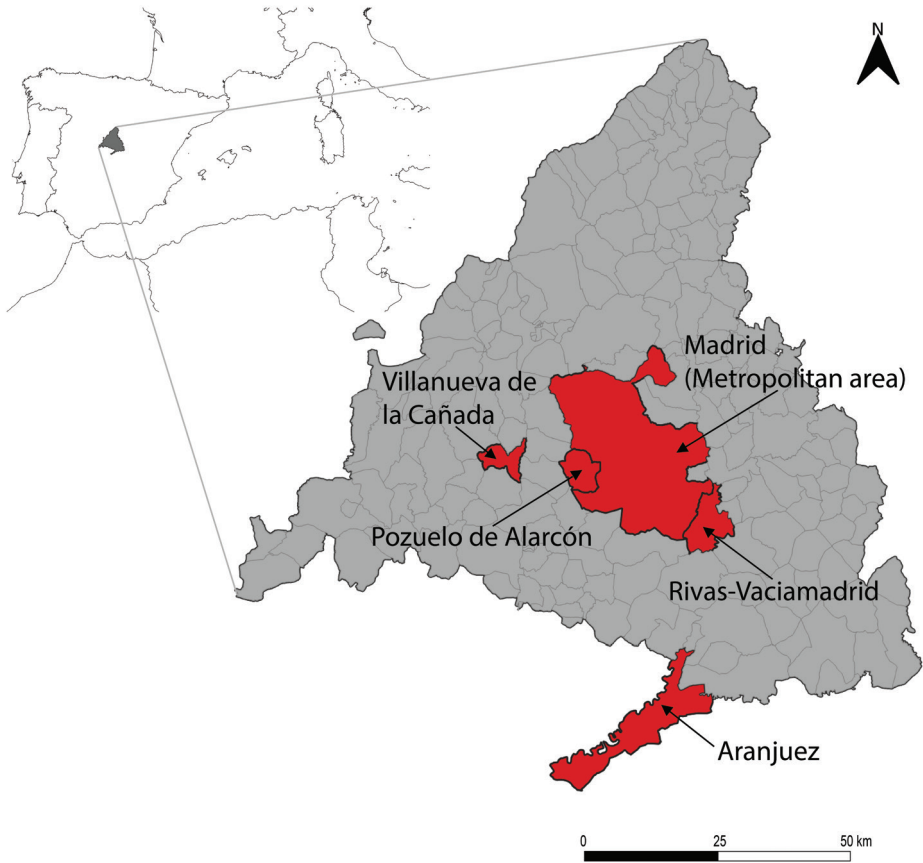


Figure 1. Municipalities (in red) where the Argentine ant has been recorded in the Community of Madrid.

S, Table 1). Six out of these nine places corresponded to green areas. Within the city limits, the species had previously been registered in a park located in the west (Casa de Campo Park; Ruiz-Heras et al. 2011) and found in two other locations in the centre and northwest of the city (BV, Table 1). *A priori*, the presence did not seem to show any geographic pattern, since they were found scattered throughout the city, although more abundant on the periphery (Fig. 2). The presences observed in other localities in Madrid and surrounding areas do not present a clear geographical pattern either but are spread over several points. The locations listed below correspond to the Argentine ant colonies observed in the city of Madrid and its surroundings.

Enrique Tierno Galván Park and Del Norte-Carmen Tagle Park

Enrique Tierno Galván Park is located in the south of the city (40°23.312'N, 3°40.961'W). With a size of 41 hectares, it is considered a large park. An Argentine

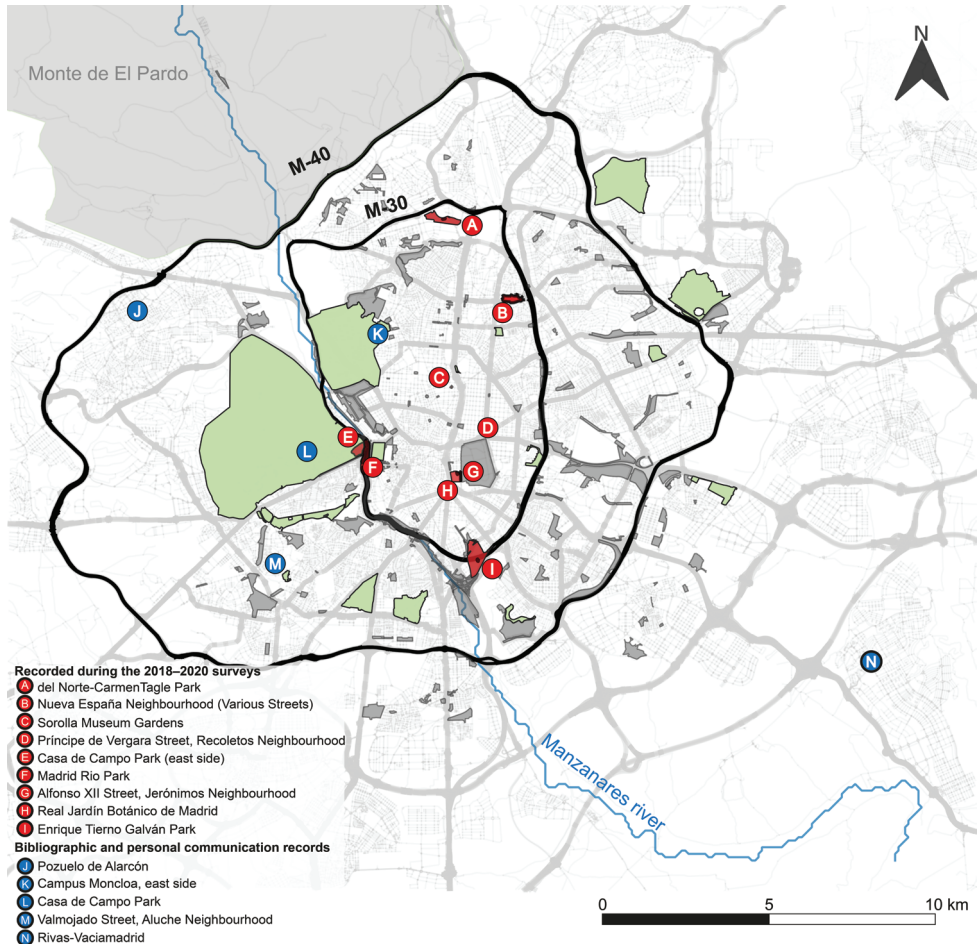


Figure 2. Locations of the Argentine ant in the city of Madrid. The letters in red circles correspond to locations where the Argentine ant has been recorded during the 2018–2020 surveys (areas in red). Letters in blue circles indicate bibliographic and personal communication records. The green areas correspond to parks and gardens that have been thoroughly sampled and where *Linepithema humile* has not been found, except for the eastern corner of the Casa de Campo Park (E). The light grey areas are green areas (parks and gardens) that have not been sampled and are capable of harbouring colonies of the Argentine ant.

ant colony was found, with its foraging tracks extending over almost 2000 square metres, where the water supply remained constant (with irrigation systems covering the grass meadows). The colony had access to plants with aphids and elements where the species could take shelter and walk easily, such as cobblestones and road gutters (Fig. 3A).

Del Norte-Carmen Tagle Park is located in the north of the city of Madrid ($40^{\circ}28.843'N$, $3^{\circ}41.734'W$), extending over 20 hectares. The colony foraging area covered approximately 380 square metres, including areas of irrigated meadows and cobblestones with ornamental shrub vegetation (Fig. 3B).

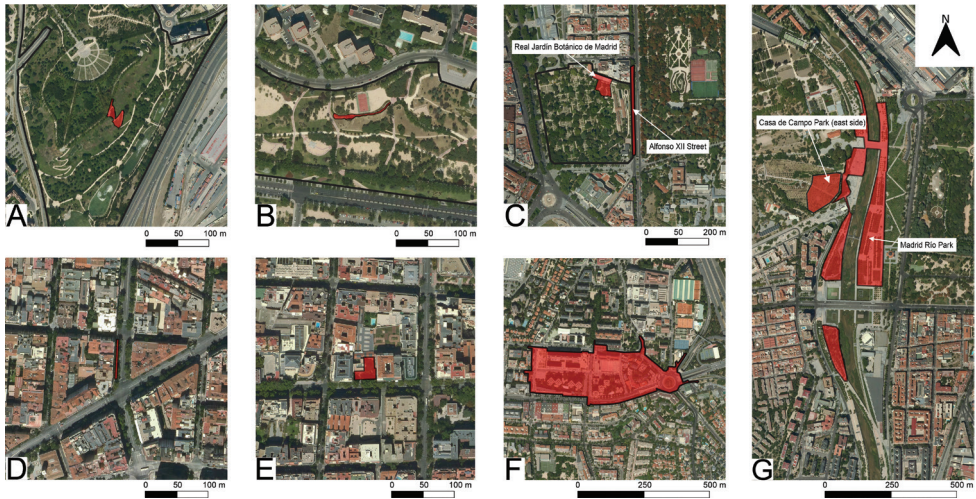


Figure 3. Colony extension and foraging areas of the Argentine ant in nine locations of Madrid. **A** Enrique Tierno Galván Park **B** del Norte-Carmen Tagle Park **C** Real Jardín Botánico de Madrid and Alfonso XII Street **D** Príncipe de Vergara Street **E** Sorolla Museum Gardens **F** Nueva España Neighbourhood **G** Casa de Campo Park (east side) and Madrid Río Park.

Real Jardín Botánico de Madrid, Alfonso XII Street and Príncipe de Vergara Street

In the Real Jardín Botánico de Madrid (Royal Botanical Garden; 40°24.660'N, 3°41.460'W), the presence of the Argentine ant confirmed a previous record (Biodiversidad Virtual 2016; Fig. 4A). To date, a single colony has been detected, with workers traversing several metres outside the exhibition greenhouse and circulating inside it in search of nectariferous plants (Fig. 3C).

A colony was also detected on Alfonso XII Street (40°24.660'N, 3°41.333'W), adjacent to the Real Jardín Botánico de Madrid. The workers may have come from inside the Jardín Botánico itself, which would act as a focal point, since several entrance trails to the possible nest were identified on a wall on the even-numbered side of the street, where a line of ants extended over approximately 300 metres (Fig. 3C). Near this location, on Príncipe de Vergara Street (40°25.382'N, 3°40.826'W), another trail of Argentine ants was spotted covering 70 metres on the sidewalk and occupying the tree pits (Fig. 3D).

Sorolla Museum Gardens

Approximately 830 square metres are occupied by the Argentine ant in the garden in front of the Sorolla museum (Fig. 3E), located near the city centre (Fig. 2; 40°26.120'N, 3°41.540'W). This green space is surrounded by walls and the ants do not occupy the adjacent street.

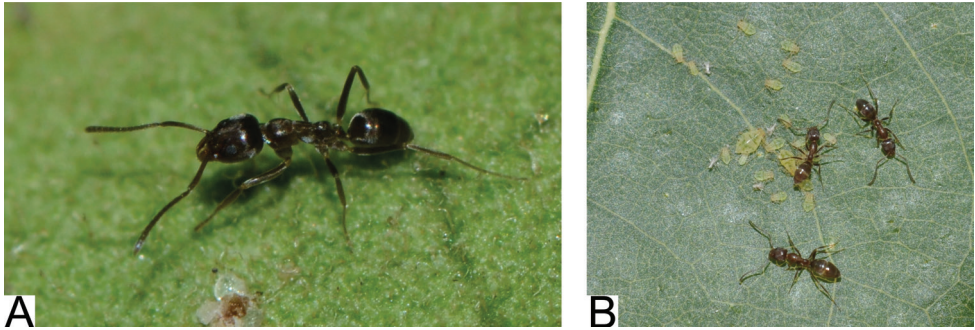


Figure 4. Argentine ant workers photographed in the city of Madrid. Both photographs belong to the citizen science platform ‘Biodiversidad Virtual’. **A** Real Jardín Botánico of Madrid, by José Fernández (Biodiversidad Virtual 2016). **B** Puerto Rico Street, Nueva España Neighbourhood, by Álvaro Izuzquiza (Biodiversidad Virtual 2011).

Nueva España Neighbourhood (Chamartín District)

A highly widespread Argentine ant population was found along the streets and gardens of Nueva España neighbourhood, in Chamartín District, with an approximate area of 9.3 hectares ($40^{\circ}27.560'N$, $3^{\circ}40.358'W$; Fig. 3F). The knowledge of this location was possible thanks to a previous record that located the sighting of *L. humile* on Puerto Rico Street (Biodiversidad Virtual 2011; Fig. 4B). Based on these data, it was possible to determine the expansion borders of this large colony, which occupies practically all the blocks in the area between Príncipe de Vergara Street, Alfonso XIII Avenue and Costa Rica Street. In addition, trails of workers were found at various points beyond these main roads. Again, private landscaped spaces, walls, urban gardens, tree pits, and ornamental shrub formations were found to be the preferred areas for the expansion and foraging habits of these ants.

Madrid Río Park

Another location where the Argentine ant is relatively abundant corresponds to a section of the Madrid Río Park, mainly between El Puente del Rey and El Puente de Segovia (two bridges over the Manzanares river), including the Virgen del Puerto Gardens, although the presence of the ant extends beyond these points ($40^{\circ}25.133'N$, $3^{\circ}43.340'W$). *Linepithema humile* presence was noticed by members of “Tecnormigas”, a group of ant fans from Madrid (M. Sierra *pers. comm.*) and verified on the ground, where numerous areas occupied by ants were detected along a wide extension on both sides of the Manzanares river (Fig. 3G).

Other records in the city of Madrid: Ciudad Universitaria, Casa de Campo Park and Aluche Neighbourhood

This ant species is cited in the bibliography on a residential area at the eastern end of Ciudad Universitaria, northwest of the city (Martínez et al. 1997; Fig. 2). According to the

authors, the colony occupied a private garden where ants could take advantage of artificial irrigation and had access to resources inside the houses. We were not able to confirm the presence today since entry was restricted. Likewise, the Argentine ant is cited in another bibliographic reference in the Casa de Campo Park (Ruiz-Heras et al. 2011; Fig. 2), although it has been found in a small portion of the park only on the east side (Fig. 3G), despite the exhaustive samplings carried out in the area in recent years. Southward, there is another *L. humile* record located on Valmojado Street (40°23.220'N, 3°45.540'W), in Aluche Neighbourhood, observed in 2004 (K. Gómez *pers. comm.*; Fig. 2).

Other records in the Community of Madrid: Villagolf-Villanueva de la Cañada residential area, Pozuelo de Alarcón, Rivas-Vaciamadrid and Aranjuez

Outside the urban district of Madrid, individuals of *L. humile* were found in private gardens in the residential area of Villagolf, 25 kilometres west of the capital (40°26.700'N, 3°59.880'W; Fig. 1), whose presence was reported to the authors by a pest control company in 2019 (N. Trotta *leg.*). In Rivas-Vaciamadrid (40°21.540'N, 3°32.820'W), in the southeast of the city, the species was observed in a landscaped street prior to 2011, according to J. Reyes (Ruiz-Heras et al. 2011 and recent *pers. comm.*; Fig. 2), but more recent surveys are needed to verify the expansion limits of this colony. Likewise, considered one of the oldest citations of this ant in the interior of the Iberian Peninsula (between 1952 and 1968), Collingwood and Yarrow (1969) had already sighted the presence of this species in the towns of Pozuelo de Alarcón and Aranjuez (Fig. 1). Its presence has recently been registered again in these two locations: in a private property in Pozuelo de Alarcón (near 40°27.500'N, 3°48.280'W; Vereda de las Columnas Street, El Paular Neighbourhood), where the owners had been noticing its presence since several years ago as the ants usually invade the garden and come indoors in winter, besides that they are spread around the neighbourhood, and in the urban environment of Aranjuez (40°2.220'N, 3°36.300'W). In this case, the ornamental trees and other typical urban elements serve as a source of resources for these ants (J. Arcos, *pers. comm.*).

Discussion

This article compiles for the first time new and previously known records of the Argentine ant in the city of Madrid and its surroundings. It shows a worrying situation that has not been previously considered and must be urgently addressed. The fact that *L. humile* has reached localities in the interior of the Iberian Peninsula, moving away from a coastal range, is unusual for a natural expansion (Espadaler and Gómez 2003). The silent expansion of *L. humile* through the different interior locations could be favoured by anthropogenic action through the movement of the species mediated by the transport of goods, gardening tools, ornamental plants, etc., as suggested by numerous authors (Suárez et al. 2001; Ward et al. 2005; Obregón and Reyes-López 2016). In general terms, the city of Madrid is undergoing a premature stage of colonisation by

the Argentine ant, although its presence has been recorded accidentally for a minimum of three decades (at least since 1991). Since observations in time and space are isolated and apparently unrelated to each other, entry and translocation of propagule-bearing elements are presented as the most probable hypothesis to explain ant dispersal, along with natural processes of spread of ants from other colonisation points.

Thus, we propose two ways in which the expansion can occur within the city itself: (i) directly, since reproduction takes place by budding (Hölldobler and Wilson 1990), so natural splits of a main colony that establishes new settlements increase the area of influence (e.g., what could be happening in a large area such as Nueva España Neighbourhood or Madrid Río Park); (ii) indirectly, due to the maintenance of green areas. Considering that many of the colonies are located in different points of the city separated in many cases by kilometres apart, a plausible explanation is the entry and translocation of garden elements, which act as vectors carrying potential colonising propagules from infested to non-infested areas. This situation enables a rapid colony expansion and facilitates the dispersal of these colonies, involving numerous zones and different sizes of green spaces (ranging from flower boxes, tree pits and patches of grass to large parks, wastelands and forest areas) as pointed out by Forte (1956) in the metropolitan areas of Western Australia. To date, the likelihood that the Argentine ant is using the sewage system to facilitate the passage from one street to another has been discarded, although it may be happening in the city of Barcelona (J. Arcos *pers. comm.*). Even so, it has been observed that in certain parks they use drains to connect foraging areas and thus avoid the paths used by vehicles and people.

The locations where the Argentine ant has been found in Madrid have a number of common characteristics that could allow it to survive and expand. Artificially irrigated areas offer an almost constant supply of moisture, which, combined with food resources that can be found in parks, gardens and even indoors, makes these areas highly valuable sites for nesting and foraging. Parks that are heavily disturbed (mowed and irrigated with sprinklers) are more likely to harbour exotic species like *L. humile* (Walters 2006) compared with more naturalized areas and urban forests (Clarke 2008). In addition, buildings and other urban elements could serve as a refuge in colder times of the year, when colonies spatially contract in winter (Heller and Gordon 2006; Abril et al. 2008). One of the possible causes of the Argentine ant persistence in cold cities of Minnesota and Illinois (United States), with a very similar latitude to Madrid, is that they overwinter in heated buildings (Gordon et al. 2001; Hartley and Lester 2003). In short, the micro-environments generated in cities, the lack of a natural vegetative structure or the Urban Heat Island effect, can lead generalist species, which often include invasive species, to colonise and better adapt to urban environments (Menke et al. 2011; Ducatez et al. 2018). In the medium to long term, cities could become 'reservoirs' from which an invasive species, such as the Argentine ant, could colonise adjacent anthropized spaces and even natural areas (Borden and Flory 2021).

The location of Nueva España Neighbourhood (Fig. 3D) can be highlighted due to the large area occupied by the Argentine ant, where an advanced level of settlement can be observed. This colony may have originated at the time of the first record (Bio-

diversidad Virtual 2011) and possibly earlier. It is in this location, as well as in Alfonso XII Street next to the Real Jardín Botánico de Madrid, Madrid Río Park and Sorolla Museum Gardens where a clear displacement of other species, relatively common in the rest of the urban environment of Madrid, can be noticed. In fact, typical urban species such as *Lasius grandis* Forel, 1909, *Messor* cf. *structor* (Latreille, 1798), *Pheidole pallidula* (Nylander, 1849), *Plagiolepis pygmaea* (Latreille, 1798), *Tapinoma* cf. *nigerimum* (Nylander, 1856) or *Tetramorium* cf. *caespitum* (Linnaeus, 1758) are again present once the expansion limits of *L. humile* become blurred. In some of these borders, fights with *T. cf. nigerrimum* were observed. This dominant species has been shown to be a competitor that offers resistance to the Argentine ant by decreasing the probability of its rapid colonisation and survival (Blight et al. 2010).

In Enrique Tierno Galván Park, Del Norte Park and Real Jardín Botánico, the colonies are relatively small in extension, but their surroundings are potentially colonisable, given the structure and elements of these green areas. In addition, it should be considered that the city of Madrid has more than 200 green areas integrated into the urban matrix that may be considered attractive for this species, with a variety of suitable places for the Argentine ant to establish, depending on the park size, the level of irrigation, the refuges, etc. In these circumstances, the invasion of this species is taking place slowly but surely.

Therefore, given the strong likelihood that the Argentine ant will continue colonising the city of Madrid and the rest of the surrounding locations and given the negative effects that its presence may have on the diversity of other ant species (Touyama et al. 2003; Holway and Suarez 2006; Stringer 2009; Achury et al. 2020) and other arthropods (Walters 2006) in urban settings, this paper calls for a joint action by researchers, managers and competent authorities to propose studies and solutions that help stop the expansion of this invasive ant.

Various methods have been used to control the Argentine ant, generally in natural environments and agricultural systems, mainly based on insecticides and toxic baits (Forschler and Evans 1994; Klotz et al. 2003; Daane et al. 2006; Choe et al. 2014). In an urban context, the greatest challenge may be the difficulty in applying treatments in a heterogeneous environment that not only involves parks and other green areas, but also a diverse set of small and inaccessible enclaves, infrastructures, buildings, houses and other private properties. Despite this, a large number of successful eradication programmes for invasive ants have been carried out in urban or industrial locations (Hoffman et al. 2016), and it is also noteworthy the progress being made in terms of improving bait treatments that reduce non-target effects (Cabrera et al. 2021).

Certainly, the best strategy that can be carried out, as mentioned by several researchers (Carpintero et al. 2004; Ward et al. 2005; Angulo et al. 2007; Stanley et al. 2008), is prevention by detecting and eliminating the propagules transported by humans, apart from an active aggressive and eradication management strategy (Silverman and Brightwell 2008; Vanderwoude et al. 2021). In this sense, preventive measures may include routine checks of agricultural or gardening equipment, work tools and transport vehicles. An option that should be seriously considered is the implementation of monitoring programmes with citizen participation in order to detect new

outbreaks and areas susceptible to invasion, observe the expansion of colonies, and study the influence on the diversity of other ants and invertebrates and vice versa (e.g., analyse whether any natural agent can decrease the expansion of the Argentine ant). Several citizen science projects have shown to be effective in the search for invasive and native ants (Lucky et al. 2014; Castracani et al. 2020) and could be applied in the case of the Argentine ant since it is a ubiquitous and conspicuous species that can be easily identified in the field and by photography. Such measures should be taken before facing a more widespread invasion.

Conclusion

The presence of the Argentine ant in Madrid and its surroundings reveals a gradual entry and a silent expansion within the city in recent years. Since it is likely that there will be new entries or movements of this species in the form of nest relocations, applying a monitoring system that involves citizens, researchers and local authorities should be really advantageous. These actions would prevent the city from becoming a 'reservoir' for the species, reducing the long-term chances of new enclaves being colonized by the Argentine ant, such as naturalized environments near the city.

Acknowledgements

We are grateful to the citizen science platform 'Biodiversidad Virtual' (especially to José Fernández and Álvaro Izuzquiza) for the georeferenced data and the photos of the Argentine ant. We also thank Javi Arcos (UAB), Kiko Gómez, Lola Martínez (UCM), Daniel Padilla (GSB), Joaquín Reyes (UCO), Mariano Sierra (Tecnormigas), Nuria Trotta (INTI, SA), M^a Ángeles Vázquez (UCM) and Josefina Cabrero for sharing information on the records referred to in this work. We are also thankful to the Community of Madrid and the Madrid City Council for the permits granted for the development of this project. We are very grateful to Xavier Espadaler for his comments and to an anonymous referee that helped us to substantially improve our manuscript.

References

- Achury R, Holway DA, Suarez AV (2020) Pervasive and persistent effects of ant invasion and fragmentation on native ant assemblages. *Ecology* 102(3): 1–14. <https://doi.org/10.1002/ecy.3257>
- Abril S, Oliveras Huix J, Gómez López C (2008) Effect of seasonal dynamics on queen densities of the Argentine Ant (*Linepithema humile*) in an invaded natural area of the NE Iberian Peninsula. *Sociobiology* 51: 1–10. <https://dugi-doc.udg.edu/handle/10256/8250?show=full>
- Agosti D, Alonso LE (2000) The all protocol. In: Agosti D, Majer DJ, Alonso LE, Schultz RT (Eds) *Ants: standard methods for measuring and monitoring biodiversity*. Smithsonian Institution Press, Washington DC, 204–206.

- Angulo E, Boulay R, Rodrigo A, Retana J, Cerdá X (2007) Efecto de una especie invasora, *Linepithema humile*, la hormiga argentina, sobre la biodiversidad del Parque Nacional de Doñana (Huelva): descripción de las interacciones con las hormigas nativas. Proyectos de investigación en parques nacionales: 2003–2006.
- Biodiversidad Virtual (2011) <https://www.biodiversidadvirtual.org/insectarium/Linepithema-humile-img258305.html> [Accessed on 09 March 2021]
- Biodiversidad Virtual (2016) [https://www.biodiversidadvirtual.org/insectarium/Linepithema-humile-\(Mayr-1868\)-img931305.html](https://www.biodiversidadvirtual.org/insectarium/Linepithema-humile-(Mayr-1868)-img931305.html) [Accessed on 09 March 2021]
- Blight O, Provost E, Renucci M, Tirard A, Orgeas J (2010) A native ant armed to limit the spread of the Argentine ant. *Biological Invasions* 12: 3785–3793. <https://doi.org/10.1007/s10530-010-9770-3>
- Borden JB, Flory SL (2021) Urban evolution of invasive species. *Frontiers in Ecology and the Environment* 19: 184–191. <https://doi.org/10.1002/fee.2295>
- Cabrera E, Rivas Fontan I, Hoffmann, BD, Josens R (2021) Laboratory and field insights into the dynamics and behavior of Argentine ants, *Linepithema humile*, feeding from hydrogels. *Pest Management Science*. <https://doi.org/10.1002/ps.6368>
- Carpintero S, Reyes-Lopez J, Arias de Reyna L (2004) Impact of human dwellings on the distribution of the exotic Argentine ant: a case study in the Doñana National Park, Spain. *Biological Conservation* 115: 279–289. [https://doi.org/10.1016/S0006-3207\(03\)00147-2](https://doi.org/10.1016/S0006-3207(03)00147-2)
- Carpintero S, Retana J, Cerdá X, Reyes-López J, Arias de Reyna L (2014) Exploitative strategies of the invasive Argentine ant (*Linepithema humile*) and native ant species in a southern Spanish pine forest. *Environmental Entomology* 36: 1100–1111. <https://doi.org/10.1093/ee/36.5.1100>
- Castracani C, Spotti FA, Schifani E, Giannetti D, Ghizzoni M, Grasso DA, Mori A (2020) Public Engagement Provides First Insights on Po Plain Ant Communities and Reveals the Ubiquity of the Cryptic Species *Tetramorium immigrans* (Hymenoptera, Formicidae). *Insects* 11: 678. <https://doi.org/10.3390/insects11100678>
- Choe DH, Tsai K, Lopez CM, Campbell K (2014) Pheromone-assisted techniques to improve the efficacy of insecticide sprays against *Linepithema humile* (Hymenoptera: Formicidae). *Journal of Economic Entomology* 107: 319–325. <https://doi.org/10.1603/EC13262>
- Clarke KM, Fisher BL, LeBuhn G (2008) The influence of urban park characteristics on ant (Hymenoptera, Formicidae) communities. *Urban Ecosystems* 11: 317–334. <https://doi.org/10.1007/s11252-008-0065-8>
- Collingwood CA, Yarrow LL (1969) A survey of Iberian Formicidae (Hymenoptera). *EOS. Revista Española de Entomología* 44: 53–101. <https://antcat.org/references/123816>
- Daane KM, Sime KR, Hogg BN, Bianchi ML, Cooper ML, Rust MK, Klotz JH, (2006) Effects of liquid insecticide baits on Argentine ants in California's coastal vineyards. *Crop Protection* 25: 592–603. <https://doi.org/10.1016/j.cropro.2005.08.015>
- Espadaler X, Collingwood C (2001) Transferred ants in the Iberian Peninsula (Hymenoptera, Formicidae). *Nouvelle Revue d'Entomologie* 1: 257–263.
- Espadaler X, Gómez C (2003) The Argentine ant, *Linepithema humile*, in the Iberian Peninsula. *Sociobiology*. 42: 187–192.

- Forschler BT, Evans GM (1994) Perimeter treatment strategy using containerized baits to manage Argentine ants, *Linepithema humile* (Mayr) (Hymenoptera: Formicidae). *Journal of Entomological Science* 29: 264–267. <https://doi.org/10.18474/0749-8004-29.2.264>
- Forte PN (1956) Some observations on the Argentine Ant campaign in Western Australia. *Journal of Agriculture of Western Australia* 5: 1–8. https://researchlibrary.agric.wa.gov.au/cgi/viewcontent.cgi?article=1745&context=journal_agriculture3
- Global Invasive Species Database (GISD) (2015) Species profile: *Linepithema humile*. <http://www.iucngisd.org/gisd/species.php?sc=127> [Accessed on 09 March 2021]
- Gómez K, Espadaler X. (2007) Hormigas.org. Asociación Ibérica de Mirmecología. Girona. <http://www.hormigas.org/> [Accessed on 09 March 2021]
- Gordon DM, Moses L, Falkovitz-Halpern M, Wong EH (2001) Effect of weather on infestation of buildings by the invasive Argentine ant, *Linepithema humile* (Hymenoptera: Formicidae). *The American Midland Naturalist* 146: 321–328. [https://doi.org/10.1674/0003-0031\(2001\)146\[0321:EOWOIO\]2.0.CO;2](https://doi.org/10.1674/0003-0031(2001)146[0321:EOWOIO]2.0.CO;2)
- Greenberg L, Klotz JH, Rust MK (2006) Liquid borate bait for control of the Argentine ant, *Linepithema humile*, in organic citrus (Hymenoptera: Formicidae). *Florida Entomologist* 89: 469–474. [https://doi.org/10.1653/0015-4040\(2006\)89\[469:LBBFCO\]2.0.CO;2](https://doi.org/10.1653/0015-4040(2006)89[469:LBBFCO]2.0.CO;2)
- Hair JF, Anderson RE, Tatham RL, Black WC (1999) *Análisis multivariante*. Prentice Hall (Madrid): 832 pp.
- Hartley S, Lester PJ (2003) Temperature-dependent development of the Argentine ant, *Linepithema humile* (Mayr) (Hymenoptera: Formicidae): a degree-day model with implications for range limits in New Zealand. *New Zealand Entomologist* 26: 91–100. <https://doi.org/10.1080/00779962.2003.9722113>
- Heller NE, Gordon DM (2006) Seasonal spatial dynamics and causes of nest movement in colonies of the invasive Argentine ant (*Linepithema humile*). *Ecological Entomology* 31: 499–510. <https://doi.org/10.1111/j.1365-2311.2006.00806.x>
- Hoffmann BD, Luque GM, Bellard C, Holmes ND, Donlan CJ (2016) Improving invasive ant eradication as a conservation tool: A review. *Biological Conservation* 198: 37–49. <https://doi.org/10.1016/j.biocon.2016.03.036>
- Holway DA, Suarez AV (2006) Homogenization of ant communities in Mediterranean California: The effects of urbanization and invasion. *Biological Conservation* 127(3): 319–326. <https://doi.org/10.1016/j.biocon.2005.05.016>
- Hölldobler B, Wilson EO (1990) *The ants*. Harvard University Press: 732 pp. <https://doi.org/10.1007/978-3-662-10306-7>
- Kaiser A, Merckx T, Van Dyck H (2016) The Urban Heat Island and its spatial scale dependent impact on survival and development in butterflies of different thermal sensitivity. *Ecology and Evolution* 6: 4129–4140. <https://doi.org/10.1002/ece3.2166>
- Kennedy TA (1998) Patterns of an invasion by Argentine ants (*Linepithema humile*) in a riparian corridor and its effects on ant diversity. *The American Midland Naturalist* 140: 343–351. [https://doi.org/10.1674/0003-0031\(1998\)140\[0343:POAIBA\]2.0.CO;2](https://doi.org/10.1674/0003-0031(1998)140[0343:POAIBA]2.0.CO;2)

- Klotz JH, Rust MK, Gonzalez D, Greenberg L, Costa H, Phillips P, Gispert C, Reiersen DA, Kido K (2003) Directed sprays and liquid baits to manage ants in vineyards and citrus groves. *Journal of Agricultural and Urban Entomology* 20: 31–40.
- Lebas C, Galkowski C, Blatrix R, Wegnez P (2017) *Guía de las hormigas de Europa occidental*. Ediciones Omega (Barcelona): 415 pp.
- Lucky A, Savage AM, Nichols LM, Castracani C, Shell L, Grasso DA, Mori A, Dunn RR (2014) Ecologists, educators, and writers collaborate with the public to assess backyard diversity in The School of Ants Project. *Ecosphere* 5: 1–23. <https://doi.org/10.1890/ES13-00364.1>
- Martínez MD, Ornos C, Gamarra P (1997) *Linepithema humile* (Mayr 1868) (Hymenoptera: Formicidae) en las viviendas de Madrid. *Boletín de la Asociación Española de Entomología* 21: 275–276. <https://www.antcat.org/references/131822>
- McGlynn TP (1999) The worldwide transfer of ants: geographical distribution and ecological invasions. *Journal of Biogeography* 26: 535–548. <https://doi.org/10.1046/j.1365-2699.1999.00310.x>
- McGlynn TP, Meineke EK, Bahlai CA, Li E, Hartop EA, Adams BJ, Brown BV (2019) Temperature accounts for the biodiversity of a hyperdiverse group of insects in urban Los Angeles. *Proceedings of the Royal Society B* 286, 20191818. <https://doi.org/10.1098/rspb.2019.1818>
- Menke SB, Guénard B, Sexton JO, Weiser MD, Dunn RR, Silverman J (2011) Urban areas may serve as habitat and corridors for dry-adapted, heat tolerant species; an example from ants. *Urban Ecosystems* 14: 135–163. n RR, Silverman J (2011) Urban areas may serve as habitat and corridors for dry-adapted, heat tolerant species; an example from ants. *Urban Ecosystems* 14: 135–163. <https://doi.org/10.1007/s11252-010-0150-7>
- Mgocheki N, Addison P (2009) Interference of ants (Hymenoptera: Formicidae) with biological control of the vine mealybug *Planococcus ficus* (Signoret) (Hemiptera: Pseudococcidae). *Biological Control* 49: 180–185. <https://doi.org/10.1016/j.biocontrol.2009.02.001>
- Obregón R, Reyes-López J (2016) Primera cita de la hormiga invasora *Linepithema humile* (Mayr, 1868) en el País Vasco (Hymenoptera, Formicidae). *Revista gaditana de Entomología* 7: 515–518. <https://www.biotaxa.org/RGDE/article/view/25651>
- Powell BE, Silverman J (2010) Population growth of *Aphis gossypii* and *Myzus persicae* (Hemiptera: Aphididae) in the presence of *Linepithema humile* and *Tapinoma sessile* (Hymenoptera: Formicidae). *Environmental Entomology* 39: 1492–1499. <https://doi.org/10.1603/EN09211>
- QGIS Development Team (2021) QGIS Geographic Information System. Open Source Geospatial Foundation Project. <http://qgis.osgeo.org>
- Roura-Pascual N, Brotons L, Peterson AT, Thuiller W (2009) Consensual predictions of potential distributional areas for invasive species: a case study of Argentine ants in the Iberian Peninsula. *Biological Invasions* 11: 1017–1031. <https://doi.org/10.1007/s10530-008-9313-3>
- Roura-Pascual N, Suarez AV, McNyset K, Gómez C, Pons P, Touyama Y, Wild AL, Gascon F, Peterson AT (2006) Niche differentiation and fine-scale projections for Argentine ants based on remotely sensed data. *Ecological Applications* 16: 1832–1841. [https://doi.org/10.1890/1051-0761\(2006\)016\[1832:NDAFPF\]2.0.CO;2](https://doi.org/10.1890/1051-0761(2006)016[1832:NDAFPF]2.0.CO;2)
- Ruiz Heras P, Martínez Ibáñez MD, Cabrero-Sañudo FJ, Vázquez Martínez MÁ (2011) Primeros datos de Formicidos (Hymenoptera, Formicidae) en parques urbanos de Madrid. *Bo-*

- letín de la Asociación Española de Entomología 35(1–2): 93–112. <https://dialnet.unirioja.es/servlet/articulo?codigo=3962684>
- Silva Dias JC (1955) Biología e ecología da Formiga Argentina (*Iridomyrmex humile* Mayr) - Notas para o seu estudo em Portugal. Separato do Boletim da Junta Nacional das Frutas, Lisbon, 118 pp.
- Silverman J, Brightwell RJ (2008) The Argentine ant: Challenges in managing an invasive unicolonial pest. *Annual Review of Entomology* 53: 231–252. <https://doi.org/10.1146/annurev.ento.53.103106.093450>
- Stanley M, Ward D, Harris R, Arnold G, Toft R, Rees J (2008) Optimizing pitfall sampling for the detection of Argentine ants, *Linepithema humile* (Hymenoptera: Formicidae). *Sociobiology* 51: 461–472.
- Stringer LD, Stephens AE, Suckling DM, Charles JG (2009) Ant dominance in urban areas. *Urban Ecosystems* 12: 503–514. <https://doi.org/10.1007/s11252-009-0100-4>
- Suárez AV, Holway DA, Case TJ (2001) Patterns of spread in biological invasions dominated by long-distance jump dispersal: insights from Argentine ants. *Proceedings of the National Academy of Sciences* 98: 1095–1100. <https://doi.org/10.1073/pnas.98.3.1095>
- Touyama Y, Ogata K, Sugiyama T (2003) The Argentine ant, *Linepithema humile*, in Japan: assessment of impact on species diversity of ant communities in urban environments. *Journal of Entomological Science* 6: 57–62. <https://doi.org/10.1046/j.1343-8786.2003.00008.x>
- UBMS (2018) <http://ubms.creaf.cat/en/> [Accessed on 13 June 2021]
- Vanderwoude C, Boudjelas S, Gruber M, Hoffmann B, Oi D, Porter S (2021) Biosecurity Plan for Invasive Ants in the Pacific Region. *Invasive Alien Species: Observations and Issues from Around the World* 2: 275–288. <https://doi.org/10.1002/9781119607045.ch25>
- Walters AC (2006) Invasion of Argentine ants (Hymenoptera: Formicidae) in South Australia: impacts on community composition and abundance of invertebrates in urban parklands. *Austral Ecology* 31: 567–576. <https://doi.org/10.1111/j.1442-9993.2006.01592.x>
- Ward DF, Harris RJ, Stanley MC (2005) Human-mediated range expansion of Argentine ants *Linepithema humile* (Hymenoptera: Formicidae) in New Zealand. *Sociobiology* 45: 401–407.
- Wetterer JK, Wild AL, Suarez AV, Roura-Pascual N, Espadaler X (2009) Worldwide spread of the Argentine ant, *Linepithema humile* (Hymenoptera: Formicidae). *Myrmecological News* 12: 187–194.

